The development of light curable biomaterials with enhanced biocompatibility for orthopaedic surgery

By

Laura Cristina Nicolae

A thesis submitted to the
University of Birmingham
for the degree of
Doctor of Philosophy

School of Dentistry
University of Birmingham
January 2016

Synopsis

Orthopaedic applications commonly involve the use of polymethylmethacrylate (PMMA)-based cements in an attempt to repair fractures, stabilise metallic prosthesis or fill gaps in bone tissue as a result of trauma. These PMMA cements, however, are encased in a fibrous capsule, in the organism, which often leads to de-bonding of the cement from the adjacent bone, requiring further surgeries and patient discomfort. Alternative materials have been tested including calcium phosphate cements and bioceramics in an attempt to provide a more suitable material for bone repair compared with PMMA-based cements; however, the cement that may successfully repair and lead to regeneration of bone tissue has still to be developed. This work used a PMMA-based cement as a starting point to develop a cement based on dimethacrylate resins with enhanced physical (degree of conversion) and mechanical characteristics (flexural strength and flexural modulus) that integrated with surrounding bone without the formation of the fibrous scar at its interface with bone and soft tissues. This new dimethacrylate-based cement will contain different types of bioactive glasses, which may provide increased viability of bone cells, differentiation of mesenchymal stem cells to bone cells and direct bonding to bone (without the formation of a fibrous capsule) .

.

Acknowledgements

I would like to extend special thanks to Professor Damien Walmsley and Dr Melisa Grant for inspiration, invaluable advice and support in writing this thesis and for their encouragement patience and time, which made it all possible.

I am also grateful to Dr Martin for his help with the synthesis of bioactive glass. I would also like to express my gratitude to the laboratory technicians, especially, Dr Gay and Dr Liu for providing help and advice when I most needed it.

Finally, I would like to express my gratitude and sincere thanks to my friends, for their patience and support throughout this PhD. My deep thanks and gratitude go to Chris and Christian, who provided immense support analysing and understanding the data, encouragement and write-up advice throughout the PhD. I would also like to extend my gratitude to Flavia, who provided invaluable help and advice in understanding and analysing data. I would also like to express my thanks to Cleo and Naveed (my fellow PhD students) for listening and trying to help.

Dedicated to my family

Abbreviations

bisGMA	bisphenol-a-glycidyldimethacrylate
UDMA	urethane dimethacrylates
TEGDMA	triethylene glycol dimethacrylate
CQ	camphorquinone
DMAEMA	2 dimethylaminoethylmethacrylate
DC	degree of conversion
RP	rate of polymerisation
FS	flexural strength
FM	flexural modulus
WS	water sorption
SO	solubility
FRC	filled resin composite

Contents

List of illustrations

List of Tables

CHAPTER 1 DEVELOPMENT OF LIGHT CURABLE DIMETHACRYLATE RESIN SYSTEMS FOR ORTHOPAEDIC APPLICATIONS

1.1 Development of materials for orthopaedic applications: a historical background

Orthopaedic applications may involve the use of autografts, allografts and artificial implants (polymeric or metallic) to repair bone defects and restore function. The use of autografts and allografts despite their limited supply, immune rejection, possibility of transmission of diseases, donor-site morbidity, donor-site pain and increased costs are still the treatment of choice in orthopaedic applications, requiring the use of transplanted bone to restore function or cover defects as a result of trauma (Kanczler and Oreffo 2008; Vakiparta et al 2005; Wang et al. 2010). Perhaps the most widely used artificial implants in orthopaedic surgeries are metallic devices such as titanium alloys employed in hip, knee and dental prosthesis. However, new materials are required for the repair of structures that contain complex shapes such as those in feet, hand, ear and spinal tissues (Schneider et al. 2010). For an implant to be considered a suitable alternative to these treatment options, it should be able to restore function and integrity in load bearing applications in the long term (Liu et al. 2011; Schneider et al. 2010), be firm enough to limit stress shielding in the adjacent bone (Zou et al. 2009) and exhibit a similar elastic modulus to that of bone to provide increased resilience (Lin et al. 2005). Consequently, with an ever increasing demand for bone replacement therapies, there is a need for the development of artificial materials capable of repairing and restoring function in bone defects and also to treat specific orthopaedic problems. Materials which may have a benefit for these latter applications include bio-resorbable polymers (polylactides, polyglycolide) and bioactive ceramics (hydroxyapatite, tricalcium phosphate, bioactive glasses). The application of bioactive materials provides the possibility of integrating the artificial material in the living tissue, leading

not only to attachment, growth, proliferation and differentiation of progenitor cells, but also enabling a strong bond of the bioactive material to the bone (Pamula et al. 2011).

1.2 Development of cement materials for orthopaedic applications and their impact on bone tissue

Bone can be classified according to its structure in cortical (compact) and trabecular bone (cancellous, spongy). Cortical bone, with a porosity of 5-10%, is found in the shaft of long bones and has a compressive strength of 120-150MPa with an elastic modulus of 10-20GPa (An, 2000; Ling et al. 2009; Rahaman et al. 2011; Rho et al. 1995). Trabecular bone, on the other hand, has a compressive strength of 2-12MPa and an elastic modulus of 0.1-5GPa; both values being considerably lower than those of cortical bone (An, 2000; Ling et al. 2009; Rahaman et al. 2011; Rho et al. 1995). The human femoral bone exhibits an ultimate compressive strength of 205MPa (Schneider et al. 2010). For a material to be successful in repairing and restoring function in orthopaedic applications, it has to closely match the mechanical properties (flexural strength and modulus) of bone to provide increased resilience and limit stress shielding in the adjacent bone.

In an era of titanium osseointegration and guided tissue regeneration, materials had to be developed to provide mechanical stability to the titanium prosthesis and to ensure screw purchase in osteoporotic bone, materials such as PMMA (Poly-methyl methacrylate), calcium phosphates and hydroxyapatite-based cements. These materials were also developed as a response to the need for a material to be used as a bone void filler for bone reconstruction in trauma or in congenital malformations. However, these materials have several shortcomings including: formation of a fibrous capsule sourrounding the implant in case of the PMMA cement, which negatively interferes with the bone repair and regeneration; brittleness and fast

resorbtion rates in the case of the calcium phosphates and hydroxyapatite-based cements which fail to provide mechanical support for enough time to allow the sorrounding bone to repair and regenerate the site of injury. A cement may be developed, which is able to provide mechanical support for bone regeneration and repair to occur (through for example a resin based component), while providing a suitable environment (free of inflamation) for migration of osteogenic stem cells to the site of injury and their proliferation and differentiation to osteoblasts (through for example the use of bioactive glass able to form a hydroxyapatite layer on the surface of the material). Such a cement may be used alongside existing cement formulations, depending on the type of surgery or reconstruction required: for example it may provide a better alternative for surgeries involving non-union fractures due to its strong bonding to bone, without the formation of a fibrous capsule.

1.2.1 Poly-methyl methacrylate (PMMA) cement

Acrylic bone cements such as PMMA have in their composition a liquid methyl methacrylate monomer and a pre-polymerised polymethyl methacrylate powder (Aita et al. 2010; Deb et al. 2005). PMMA bone cements were first developed by Charnley to help immobilise prosthesis (Charnley, 1960). It has become one of the most commonly employed alloplastic materials in orthopaedic surgery, and it is used in the repair of skull defects and spinal injuries, amongst other applications (Chang et al. 2010; Deb et al. 2005). Commercially available cements based on PMMA include: Cobalt (Biomet, Inc.), Simplex (Stryker, Inc.) and Palacos (Heraeus Company). In orthopaedic surgery, PMMA's main role is as an anchoring agent in cemented joint replacement of the hip and knee to transfer the service loads and stabilise the prosthesis (when pressed between the femoral stem and the bone) (Aita et al. 2010; Deb et al. 2005; Lewis, 1997; Lewis et al. 1997; Peltola et al. 2012; Saito et al. 1994). Bone cementation is achieved through the injection of the fluid material (such as PMMA) into the bone defect leading to its

hardening within the target area, thus not only providing mechanical stability but also facilitating pain relief and increased mobility post-operatively (Chang et al. 2010). Other roles in orthopaedics include screw purchase in osteoporotic bone and stability of bone construct implant of metaphyseal fractures in osteoporotic patients (Larsson 2006).

The advantages of using this type of cement include: a density similar to that of bone, decreased thermal conductivity (Peltola et al. 2012), cost efficiency and ease of manufacture (Pryor et al. 2009). Disadvantages of using PMMA in orthopaedic applications relate to shrinkage (Lewis, 1997; Lewis et al. 1997), brittleness, poor radiopacity and mechanical strength, an inability to be remodelled (Larsson 2006; Pryor et al. 2009), non-degradability (Chang et al. 2010) and stiffness (Pryor et al. 2009). PMMA is, moreover, a water-free hydrophobic compound, thus it can only be observed indirectly as a lack of signal on magnetic resonance imaging scan (which works by visualising free protons) (Wichlas et al. 2010). The weak radiopacity makes it difficult to identify the cement mantle, the interface between the cement and bone and the interface between the implant and cement on either an X-ray or a magnetic resonance imaging scan (Lewis, 1997; Lewis et al. 1997; Pryor et al. 2009). This cement can be made radiopaque through the incorporation of $BaSO_4$ or ZrO_2 particles, which may, however, severely limit the mechanical properties of the PMMA cement (Pryor et al. 2009). The low mechanical properties and increased degradation of such cements containing $BaSO_4$ or ZrO_2 particles compared with PMMA cements are due to the phase separation of the cement compounds, between the high polar ionic radiopaque salt and the low polarity of the resin (Khaled et al. 2011).

Other shortcomings of employing PMMA in orthopaedic applications include foreign-body reactions, significantly high polymerisation exotherm, poor osseo-integration (inability to chemically attach to bone and soft tissue), possibility of leaching out, risk of inhibiting the healing of fractures of extremities (when located between fracture surfaces), complexity in

removal if the patient has to undergo revision surgery and the lifelong possibility of infection or extrusion (Aita et al. 2010; Deb et al. 2005; Fukuda et al. 2011; Ha et al. 2011; Larsson 2006; Liu et al. 2010; Peltola et al. 2012; Pryor et al. 2009; Saito et al. 1994). Foreign body reactions occur due to cement particles interacting with the living tissue, which may lead to an inflammatory peri-prosthetic tissue response, resulting in bone destruction (Lewis, 1997; Lewis et al. 1997). The high polymerisation exotherm (with a temperature increase of ≥45°C) may lead to denaturation of proteins and necrosis of cells when implanted in the human body (Baroud et al. 2004; Belkof and Molloy, 2003; Deramond et al. 1999; Luo et al. 2007; Uchiyama et al. 1989), also resulting in bone resorption. Poor osseo-integration may lead to the formation of a fibrous tissue at the interface between the cement and the bone, which may play a role in the aseptic loosening of the prosthesis together with interfacial, bone and cement failure (Chang et al. 2010; Fukuda et al. 2011; He et al. 2012; Lewis, 1997; Lewis et al. 1997; Saito et al. 1994), which also leads to bone resorption. The leakage of unreacted methyl methacrylate monomer into surrounding tissue may lead to chemical necrosis and resorption of bone and to the compression and thermal necrosis of the host tissues in percutaneous vertebroplasty (employed to treat painful osteoporotic vertebral compression fractures and malignant bone tumours) (Anselmetti et al. 2009; Chang et al. 2010; Larsson 2006; Lewis, 1997; Lewis et al. 1997). Due to its high exothermic reaction during polymerization (which can range between 67-124°C, depending on the body site where used and amount of cement), PMMA has also been shown to cause thermal necrosis of bone and neural tissues, with the formation of a zone of adjacent necrosis (Anselmetti et al. 2009; Chang et al. 2010; Saito et al. 1994), restricted local blood flow, and formation of a fibrous tissue at the cement-bone interface (Lewis, 1997; Lewis et al. 19977). In bone tissues thermal necrosis occurs when there is an increase in temperature (>50°C) lasting for more than one minute, such as that exhibited by PMMA during

polymerisation (which can range between 67-124°C, depending on the body site where used and amount of cement) (Anselmetti et al. 2009; Berman et al. 1984; Eriksson et al. 1984; Lewis, 1997). Another disadvantage of PMMA cement is due to the mismatch in stiffness between the PMMA cement and the contiguous bone (Lewis, 1997; Lewis et al. 1997). Moreover, a recent study has shown a correlation between PMMA cement extract exposure and significantly decreased functionality of osteoblasts and a marked cell death (Aita et al. 2010).

The mechanism through which PMMA bonds to bone is via mechanical interlocking, which requires an irregular, rough bone surface. However, as mentioned previously a fibrous tissue layer forms at the interface of the PMMA cement with the bone, which can result in loosening of the prosthesis. For this reason, methods have been developed to improve the reaction of the PMMA cement with the bone including: the addition of bio-ceramics such as glass and calcium phosphate compounds (hydroxyapatite and tricalcium phosphate) (He et al. 2012; Mousa et al. 2000).

Notably, when ceramics were incorporated into PMMA, the mechanical and handling characteristics of the final product were severely reduced. Conversely the incorporation of up to 20wt% hydroxyapatite to PMMA cement increased its mechanical properties (Mousa et al. 2000). When bioactive components (which bond to bone through an apatite layer) were added to the PMMA cement, it led to increased bone resorption, which ultimately loosen the implant. This loosening of the implant may have been due to free cement particles and to the calcium phosphorous layer formation on the cement, which promoted bone resorption (He et al. 2012; Mousa et al. 2000). A further study, however, reported that, the incorporation of bioactive titania (>20wt%) into PMMA cement led to increased bonding to bone (Fukuda et al. 2011). By incorporating bioactive fillers into the PMMA cement, the heat released during polymerisation was also reduced, which may have led to better mechanical properties and

decreased shrinkage of the final product (Mousa et al. 2000). Table 1.1 presents a summary regarding how the cements to be developed based on dimethacrylate resins and bioactive glass filler can compete and improve the existing PMMA cements (Table 1.1).

	PMMA	Cements to be developed
Advantages	Low thermal conductivity	=
	Cost efficiency	+
	Ease of manufacture	+
Disadvantages	Shrinkage	=
	Brittleness	+
	Poor radiopacity	+
	Poor mechanical strength	+
	Poor elasticity	+
	Time to set	+
	Non-degradability	=
	High polymerisation exotherm	+
	Infection	+
	Foreign-body reactions	+
	Poor osseo-integration	+
	Inability to be remodeled	+

Table 1.1 The advantages and disadvantages of using PMMA in orthopaedic applications and how the cements to be developed can either compete (=) or improve (+) the PMMA cements.

1.2.2 Calcium phosphate cements

Alternative materials such as calcium phosphate cements (which produce hydroxyapatite or brushite (dicalcium phosphate dihydrate) (Figure 1.1) as the end product have been developed for fracture augmentation involving crushed cancellous bone or osteoporotic bone and offer improved biological, chemical and physical properties when compared with standard PMMA cements (Larsson 2006; Young et al. 2008).

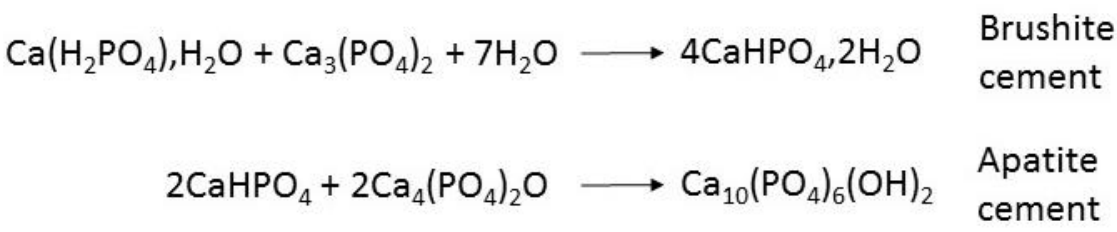

Figure 1.1 The composition of calcium phosphate cements that forms either hydroxyapatite or brushite as the end product.

The most important difference between the hydroxyapatite and brushite forming cements lies in the fact that the hydroxyapatite forming calcium phosphate cements are non-degradable (which prevents their complete replacement with bone tissue), whereas brushite forming ones are resorbable. Moreover, the brushite cements have rapid, water-consuming setting times and decreased mechanical strength compared with the hydroxyapatite cements (Hofmann et al. 2009; Young et al. 2008).

Commercially available calcium phosphate cements include BoneSource (chemically cured) which is used in facial skeleton augmentation (Pryor et al. 2009), Norian SRS which has similar characteristics to BoneSource and Alpha-BSM (ETEX Corp) (Larsson 2006). Calcium phosphate cements were first synthesised by Brown and Chow in the early eighties and compared with PMMA, were mouldable and osteo-conductive (Stadelmann et al. 2010; Wang et al. 2010). These calcium phosphate cements consist of two elements: a powder (a mixture of monocalcium phosphate, monohydrate, tricalcium phosphate and calcium carbonate) and a fluid (sodium phosphate solution). During surgery, these two elements are mixed to form an injectable paste which sets in a relatively short time-frame (approximately 15min) resulting in the production of a carbonated calcium-phosphate apatite (comparable to the mineral portion of bone) (Wang et al. 2010; Zou et al. 2009) (Figure 1.1). This cement forms a strong bond with the adjacent bone; however, it exhibits decreased tensile and shear strength compared with cancellous bone. Nonetheless, its compressive strength is between that of cancellous and

cortical bone (Larsson 2006). These features made these cements a suitable alternative to PMMA cement since 1990s for the use as bone substitutes to repair defects of the facial skeleton and also to fill calvarial defects. Thus, their ability to be easily molded to fit the defect has made them a popular choice for craniofacial surgeries. Their porous three dimensional arrangement also makes these cements a suitable choice for bone tissue repair (Mori et al. 2011; Wang et al. 2010). Furthermore, animal studies have also demonstrated their osteo-conductivity, angiogenic ability, osteoblast adhesion and proliferation and non-toxicity (Chang et al. 2010; Larsson 2006; Mori et al. 2011; Wang et al. 2010).

Nonetheless, these cements also have limitations including low tensile strength (50-70MPa), Young's modulus (35-120GPa), fracture toughness (0.5-1.5MN/$m^{3/2}$) and brittle fracture, which severely hinder their use in orthopaedic surgeries, making them unsuitable for stress bearing applications (Harper 1998; Pryor et al. 2009; Wang et al. 2010). Other limitations of these cements are due to their relatively long setting time and inability to attain complete haemostasis, which may lead to cement washout upon contact with physiological fluids (Wang et al. 2010). Table 1.2 presents a summary regarding how the cements to be developed based on dimethacrylate resins and bioactive glass fillers can compete and improve the existing calcium phosphate cements (Table 1.2).

	Calcium phosphate cements	Cements to be developed
Advantages	Osteo-conductivity	=
	Osseo-integration	=
	Angiogenic ability	=
	Non-toxicity	=
	Ability to be molded in required shape	+
Disadvantages	Low setting time	+
	Low mechanical strength	+

Table 2.2 The advantages and disadvantages of calcium phosphate cements for orthopaedic applications and how the cements to be developed can either compete (=) or improve (+) these cements.

1.2.3 Bioactive glass

A bioactive material (such as bioactive glass) was initially described by Hench et al. (1971) as one that "elicits a specific biological response at the interface of the material that results in the formation of a bond between the tissues and the material" (Hench et al. 1971; Hattar et al. 2002; Valimaki and Aro 2006). Bioactive glasses were formed as possible suitable replacements for existing orthopaedic materials to repair and regenerate the cells and tissues that make up the skeletal system (Silver et al. 2001). Bioactive glasses such as 45S5 are part of bio-ceramics, a group of materials based on amorphous silicate elements that exhibit a reactive surface, bioactivity, osteo-conductivity and osteo-inductivity. Bioglass 45S5 forms part of a family of melt-derived, soda-lime-phosphosilicate glasses and was first developed by Hench in 1971 (Hench et al. 1971). The chemical structure of 45S5 Bioglass consists of: 45% silica, 24.5% CaO, 24.5% Na_2O and 6% P_2O_5 in weight percent. These compounds are combined to form a homogeneous silica network when subjected to a temperature of 1350°C. These types of glasses have been demonstrated to bond to bone through the formation of a carbonate hydroxyapatite layer (composed of CaO and P_2O_5) on their surface that stimulates bone apposition by attachment of osteoblasts (Bachar et al. 2013; Cerruti et al. 2005; Huang et al. 2006; Ling et al.

2009; Soundrapandian et al. 2010). The formation of this hydroxyapatite layer *in vitro* may be indicative of these glasses bioactivity *in vivo* (Bachar et al. 2013; Huang et al. 2006; Rahaman et al. 2011; Vakiparta et al. 2005). The mechanism of bioactivity may be due to 45S5 Bioglass's ability to generate a crystalline apatite layer similar to that of bone on its surface upon contact with physiological fluids leading to the formation of a bond with the bone (Lusvardi et al. 2009; Rahaman et al. 2011). This layer also implies the formation of apatite nuclei, which grow using calcium and phosphate ions from the medium (a process called biomimetic mineralisation) (Lusvardi et al. 2009; Pryor et al. 2009; Rahaman et al. 2011). Notably its silica and phosphate compounds are in the range suitable for the formation of calcium phosphate on its surface upon dissolution, while still exhibiting an appropriate rate of degradability (Reilly et al. 2007). Another reason for the bioactivity of 45S5 Bioglass may be due to its potential for alkalinisation of the physiological environment. Its low SiO_2 content, thus reduced network connectivity, helps promote dissolution of elements from its structure when placed in a physiological environment (Martin et al. 2009; Ouis et al. 2012). Thus, when placed in a biological environment, 45S5 Bioglass is capable of leaching Na^+ and Ca^{2+} ions, which in turn make the local pH more alkaline. This process may also lead to the production of hydroxyapatite due to dissolution of calcium, which in turn may promote bone formation and repair (Lin et al. 2005; Martin et al. 2009). The production of hydroxyl calcium apatite possibly occurs through cation exchange between the H^+ or H_3O^+ ions from the physiological environment and the Ca^{2+} ions of the 45S5 Bioglass (Martin et al. 2009). The formation of bone in the presence of 45S5 Bioglass may be due to either its high surface reactivity or elution of ionic dissolution products in physiological environments (Misra et al. 2010). To summarise, the bioactivity of 45S5 Bioglass is resultant of its low SiO_2 composition, its high Na_2O/CaO and CaO/P_2O_5 ratios (Rahaman et al. 2011).

Therefore, bone substitutes based on bioactive glasses such as 45S5 bioglass have previously been shown to promote osteoblast proliferation (Xynos et al. 2000). 45S5 Bioglass has previously been shown to control the osteogenic precursor cell cycle and the subsequent differentiated cell population through dissolution of specific biologically active soluble Si and Ca ions (Hattar et al. 2002). The presence of these ions in the physiological medium at concentrations of 15-30ppm for Si and 60-90ppm for Ca led to promotion of bone formation (Rahaman et al. 2011). The cells unable to fully differentiate to mature osteoblasts underwent apoptosis when cultured in the presence of bioactive glasses. The cells that were capable of differentiating into mature osteoblasts formed mineralized bone nodules in culture in the presence of bioactive glass even in the absence of growth factors such as bone morphogenetic proteins (BMPs) (Hench 2009; Rahaman et al. 2011). A less than 30ppm release of phosphorus from bioactive glasses in the physiological solution induced the expression of osteogenic messenger RNA transcripts, while release of higher amounts of phosphorous had deleterious effects on cells (Goel et al. 2011). Interestingly bioactive glasses have also been shown to be able to promote tissue infiltration into implants *in vivo* in subcutaneous pockets in the dorsum of rats (Liu et al. 2011). Furthermore, a mixture of bioactive glass, autogeneous bone particles and demineralised bone matrix has been demonstrated to significantly increase bone healing when compared with bone grafting (Pryor et al. 2009).

Conclusively, its bioactivity and positive, non-toxic biological response, has made 45S5 Bioglass a suitable material as a synthetic bone graft substitute for a variety of applications including middle ear prostheses, endosseous ridge implants and periodontal defect fillers (Brauer et al. 2010; Cerruti et al. 2005; Lin et al. 2005; Reilly et al. 2007). There are several commercially available products based on Bioglass including NovaBone, NovaBone-C/M and PerioGlass, which have been employed in orthopaedic and cranio-maxillo-facial surgery in the

last 10 years (Hu and Zhong 2009; Martin et al. 2009). The main drawback of these materials, however, is that due to the brittle nature of Bioglass, they cannot be drilled, bent or shaped in surgery (Peltola et al. 2012). Moreover, from a mechanical point of view, the stiffness of Bioglass has to be similar to that of adjacent bone to permit transfer of stress in load bearing situations between the two (Lin et al. 2005). The advantages of using 45S5 Bioglass include its controlled degradation, ability to form hydroxyapatite to bond to soft and hard tissues and release of ionic dissolution products (Rahaman et al. 2011). A limitation of Bioglass is due to its crystallisation during sintering, which means that it cannot be made into amorphous bioactive glass scaffolds as can other bio-ceramics. Several new glasses have been developed by changing the chemical structure of the 45S5 Bioglass with the aim of improving its mechanical, physical and bioactive characteristics. Several studies have reported positive effects on bone growth when trace amounts of elements such as copper, zinc and strontium were incorporated into bioactive glasses (Rahaman et al. 2011).

Mechanical properties of 45S5 Bioglass such as strength can also be improved by addition of nitrogen into the silicate network. By substituting oxygen with nitrogen, the density, elastic modulus and hardness of these glasses increased with increasing nitrogen content, with the density increasing up to 1.7%, elastic modulus up to 45% and hardness up to 24% (Bachar et al. 2013). This improvement in mechanical properties may be due to the fact that nitrogen acts as a network forming anion. Nitrogen addition to these glasses results in an increase (up to 60%) in the stiffness of the network structure due to the extra cross-linking offered by the replacement of the divalent O^{2-} ion with the trivalent N^{3-} ion (Bachar et al. 2013). This substitution leads to the generation of SiO_3N and SiO_2N_2 tetrahedra which exhibit extra bridging anions compared with the SiO_4 ones found in 45S5 Bioglass. Furthermore, a recent study demonstrated that the incorporation of fluoride in these nitrogen containing bioglasses led to additional increase in

their mechanical strength (Bachar et al. 2013). Notably however the addition of calcium and fluoride to bioactive glasses had no impact on their network connectivity and bioactivity as long as the ratio of network formers to network modifiers was kept constant. It was also demonstrated that in these glasses the fluorine preferentially complexed calcium. However, the substitution of CaO or Na_2O with calcium fluoride led to decreased reactivity and bioactivity because of increased connectivity and cross-linking of the network (Brauer et al. 2009).

The Na_2O molecule has been replaced with CaF_2 in several bioactive glasses in an attempt to produce a material with reinforced networks due to generation of Si-O-Ca-Si groups. The substitution of CaO by CaF_2 resulted in the formation of a glass with decreased mechanical strength, possibly because of the production of nano-aggregates of Na^+F^- and $Ca^{2+}F^-$, which weakened the chemical structure of the glass. The glasses generated also exhibited a decreased reactivity and solubility due to their lower sodium content (Lusvardi et al. 2009).

The incorporation of strontium into bioactive glasses has resulted in decreased dissolution and bioactivity due to increased network connectivity of the glass. The chemical degradation of such glasses has been demonstrated to decrease with increasing strontium content. The lower ability of bioactive glasses containing strontium to form an apatite layer may be due to the greater metal oxygen bond strength (389kJ/mol for Sr-O compared with 351kJ/mol for Ca-O) and decreased electronegativity (0.99 for Sr^{2+} compared with 1.04 for Ca^{2+}). These factors decrease the ability of Sr^{2+} to be replaced with H^+ in the physiological solution. A concentration of between 8.7 to 87.1ppm of Sr^{2+} has been demonstrated to have a stimulatory effect on osteoblasts viability; however, a concentration of 8.7 to 2102.8ppm of Sr^{2+} had an inhibitory effect on osteoclasts viability. Nonetheless, strontium-containing bioglasses did produce a silica-rich gel layer on their surface, which aided bone regeneration and repair (Goel et al. 2011).

The addition of fluoride to 45S5 Bioglass has been demonstrated to help patients suffering from osteoporosis and prevent fractures in these patients through the release of fluoride ions. These features make these glasses suitable biomaterials (by formation of fluoroapatite) for the repair of bone tissue (Bachar et al. 2013; Brauer et al. 2010).

When the SiO_2 content in the Bioglass was changed, it was discovered that glasses with content of SiO_2 higher than 60% do not form a bond with bone (Hench 2006; Martin et al. 2009; Valimaki and Aro 2006), while those with a SiO_2 content of between 52-60% exhibited decreased bonding to bone (Martin et al. 2009). The strongest bond to bone was achieved in glasses with a SiO_2 content between 45-52% in weight (Valimaki and Aro 2006).

Borate-based glasses have been recently found to stimulate bone growth and formation, through enhanced osteoblast activity, leading to their employment as osseous implants and tissue-engineering bone scaffolds (Gorustovich et al. 2006; Rahaman et al. 2011). A bioactive glass based on 45S5 composition but where the silica content was replaced with boron stimulated the growth and differentiation of human mesenchymal stem cells into cells of the skeletal system (Huang et al. 2006; Li et al. 2013; Yao et al. 2007). However, borate-based glasses exhibit decreased chemical durability, thus increased dissolution rate when compared with 45S5 Bioglass (Huang et al. 2006). Table 1.3 presents a summary regarding how the cements to be developed containing dimethacrylate resins and bioactive glass filler can compete and improve existing Bioactive glass cements (Table 1.3).

	Bioactive glass	Cements to be developed
Advantages	Osteo-conductivity	=
	Osseo-integration	=
	Osteo-inductivity	=
	Controlled degradation	=
Disadvantages	Brittleness	+
	Inability to be molded in required shape	+

Table 1.3 The advantages and disadvantages of using bioactive glass for orthopaedic applications and how the developed cements can either compete (=) or improve (+) the bioactive glass.

1.2.3 The potential of dental resin composite chemistry for orthopaedic applications

1.3.1 Photo-polymerisable resins used in orthopaedic applications

Photo-polymerisable resins are not only used as dental restorative materials, but are also, now, the subject of research and development of bone restorative materials, due to their benefits from a command set initiation of the polymerisation (or hardening) process. Such materials include bisphenol-a-glycidyldimethacrylate/triethylene glycol dimethacrylate (bisGMA/TEGDMA) formulations for use as bone substitutes, with the material exhibiting decreased toxicity compared with PMMA cement (Harper 1998; Saito et al. 1994; Schneider et al. 2010). These bisGMA/TEGDMA based cements exhibit water uptake similar to the PMMA cement; moreover, they possess a decreased exothermic reaction and shrinkage after curing. These cements also permit the incorporation of increased amounts of filler particles compared with PMMA due to the lack of polymer beads in their structure. Nonetheless, the end product is difficult to handle due to its increased viscosity given by the increased amount of filler present in the bisGMA/TEGDMA cement. However, the use of bisGMA to augment metal screws in the treatment of ankle fractures in osteopenic patients, was shown to be a suitable alternative to the use of PMMA cement, with reduced rates of failure. Spinal fractures and fractures involving

extremities have been successfully treated with bisGMA/TEGDMA composites containing combeite (available commercially under the names of Cortoss, Orthovita Inc., Malvern USA) (Larsson 2006). However, due to the higher release of residual monomer, brittleness and increased modulus (which may lead to higher stress in the cement adjacent to an implanted prosthesis), bisGMA-based cements containing fillers are at a clinical disadvantage to PMMA cements (Harper 1998; Mousa et al. 2000).

The incorporation of nano-sized bioactive glass fillers has resulted in increased mechanical strength and surface adsorption of proteins to these bisGMA-based composites. The increased surface adsorption of proteins and the rough surface of the composites has also led to increased cell attachment (Misra et al. 2010). These composites also exhibited increased water uptake and weight loss which can be due to increased hydrophilicity (because of the incorporation of nano-sized bioactive fillers) and dissolution of these filler particles, respectively (Misra et al. 2010). Table 1.4 represents a summary regarding how the cements to be developed containing dimethacrylate resins and bioactive glass filler can compete and improve the existing bisGMA-based cements.

	bisGMA-based cements	Cements to be developed
Advantages	Low toxicity	=
	Low exothermicity	=
	Cell attachment	+
Disadvantages	Difficulty in handling	+
	Addition of filler particles	+
	Brittleness	+
	High modulus	+
	Low mechanical strength	+

Table 1.4 The advantages and disadvantages of using bisGMA-based cements in orthopaedic applications and how the cements to be developed can either compete (=) or improve (+).

1.3.2 Constituents of photo-polymerisable resins

Photo-polymerised resin-based composites most commonly contain an organic resin matrix, inorganic filler and a ketone-amine initiator-co-initiator system. Upon light irradiation these formulations are transformed into a cross-linked polymer structure. A polymer is a macromolecule formed through the linkage of large amounts of monomer molecules. Polymers can typically be described according to the polymerisation reaction by which crosslinking is achieved as either condensation or addition cured. The condensation polymers are produced from poly-functional monomers through the elimination of a small molecule and include polyamides and diacides. Addition polymers (such as dimethacrylates), on the other hand, are produced by polymerisation of monomers containing carbon double bonds (referred to as vinyl (CH_2=CH- groups) monomers) without the loss of a small molecule.

Resin matrix chemistry

Monomers used in resin composites include: bisGMA, TEGDMA, UDMA (urethane dimethacrylate), ethylene- and hexamethylene-glycoldimethacrylate employed to dilute the former viscous materials whereas the inorganic filler particles consist of mainly silicate glass (Azzopardi et al. 2009; Bouillaguet 2004; Ensaff et al. 2001; Ferracane 1995; Floyd and Dickens 2006; Goncalves et al. 2009; Lee et al. 2004; Sideridou et al. 2002).

The most commonly employed base monomer in composite restorative materials is bisGMA. This monomer was developed by Bowen in 1956 through the attachment of methacrylate groups to the epoxy monomer, thereby producing bisphenol A-glycidyl methacrylate (bisGMA) (Bowen, 1963). The bisGMA molecular structure consists of both hydrophilic and hydrophobic components, with its hydrophilicity provided by its two hydroxyl groups and its hydrophobicity due to its diphenyl-isopropane core (which contains two aromatic phenol rings exhibiting π-π

interactions) (Deb et al. 2005; Sauro et al. 2013). These two aromatic phenol rings and the pendant hydroxyl groups are held together by strong intermolecular hydrogen bonds, which make bisGMA a highly rigid molecule due to the limited bond rotation (steric hindrance) around its aromatic ring structure (Emami and Soderholm 2009). The presence of the two aromatic rings and hydroxyl groups make bisGMA a large methacrylate molecule, which also results in bisGMA having high viscosity (η=1,200Pa); limiting its degree of conversion to values not higher than 42% when used alone or 55-75% when employed as the base monomer in composite resins (Elliott et al. 2001; Gajewski et al. 2012; Harper 1998; Pfeifer et al. 2009). Its high reactivity is due to the presence of reactive carbon double bonds in the molecular structure. Its high molecular weight, rigidity, decreased shrinkage following polymerisation and high refractive index (1.55) make it a frequent monomer choice in composite resins (Azzopardi et al. 2009; Sideridou et al. 2002). However, bisGMA has several shortcomings including: cytotoxicity (due to potential leakage into the surrounding environment) and, as already mentioned, increased viscosity (which hinders the mobility of the free radicals during polymerisation), lower conversion of carbon double bonds (Elliott et al. 2001) and increased stickiness, which affects handling.

An alternative monomer that can either replace or be used in combination with bisGMA is UDMA, which has a lower molecular weight and decreased viscosity (approximately 11,000mPa) due to the absence of aromatic groups compared with bisGMA (Deb et al. 2005; Sauro et al. 2013). The UDMA chemical structure comprises of methacrylates, which are held together by aliphatic spacer groups and –NHCOO- or urethane groups (Sideridou et al. 2002). The presence of urethane groups also confers increased functionality on UDMA, resulting in increased toughness and flexibility of the monomer's backbone structure; which may also lead to increased conversion of the monomer to polymer during the polymerisation reaction. When

compared with bisGMA, UDMA has in its structure imino (-NH-) rather than hydroxyl groups and exhibits greater flexibility due to lower strength hydrogen bonding interactions; however, it has a lower refractive index (1.48), which may limit the depth of cure based on the co-monomer blend and type of filler incorporated in the UDMA based resins (Azzopardi et al. 2009; Barszczewska-Rybarek 2009; Gajewski et al. 2012). Consequently, UDMA has the following advantages over bisGMA: a lower viscosity and a highly flexible urethane linkage, which may improve the toughness and degree of conversion of resin composites based on this monomer (Asmussen and Peutzfeldt 1998; Barszczewska-Rybarek 2009).

As the majority of resin composites use either bisGMA and/or UDMA as the base monomers, a diluent monomer such as TEGDMA is usually required to decrease viscosity. This monomer has a low molecular weight and decreased viscosity (approximately 10mPa), which gives TEGDMA its high reactivity. TEGDMA is also used to increase the conversion of carbon double bonds to carbon single bonds (conversion of the monomer to a polymer). This monomer not only acts as diluent for bisGMA or UDMA but also makes the addition of filler particles in composite resins easier by decreasing viscosity (Khatri et al. 2003) and may improve handling. However, because of the absence of aromatic rings and the presence of ether groups (C-O-C), this may lead to low mechanical properties of the polymer after the polymerisation reaction. Therefore, due to its flexible structure, decreased refractive index (1.46), low molecular weight, decreased viscosity (given by the lack of intermolecular hydrogen interactions) and its ability for cyclisation (to form ring structures) (for full description of cyclisation refer to Section 1.4.3 Polymerisation kinetics and chemistry of light-activated dental composites, below), TEGDMA increases radical mobility during the polymerisation reaction, however, it does not lead to network formation (Azzopardi et al. 2009; Gajewski et al. 2012). Due to the increased amounts of carbon double bonds in their molecular structure, composite resins containing TEGDMA

exhibit higher degree of conversion (Gajewski et al.2012). The disadvantages of using TEGDMA in composite resins include its increased water sorption and ability to elute in the surrounding environment, resulting in a possible negative impact on cells (Atai et al. 2005; Ferracane 1995).

Photo-initiators

There are three main types of initiators classified according to the nature of the polymerisation reaction: free radical, cationic and anionic (Andrzejewska 2001). As this study involves free radical polymerisation, the following section covers free radical initiators (referred to as photo-initiators), which are relevant to the studies presented here.

Free radical photo-polymerisation can occur through the absorption of an appropriate wavelength of light by a photo-initiator molecule, which starts the polymerisation reaction by direct light absorption or an indirect mechanism via a co-initiator to produce reactive free radical species (Ogunyinka et al. 2007). When the photo-initiator absorbs light at the appropriate wavelength, its carbonyl group with the non-bonding electrons is promoted to a π^* anti-bonding orbital. This leads to an overlap between the lower energy bonding and higher energy anti-bonding molecular orbitals, resulting in the initiation of polymerisation (Ikemura and Endo 2010; Stansbury 2000). Therefore, a photo-initiator is a species capable of initiating the polymerisation reaction through the absorption of external energy (which may include, for example, light or heat).

There are two types of radical photo-initiators depending on how the free radical intermediates are produced following light activation of the initiators: Type I and Type II (Andrzejewska 2001). Type I initiators consist of aromatic carbonyl elements that exhibit haemolytic carbon bond scission following ultraviolet or short wavelength visible light irradiation. Such initiators

(benzyl ketals, acyclophosphine oxides, benzoin ether derivatives to give some examples) start polymerisation through a photo-fragmentation method, where radicals are produced by a successful α-cleavage process (Andrzejewska 2001; Fairbanks et al. 2009). Type II initiators (those used in this thesis) require two compounds to begin polymerisation: aromatic diketones being commonly used together with a weak-covalent bond exhibiting radical precursor. Camphorquinone and benzophenones are other examples of such initiators, which start polymerisation through a mechanism of "hydrogen abstraction from donor molecules" (Fairbanks et al. 2009). There are also initiators that do not belong to this classification such as borate salt, which initiates polymerisation through either inter- or intra-molecular electron transfer (Andrzejewska 2001).

Current composite resins usually employ Type II initiators to start the polymerisation reaction, with camphorquinone being commonly used as the visible light activated source of free-radicals due to its excellent characteristics since its development in 1971 by Dart and Nemcek. This photo-initiator requires a co-initiator such as tertiary aliphatic amines photo-reductants (eg DMAEMA (dimethylaminoethyl methacrylate)) to act as electron donors to successfully start the polymerisation reaction (Leprince et al. 2013; Ogunyinka et al. 2007; Pagoria et al. 2005). These tertiary amines are a popular choice of co-initiators for light curable composite resins due to their reactivity with the carbon double bonds of the monomers and ability to generate α–amino alkyl radicals (Andrzejewska 2001). These co-initiators do not play a role in light absorption, but interact with the photo-initiator to generate reactive species. Therefore, camphorquinone initiates polymerisation through a hydrogen abstraction method, where, following light irradiation it absorbs light to create a photo-excitation structure with its hydrogen donating tertiary amine co-initiator. This results in the formation of amine-derived

free radicals (Fairbanks et al. 2009; Ikemura and Endo, 2010; Nugent et al. 2010, Ogunyinka et al. 2007).

Camphorquinone, due to its α-dicarbonyl group, is capable of absorbing light in the blue visible region (400-550nm) at a peak wavelength of 468nm resulting in a transition from n to π^* of its dicarbonyl group (Arikawa et al. 2009; Ikemura and Endo 2010; Ogunyinka et al. 2007; Pagoria et al. 2005). The non-bonding electrons of the carbonyl groups are then promoted to a π^* anti-bonding orbital, creating a short-lived excited energy state, with a half-life of approximately 0.05ms. When this excited $n \rightarrow \pi^*$ transition, then, comes into contact with an amine molecule through charge transfer, diffusion or prior association, an excited short-lived complex (an exciplex) is created as it is shown in Figure 1.2 (Alvim et al. 2007; Asmussen et al. 2009; Ikemura and Endo 2010; Stansbury 2000; Watts 2005).

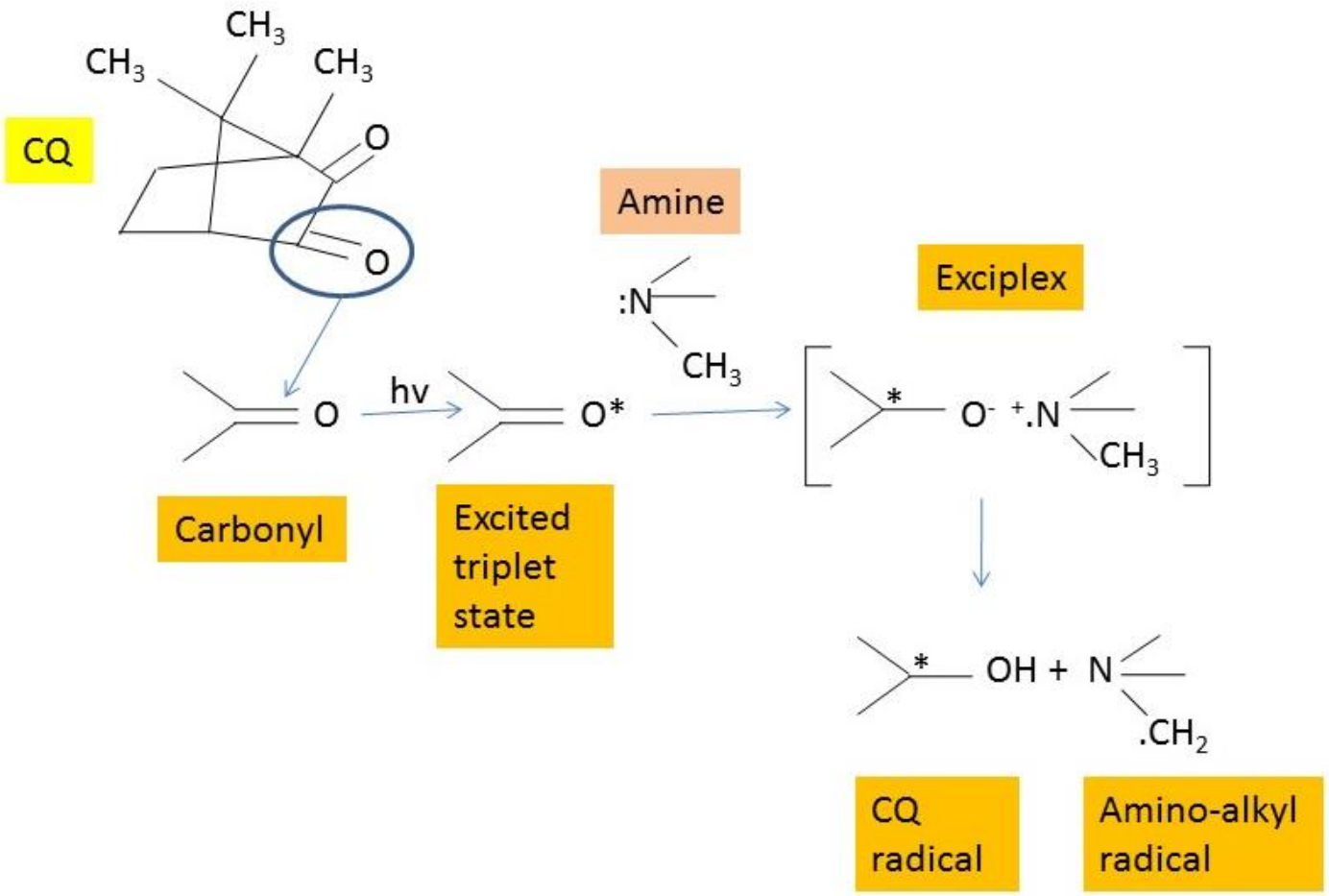

Figure 1.2 The molecular structure of CQ and photo-activation mechanism to start the initiation of the polymerisation reaction (adapted from Stansbury, 2000).

In the excited short-lived complex, an electron is donated by the amine to the camphorquinone to generate the radical ion pair and, then, the camphorquinone abstracts a proton from the amine to form the free radical species (or the primary radical) (Figure 1.1) (Pagoria et al. 2005; Stansbury, 2000). The former CQ radical has the ability to inhibit polymerisation via termination reactions by interacting with the growing polymer chains. The latter radical is able to attack the carbon double bonds in the monomers leading to a chain reaction process where many hundreds of monomer units can be added to the polymer network through the light activation of a single photon by the camphorquinone initiator (Alvim et al. 2007; Asmussen et al. 2009; Ikemura and Endo 2010; Stansbury 2000; Watts 2005).

Fillers impact on dimethacrylate resins

Resin composites consist of a polymerised resin network and fillers, which are mixed in to form a chemical or photo-polymerised cured resin (Bouillaguet 2004; Ferracane 1995; Shirai et al. 2000). Fillers may include micron- or nano-sized particles of SiO_2, ZrO_2 and Al2O3. However, an increased volume of monomer is needed to form a homogenous mixture, when nano-particle sized fillers are incorporated into composites, mainly due to the nano-particles large surface-area to volume ratio (Ensaff et al. 2001; Ferracane 1995). Nano-particles may also form aggregates within the resin composite due to agglomeration of the particles within the resin matrix. This occurs when inter-particulate forces of attraction exceed the particulate weight and this may have a negative impact on the mechanical properties of the final resin composite containing nano-particles (Chen et al. 2006).

The addition of micro-sized fillers to the resin network has the role of reinforcing the resin composite by improving its mechanical properties. An increase in the amount of filler present also results in a decrease in the polymerisation shrinkage, which is due to decreased amount of

monomers and increased amount of filler particles present in the composite. Nonetheless, the maximum amount of filler that can be incorporated into a resin mixture is restricted by the viscosity of the monomers (Ling et al. 2009). One method to aid the incorporation of fillers in resin mixtures is through the addition of TEGDMA, which decreases the viscosity of the base monomers bisGMA or UDMA as previously described.

When these inorganic glassy fillers were initially incorporated into the organic resin mixture, it was identified that these two compounds had to form a strong bond in order to produce a composite with acceptable physical and mechanical properties. This bond was achieved through the coating of the filler particles with a coupling molecule (silane). This molecule has in its structure silanol groups (Si-OH), which bond to the silicon-oxygen groups in the glassy fillers and methacrylate groups (comprising of C=C), which provide bonding to the methacrylate groups of the resin monomers as it is shown in Figure 1.3 (Ferracane 1995).

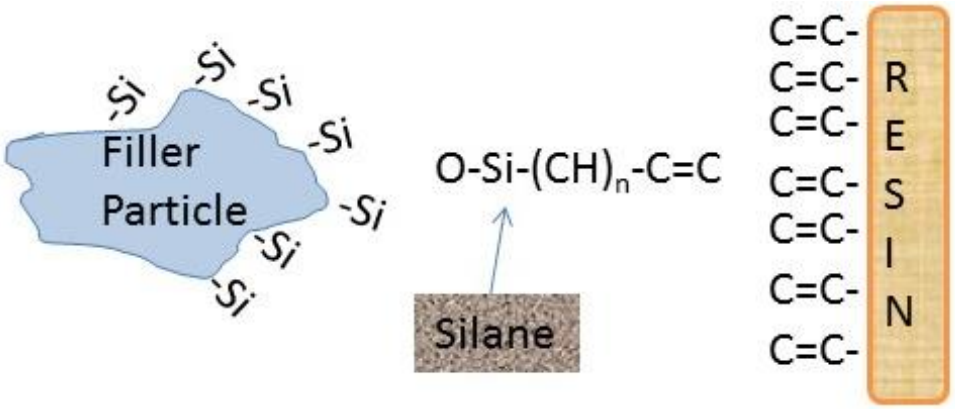

Figure 1.3 Illustration of the bonding between the silane coupling agent with the filler particles and the resin matrix in resin-based materials. The silane coupling agent may lead to better chemical bonding between the filler particles and the resin matrix (adapted from Ferracane, 1995).

This coupling molecule and an efficient silanisation process also increase fracture toughness by modifying crack propagation by transgranular strengthening. Another role played by the silane molecule involves the transmission of stress between the soft resin matrix and the harder filler

particles (Ferracane 1995; Shirai et al. 2000). Successful coating of fillers with the silane would also slow the degradation process of resin composites due to the inevitable failure of the bond between the fillers and the resin matrix (Shirai et al. 2000).

1.3.3 Polymerisation kinetics and chemistry of light-activated dental composites

Light-curable dimethacrylate resin composites undergo free radical photo-polymerisation in response to visible, blue light (wavelength of 400-550nm) curing (500-800mW/cm^2 of light) for approximately 30-40sec (at 15-24Jcm^{-2}) (Bouillaguet 2004). Thus, as previously mentioned, the photo-polymerisation reaction employs photo-initiators capable of absorbing irradiated light at specific wavelength to produce primary radicals, which can, then, convert monomers into a polymeric network (Figure 1.4) (Ikemura and Endo 2010). These free radicals open the carbon double bonds of the methacrylate groups of the monomers, initiating a chain polymerisation reaction. This reaction includes three steps: initiation, propagation and termination (Figure 1.5), where formation of radicals, initiation and growth of the polymer chain and removal of radicals occurs, resulting in the formation of a high molecular weight, cross-linked polymer network (Rosentritt et al. 2010).

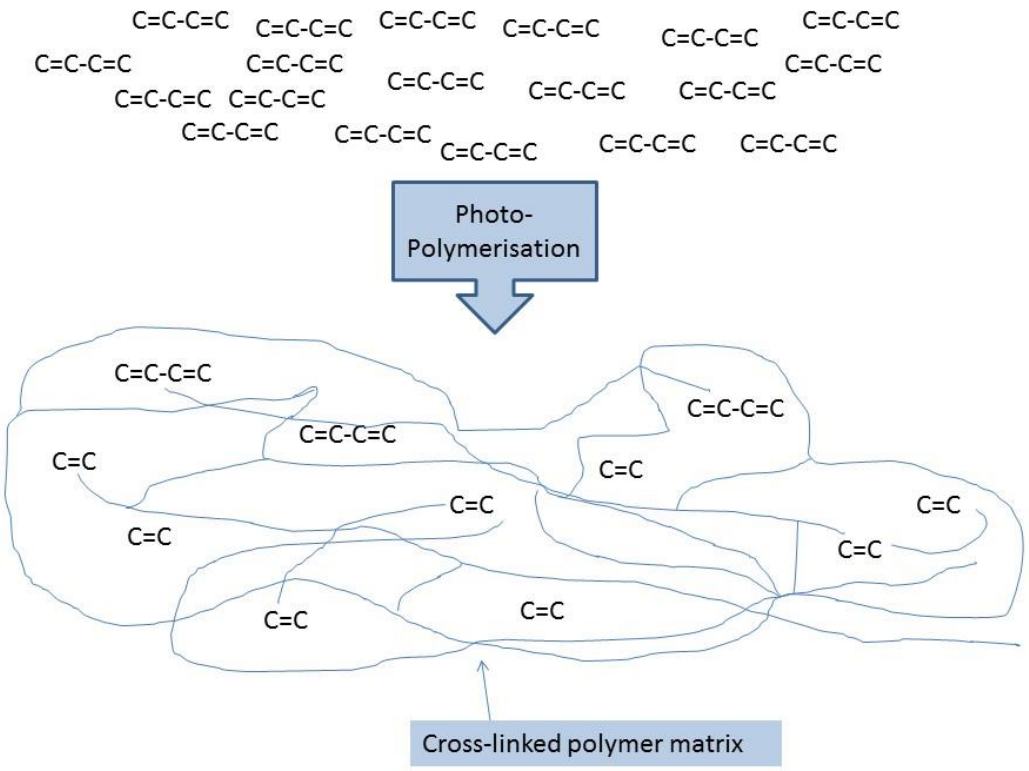

Figure 1.4 The conversion of carbon double bonds to carbon single bonds following photo-polymerisation of dimethacrylate resin monomers to form a cross-linked polymer matrix containing small amounts of unreacted monomers and many pendant methacrylate groups (C=C) (adapted from Ferracane, 1995).

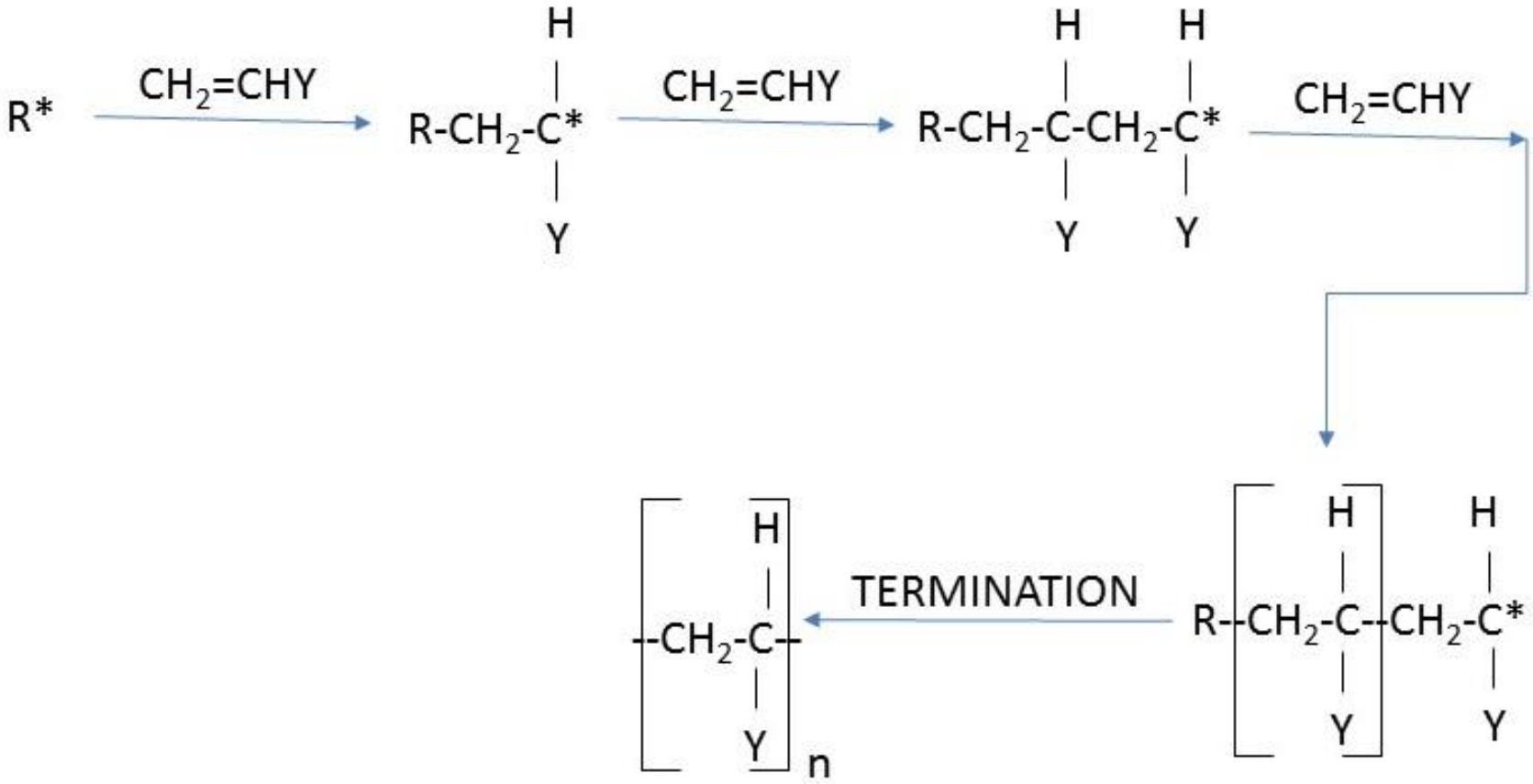

Figure 1.5 Polymerisation of dimethacrylate resins. The polymerisation reaction ensues through the incorporation of large amounts of monomer molecules (CH_2=CHY) to the reactive centre R* resulting in the formation of a highly cross-linked polymer network (adapted from LePrince et al. 2013).

As previously mentioned, during initiation the photo-initiator is decomposed leading to the formation of free radicals, which in turn open the carbon double bonds of the monomer molecule resulting in the conversion of the monomer to the polymer. This process leads to an increase in the viscosity of the resin, thus a decrease in the termination rate, which is known as auto-acceleration (gel effect) (Rosentritt et al. 2010; Watts 2005). This effect is produced by the rapid conversion of the carbon double bonds to single bonds (monomer to polymer), resulting in increased viscosity (Dewaele et al. 2006; LePrince et al. 2013). This increased viscosity due to polymer formation and increased cross-link density leads to a decrease in the mobility of the radicals, resulting in diffusion controlled propagation (Atai et al. 2005). During propagation, the free radical continues attacking the π-bond of a monomer creating an active (also referred to as reactive) centre to which monomer molecules are then rapidly added leading to the growth of the polymer chain (Watts 2005). Thus, this step implies the interaction of monomer molecules (as units consisting of pendant double bonds), resulting in this step being the least limited by diffusion in the polymerisation reaction. Propagation continues through the incorporation of another monomer molecule to the active centre and through attack of the pendant double bond by the radical through cyclisation, inter- or intra- molecular cross-linking. Therefore, cyclisation reactions occur during the polymerisation of dimethacrylate resins and are of two types: primary or secondary cyclisation. During the primary cyclisation reactions, the pendant double bonds of the monomer molecules react with their radical centre leading to the growth of the polymer chain, whereas during secondary cyclisation (multiple cross-linking) reactions, the pendant double bonds react with a radical located on a different polymer chain (Elliott et al. 2001; Lovell et al. 1999, Lovell et al. 2001). Primary cyclisation reactions, thus, limit the density of the cross-linked polymer network. Moreover, during the polymerisation

reaction, primary cyclisation is reduced with increased conversion of the monomer to a polymer network, with an increase in cross-linking reactions (Lovell et al. 2001).

Thus, the pendant double bonds may interact with propagating radicals to generate primary cycles, secondary cycles (multiple cross-links) and cross-links. Cross-linking occurs between pendant double bonds and a radical situated on a different growing chain (Lovell et al. 2001). On one hand, cyclisation may increase conversion (due to having no negative impact on mobility of radicals), nonetheless, on the other hand, this may have a detrimental effect on density of the cross-linked polymeric network, because cycles do not play a role in the formation of the polymeric system (Elliott et al. 2001; Lovell et al. 2001). Due to the high number of monomeric double bonds near the radical site, widespread cyclisation occurs, resulting in the formation of micro-gels (which are compact structures). This cyclisation leads to a delay in the time required to reach the gel point conversion in the polymerisation reaction. It is in these micro-gels that the remaining unreacted pendant double bonds of the monomer molecule become entrapped resulting in decreased reactivity through steric hindrance.

Micro-gel formation is also one of the reasons why conversion of carbon double bonds to single bonds never reaches 100%, this being due to the network inhomogeneity created by these micro-gel structures. This inhomogeneity of the polymeric network may also have a detrimental effect on the mechanical properties of the resin. Micro-gels are generated during primary cyclization, with the polymeric network consisting of loosely cross-linked regions interspersed between highly cross-linked regions (Lovell et al. 2001). Consequently, polymerisation proceeds through the chemical interaction of the micro-gel structures, resulting in the generation of macro-gels. During this step, the polymeric chains become trapped in the network. A limited amount of radicals are still able to interact by segmental diffusion or propagation, with the radicals already trapped in the micro-gels becoming inaccessible for further reaction.

There are three main species of radicals in a polymerisation reaction: the free radicals which are not bound to the network, the mobile radicals that, although bound to loosely cross-linked parts of the network, can still react with others and the trapped radicals, which are terminated. However, as the polymeric network becomes increasingly cross-linked the mobility of radical sites is governed by propagation, with trapped radicals constituting another method of radical deactivation (Elliott et al. 2001; Lovell et al. 2001).

Therefore, reaction termination may occur through two methods: bimolecular termination of polymer radicals (when mobility of the system is high; irreversible) and monomolecular termination (here, only one polymer radical is required) (reversible, when network mobility is decreased). This step in the polymerisation reaction ensues due to radical-radical interaction and entrapment of radicals in an increasingly cross-linked network, which hinders any further reaction with the vinyl double bonds. The termination step of the polymerisation reaction is dependent on the amount of carbon double bond conversion to single bonds and the conditions in which the reaction occurs such as: temperature, the chemical structure of monomers and the density of the cross-linked network. Diffusion controlled termination constitutes the main method of termination in the polymerisation of light-curable dimethacrylate resins (Elliott et al. 2001; Lovell et al. 2001). This diffusion controlled reaction has a negative impact on the physical (degree of conversion) and mechanical (flexural strength and flexural modulus) properties of dimethacrylate resins because the reaction is terminated before all the monomer is converted into polymer (Lovell et al. 1999). Therefore, the early termination of free radicals leads to decreased degree of conversion, which may also have a detrimental impact on the mechanical characteristics of the final resin and filled composite. However, when bimolecular termination (interaction between two radicals attached to long, polymer chains) is severely hindered, termination can also occur through chain transfer, which reduces both the rate of

polymerisation and the lifetime of radicals, leading to a decrease in the monomolecular rate of termination (Andrzejewska 2001). As the polymerisation reaction proceeds the movement of the free radicals and their interaction with the monomer molecules becomes more and more restricted, with a sudden decrease in the rate of polymerisation, a phenomenon known as auto-deceleration. During this stage, the monomer movement to the reactive sites is severely limited leading to a drop in the polymerisation rate (Goodner and Bowman 1999). This eventually leads to vitrification (transition from a rubber to a glass state) where the mobility of the radicals is restricted leading to the formation of a polymer network where residual monomer and unreacted pendant groups bound to the polymer chain remain pres,ent (Atai et al. 2005; Lee et al. 2004; LePrince et al. 2010; Rosentritt et al. 2010; Sideridou et al. 2002).

Polymerisation does not, however, stop with the cessation of light irradiation, but it continues in the absence of further irradiation. The primary radicals formed during light irradiation keep interacting with growing polymer chains or terminate micro-radicals. Therefore, chain propagation will continue, but at a significantly reduced rate compared with that during light irradiation (Goodner and Bowman 1999).

To summarise, during polymerisation, an increase in the degree of conversion and the density of the polymeric network occurs. As the cross-linked network is generated, the viscosity increases resulting in gelation (transition from a liquid to a rubber state) of the medium. During gelation, which occurs at the beginning of the polymerisation reaction, the mobility of radicals interacting with the growing polymer chain becomes restricted due to an increase in density, however, the small monomer molecules are still able to diffuse easily (Atai et al. 2005; Rosentritt et al. 2010). This results in a significant decrease of the termination step, with initiation producing new growth centres. This subsequently leads to auto-acceleration, where the rate of polymerisation and the amount of free radicals are increased reaching a maximum

rate of polymerisation. Auto-deceleration then occurs, when the viscosity of the systems hinders even the movement of the small monomer molecules, leading to a significant drop in the rate of polymerisation (Atai et al. 2005). At this stage, vitrification occurs with the transition from rubber to glass of the polymeric system. Vitrification is also the main reason why the degree of conversion of monomer to polymer can never reach 100%, with up to 50% of the monomer carbon double bonds remaining unreacted (Asmussen and Peutzfeldt 2001; Bouillaguet 2004; Floyd and Dickens 2006; Lee et al. 2004; LePrince et al. 2013; Sideridou et al. 2002).

The main problem encountered with free radical polymerisation is shrinkage. This phenomenon occurs when monomers are converted into polymers, due to a density change from the liquid monomer (lower density) to the highly cross-linked polymer (higher density) (Gilbert et al. 2000). Another limitation of photo-polymerisation is given by the presence of atmospheric oxygen. Not only does oxygen quench the excited states of the photo-initiator (thus decreasing the amount of initiating radicals), but it, also, has the ability to form peroxy radicals with the carbon-based polymerising radicals (preventing them from reacting with the carbon double bonds of the monomers) resulting in a decrease in the effectiveness of initiation. This may either lead to the complete inhibition or a significant reduction of the polymerisation reaction (Andrzejewska 2001).

Therefore, a thorough understanding of appropriate resin chemistry is required for the development of bioactive glass containing materials based on such resins, for orthopaedic applications. By changing the concentration, composition and amount of either the resin component or the bioactive glass component in these materials, cements can be developed that have enhanced mechanical, physical and biological properties compared with current materials, which could further lead to the generation of versatile bone substitutes for orthopaedic repair.

1.4 Study aims

This work aimed to develop a material based on dimethacrylate resins and bioactive glasses that provides enhanced physical and mechanical characteristics (degree of conversion, flexural strength, flexural modulus, water sorption and water solubility) as well as improved viability of bone marrow stromal cells compared with existing cement materials based on PMMA cement. Studies aimed to investigate various resin types and monomer blends (in terms of degree of conversion, rate of polymerisation, hardness, flexural strength and flexural modulus) (Chapter 3) to provide a versatile system in regard to physical, mechanical and biological characteristics to be used for different orthopaedic applications. Subsequently, the impact of the addition of different sizes and concentrations of bioactive glass to resin systems on the mechanical and physical properties of the final resin composites (in terms of degree of conversion, flexural strength and flexural modulus) was analysed (Chapter 4). Further, the impact of water immersion on the mechanical properties (bi-axial flexural strength, flexural strength and flexural modulus) as well as the water sorption and solubility of the optimum formulations of resin composites (Chapter 5 and 6) were determined. Finally, the impact of these resin composites on bone marrow stromal cells viability as well as changes in the acidity of the culture media were analysed (Chapter 7).

References

Aita, H., Tsukimura, N., Yamada, M., Hori, N., Kubo, K., Sato, N., Maeda, H., Kimoto, K., Ogawa, T. 2010. N-Acetyl cysteine prevents polymethyl methacrylate bone cement extract-induced cell death and functional suppression of rat primary osteoblasts. *Journal of Biomedical Materials Research Part A*, 92A, (1) 285-296

Alvim, H.H., Alecio, A.C., Vasconcellos, W.A., Furlan, M., de Oliveira, J.E., Saad, J.R.C. 2007. Analysis of camphorquinone in composite resins as a function of shade. *Dental Materials*, 23, (10) 1245-1249

An, Y.H., Draughn, R.A., Mechanical testing of bone and the bone-implant interface. CRC Press; Boca Raton, FL:2000, p.51

Andrzejewska, E. 2001. Photopolymerization kinetics of multifunctional monomers. *Progress in Polymer Science*, 26, (4) 605-665

Anselmetti, G.C., Manca, A., Kanika, K., Murphy, K., Eminefendic, H., Masala, S., Regge, D. 2009. Temperature Measurement During Polymerization of Bone Cement in Percutaneous Vertebroplasty: An In Vivo Study in Humans. *Cardiovascular and Interventional Radiology*, 32, (3) 491-498

Arikawa, H., Takahashi, H., Kanie, T., Ban, S. 2009. Effect of various visible light photoinitiators on the polymerization and color of light-activated resins. *Dental Materials Journal*, 28, (4) 454-460

Asmussen, S., Arenas, G., Cook, W.D., Vallo, C. 2009. Photobleaching of camphorquinone during polymerization of dimethacrylate-based resins. *Dental Materials*, 25, (12) 1603-1611

Asmussen, E., Peutzfeldt, A. 1998. Influence of UEDMA, BisGMA and TEGDMA on selected mechanical properties of experimental resin composites. *Dental Materials*, 14, (1) 51-56

Asmussen, E., Peutzfeldt, A. 2001. Influence of selected components on crosslink density in polymer structures. *European Journal of Oral Sciences*, 109, (4) 282-285

Atai, M., Watts, D.C., Atai, Z. 2005. Shrinkage strain-rates of dental resin-monomer and composite systems. *Biomaterials*, 26, (24) 5015-5020

Azzopardi, N., Moharamzadeh, K., Wood, D.J., Martin, N., van Noort, R. 2009. Effect of resin matrix composition on the translucency of experimental dental composite resins. *Dental Materials*, 25, (12) 1564-1568

Bachar, A., Mercier, C., Tricoteaux, A., Hampshire, S., Leriche, A., Follet, C. 2013. Effect of nitrogen and fluorine on mechanical properties and bioactivity in two series of bioactive glasses. *Journal of the Mechanical Behavior of Biomedical Materials*, 23, 133-148

Baroud, G., Samara, M., Steffen, T. 2004. Influence of mixing method on the cement temperature-mixing time history and doughing time of three acrylic cements for vertebroplasty. *Journal of Biomedical Material Research Part B: Applied Biomaterials,* 68, (1) 112-116

Barszczewska-Rybarek, I.M. 2009. Structure-property relationships in dimethacrylate networks based on Bis-GMA, UDMA and TEGDMA. *Dental Materials*, 25, (9) 1082-1089

Berman, A.T., Reid, J.S., Yanicko, D.R., Sih, G.C., Zimmerman, M.R. 1984. Thermally induced bone necrosis in rabbits. Relation to implant failure in humans. *Clinical Orthopeadics and Related Research,* 186, (1) 284-292

Bouillaguet, S. 2004. Biological risks of resin-based materials to the dentin-pulp complex. *Critical Reviews in Oral Biology and Medicine*, 15, (1) 47-60

Bowen, R.L. 1963. Properties of a silica-reinforced polymer for dental restorations. *The Journal of the American Dental Association,* 66, (1) 57-64

Brauer, D.S., Karpukhina, N., Law, R.V., Hill, R.G. 2009. Structure of fluoride-containing bioactive glasses. *Journal of Materials Chemistry*, 19, (31) 5629-5636

Brauer, D.S., Karpukhina, N., O'Donnell, M.D., Law, R.V., Hill, R.G. 2010. Fluoride-containing bioactive glasses: Effect of glass design and structure on degradation, pH and apatite formation in simulated body fluid. *Acta Biomaterialia*, 6, (8) 3275-3282

Cerruti, M., Greenspan, D., Powers, K. 2005. Effect of pH and ionic strength on the reactivity of Bioglass((R)) 45S5. *Biomaterials*, 26, (14) 1665-1674

Chang, C.H., Liao, T.C., Hsu, Y.M., Fang, H.W., Chen, C.C., Lin, F.H. 2010. A poly(propylene fumarate) - Calcium phosphate based angiogenic injectable bone cement for femoral head osteonecrosis. *Biomaterials*, 31, (14) 4048-4055

Charnley, J. 1960. Anchorage of femoral head prosthesis to the shaft of the femur. *The Journal of Bone and Joint Surgery,* 42-B, () 28-30

Chen, M.H., Chen, C.R., Hsu, S.H., Sun, S.P., Su, W.F. 2006. Low shrinkage light curable nanocomposite for dental restorative material. *Dental Materials*, 22, (2) 138-145

Deb, S., Aiyathurai, L., Roether, J.A., Luklinska, Z.B. 2005. Development of high-viscosity, two-paste bioactive bone cements. *Biomaterials*, 26, (17) 3713-3718

Deramond, H., Wright, N.T., Belkoff, S.M. 1999. Temperature elevation caused by bone cement polymerisation during vertebroplasty. *Bone,* 25, (2 Supplement) 17S-21S

Dewaele, M., Truffier-Boutry, D., Devaux, J., Leloup, G. 2006. Volume contraction in photocured dental resins: The shrinkage-conversion relationship revisited. *Dental Materials*, 22, (4) 359-365

Elliott, J.E., Lovell, L.G., Bowman, C.N. 2001. Primary cyclization in the polymerization of bis-GMA and TEGDMA: a modeling approach to understanding the cure of dental resins. *Dental Materials*, 17, (3) 221-229

Emami, N., Soderholm, K. 2009. Young's Modulus and Degree of Conversion of Different Combination of Light-Cure Dental Resins. *The Open Dentistry Journal*, 3, 202-207

Ensaff, H., O'Doherty, D.M., Jacobsen, P.H. 2001. Polymerization shrinkage of dental composite resins. *Proceedings of the Institution of Mechanical Engineers Part H-Journal of Engineering in Medicine*, 215, (H4) 367-375

Eriksson, R.A., Albrektsson, T., Magnasson, B. 1984. Assesment of bone viability after heat trauma. A histological, histochemical and vital microscopic study in the rabbit. *Scandinavian Journal of Plastic and Reconstructive Surgery,* 18, (3) 261-268

Fairbanks, B.D., Schwartz, M.P., Bowman, C.N., Anseth, K.S. 2009. Photoinitiated polymerization of PEG-diacrylate with lithium phenyl-2,4,6-trimethylbenzoylphosphinate: polymerization rate and cytocompatibility. *Biomaterials*, 30, (35) 6702-6707

Ferracane, J.L. 1995. Current Trends in Dental Composites. *Critical Reviews in Oral Biology and Medicine*, 6, (4) 302-318

Floyd, C.J.E., Dickens, S.H. 2006. Network structure of bis-GMA- and UDMA-based resin systems. *Dental Materials*, 22, (12) 1143-1149

Fukuda, C., Goto, K., Imamura, M., Neo, M., Nakamura, T. 2011. Bone bonding ability and handling properties of a titania-polymethylmethacrylate (PMMA) composite bioactive bone cement modified with a unique PMMA powder. *Acta Biomaterialia*, 7, (10) 3595-3600

Gajewski, V.E.S., Pfeifer, C.S., Froes-Salgado, N.R.G., Boaro, L.C.C., Braga, R.R. 2012. Monomers used in resin composites: degree of conversion, mechanical properties and water sorption/solubility. *Brazilian Dental Journal*, 23, (5) 508-514

Gilbert, J.L., Hasenwinkel, J.M., Wixson, R.L., Lautenschlager, E.P. 2000. A theoretical and experimental analysis of polymerization shrinkage of bone cement: A potential major source of porosity. *Journal of Biomedical Materials Research*, 52, (1) 210-218

Goel, A., Rajagopal RR FAU - Ferreira, J., Ferreira, J.M. 2011. Influence of strontium on structure, sintering and biodegradation behaviour of CaO-MgO-SrO-SiO(2)-P(2)O(5)-CaF(2) glasses. *Acta Biomaterialia,* 11, (7) 4071-4080

Goncalves, F., Kawano, Y., Pfeifer, C., Stansbury, J.W., Braga, R.R. 2009. Influence of BisGMA, TEGDMA, and BisEMA contents on viscosity, conversion, and flexural strength of experimental resins and composites. *European Journal of Oral Sciences*, 117, (4) 442-446

Goodner, M.D., Bowman, C.N. 1999. Modeling primary radical termination and its effects on autoacceleration in photopolymerization kinetics. *Macromolecules*, 32, (20) 6552-6559

Gorustovich, A.A., Lopez, J.M.P., Guglielmotti, M.B., Cabrini, R.L. 2006. Biological performance of boron-modified bioactive glass particles implanted in rat tibia bone marrow. *Biomedical Materials*, 1, (3) 100-105

Ha, J.Y., Kim, S.H., Kim, K.H.,Kwon, T.Y. 2011. Influence of the volumes of bis-acryl and poly(methyl methacrylate) resins on their exothermic behaviour during polymerisation. *Dental Materials,* 30, (3) 336-342

Harper, E.J. 1998. Bioactive bone cements. *Proceedings of the Institution of Mechanical Engineers Part H-Journal of Engineering in Medicine*, 212, (H2) 113-120

Hattar, S., Berdal, A., Asselin, A., Loty, S., Greenspan, D., Sautier, J. 2002. Behaviour of moderately differentiated osteoblast-like cells cultured in contact with bioactive glasses. *European Cells and Materials*, 4, 61-69

He, Q., Chen, H.L., Huang, L., Dong, J.J., Guo, D.G., Mao, M.M., Kong, L., Li, Y., Wu, Z.X., Lei, W. 2012. Porous Surface Modified Bioactive Bone Cement for Enhanced Bone Bonding. *Plos One*, 7, (8) e42525-e42536

Hench, L.L. 2006. The story of Bioglass (R). *Journal of Materials Science-Materials in Medicine*, 17, (11) 967-978

Hench, L.L. 2009. Genetic design of bioactive glass. *Journal of the European Ceramic Society*, 29, (7) 1257-1265

Hench, L.L., Splinter, R.J., Allen, W.C., Greenlee, T.K. 1971. Bonding mechanisms at the interface of ceramic prosthetic materials. *Journal of Biomedical Materials Research,* 5, (6) 117-141

Hofmann, M.P., Mohammed, A.R., Perrie, Y., Gbureck, U., Barralet, J.E. 2009. High-strength resorbable brushite bone cement with controlled drug-releasing capabilities. *Acta Biomaterialia*, 5, (1) 43-49

Hu, Y.C., Zhong, J.P. 2009. Osteostimulation of bioglass. *Chinese Medical Journal*, 122, (19) 2386-2389

Huang, W.H., Day, D.E., Kittiratanapiboon, K., Rahaman, M.N. 2006. Kinetics and mechanisms of the conversion of silicate (45S5), borate, and borosilicate glasses to hydroxyapatite in dilute phosphate solutions. *Journal of Materials Science-Materials in Medicine*, 17, (7) 583-596

Ikemura, K., Endo, T. 2010. A review of the development of radical photopolymerization initiators used for designing light-curing dental adhesives and resin composites. *Dental Materials Journal*, 29, (5) 481-501

Kanczler, J.M., Oreffo, R.O. 2008. Osteogenesis and angiogenesis: the potential for engineering bone. *European Cells and Materials,* 15, (2) 100-114

Khaled, S.M.Z., Charpentier, P.A., Rizkalla, A.S. 2011. Physical and Mechanical Properties of PMMA Bone Cement Reinforced with Nano-sized Titania Fibers. *Journal of Biomaterials Applications*, 25, (6) 515-537

Khatri, C.A., Stansbury, J.W., Schultheisz, C.R., Antonucci, J.M. 2003. Synthesis, characterization and evaluation of urethane derivatives of Bis-GMA. *Dental Materials*, 19, (7) 584-588

Larsson, S. 2006. Cement augmentation in fracture treatment. *Scandinavian Journal of Surgery*, 95, (2) 111-118

Lee, J.K., Choi, J.Y., Lim, B.S., Lee, Y.K., Sakaguchi, R.L. 2004. Change of properties during storage of a UDMA/TEGDMA dental resin. *Journal of Biomedical Materials Research Part B-Applied Biomaterials*, 68B, (2) 216-221

Leprince, J.G., Lamblin, G., Devaux, J., Dewaele, M., Mestdagh, M., Palin, W.M., Gallez, B., Leloup, G. 2010. Irradiation Modes' Impact on Radical Entrapment in Photoactive Resins. *Journal of Dental Research*, 89, (12) 1494-1498

Leprince, J.G., Palin, W.M., Hadis, M.A., Devaux, J., Leloup, G. 2013. Progress in dimethacrylate-based dental composite technology and curing efficiency. *Dental Materials*, 29, (2) 139-156

Lewis, G. 1997. Properties of acrylic bone cement: State of the art review. *Journal of Biomedical Materials Research*, 38, (2) 155-182

Lewis, G., Nyman, J.S., Trieu, H.H. 1997. Effect of mixing method on selected properties of acrylic bone cement. *Journal of Biomedical Materials Research*, 38, (3) 221-228

Lin, C.C., Huang, L.C., Shen, P.Y. 2005. Na2CaSi2O6-P2O5 based bioactive glasses. Part 1: Elasticity and structure. *Journal of Non-Crystalline Solids*, 351, (40-42) 3195-3203

Ling, L., Xu, X., Choi, G.Y., Billodeaux, D., Guo, G., Diwan, R.M. 2009. Novel F-releasing Composite with Improved Mechanical Properties. *Journal of Dental Research*, 88, (1) 83-88

Liu, W.C., Wong, C.T., Fong, M.K., Cheung, W.S., Kao, R.Y.T., Luk, K.D.K., Lu, W.W. 2010. Gentamicin-loaded strontium-containing hydroxyapatite bioactive bone cement-An efficient bioactive antibiotic drug delivery system. *Journal of Biomedical Materials Research Part B-Applied Biomaterials*, 95B, (2) 397-406

Liu, X., Rahaman, M.N., Fu, Q.A. 2011. Oriented bioactive glass (13-93) scaffolds with controllable pore size by unidirectional freezing of camphene-based suspensions: Microstructure and mechanical response. *Acta Biomaterialia*, 7, (1) 406-416

Lovell, L.G., Lu, H., Elliott, J.E., Stansbury, J.W., Bowman, C.N. 2001. The effect of cure rate on the mechanical properties of dental resins. *Dental Materials*, 17, (6) 504-511

Lovell, L.G., Stansbury, J.W., Syrpes, D.C., Bowman, C.N. 1999. Effects of composition and reactivity on the reaction kinetics of dimethacrylate dimethacrylate copolymerizations. *Macromolecules*, 32, (12) 3913-3921

Luo, J., Skrzypiec, D.M., Pollintine, P., Adams, M.A., Annesley-Williams, D.J., Dolan, P. 2007. Mechanical efficacy of vertebroplasty: Influence of cement type, BMD, fracture severity, and disc degeneration. *Bone,* 40, (4) 1110-1119

Lusvardi, G., Malavasi, G., Menabue, L., Aina, V., Morterra, C. 2009. Fluoride-containing bioactive glasses: Surface reactivity in simulated body fluids solutions. *Acta Biomaterialia*, 5, (9) 3548-3562

Martin, R.A., Twyman, H., Qiu, D., Knowles, J.C., Newport, R.J. 2009. A study of the formation of amorphous calcium phosphate and hydroxyapatite on melt quenched Bioglass(A (R)) using surface sensitive shallow angle X-ray diffraction. *Journal of Materials Science-Materials in Medicine*, 20, (4) 883-888

Misra, S.K., Ansari, T., Mohn, D., Valappil, S.P., Brunner, T.J., Stark, W.J., Roy, I., Knowles, J.C., Sibbons, P.D., Jones, E.V., Boccaccini, A.R., Salih, V. 2010. Effect of nanoparticulate bioactive glass particles on bioactivity and cytocompatibility of poly(3-hydroxybutyrate) composites. *Journal of the Royal Society Interface*, 7, (44) 453-465

Mori, R., Nakai, T., Enomoto, K., Uchio, Y., Yoshino, K. 2011. Increased Antibiotic Release from a Bone Cement Containing Bacterial Cellulose. *Clinical Orthopaedics and Related Research*, 469, (2) 600-606

Mousa, W.F., Kobayashi, M., Shinzato, S., Kamimura, M., Neo, M., Yoshihara, S., Nakamura, T. 2000. Biological and mechanical properties of PMMA-based bioactive bone cements. *Biomaterials*, 21, (21) 2137-2146

Nugent, M., McLaren, A., Vernon, B., McLemore, R. 2010. Strength of Antimicrobial Bone Cement Decreases with Increased Poragen Fraction. *Clinical Orthopaedics and Related Research*, 468, (8) 2101-2106

Ogunyinka, A., Palin, W.M., Shortall, A.C., Marquis, P.M. 2007. Photoinitiation chemistry affects light transmission and degree of conversion of curing experimental dental resin composites. *Dental Materials*, 23, (7) 807-813

Ouis, M.A., Abdelghany, A.M., ElBatal, H.A. 2012. Corrosion mechanism and bioactivity of borate glasses analogue to Hench's bioglass. *Processing and Appplication of Ceramics,* 6, (3) 141-149

Pagoria, D., Lee, A., Geurtsen, W. 2005. The effect of camphorquinone (CQ) and CQ-related photosensitizers on the generation of reactive oxygen species and the production of oxidative DNA damage. *Biomaterials*, 26, (19) 4091-4099

Pamula, E., Kokoszka, J., Cholewa-Kowalska, K., Laczka, M., Kantor, L., Niedzwiedzki, L., Reilly, G.C., Filipowska, J., Madej, W., Kolodziejczyk, M., Tylko, G., Osyczka, A.M. 2011. Degradation, Bioactivity, and Osteogenic Potential of Composites Made of PLGA and Two Different Sol-Gel Bioactive Glasses. *Annals of Biomedical Engineering*, 39, (8) 2114-2129

Peltola, M.J., Vallittu, P.K., Vuorinen, V., Aho, A.A.J., Puntala, A., Aitasalo, K.M.J. 2012. Novel composite implant in craniofacial bone reconstruction. *European Archives of Oto-Rhino-Laryngology*, 269, (2) 623-628

Pfeifer, C.S., Silva, L.R., Kawano, Y., Braga, R.R. 2009. Bis-GMA co-polymerizations: Influence on conversion, flexural properties, fracture toughness and susceptibility to ethanol degradation of experimental composites. *Dental Materials*, 25, (9) 1136-1141

Pryor, L.S., Gage, E., Langevin, C.J., Herrera, F., Breithaupt, A.D., Gordon, C.R., Afifi, A.M., Zins, J.E., Meltzer, H., Gosman, A., Cohen, S.R., Holmes, R. 2009. Review of bone substitutes. *Craniomaxillofacial Trauma and Reconstruction*, 2, (3) 151-160

Rahaman, M.N., Day, D.E., Bal, B.S., Fu, Q., Jung, S.B., Bonewald, L.F., Tomsia, A.P. 2011. Bioactive glass in tissue engineering. *Acta Biomaterialia*, 7, (6) 2355-2373

Reilly, G.C., Radin, S., Chen, A.T., Ducheyne, P. 2007. Differential alkaline phosphatase responses of rat and human bone marrow derived mesenchymal stem cells to 45S5 bloactive glass. *Biomaterials*, 28, (28) 4091-4097

Rho, J.Y., Hobatho, M.C., Ashman, R.B. 1995. Relations of densitty and CT numbers to mechanical properties for human cortical and cancellous bone. *Medical Engineering and Physics*, 17, (5) 347-355

Rosentritt, M., Shortall, A.C., Palin, W.M. 2010. Dynamic monitoring of curing photoactive resins: A methods comparison. *Dental Materials*, 26, (6) 565-570

Saito, M., Maruoka, A., Mori, T., Sugano, N., Hino, K. 1994. Experimental Studies on A New Bioactive Bone-Cement - Hydroxyapatite Composite Resin. *Biomaterials*, 15, (2) 156-160

Sauro, S., Osorio, R., Fulgencio, R., Watson, T.F., Cama, G., Thompson, I., Toledano, M. 2013. Remineralisation properties of innovative light-curable resin-based dental materials containing bioactive micro-fillers. *Journal of Materials Chemistry B*, 1, (48) 6670

Schneider, O.D., Stepuk, A.F., Mohn, D.F., Luechinger NA FAU - Feldman, K., Feldman, K.F., Stark, W.J. 2010. Light-curable polymer/calcium phosphate nanocomposite glue for bone defect treatment. *Acta Biomaterialia,* 6, (7) 2704-2710

Shirai, K., Yoshida, Y., Nakayama, Y., Fujitani, M., Shintani, H., Wakasa, K., Okazaki, M., Snauwaert, J., Van Meerbeek, B. 2000. Assessment of decontamination methods as pretreatment of silanization of composite glass fillers. *Journal of Biomedical Materials Research*, 53, (3) 204-210

Sideridou, I., Tserki, V., Papanastasiou, G. 2002. Effect of chemical structure on degree of conversion in light-cured dimethacrylate-based dental resins. *Biomaterials*, 23, (8) 1819-1829

Silver, I.A., Deas, J., Erecinska, M. 2001. Interactions of bioactive glass with osteoblasts in vitro: effects of 45S5 Bioglass, and 58S and 77S bioactive glasses on metabolsim, intracellular ion concentrations and cell viability. *Biomaterials,* 22, (2) 175-185

Soundrapandian, C., Datta, S., Kundu, B., Basu, D., Sa, B. 2010. Porous Bioactive Glass Scaffolds for Local Drug Delivery in Osteomyelitis: Development and In Vitro Characterization. *Aaps Pharmscitech*, 11, (4) 1675-1683

Stadelmann, V.A., Bretton, E., Terrier, A., Procter, P., Pioletti, D.P. 2010. Calcium phosphate cement augmentation of cancellous bone screws can compensate for the absence of cortical fixation. *Journal of Biomechanics*, 43, (15) 2869-2874

Stansbury, J.W. 2000. Curing dental resins and composites by photopolymerization. *Interrnational Journal of Esthetic Dentistry,* 12, (6) 300-308

Uchiyama, S., Yashiro, K., Takahashi, H., Homma, T. 1989. An experimental study of spinal cord evoked potentials and histologic changes following spinal cord heating. *Spine,* 14, (11) 1215-1219

Vakiparta, M., Forsback AP, F.A.U., Lassila LV, F.A.U., Jokinen, M.F., Yli-Urpo AU FAU-Vallittu, Vallittu, P.K. 2005. Biomimetic mineralization of partially bioresorbable glass fiber reinforced composite. *Journal of Materials Science-Materials in Medicine*, 16, (9) 873-879

Valimaki, V.V. Aro, H.T. 2006. Molecular basis for action of bioactive glasses as bone graft substitute. *Scandinavian Journal of Surgery*, 95, (2) 95-102

Wang, J., Liu, C.S., Liu, Y.F., Zhang, S. 2010. Double-Network Interpenetrating Bone Cement via in situ Hybridization Protocol. *Advanced Functional Materials*, 20, (22) 3997-4011

Watts, D.C. 2005. Reaction kinetics and mechanics in photo-polymerised networks. *Dental Materials*, 21, (1) 27-35

Wichlas, F., Bail, H.J., Seebauer, C.J., Schilling, R., Pflugmacher, R., Pinkernelle, J., Rump, J., Streitparth, F., Teichgraber, U.K. 2010. Development of a signal-inducing bone cement for magnetic resonance imaging. (vol 31, pg 636, 2010). *Journal of Magnetic Resonance Imaging*, 32, (5) 1269

Xynos, I.D., Hukkanen, M.V.J., Batten, J.J., Buttery, L.D., Hench, L.L., Polak, J.M. 2000. Bioglass (R) 45S5 stimulates osteoblast turnover and enhances bone formation in vitro: Implications and applications for bone tissue engineering. *Calcified Tissue International*, 67, (4) 321-329

Yao, A.H., Wang, D.P., Huang, W.H., Fu, Q., Rahaman, M.N., Day, D.E. 2007. In vitro bioactive characteristics of borate-based glasses with controllable degradation behavior. *Journal of the American Ceramic Society*, 90, (1) 303-306

Young, A.M., Ng, P.Y.J., Gbureck, U., Nazhat, S.N., Barralet, J.E., Hofmann, M.P. 2008. Characterization of chlorhexidine-releasing, fast-setting, brushite bone cements. *Acta Biomaterialia*, 4, (4) 1081-1088

Zou, Q., Li, Y.B., Zhang, L., Zuo, Y., Li, J.F., Li, J.D. 2009. Antibiotic delivery system using nano-hydroxyapatite/chitosan bone cement consisting of berberine. *Journal of Biomedical Materials Research Part A*, 89A, (4) 1108-1117

CHAPTER 2 MATERIALS AND METHODS COMMON TO CHAPTERS CONTAINING EXPERIMENTAL DATA

2.1 Synthesis of unfilled resin systems containing 60/40wt% UDMA/TEGDMA

Unfilled resins systems were made containing 60/40wt% UDMA/TEGDMA, 0.2wt% CQ (photo-initiator) and 0.8wt% DMAEMA (co-initiator). Each substance was, accurately measured using a balance accurate to 0.0001mg (TS400D, Ohaus, USA). TEGDMA was carefully placed into a beaker, then the photo-initiator and co-initiator carefully added and gently mixed with a spatula for 15sec to reach a homogenous texture. UDMA was added to this mixture. The resulting resin formulation was mixed in a beaker covered with aluminium foil (to avoid photo-curing as a result of ambient light) on a magnetic stirrer at 60°C for 30min to obtain a homogenous solution. The resulting resin formulation was stored in a lightproof container at 4°C to avoid premature photo-curing prior to further testing.

The synthesis of 60/40wt% UDMA/TEGDMA was required in Chapters 4, 5, 6 and 7.

2.2 Synthesis of 45S5 bioactive glass

SiO_2 was employed to make melt-quenched glass samples (Alfa Aesar, 99.5%), P_2O_5 (Sigma-Aldrich, 98.5%), $CaCO_3$ (Alfa Aesar, 99.95–100.5%) and Na_2CO_3 (Sigma-Aldrich, 99.5%). A BRF16/5 chamber furnace (Elite furnaces) was used to heat a platinum-rhodium crucible, which contained the precursors to 1400°C following mixing for 5min with a spatula at 10°Cmin^1 and held at temperature for 1.5h. The molten glass was poured into a pre-heated split graphite mould (length: 6cm; diameter: 10mm) (350°C) and annealed at this temperature for 12h. The glass was then allowed to slowly cool inside the insulated furnace at room temperature by switching off the chamber furnace. This glass had the following composition $(CaO)_{26.9}(Na_2O)_{24.4}(SiO_2)_{46.1}(P_2O_5)_{2.6}$. The Bioglass was then gently and carefully manually

ground using a ceramic pestle and mortar (to avoid the possible contamination and over-heating of the bioactive glass as it may occur in the speedmixer/zirconia balls method) and subsequently sieved (using 100µm and 50µm sieves) (Fisherbrand, Fisher Scientific, UK) to ≤50µm particle diameter size (Martin et al. 2009).

The synthesis of 45S5 bioactive glass was required in Chapters 4, 5, 6 and 7.

2.3 Synthesis of filled resin composites containing bioactive glass and barium silicate filler

Filled resin composites (FRC) were synthesised containing the unfilled resin system (refer to Section 2.1 Synthesis of unfilled resin systems), barium silicate glass and bioactive glass fillers. Barium silicate glass filler (G018-186) was purchased from Schott Glass (Landshut, Germany) and had the composition: $(Al_2O_3)_{10}(B_2O_3)_{10}(BaO)_{35}(SiO_2)_{45}(F)_{<2}$ with a Silane content of 6.0%. The size of the particles was approximately 0.7µm. There were three types of bioactive glass fillers tested. There were two types of bioactive glass fillers (G018-144) purchased from Schott Glass (Landshut, Germany): silanated (silane content of 0.5%) (Type I) and non-silanated (Type II). The third bioactive glass filler (45S5) was synthesised in the laboratory and it was non-silanated (Type III) (Table 2.1 and 2.2) (refer to Section 2.2 Synthesis of bioactive glass, above).

FRC	Low filler		High filler	
wt%	20	40	23	45
Type I	SIL20	SIL40	SIL23	SIL45
Type II	NS20	NS40	NS23	NS45
Type III	AB20	AB40	AB23	-

Table 2.1 Filled resin composite (FRC) compositions in wt% for both low filler (46vol% filler) and high filler (60vol% filler) content.

The Type I and Type II fillers had an average particle size diameter of 10µm, whereas Type III fillers had a particle size diameter <50µm (Table 2.2).

	Composition	Filler type	Filler size (µm)
Type I	$(CaO)_{25}(Na_2O)_{25}(SiO_2)_{45}(P_2O_5)_5 + (Silane)_{0.5}$	Silanated	10
Type II	$(CaO)_{25}(Na_2O)_{25}(SiO_2)_{45}(P_2O_5)_5$	Non-silanated	10
Type III	$(CaO)_{26.9}(Na_2O)_{24.4}(SiO_2)_{46.1}(P_2O_5)_{2.6}$	Non-silanated	<50

Table 2.2 The type and size of bioactive glass filler particles present in each filled resin composite.

Low and high viscosity FRCs (with low and high filler content) were made containing 60/40wt% UDMA/TEGDMA; 20, or 40wt% bioactive glass and barium silicate glass to a ratio of resin to filler in the final FRC at 30:70wt% (low filler content) or 60/40wt% UDMA/TEGDMA; 23, or 45wt% bioactive glass and barium silicate glass to a ratio of resin to filler in the final FRC at 20:80wt% (high filler content) (Table 2.3). FRCs containing barium silicate glass filler only (70 or 80wt%, low and high filler content, respectively) were used as positive control. The FRCs were synthesised to form either a low viscosity or a high viscosity filler content in the final filled resin composite keeping the ratio of resin to filler at 30:70wt% (low filler content) or 20:80wt% (high filler content) (Table 2.2). All the substances were measured using a balance accurate to 0.0001mg (TS400D, Ohaus, USA). The bioactive glass and barium silicate filler particles were placed in a container and gently mixed with a spatula. The resin mixture was then added to this bioactive glass, barium silicate mixture. This formulation was, then, mixed in a Speed Mixer (DAC 150 FV2-K, Hauschild Engineering, Germany) for 90s at low speed (1000rpm) and 180s at high speed (3000rpm). The mixed formulations were subsequently stored in a lightproof container at 4°C to avoid premature photo-curing prior to further testing.

The synthesis of filled resin composites was required in Chapters 5, 6 and 7.

	Low viscosity			High viscosity			
60/40 UT	wt%	0	20	40	0	22.72	45.29	Bioglass
	vol%	0	14.44	28.48	0	18.33	35.82	
	wt%	70	50	30	80.31	56.97	34.02	Barium Silicate
	vol%	46.17	32.50	19.22	60	41.27	24.02	

Table 2.3 Filled resin composites compositions in wt% for both low filler (46vol% filler) and high filler (60vol% filler) content. 60/40 UT represents the unfilled resin formulation containing 60/40wt% UDMA/TEGDMA. Bioglass represents the three different types of bioactive glass used: Type I, Type II and Type III. Barium Silicate refers to barium silicate glass filler.

2.4 Synthesis of polymethylmethacrylate

Polymethylmethacrylate (PMMA) cement (Palamed, Hereus Medical GMBH, Germany), a commercially available material for hip and knee arthroplasties, was used as a control for the experimentally developed FRCs. The PMMA constituents were measured with a balance accurate to 0.0001mg (TS400D, Ohaus, USA) to obtain a ratio of 2:40 powder to liquid monomer, which was, then, manually mixed with a plastic spatula for 30sec, at room temperature. The mixed cement was then carefully placed at the bottom of the mould, avoiding the inclusion of air bubbles, flattened with a glass slide and allowed to set for 10min. Disc shaped molds (diameter: 10mm and height 2mm) were used for testing the degree of conversion, whereas disc shaped molds (diameter: 15mm and height: 1mm) were used for water sorption, solubility and bi-axial flexural testing. Split aluminium rectangular shaped molds (25mmx2mmx2mm) were used for three point bend testing. The cement was, then, carefully removed from the mold and stored in Petri dishes prior to use.

The synthesis of PMMA cement was required in Chapters 4, 5, 6 and 7.

2.5 Preparation and light curing of unfilled resin systems and filled resin composite samples

For mechanical (three point bend) testing, rectangular bars (n=10 for each sample condition) of unfilled resin systems and FRCs were made using a rectangular aluminium split mold. Each resin bar was carefully polished manually with 1000 grit silicon carbide paper (Struers, UK) to the dimensions of 25(length)x2(height)x2(width)mm; to obtain a flat surface, with no poorly-polymerised layer due to oxygen inhibition (Sauro et al. 2013; Tian et al. 2008). For water sorption, solubility and bi-axial flexure strength testing, disks of FRCs (n=10 for each sample condition) were made using a black Teflon disc shaped mold (15mm diameter and 1mm thickness). For bone marrow stromal cell viability studies (n=9 for each sample condition; 3

biological replicates), disks of unfilled resin systems and FRCs were made using a black Teflon disk shaped mold (10mm diameter, 2mm thickness). A thin layer of Vaseline (Unilever, UK) (release agent) was used to cover the surfaces of the mold that came into contact with the unfilled resin systems/FRCs formulation. The unfilled resin systems/FRCs formulations were carefully pipetted at the bottom of each mold, which was placed on a glass microscope slide. Each mold was, then, covered with acetate film (to prevent oxygen inhibition) and another glass slide in order to achieve a flat specimen.

Each mixture was, then, irradiated from the top for 40sec with a blue light (spectral range of 400-500nm) using a Quarts-Tungsten-Halogen light curing unit (tip diameter 10mm) (Optilux 501, Sybron Dental Specialists Kerr, USA). The spectral irradiance of the Optilux 501 light curing unit was 695±43mW/cm^2, which was measured using a fibre-coupled UV-Vis spectrometer and 3.9mm cosine corrector sensor (Ocean Optics) calibrated with a NIST-traceable halogen-deuterium lamp (DH-2000; Ocean Optics). The curing light tip was aligned centrally, 0mm above the sensor using a universal joint and clamp securely fixed to an optical breadboard. The irradiance of the curing unit was determined prior to each experiment to ensure the output did not vary significantly (695±43mW/cm^{-2}). For the preparation of specimens for mechanical testing, an overlapping curing protocol was used, which was necessary as a consequence of the diameter of the curing tip (10mm) being less than the length of the specimens. For the preparation of specimens for water sorption, solubility and bi-axial flexure testing, FRCs formulations were photo-activated with 5 overlapping exposures for 40sec each, with a total of 200sec curing time (according to the ISO standard protocol for polymer based restorations (ISO 4049)). The cured unfilled resin systems or filled resin composite specimens were then placed in Petri dishes covered with aluminium foil (to allow dark polymerisation to

occur) and stored overnight at room temperature to ensure completion of the polymerisation reaction prior to further testing.

2.6 Physical testing of unfilled resin systems and filled resin composites

The degree of conversion of a substance provides an evaluation of the amount of monomer converted to a three dimensional polymer network, during the polymerisation reaction. DC may also indirectly provide details about the mechanical, fatigue and elution properties of the substance tested (Dewaele et al. 2006). The degree of conversion of unfilled resin systems and filled resin composites is commonly tested using spectroscopic methods such as Fourier transform and Raman spectroscopy. These spectroscopic methods can be employed to acquire infrared (IR) spectra of light polymerisable materials such as dimethacrylate resins. These methods are commonly based on absorption spectroscopy of the electromagnetic spectrum in the infrared region. This infrared region is composed of three main sub-regions: the far (wavenumber: 25-400cm^{-1}), mid (wavenumber: 400-4000cm^{-1}) and near IR (wavenumber; 4000-14000cm^{-1}) according to their connection to the visible spectrum of light (Guerra et al. 1996). The degree of conversion and polymerisation rate (for unfilled resin systems) of each sample were recorded at an acquisition rate of 10s^{-1} and spectra taken at an 8cm^{-1} wavenumber resolution, 3scans to average for 180sec.

2.6.1 Real-time near infrared spectroscopy

The real-time near infrared spectroscopy was used to analyse the degree of conversion and rate of polymerisation of unfilled resin systems using a Fourier transform infrared spectrometer (FT-IR) (Nicolet 6700, Thermo Scientific). There were two types of unfilled resin systems analysed based on the chemical structure of the monomers used: a system based on bisGMA as the main monomer and another system based on UDMA as the main monomer. The uncured unfilled resin system formulation was gently pipetted at the base of a disc shaped mould (diameter:

10mm, height: 2mm) (which was placed on a glass slide) and carefully covered with another glass slide to avoid air inclusion and attain a flat surface for the specimen. This resin mixture was then exposed to a curing light for 40sec (Optilux 501, Sybron Dental Specialists Kerr, USA), to polymerise the resin monomer. Real time near infrared spectroscopy was used to measure the continuous change in absorbance of the =C-H group of monomers (wavenumber: 6165cm^{-1}) for bisGMA/TEGDMA unfilled resin systems and the C=O group (wavenumber: 1730cm^{-1}) for UDMA/TEGDMA unfilled resin systems (Guerra et al. 1996; Podgorski, 2010; Stansbury and Dickens, 2001) at room temperature, for 3min, with 3scans/spectrum and 8cm^{-1} wavenumber resolution, utilising series run. During the measurement of the polymerisation of each unfilled resin system formulation, the infrared spectra were collected every 3sec (in this study). The light curing unit was manually switched on at 10sec (Figure 2.1). Then the conversion of the monomer to polymer was calculated for each unfilled resin system containing bisGMA/TEGDMA, UDMA/TEGDMA (Equation 2.1):

Equation 2.1 $DC\% = 1 - \frac{Final\ absorbance}{Initial\ absorbance} x100$

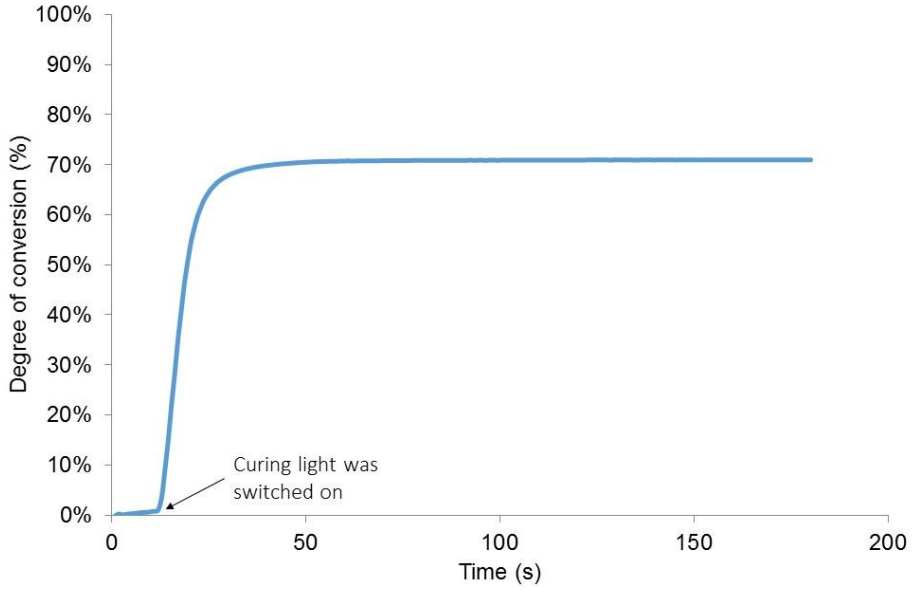

Figure 2.1 Schematic representation of a typical curve of the degree of conversion (%) of light curable dimethacrhylate resins over time (s).

The rate of polymerisation was also calculated by dividing the change in the degree of conversion of the unfilled resin systems with the change in time (Figure 2.2).

Equation 2.2 $Rp=\frac{DC_n - DC_{n-1}}{T_n - T_{n-1}}$, where DC_n representes the degree of conversion at time n, and T_n represents time at each point of analysis.

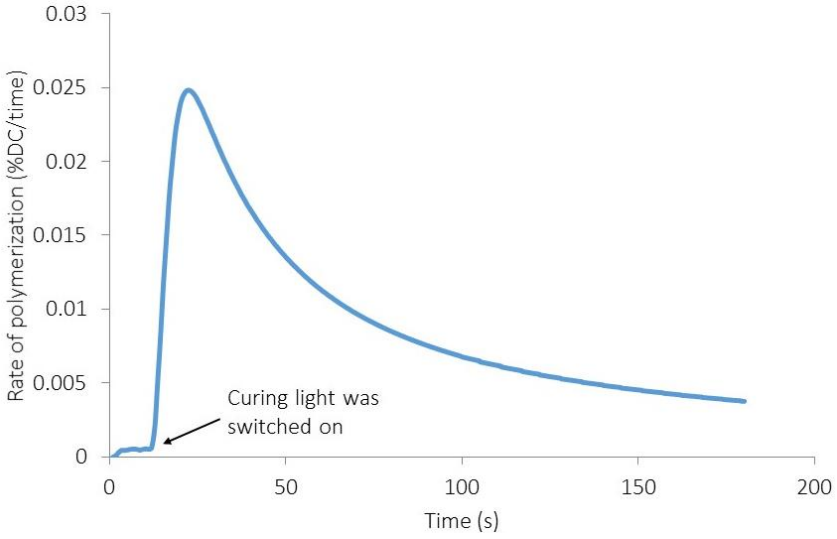

Figure 2.2 Schematic representation of a typical curve of the rate of polymerisation of light curable dimethacrylate resins over time (s).

2.6.2 Mid infra-red spectroscopy

Fourier transform infrared spectra in the mid-IR region was used to analyse the conversion of carbon double bonds to carbon single bonds of FRCs. This spectra was obtained using attenuated total reflection from un-polymerised 2mm thick FRC formulations. This ATR method can be employed with infrared spectroscopy to analyse samples in liquid or solid state. The Fourier transform mid-IR method employs the reflection of the infrared radiation at the lower specimen surface to calculate the DC of a material, in this case, the filled resin composites (Stansbury and Dickens, 2001). This method also requires reference bands, which are stable during polymerisation to normalise the spectra of the monomer and polymer. In this study, the reference band at 1716cm^{-1} (corresponding to the C=O group of urethane dimethacrylates) was used (Nomoto and Hirasawa 1999; Stansbury and Dickens). The same reference bands were used to determine the degree of conversion of PMMA. The uncured FRC formulation for each condition was carefully pipetted at the base of a disc shaped mould (diameter: 10mm; thickness 2mm) (which was placed on the diamond tip of the FT-IR machine) and covered with acetate film (to prevent oxygen inhibition and attain a flat specimen). The uncured filled resin composite formulation was then exposed to a curing light for 40sec (Optilux 501, Sybron Dental Specialists Kerr, USA), to allow polymerisation of the resin monomer. Then, the conversion of the monomer to polymer of each FRC condition was calculated from the intensity at each band (Dewaele et al. 2006) (Equation 2.3):

Equation 2.3 $$DC\% = \frac{1730cm^{-1}/1716cm^{-1}\ \text{cured}}{1730cm^{-1}/1716cm^{-1}\ \text{uncured}} x100$$

This method was used in Chapters 3 and 4.

2.7 Mechanical testing of unfilled resin systems and filled resin composites

The mechanical properties of the unfilled resin systems, filled resin composites and PMMA were determined using the three point bend test, as described in the ISO standard protocol for polymer based restorations (ISO 4049). Each specimen bar was placed centrally on a support span of 20mm and loaded centrally using a blunt point tip. Each specimen bar was, then, subjected to load using a universal testing instrument (Instron 5544, UK) at a cross head speed of 1mm/min with a 2kN load cell to determine the strain and stress levels within each sample. Failure was initiated by tensile stresses acting on the lower convex surface of the specimen, when the specimen bars were subjected to loading (Hosseinalipour et al. 2010; Palin et al. 2005). By producing a stress-strain graph, the fracture stress, the yield stress and the flexural modulus were determined for each sample. The elastic value provided information regarding the rigidity of a particular sample (the steeper the slope of the stress-strain graph, the more rigid the sample was). The width and the thickness of each sample bar were also measured using a micrometre scale accurate to 10μm. Equation 2.4 was employed for the calculation of the flexural stress of each sample condition:

Equation 2.4 $\sigma = 3PL/2bd;$

The strain of each sample was calculated using Equation 2.5*:*

Equation 2.5 $\varepsilon = 6Dd/L^2 * 100;$

where P=load at fracture, L=support span, b=specimen width, d=specimen thickness, D=midspan deflection.

The calculation of the flexural modulus of each sample condition was calculated using Equation 2.6:

Equation 2.6 $E = \sigma/\varepsilon$;

where σ=stress and ε=strain (Palin et al. 2005).

This method was employed in Chapters 3, 4 and 6.

References

Dewaele, M., Truffier-Boutry, D., Devaux, J., Leloup, G. 2006. Volume contraction in photocured dental resins: The shrinkage-conversion relationship revisited. *Dental materials*, 22, (4) 359-365

Guerra, R.M., Duran, I., Ortiz, P. 1996. FTIR monomer conversion analysis of UDMA-based dental resins. *Journal of Oral Rehabilitation*, 23, (9) 632-637

Hosseinalipour, M., Javadpour, J., Rezaie, H., Dadras, T., Hayati, A.N. 2010. Investigation of mechanical properties of experimental Bis-GMA/TEGDMA dental composite resins containing various mass fractions of silica nanoparticles. *Journal of Prosthodontics-Implant Esthetic and Reconstructive Dentistry*, 19, (2) 112-117

International Standard Organisation: ISO 4049, Dentistry-Polymer-Based Filling, Restorative and Luting Materials (ed 3). Geneva, ISO, 2000, pp. 15-18

Nomoto, R., Hirasawa, T. 1999. Evaluation of the amount of residual monomer on UDMA-based resins by FTIR. *Dental Materials Journal*, 18, (2) 176-183

Palin, W.M., Fleming, G.J.P., Marquis, P.M. 2005. The reliability of standardized flexure strength testing procedures for a light-activated resin-based composite. *Dental Materials*, 21, (10) 911-919

Podgorski, M. 2010. Synthesis and characterisation of novel dimethacrylates of different chain lengths as possible dental resins. *Dental Materials,* 26, (6) e188-e194

Sauro, S., Osorio, R., Fulgencio, R., Watson, T.F., Cama, G., Thompson, I., Toledano, M. 2013. Remineralisation properties of innovative light-curable resin-based dental materials containing bioactive micro-fillers. *Journal of Materials Chemistry B*, 1, (48) 2624-2638

Stansbury, J.W., Dickens, S.H. 2001. Determination of double bond conversion in dental resins by near infrared spectroscopy. *Dental Materials,* 17, (1) 71-79

Tian, M., Gao, Y., Liu, Y., Liao, Y., Hedin, N.E., Fong, H. 2008. Fabrication and evaluation of Bis-GMA/TEGDMA dental resins/composites containing nano fibrillar silicate. *Dental Materials,* 24, (2) 235-243

CHAPTER 3 DEVELOPMENT OF UNFILLED RESIN SYSTEMS FOR ORTHOPAEDIC RESIN-BASED COMPOSITE CEMENTS

3.1 Introduction

The majority of orthopaedic cements are chemically cured by the mixture of two or more components using a set curing time relevant for different specific applications. For example a cement that hardens in less than 5 minutes after the mixture of components may be suitable for spinal repair, however, it may be unsuitable for the repair of cranial injuries where more time may be required by the surgeon to mould the cement in the desired shape. By introducing a material that command sets following exposure to intense blue light, this time constraint may be removed. The surgeon is then able to harden the material only when the desired shape and appropriate placement have been achieved. Such materials that harden upon light exposure are frequently used in dental applications as components in tooth filling materials, adhesives and sealants. These materials are monomers (including bisGMA (bisphenol-a-glycidyldimethacrylate), UDMA (urethane dimethacrylates), TEGDMA (triethylene glycol dimethacrylate)), which by the addition of suitable photo-initiator systems (such as diketone/amine) form a cross-linked polymer network following light activation (chemical structures of those used in the current study are presented in Figure 3.1) (Sideridou et al. 2002). Resins systems can be further developed by varying the amount and type of monomers used to enable modification of viscosity that may enable suitability for different orthopaedic applications such as bone void fillings or cranio-facial repair surgeries. The viscosity of the resin systems is influenced by the chemical structure and molecular weight of the monomers and has an impact on the polymerisation kinetics and the cross-linkage of the polymer network (Cornelio et al. 2013; Ferracane et al. 1985; Floyd and Dickens 2006; Kalachandra et al. 1997).

Moreover, adjusting the viscosity of the resin system by varying the monomer ratios may have an impact on the mechanical and physical properties of the set composite materials (Gajewski et al. 2012; Goncalves et al. 2009).

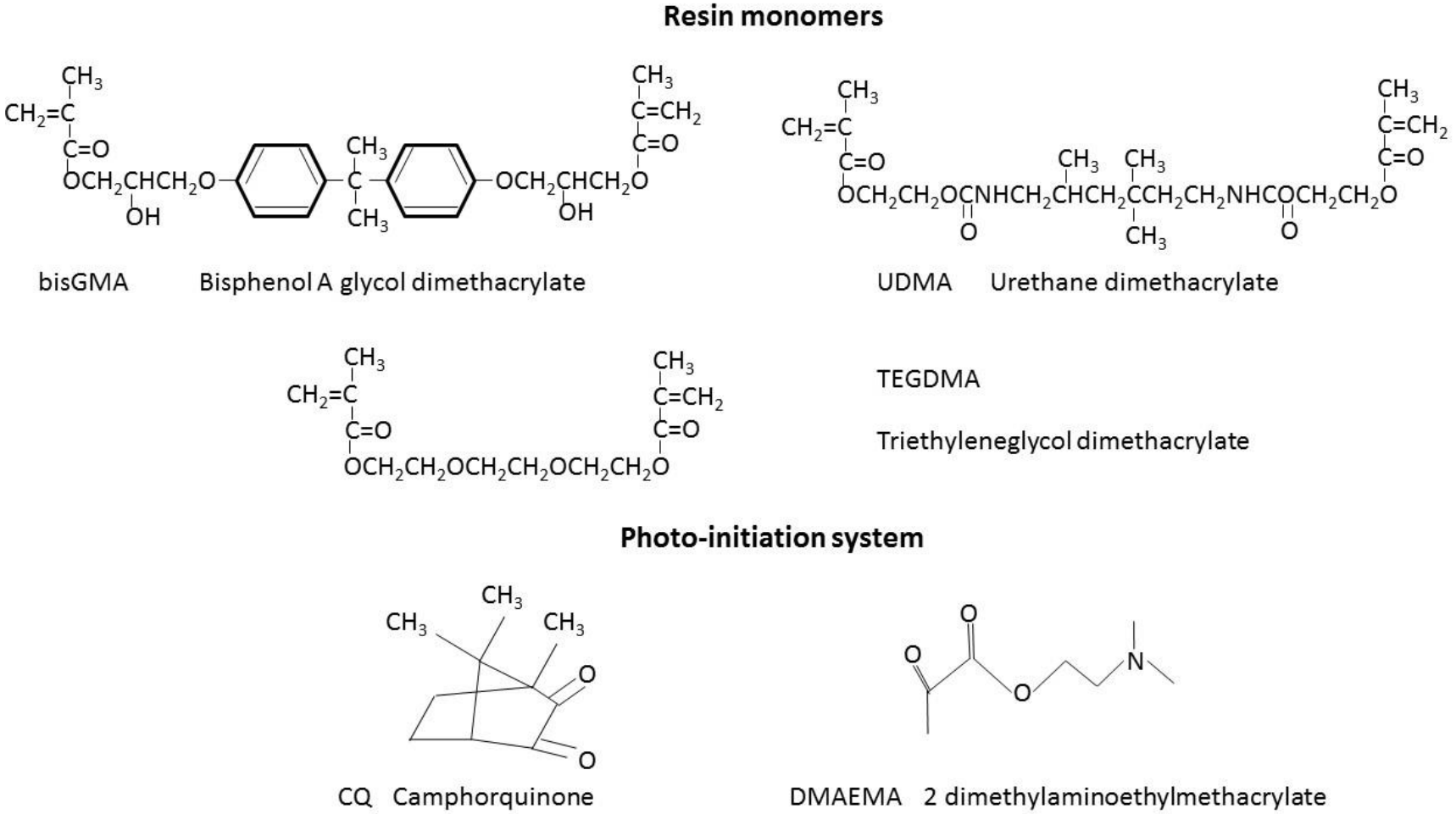

Figure 3.1 Chemical structures of the 3 different monomers and the photo-initiator system employed in this study (adapted from Asmussen et al. 2009; Ikemura and Endo, 2010).

By increasing the concentration of TEGDMA in unfilled resin systems containing bisGMA/TEGDMA monomers, the viscosity of the system is reduced and the concentration of double bonds available for conversion increased, resulting in increased degree of conversion (DC) (percentage of carbon double bonds converted to carbon single bonds during polymerisation) of the monomer to a three dimensional polymer network (Cornelio et al. 2013; Ferracane et al. 1985). However, an increase in TEGDMA concentration in bisGMA/TEGDMA unfilled resin systems may lead to a decrease in mechanical strength due to a decrease in aromatic rings (present in the bisGMA molecule) and an increase in ether groups (present in the TEGDMA molecule) (Asmussen and Peutzfeldt 1998; Barszczewska-Rybarek 2009; Emami and Soderholm 2009; Floyd and Dickens 2006; Gajewski et al. 2012; Goncalves et al. 2009; Lovell et al. 1999). For unfilled resin systems containing UDMA and TEGDMA monomers, an increase in UDMA concentration results in increased mechanical strength and possibly degree of conversion due to the presence of urethane groups, which lead to increased flexibility of such unfilled resin systems (Asmussen and Peutzfeldt 1998; Barszczewska-Rybarek 2009; Emami and Soderholm 2009; Floyd and Dickens 2006; Gajewski et al. 2012; Goncalves et al. 2009; Lovell et al. 1999).

The aims of this chapter were to analyse the effect of different concentrations of three commonly used monomers in dental applications (namely bisGMA, UDMA, TEGDMA) on their physical and mechanical properties to determine whether comparable results with the ones conducted in previous studies are obtained and to develop the basis for possible formulations that may be employed as the base for cements in orthopaedic applications. The degree of conversion, rate of polymerisation (RP), hardness (physical characteristics) and the flexural strength (FS) and modulus (FM) (mechanical properties) were analysed to determine suitable formulations for filled resin composites that may have usage in orthopaedic applications.

3.2 Materials and Methods

3.2.1 Synthesis of unfilled resin systems

All monomers were sourced from Sigma Aldrich, UK and used without modification unless otherwise stated (Table 3.1).

Monomer	Molecular mass	Concentration of double bonds (mol/kg)	Viscosity (Pas)	Density (g/mL)
UDMA	471	4.25	28	1.129
bisGMA	512	3.90	1369	1.140
TEGDMA	286	6.99	0.05	1.073

Table 3.1 Properties of monomers used in this study. The viscosity, concentration of double bonds, molecular mass and density, all have an impact on the mechanical and physical properties of the final unfilled resin system.

Three types of unfilled resin systems were synthesised for analysis: two co-monomers containing UDMA/TEGDMA or bisGMA/TEGDMA and a ter-monomer containing bisGMA/UDMA/TEGDMA to determine a suitable unfilled resin system by mixing different concentrations of the most common monomers (Ekworapoj et al. 2002) in different concentrations to which bioactive glass can be added to form a filled resin composite for use in orthopaedic applications. The ter-monomer system was tested to determine whether the addition of UDMA (which exhibits increased flexibility and decreased viscosity) to resins containing bisGMA/TEGDMA can enhance the degree of conversion, flexural strength and flexural modulus of such resins. The photo-initiator system was composed of CQ (camphorquinone) and a co-initiator (DMAEMA (2 dimethylaminoethylmethacrylate)). The concentrations used to synthesise the organic matrix of the unfilled resin systems were: 20/80; 30/70; 40/60; 50/50; 60/40; 70/30; 80/20wt% UDMA/TEGDMA or bisGMA/TEGDMA or 30/60/10; 20/60/20; 10/60/30; 40/50/10; 30/50/20; 20/50/30; 10/50/40; 50/40/10; 50/30/20;

50/20/30; 50/10/40wt% bisGMA/UDMA/TEGDMA. 100wt% UDMA, 100wt% bisGMA and 100wt% TEGDMA were used as controls. The photo-initiator system was added to either UDMA/TEGDMA, bisGMA/TEGDMA, or bisGMA/UDMA/TEGDMA formulations in proportion of 0.2wt% CQ (this value was selected to ensure the initiator was completely consumed during the polymerisation reaction (Lovell et al. 2003) and 0.8wt% DMAEMA. Each unfilled resin system formulation was mixed in a beaker on a magnetic stirrer at 60°C for 30min covered with aluminium foil (to avoid photo-curing as a result of ambient light). The unfilled resin system formulations were stored in a lightproof container at 4°C to avoid premature photo-curing prior to further testing.

For the analysis of the degree of conversion and rate of polymerisation of unfilled resin systems refer to Chapter 2, Section 2.6

3.2.2 Mechanical properties: Hardness testing of unfilled resin systems

Hardness testing refers to the property of a given material to resist surface plastic deformation. The unfilled resin systems mixture was placed into disc shaped molds (diameter: 10mm, height: 2mm) between acetate sheets (to minimise the effects of oxygen inhibition) and cured using blue light (Optilux 501, Sybron Dental Specialists Kerr, USA) for 40sec (Figure 3.2).

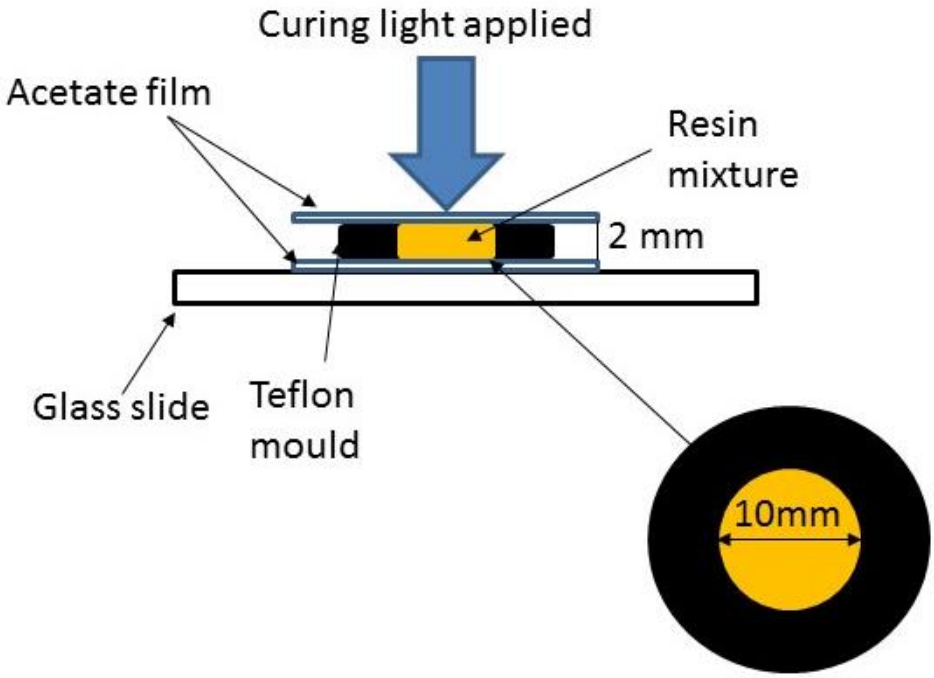

Figure 3.2 Experimental set-up for synthesis of disc shaped specimens. Each disc shaped specimen was cured for 40s using visible blue light curing and stored in a light proof container to avoid premature photo-curing prior to testing.

Three discs containing unfilled resin systems were tested for each sample condition on both the upper (curing light applied to this surface of the disc) (n=3) and lower surface (n=3) and an average taken by using a hardness tester (Struers-Duramin, Glasgow, UK) to perform 6 Vickers indentations on each disc. This test assessed the hardness of specimens by determining the size of these indentations left on the surface of the specimen using a pyramid-shaped diamond indenter, which has a square base and a 136^0 apex angle. Each unfilled resin system specimen disk was subjected to a load of 1.96N for 10sec applied to the pyramid indenter causing indentations that appeared as dark squares on a lighter background, when visualised using a microscope (integral to the equipment) (Hosseinalipour et al. 2010). The two diagonals of each square were measured and an average calculated as shown in Figure 3.3.

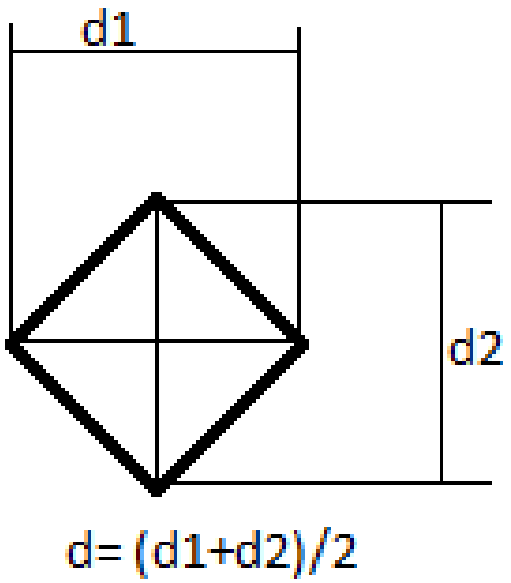

Figure 3.3 Diagram of Vickers hardness indentation appearance on the surface of a material (used to calculate the hardness value of each resin specimen).

Equation 3.1 was applied to calculate the Vickers hardness values of the unfilled resin systems:

Equation 3.1 $HV = 1.854xF/d^2$;

where HV is the hardness Vickers number in kg/mm^2, F is the force applied to the specimen and d^2 represents the surface area determined by taking the average of the 2 diagonals of the square left by the indenter in µm (Hosseinalipour et al. 2010). The hardness value of each disc containing unfilled resin systems was calculated on both the upper surface and the lower surface to determine the extent of cure of each unfilled resin system formulation condition.

For the preparation and light curing of specimens for mechanical testing and the analysis of flexural strength and modulus using the three point bend test refer to Chapter 2, Section 2.5 and Section 2.7.

3.2.3 Statistical analysis

Minitab statistical software (Minitab, UK) was used to analyse the data using one-way analysis of variance (ANOVA) test. An Anderson-Darling test was used to determine whether the data

followed a normal distribution. Tukey's post hoc tests were used for pair-wise comparison using a significance value of P=0.05.

3.3 Results

3.3.1 Physical properties: degree of conversion and rate of polymerisation of unfilled resin systems

For analysis of significant differences between the degree of conversion of unfilled resin systems refer to Appendix 1, Tables 1.1-1.3. The DC of bisGMA/TEGDMA unfilled resin systems was significantly lower compared with the DC of UDMA/TEGDMA unfilled resin systems ($p<0.005$) (Figure 3.4). The bisGMA/TEGDMA unfilled resin system formulation concentrations that exhibited the highest DC were 30/70 (statistically higher compared with 20/80 bisGMA/TEGDMA and 80/20 bisGMA/TEGDMA ($p<0.001$, $p<0.001$, respectively) and 50/50wt% (statistically higher compared with 20/80 bisGMA/TEGDMA ($P<0.001$), 70/30 bisGMA/TEGDMA ($p=0.002$) and 80/20 bisGMA/TEGDMA ($p<0.001$)); whereas the UDMA/TEGDMA unfilled resin systems exhibited a similar DC irrespective of the concentration of base monomers (Figure 3.4). The UDMA/TEGDMA unfilled resin systems exhibited a significantly higher DC compared with TEGDMA control resins ($p<0.001$). The bisGMA/TEGDMA unfilled resin systems, also, exhibited significantly higher DC compared with bisGMA control and TEGDMA control resins ($p<0.001$) (Figure 3.4).

The DC of bisGMA/UDMA/TEGDMA unfilled resin systems increased with increasing concentration of TEGDMA and decreasing concentration of bisGMA. The unfilled resin system formulation containing 40/10/50wt% bisGMA/UDMA/TEGDMA exhibited significantly higher DC compared with all the ternary monomer unfilled resin systems studied ($p<0.005$) (Figure 3.5). The DC of each unfilled resin system containing the highest amount of TEGDMA (30 or 40wt%) was significantly higher compared with the other unfilled resin system mixtures in each group tested (unfilled resin systems containing either 60wt%, 50wt% UDMA or 50wt% bisGMA) ($p<0.035$). Similarly, the DC of each unfilled resin systems containing the highest

amount of bisGMA (30 or 40wt%) was significantly lower compared with the other unfilled resin system mixtures in each group tested (unfilled resin systems containing either 60wt% or 50wt% UDMA) ($p<0.010$). The highest DC in the present study was found to be 89%, which was exhibited by an unfilled resin system containing 40/60wt% UDMA/TEGDMA (Figure 3.4). This value was also much higher than that of the DC of bisGMA/TEGDMA unfilled resin systems (75.1 for 30/70 bisGMA/TEGDMA unfilled resin system formulation) and bisGMA/UDMA/TEGDMA unfilled resin systems (82.02 for 10/50/40 bisGMA/UDMA/TEGDMA unfilled resin system formulation) (Figures 3.4, 3.5).

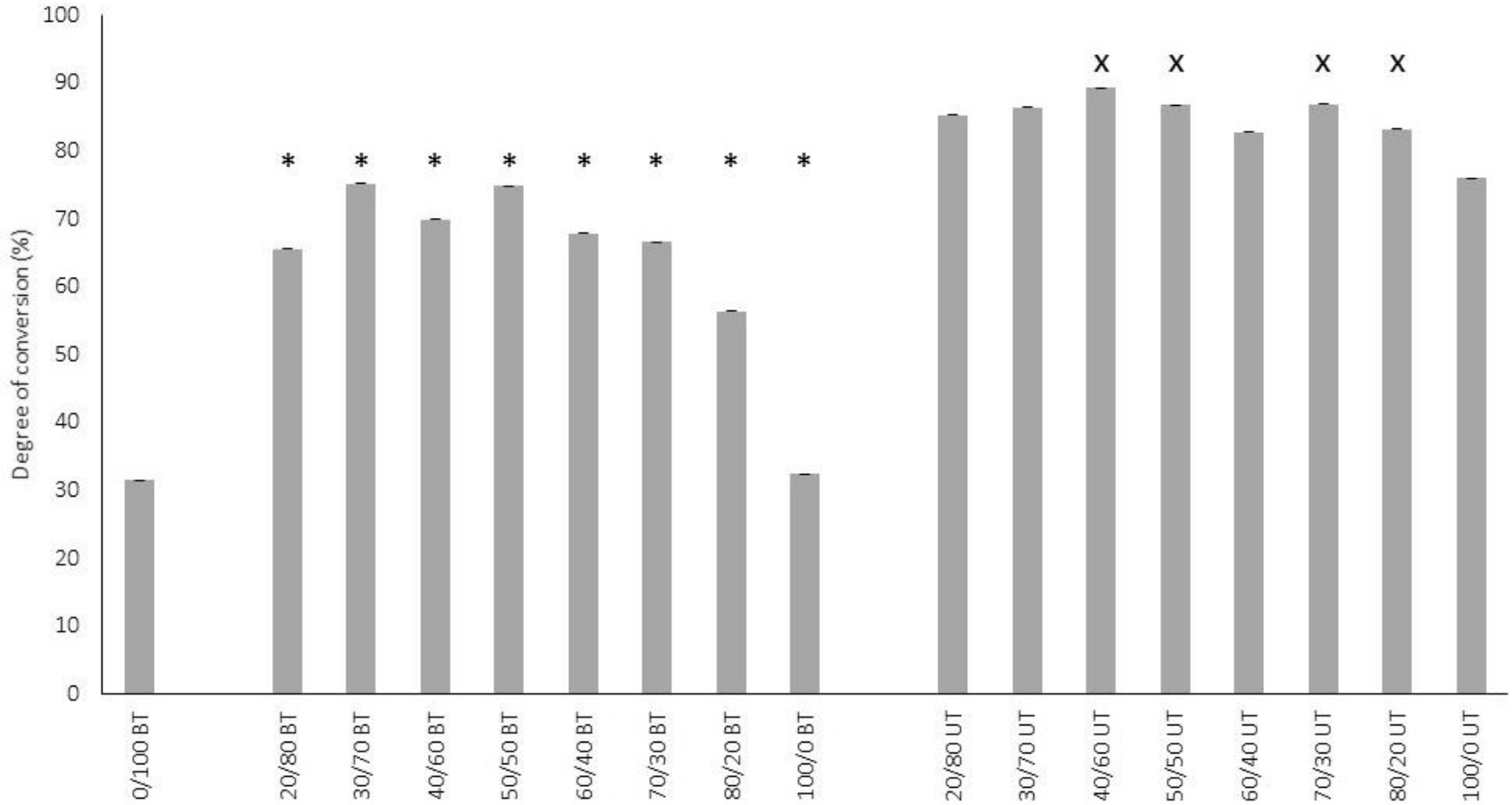

Figure 3.4 Degree of conversion of TEGDMA based unfilled resin systems containing increasing concentration of either bisGMA or UDMA (BT or UT). Unfilled resin system percentage inclusions are shown within bar labels. * denotes statistical differences with unfilled resin systems containing 100wt% bisGMA; X denotes statistical differences with unfilled resin systems containing 100wt% UDMA. UDMA/TEGDMA unfilled resin systems exhibited increased degree of conversion compared with bisGMA/TEGDMA unfilled resin systems. Error bars indicate standard deviation over mean average of 3 samples.

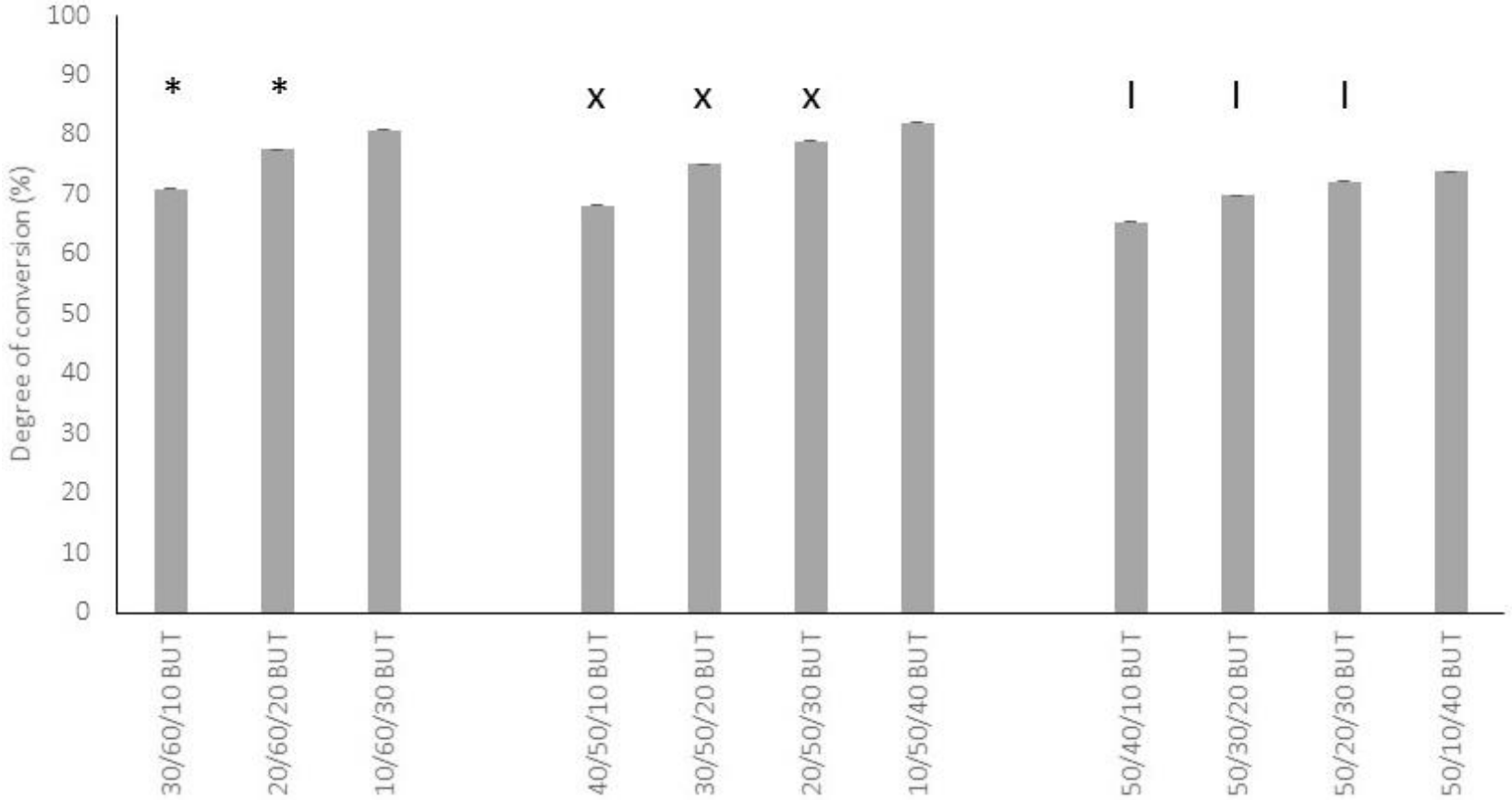

Figure 3.5 Degree of conversion of unfilled resin systems containing bisGMA/UDMA/TEGDMA resins (BUT). Unfilled resin system percentage inclusions are shown within bar labels. * denotes statistical differences with unfilled resin systems containing 10/60/30wt% bisGMA/UDMA/TEGDMA; X denotes statistical differences with unfilled resin systems containing 10/50/40wt% bisGMA/UDMATEGDMA and l denotes statistical differences with unfilled resin systems containing 50/10/40wt% bisGMA/UDMA/TEGDMA. The degree of conversion increased with increasing concentration of TEGDMA. Error bars indicate standard deviation over mean average of 3 samples.

For analysis of significant differences between the rate of polymerisation (RP) of unfilled resin systems refer to Appendix 1, Tables 1.4-1.6. The RP was significantly higher for UDMA/TEGDMA unfilled resin systems compared with bisGMA/TEGDMA unfilled resin systems ($p<0.005$). The addition of TEGDMA significantly increased the RP of unfilled resin systems containing bisGMA ($p<0.001$); compared with unfilled resin systems containing UDMA, which was only statistically smaller compared with 30/70 UDMA/TEGDMA ($p=0.007$) and 60/40 UDMA/TEGDMA ($p<0.001$). UDMA/TEGDMA unfilled resin systems exhibited an increasing RP with decreasing concentrations of TEGDMA used, whereas bisGMA/TEGDMA unfilled resin systems exhibited a similar RP regardless of the amount of TEGDMA present. The bisGMA/TEGDMA unfilled resin systems exhibited significantly higher RP compared with bisGMA and TEGDMA control resins ($p<0.001$); whereas UDMA/TEGDMA unfilled resin systems exhibited significantly higher RP compared with TEGDMA control resins ($p<0.001$). The maximum RP was achieved faster for bisGMA/TEGDMA unfilled resin systems compared with UDMA/TEGDMA unfilled resin systems in the co-monomer based resins (Table 3.2).

BisGMA/UDMA/TEGDMA unfilled resin systems containing the highest concentration of UDMA exhibited the highest RP. The RP increased with increasing concentration of TEGDMA up to 30wt% TEGDMA for bisGMA/UDMA/TEGDMA unfilled resin systems containing 50wt% UDMA, whereas, the RP decreased with increasing concentration of TEGDMA for bisGMA/UDMA/TEGDMA unfilled resin systems containing either 60wt% UDMA, or 50wt% bisGMA (Table 3.3). The unfilled resin system group containing the highest amount of bisGMA (50wt%) exhibited a significantly lower RP compared with all the bisGMA/UDMA/TEGDMA unfilled resin systems studied ($p<0.033$). The unfilled resin system containing 50/10/40wt% bisGMA/UDMA/TEGDMA exhibited significantly lower RP compared with all the

bisGMA/UDMA/TEGDMA unfilled resin systems studied ($p<0.030$), with the exception of the unfilled resin system containing 50/20/30wt% bisGMA/UDMA/TEGDMA ($p=0.063$). The RP was achieved faster for the bisGMA/UDMA/TEGDMA unfilled resin systems containing the highest amount of bisGMA (Table 3.3).

Resin (wt%)	Time (s) to RP max	Max RP (s^{-1})	Max DC (%)
B/T			
20/80	47.0 (1.0)	0.036 ($3x10^{-3}$)	65.5 ($3x10^{-2}$)
30/70	36.8 (1.0)	0.041 ($1x10^{-3}$)	75.1 ($3x10^{-2}$)
40/60	30.6 (0.0)	0.040 ($1x10^{-4}$)	69.9 ($6x10^{-3}$)
50/50	28.3 (1.0)	0.044 ($1x10^{-3}$)	74.8 ($5x10^{-3}$)
60/40	31.2 (1.0)	0.043 ($1x10^{-4}$)	67.8 ($8x10^{-3}$)
70/30	22.1 (1.7)	0.038 ($4x10^{-4}$)	66.5 ($3x10^{-3}$)
80/20	17.0 (1.7)	0.037 ($5x10^{-4}$)	56.3 ($1x10^{-2}$)
100/0	27.8 (4.3)	0.013 ($2x10^{-3}$)	56.3 ($1x10^{-2}$)
U/T			
20/80	45.6 (0.5)	0.051 ($1x10^{-3}$)	85.3 ($1x10^{-2}$)
30/70	37.4 (4.0)	0.058 ($2x10^{-3}$)	86.4 ($5x10^{-2}$)
40/60	34.6 (0.5)	0.061 ($2x10^{-3}$)	89.3 ($2x10^{-5}$)
50/50	32.0 (0.5)	0.058 ($6x10^{-4}$)	86.7 ($9x10^{-3}$)
60/40	26.1 (0.5)	0.061 ($7x10^{-4}$)	82.7 ($1x10^{-2}$)
70/30	23.8 (0.0)	0.069 ($7x10^{-4}$)	86.9 ($3x10^{-3}$)
80/20	20.4 (0.0)	0.077 ($3x10^{-3}$)	83.2 ($1x10^{-2}$)
100/0	16.7 (0.5)	0.087 ($6x10^{-3}$)	76.0 ($3x10^{-2}$)
0/100	50.7 (0.5)	0.011 ($4x10^{-4}$)	31.4 ($3x10^{-3}$)

Table 3.2 The average time to the maximum RP and maximum DC of bisGMA/TEGDMA (B/T) or UDMA/TEGDMA (U/T) unfilled resin systems. The bisGMA/TEGDMA unfilled resin systems exhibited lower DC and RP compared with the UDMA/TEGDMA unfilled resin systems.

Resin (wt%) (BUT)	Time (s) to RP max	Max RP (s^{-1})	Max DC (%)
30/60/10	15.3 (0.0)	0.084 ($3x10^{-4}$)	80.0 ($9x10^{-3}$)
20/60/20	18.7 (0.0)	0.083 ($5x10^{-4}$)	77.5 ($1x10^{-3}$)
10/60/30	20.4 (0.0)	0.083 ($2x10^{-4}$)	80.9 ($4x10^{-3}$)
40/50/10	15.9 (1.0)	0.076 ($3x10^{-3}$)	68.2 ($5x10^{-3}$)
30/50/20	18.1 (1.0)	0.077 ($9x10^{-4}$)	75.0 ($3x10^{-3}$)
20/50/30	19.8 (1.0)	0.077 ($2x10^{-3}$)	78.9 ($4x10^{-3}$)
10/50/40	22.1 (0.0)	0.076 ($2x10^{-4}$)	82.0 ($7x10^{-4}$)
50/40/10	17.0 (0.0)	0.065 ($4x10^{-4}$)	65.3 ($4x10^{-3}$)
50/30/20	17.0 (0.0)	0.061 ($7x10^{-4}$)	70.0 ($2x10^{-3}$)
50/20/30	20.1 (1.0)	0.056 ($2x10^{-4}$)	72.1 ($5x10^{-3}$)
50/10/40	25.5 (1.7)	0.048 ($5x10^{-4}$)	73.8 ($6x10^{-3}$)

Table 3.3 The average time to the maximum RP and maximum DC of bisGMA/UDMA/TEGDMA (BUT) unfilled resin systems. The unfilled resin systems containing the highest amount of bisGMA exhibited lower RP compared with all the TEGDMA/bisGMA/UDMA unfilled resins systems studied.

3.3.2 Mechanical properties: Vickers hardness of unfilled resin systems

For analysis of significant differences between the hardness values of unfilled resin systems refer to Appendix 1, Tables 1.7-1.15. Hardness values were analysed for both the upper and lower surface of the unfilled resin system specimen (Figure 3.6). The UDMA/TEGDMA unfilled resin system exhibited higher hardness values on their upper and lower surface compared with bisGMA/TEGDMA unfilled resin systems. The bisGMA/TEGDMA unfilled resin system exhibited significantly different values for hardness compared with each other, with the 60/40 bisGMA/TEGDMA unfilled resin system exhibiting the highest value of hardness of all unfilled resin systems containing bisGMA tested ($p<0.001$). Unfilled resin systems containing 70/30wt% UDMA/TEGDMA exhibited the highest hardness value of all unfilled resin systems specimens tested on both the upper and lower surface ($p<0.033$), with the exception of 70/30 UDMA/TEGDMA (lower surface), which was statistically similar ($p=0.532$). 100wt% bisGMA control resin exhibited the lowest value for hardness, when both surfaces were tested ($p<0.001$) (Figure 3.6). BisGMA/TEGDMA unfilled resin systems exhibited significantly lower hardness values compared with TEGDMA control resins ($p<0.001$); whereas UDMA/TEGDMA unfilled resin systems exhibited significantly higher hardness values compared with the TEGDMA control resins ($p<0.001$) (Figure 3.6). The 60/40 bisGMA/TEGDMA unfilled resin system exhibited the highest value of hardness of all unfilled resin systems containing bisGMA ($p<0.001$). BisGMA/TEGDMA unfilled resin systems exhibited significantly lower hardness values compared with TEGDMA control resins ($p<0.001$); whereas UDMA/TEGDMA unfilled resin systems exhibited significantly higher hardness values compared with the TEGDMA control resins ($p<0.001$) (Figure 3.6).

The lowest hardness value of bisGMA/UDMA/TEGDMA unfilled resin systems containing 60wt% UDMA was exhibited by the unfilled resin system containing the smallest amount of

TEGDMA (10wt%) on both the upper and lower surface ($p<0.001$). The hardness value increased with increasing concentration of TEGDMA up to 30wt%, which was significantly higher compared with all the ter-monomer unfilled resin systems containing 50wt% UDMA ($p<0.001$) (Figure 3.7). The hardness value of the ter-monomer unfilled resin systems containing 50wt% bisGMA followed a similar trend to the unfilled resin systems containing 50wt% UDMA. Thus, the hardness value increased with increasing concentration of TEGDMA up to 30wt%, which was significantly higher compared with all the ter-monomer unfilled resin systems containing 50wt% bisGMA ($p<0.001$) (Figure 3.7).

The hardness values were significantly higher on the upper side compared with the lower side of bisGMA/TEGDMA, UDMA/TEGDMA and bisGMA/UDMA/TEGDMA unfilled resin systems ($p<0.001$) (Figures 3.6, 3.7).

For analysis of correlation between the degree of conversion and hardness values of unfilled resin systems refer to Appendix 6, Tables 6.1-6.28. There was a strong positive correlation between the degree of conversion and hardness values (upper surface) of unfilled resin systems containing 20/80wt% UDMA/TEGDMA ($r=0.630$), 40/60wt% UDMA/TEGDMA ($r=0.907$), 50/50wt% UDMA/TEGDMA ($r=0.956$), 60/40wt% UDMA/TEGDMA ($r=0.870$), 40/60/0wt% bisGMA/TEGDMA ($r=0.905$), 50/50wt% bisGMA/TEGDMA ($r=0.998$), 80/20wt% bisGMA/TEGDMA ($r=0.816$), 100wt% bisGMA ($r=0.807$), 40/50/10wt% bisGMA/UDMA/TEGDMA ($r=0.811$), 30/50/20wt% bisGMA/UDMA/TEGDMA ($r=0.860$), 20/50/30wt% bisGMA/UDMA/TEGDMA ($r=0.958$) (Figure 3.8).

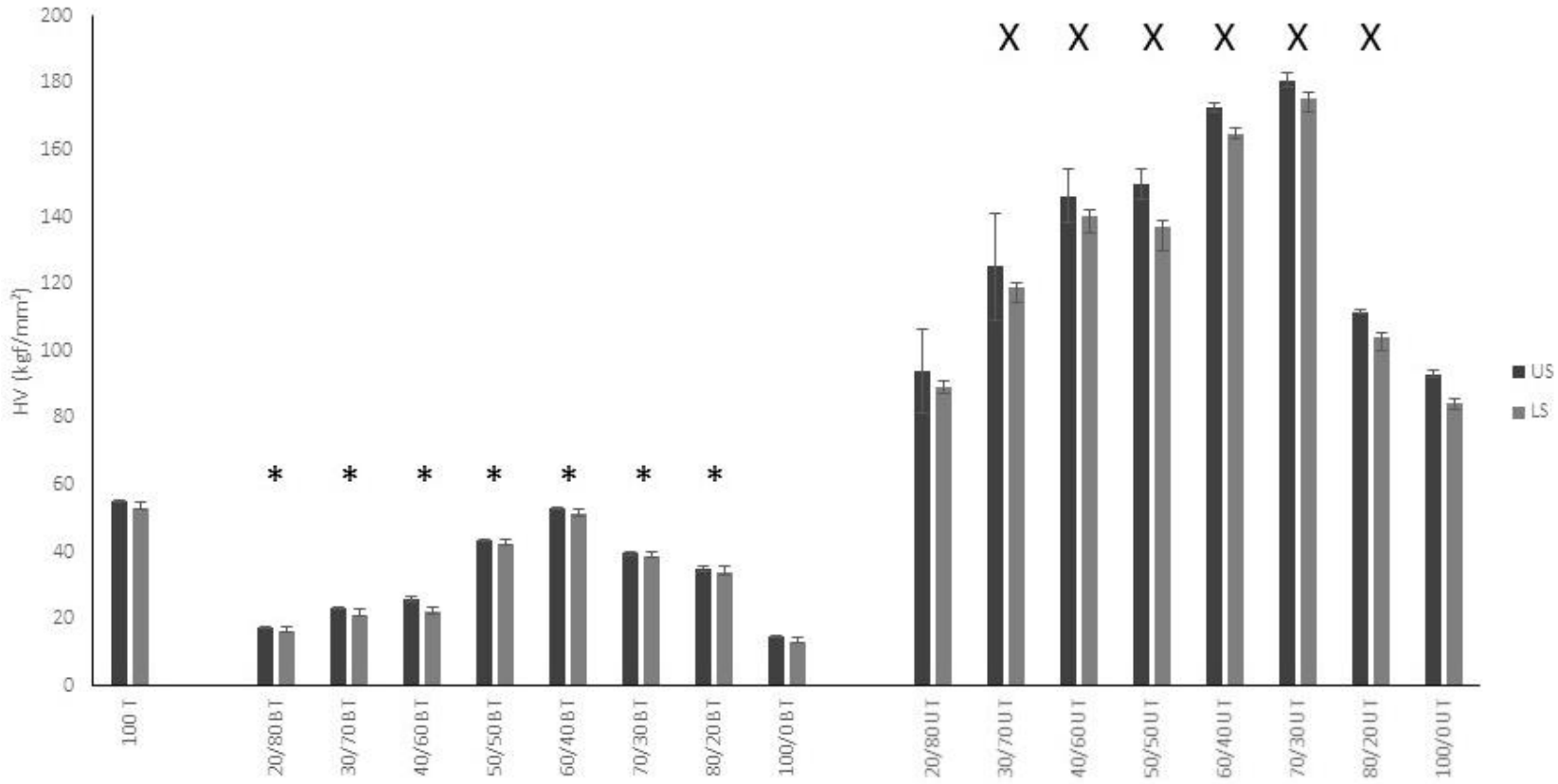

Figure 3.6 Hardness values of the upper (US) and lower (LS) surfaces of TEGDMA based unfilled resin systems containing increasing concentration of bisGMA (BT) or UDMA (UT). Unfilled resin system percentage inclusions are shown within bar labels. * denotes statistical differences with unfilled resin systems containing 100wt% bisGMA; X denotes statistical differences with unfilled resin systems containing 100wt% UDMA (for both upper and lower surfaces). bisGMA/TEGDMA unfilled resin systems exhibited similar hardness values on both surfaces, whereas UDMA/TEGDMA unfilled resin systems exhibited increased hardness on the upper surface compared with the lower surface. Error bars indicate standard deviation of a mean average of 3 samples.

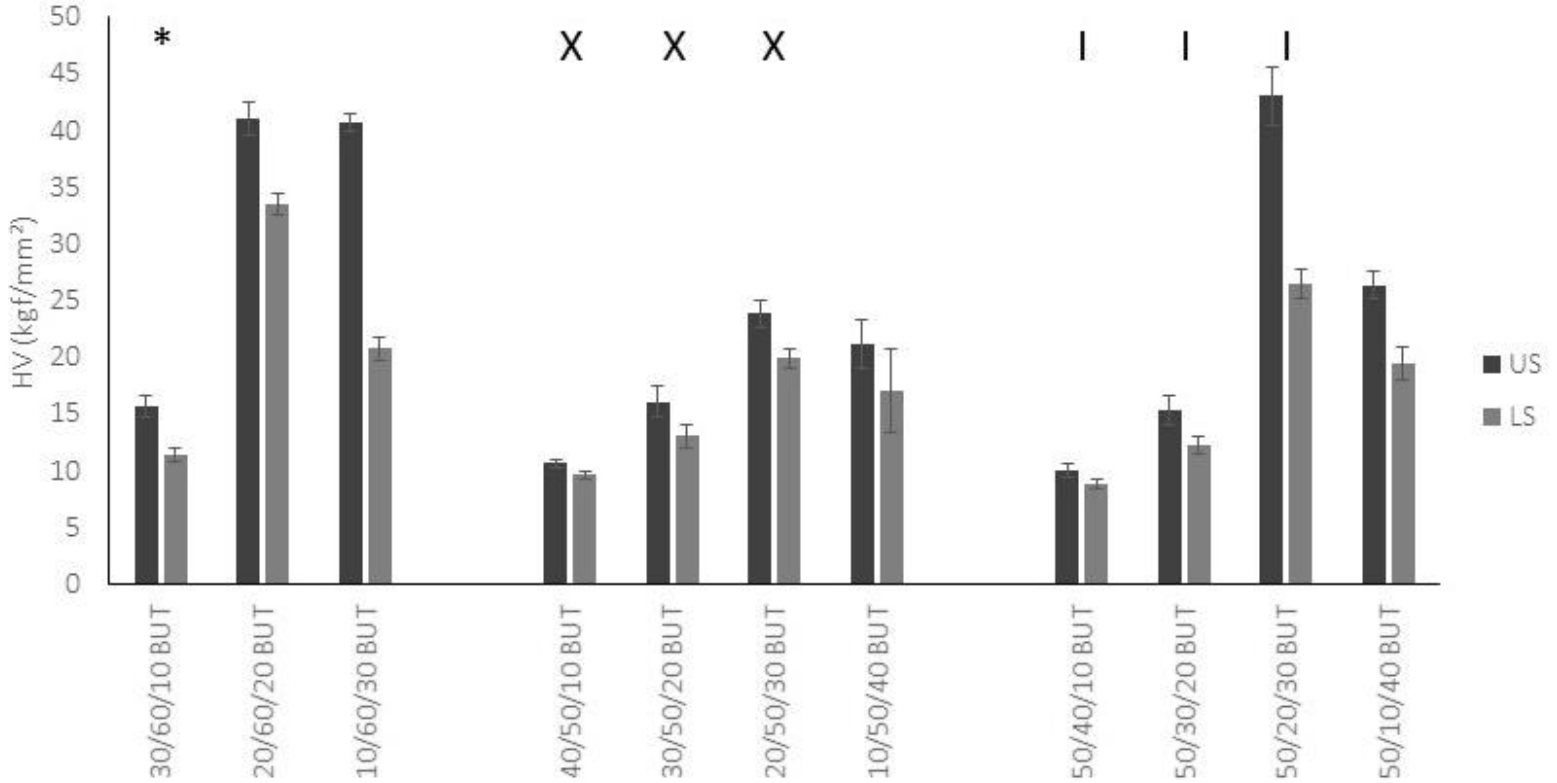

Figure 3.7 Hardness values of the upper (US) and lower (LS) surfaces of bisGMA/UDMA/TEGDMA unfilled resin systems (BUT). Unfilled resin system percentage inclusions are shown within bar labels. * denotes statistical differences with unfilled resin systems containing 10/60/30wt% bisGMA/UDMA/TEGDMA; X denotes statistical differences with unfilled resin systems containing 10/50/40wt% bisGMA/UDMATEGDMA and l denotes statistical differences with unfilled resin systems containing 50/10/40wt% bisGMA/UDMA/TEGDMA (for both upper and lower surfaces). Increased concentration of TEGDMA resulted in increased hardness on the upper surface of these unfilled resin systems up to 30wt% TEGDMA. Error bars indicate standard deviation of a mean average of 3 samples.

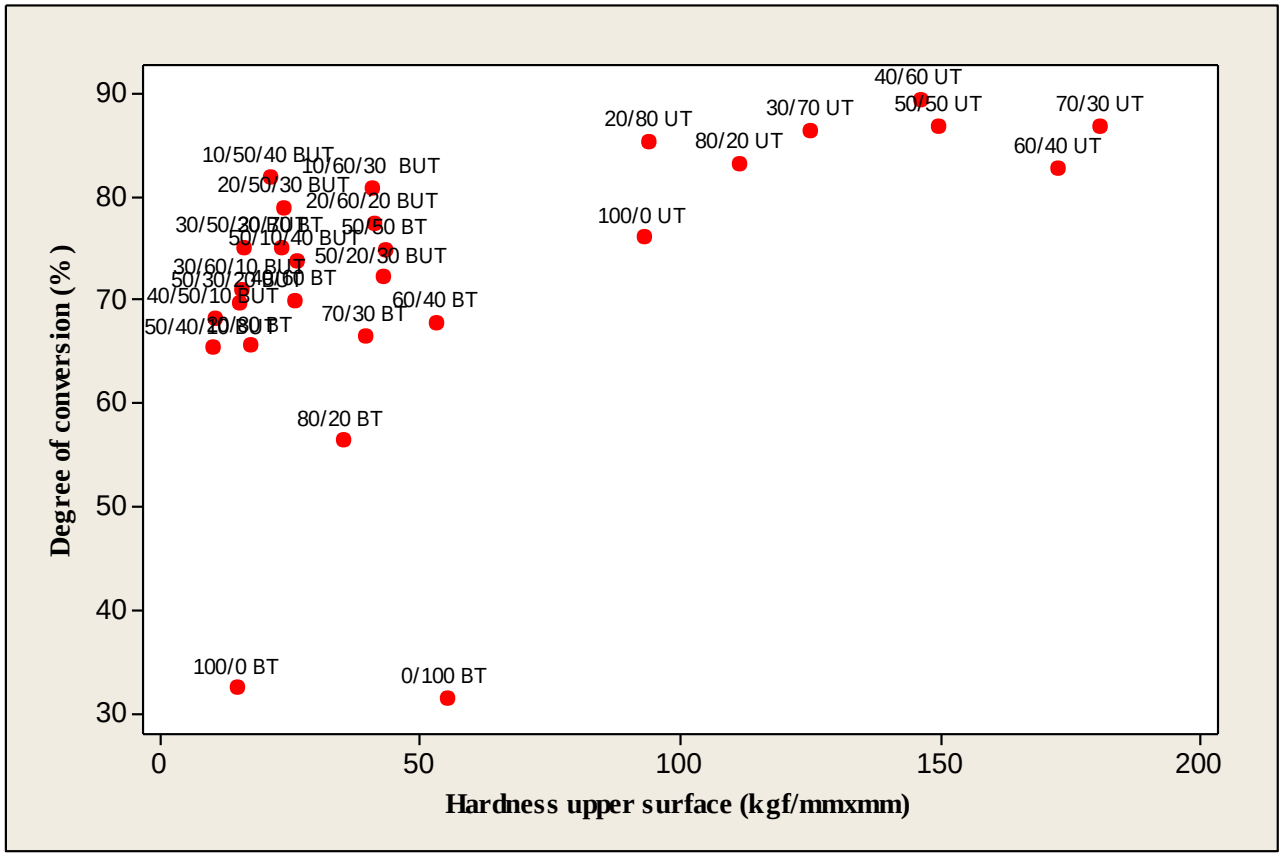

Figure 3.8 Pearson correlation between the degree of conversion and hardness values of unfilled resin systems containing bisGMA/TEGDMA (BT), UDMA/TEGDMA (UT), or bisGMA/UDMA/TEGDMA (BUT). Unfilled resin system percentage inclusions are shown within labels. There was a strong positive correlation between the degree of conversion and hardness values of unfilled resin systems containing 60/40 UDMA/TEGDMA (r=0.870).

3.3.3 Mechanical properties: flexural strength and modulus analysis of unfilled resin systems

For analysis of significant differences between the flexural strength (FS) of unfilled resin systems refer to Appendix 1, Tables 1.16-1.18. The highest FS value of bisGMA/TEGDMA unfilled resin systems was exhibited by those containing 70/30 bisGMA/TEGDMA (only significantly higher compared with 20/80 bisGMA/TEGDMA ($p<0.001$) and 80/20 bisGMA/TEGDMA ($p=0.001$)); whereas 50/50 UDMA/TEGDMA unfilled resin system exhibited the highest FS values of UDMA/TEGDMA unfilled resin systems (significantly higher compared with 80/20 UDMA/TEGDMA ($p=0.012$), 40/60 UDMA/TEGDMA ($p=0.023$), 60/40 UDMA/TEGDMA ($p=0.007$), 70/30 UDMA/TEGDMA ($p<0.001$) and 80/20 UDMA/TEGDMA ($p<0.001$). The FS of bisGMA/TEGDMA unfilled resin systems was significantly higher compared with the bisGMA control resin ($p<0.001$). The 40/60, 50/50, 60/40 and 70/30 bisGMA/TEGDMA unfilled resin systems exhibited significantly higher FS values compared with TEGDMA control resin ($p<0.005$). All the UDMA/TEGDMA unfilled resin systems exhibited higher FS values compared with TEGDMA control resin ($p<0.005$), with the exception of 20/80 (which was significantly lower: $p<0.001$) and 80/20 (statistically similar: $p=615$) UDMA/TEGDMA unfilled resin systems. The FS of all UDMA/TEGDMA unfilled resin systems was significantly higher compared with UDMA control resin ($p<0.001$), with the exception of 20/80 (significantly lower: $p<0.001$) and 80/20 (statistically similar: $p=0.561$) UDMA/TEGDMA resins (Figure 3.9).

Except of 20/80wt% UDMA/TEGDMA, the bisGMA/UDMA/TEGDMA unfilled resin systems exhibited decreased FS compared with UDMA/TEGDMA unfilled resin systems (Figures 3.9, 3.10). For the ter-monomer unfilled resin systems containing 60wt% UDMA, the

highest FS was exhibited by the unfilled resin system containing equal amount of bisGMA and TEGDMA monomers ($p<0.048$) (Figure 3.10).

For analysis of correlation between the degree of conversion and flexural strength values of unfilled resin systems refer to Appendix 6, Tables 6.1-6.28. There was a strong positive correlation between the degree of conversion and flexural strength values of unfilled resin systems containing 20/80wt% bisGMA/TEGDMA (r=0.980), 30/70wt% bisGMA/TEGDMA (r=1.000), 50/50wt% bisGMA/TEGDMA (r=1.000), 80/20wt% bisGMA/TEGDMA (r=0.651), 100wt% bisGMA (r=0.983), 20/60/20wt/% bisGMA/UDMA/TEGDMA (r=0.955), 20/50/30wt% bisGMA/UDMA/TEGDMA (r=0.867), 50/20/30wt% bisGMA/UDMA/TEGDMA (r=0.931) (Figure 3.11).

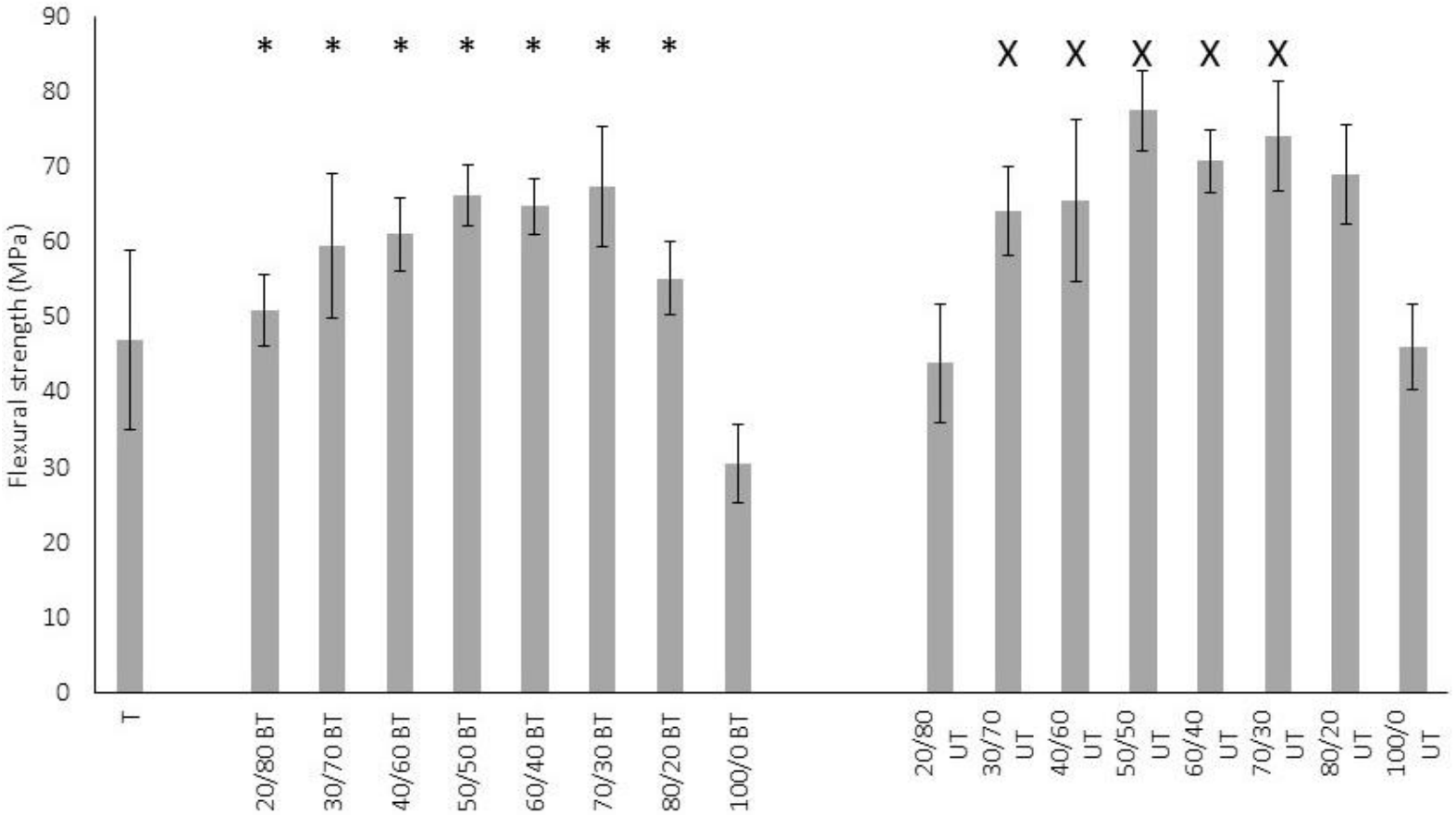

Figure 3.9 Flexural strength of TEGDMA based resins containing increasing concentration of bisGMA or UDMA. Unfilled resin system percentage inclusions are shown within bar labels. Error bars indicate standard deviation of a mean average of 10 samples. * denotes statistical differences with unfilled resin systems containing 100wt% bisGMA; X denotes statistical differences with unfilled resin systems containing 100wt% UDMA. UDMA/TEGDMA unfilled resin systems exhibited higher flexural strength compared with bisGMA/TEGDMA unfilled resin systems.

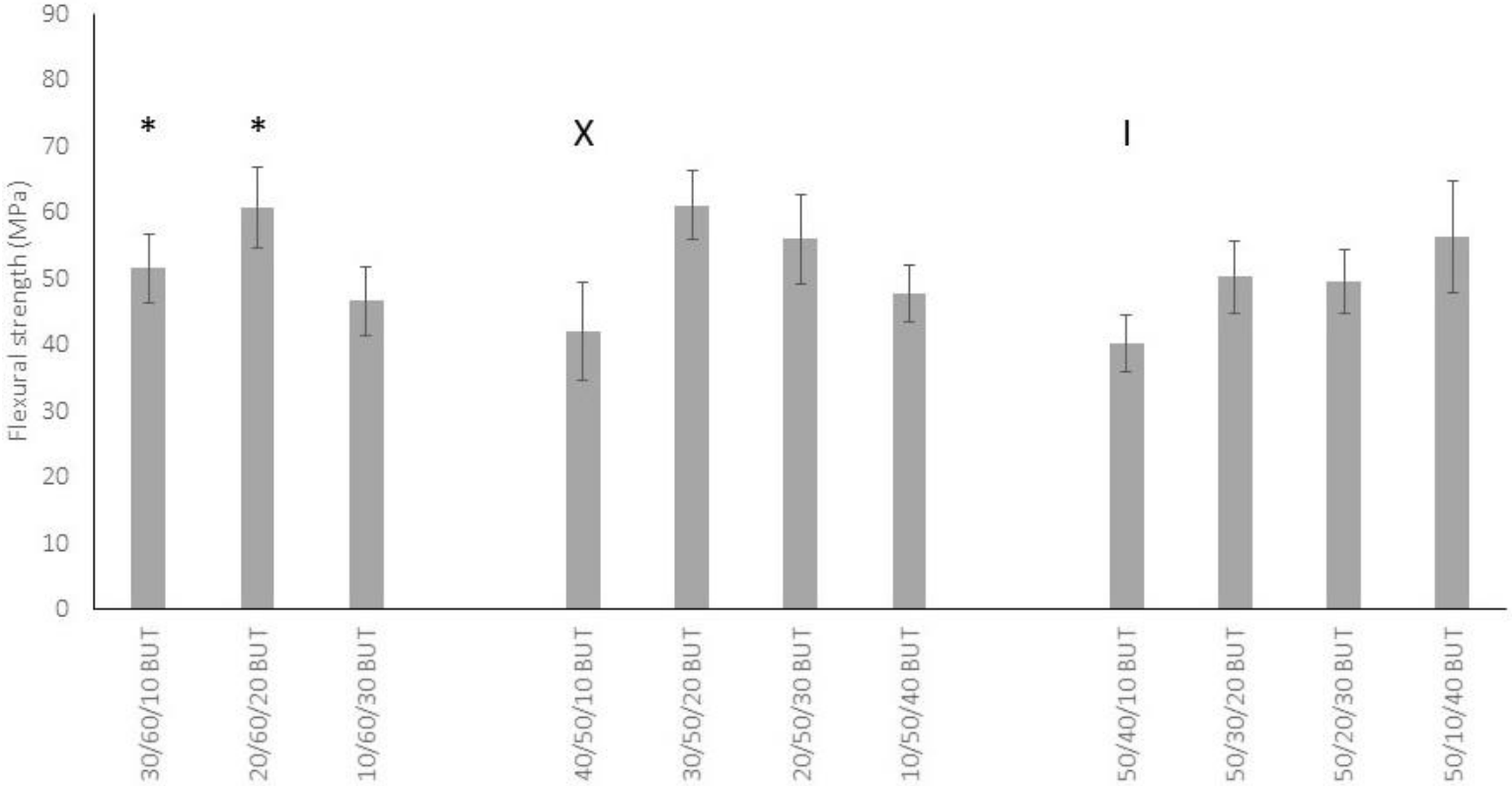

Figure 3.10 Flexural strength of bisGMA/UDMA/TEGDMA unfilled resin systems (BUT). Unfilled resin system percentage inclusions are shown within bar labels. Error bars indicate standard deviation of a mean average of 10 samples. For the unfilled resin systems containing 60 or 50wt% UDMA, the flexural strength increased with increasing concentration of TEGDMA up to 20wt%.* denotes statistical differences with unfilled resin systems containing 10/60/30wt% bisGMA/UDMA/TEGDMA; X denotes statistical differences with unfilled resin systems containing 10/50/40wt% bisGMA/UDMATEGDMA and l denotes statistical differences with unfilled resin systems containing 50/10/40wt% bisGMA/UDMA/TEGDMA 0wt% TEGDMA.

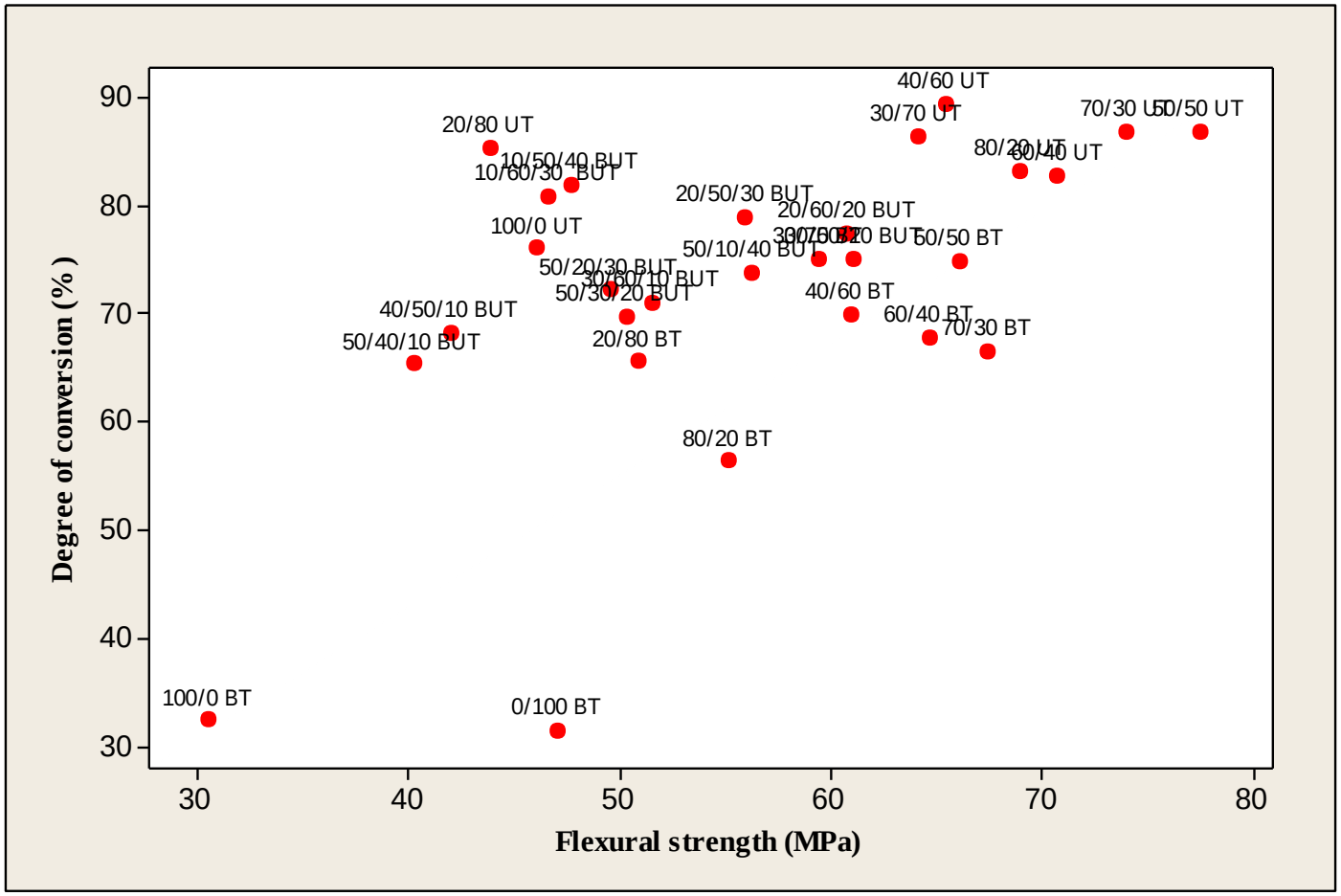

Figure 3.11 Pearson correlation between the degree of conversion and flexural strength values of unfilled resin systems containing bisGMA/TEGDMA (BT), UDMA/TEGDMA (UT), or bisGMA/UDMA/TEGDMA (BUT). Unfilled resin system percentage inclusions are shown within labels. There was a strong negative correlation between the degree of conversion and flexural strength values of unfilled resin systems containing 60/40 UDMA/TEGDMA (r=-0.999).

For analysis of significant differences between the flexural modulus (FM) of unfilled resin systems refer to Appendix 1, Tables 1.19-1.21. The highest FM value of bisGMA/TEGDMA unfilled resin systems was exhibited by those containing 70/30 bisGMA/TEGDMA (significantly higher compared with 20/80 bisGMA/TEGDMA ($p=0.001$)); whereas 50/50 UDMA/TEGDMA exhibited the highest FM values of UDMA/TEGDMA unfilled resin systems (statistically higher compared with 20/80 UDMA/TEGDMA ($p=0.006$), 60/40 UDMA/TEGDMA ($p=0.012$), 70/30 UDMA/TEGDMA ($p<0.001$) and 80/20 UDMA/TEGDMA ($p<0.001$)). The FM of bisGMA/TEGDMA unfilled resin systems was significantly higher compared with the bisGMA control resin ($p<0.001$). All the bisGMA/TEGDMA unfilled resin systems exhibited higher FM values compared with TEGDMA control resins ($p<0.005$) with the exception of 20/80 (statistically similar: $p=0.222$) and 80/20 (statistically similar: $p=0.145$,) bisGMA/TEGDMA unfilled resin system. All the UDMA/TEGDMA unfilled resin systems exhibited higher FM values compared with TEGDMA control resin ($p<0.050$), with the exception of 80/20 (statistically similar: $p=0.387$) UDMA/TEGDMA unfilled resin systems. The FM of all UDMA/TEGDMA unfilled resin systems was significantly higher compared with UDMA control resin ($p<0.005$), with the exception of 80/20 (statistically similar: $p=0.511$) UDMA/TEGDMA unfilled resin system (Figure 3.12).

However, the bisGMA/UDMA/TEGDMA unfilled resin systems exhibited decreased FM compared with UDMA/TEGDMA unfilled resin systems (Figure 3.11). For the ter-monomer unfilled resin systems containing 60wt% UDMA, the highest FM was exhibited by the unfilled resin system containing equal amount of bisGMA and TEGDMA monomers ($p<0.005$) (Figure 3.13).

For analysis of correlation between the degree of conversion and flexural modulus values of unfilled resin systems refer to Appendix 6, Tables 6.1-6.28. There was a strong positive correlation between the degree of conversion and flexural modulus values of unfilled resin systems containing 60/40wt% UDMA/TEGDMA (r=0.788), 20/80wt% bisGMA/TEGDMA (r=0.999), 30/70wt% bisGMA/TEGDMA (r=0.995), 80/20wt% bisGMA/TEGDMA (r=0.619), 100wt% bisGMA (r=0.998), 20/6020wt% bisGMA/UDMA/TEGDMA (r=0.996), 30/50/20wt% bisGMA/UDMA/TEGDMA (r=0.632), 50/30/20wt% bisGMA/UDMA/TEGDMA (r=0.816) (Figure 3.14).

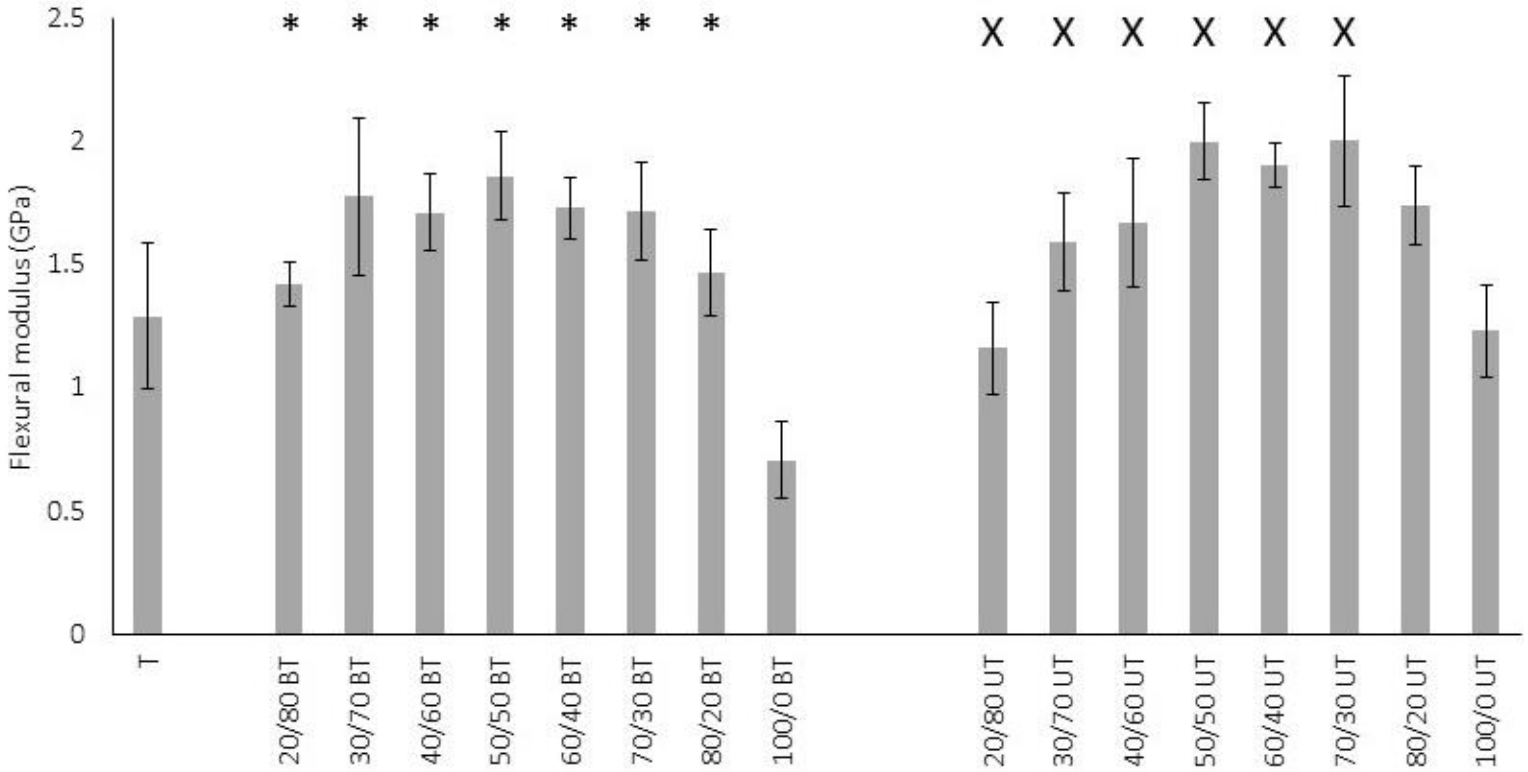

Figure 3.12 Flexural modulus of TEGDMA based unfilled resin systems containing increasing concentration of either bisGMA (BT) or UDMA (UT). Unfilled resin system percentage inclusions are shown within labels. Error bars indicate standard deviation of a mean average of 10 samples. * denotes statistical differences with unfilled resin systems containing 100wt% bisGMA; X denotes statistical differences with unfilled resin systems containing 100wt% UDMA. The bisGMA/TEGDMA unfilled resin systems exhibited similar values for flexural modulus compared with UDMA/TEGDMA unfilled resin systems.

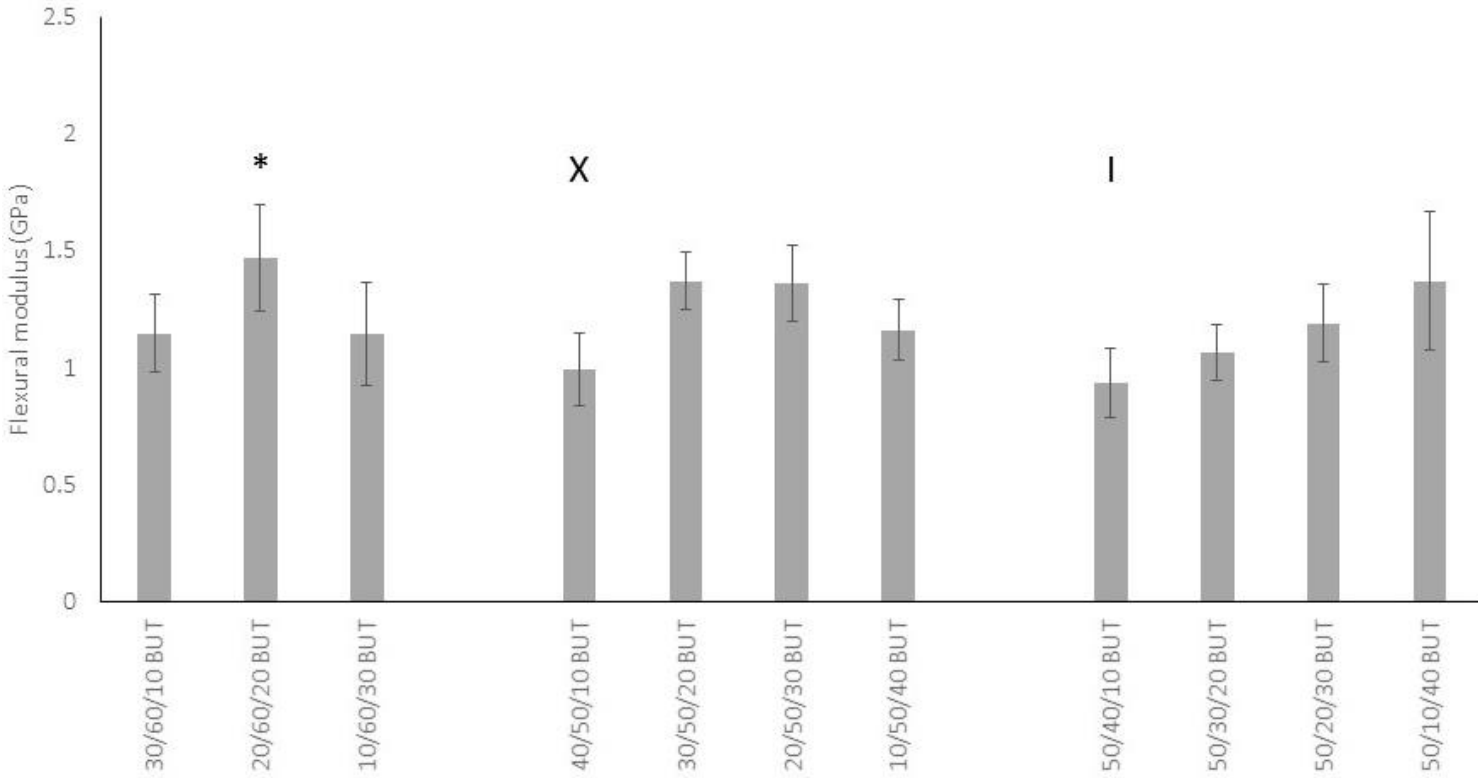

Figure 3.13 Flexural modulus of bisGMA/UDMA/TEGDMA unfilled resin systems (BUT). Unfilled resin system percentage inclusions are shown within bar labels. Error bars indicate standard deviation of a mean average of 10 samples. * denotes statistical differences with unfilled resin systems containing 10/60/30wt% bisGMA/UDMA/TEGDMA; X denotes statistical differences with unfilled resin systems containing 10/50/40wt% bisGMA/UDMATEGDMA and l denotes statistical differences with unfilled resin systems containing 50/10/40wt% bisGMA/UDMA/TEGDMA. The flexural modulus increased with increasing concentration of TEGDMA for the unfilled resin systems containing 50wt% bisGMA.

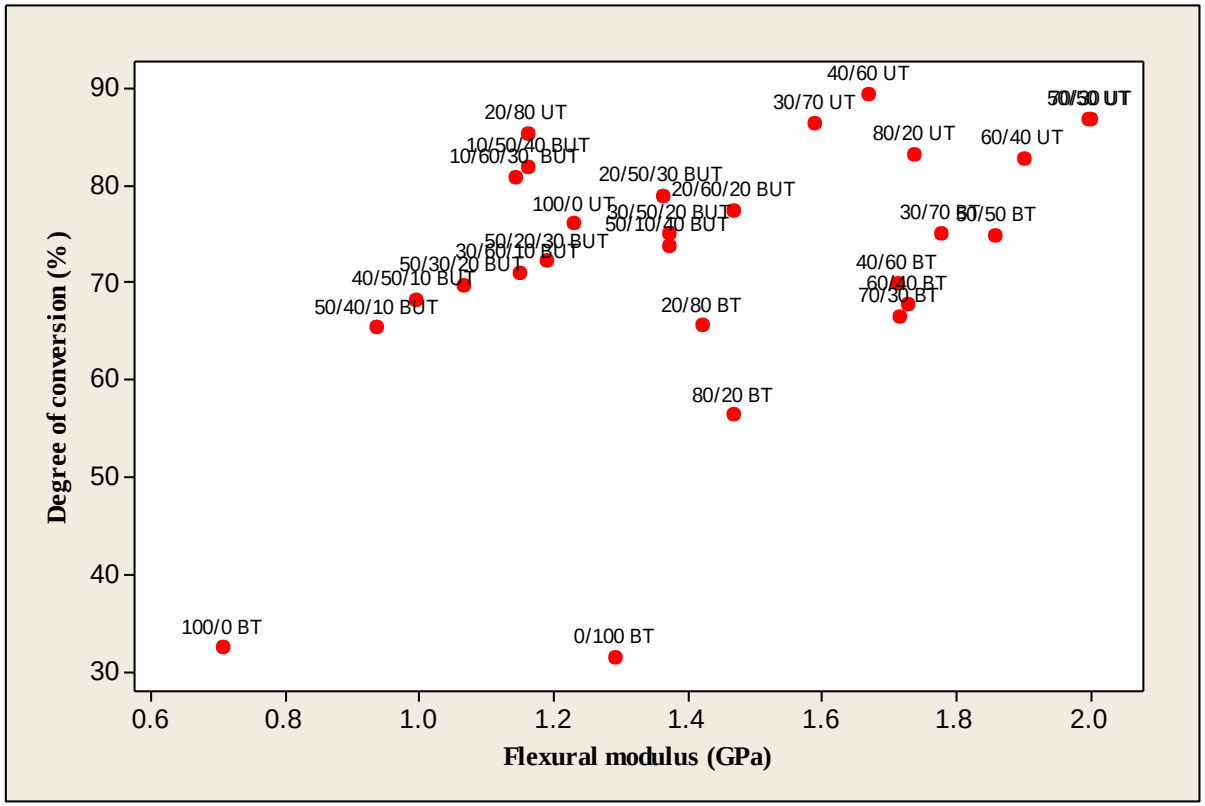

Figure 3.14 Pearson correlation between the degree of conversion and flexural modulus values of unfilled resin systems containing bisGMA/TEGDMA (BT), UDMA/TEGDMA (UT), or bisGMA/UDMA/TEGDMA (BUT). Unfilled resin system percentage inclusions are shown within labels. There was a strong positive correlation between the degree of conversion and flexural modulus values of unfilled resin systems containing 60/40 UDMA/TEGDMA (r=0.788).

3.4 Discussion

3.4.1 Physical properties of the unfilled resin systems

DC is dependent upon the structure and concentration of the monomers present, with monomers exhibiting increased flexibility in their molecular structure having higher degree of conversion values (Asmussen and Peutzfeldt 1998). Due to the formation of a highly cross-linked polymer network that limits the mobility of reacting radicals following polymerisation, the DC of unfilled photo-polymerisable dimethacrylate resin systems can never reach 100% without increased temperature and pressure and is normally in the range of 55-75% (Cornelio et al. 2013; Emami and Soderholm 2009; Ferracane et al. 1985). The conversion of such unfilled resin systems as those analysed in the current study (Tables 3.2, 3.3) might have been due to the chemical structure of the monomers (Figure 3.1) and the kinetics of the polymerisation reaction. Incomplete conversion of carbon double to single bonds shows that there is a significant amount of residual monomer (in the range of 20 to 50%) in the polymeric network following photo-curing (Cornelio et al. 2013; Lovell et al. 2003). The chemical structure and viscosity of the unfilled resin system mixtures significantly affected not only the DC, but also the RP of these unfilled resin systems.

The molecular structure of monomers also had an impact on the DC, with monomers that had decreased size such as UDMA and TEGDMA (Figure 3.1) exhibiting lower molecular weight and increased concentration of double bonds compared with bisGMA monomers (Moszner et al. 2008). bisGMA consists of a relatively stiff isopropylidene-diphenoxy central core and hydroxyl groups that caused steric hindrance and lack of chain mobility causing diffusion controlled kinetics directly following light irradiation (Floyd and Dickens 2006; Lovell et al. 1999). For this reason and due to the rigidity of bisGMA molecules, DC was limited prior to the maximum RP for unfilled resin systems containing 100wt% bisGMA, which occurred less

for unfilled resin systems containing 100wt% UDMA, the latter also exhibited the highest DC compared with resins containing 100wt% bisGMA or 100wt% TEGDMA (Figure 3.4, Table 3.2).

The higher DC of unfilled resin systems containing 100wt% UDMA compared with that of 100wt% TEGDMA (DC = 76 and 30%, respectively) (Figure 3.4) might be explained by the chain transfer reactions of the NH groups of the UDMA molecule (Equation 3.2):

Equation 3.2 $M_n + -NH- \rightarrow M_nH + -N-$; where M_n is a microradical, $-NH-$ can be part of either a monomer or polymer molecule and $-N-$ is the newly formed radical (Pfeifer et al. 2009; Sideridou et al. 2002).

The presence of NH groups in the UDMA molecule also led to increased viscosity of the UDMA/TEGDMA unfilled resin systems during polymerisation (Pfeifer et al. 2009; Sideridou et al. 2002).

The increased polymerisation reactivity of unfilled resin systems containing UDMA (Tables 3.2, 3.3) might have also been due to these chain transfer reactions (Sideridou et al. 2002). Moreover, increased concentration of UDMA (up to 70wt%) (Figure 3.4) resulted in higher DC due to the presence of aliphatic spacer groups, which led to stronger hydrogen bonding interactions between the imino group of UDMA and the carbonyl group of the co-monomer (Pfeifer et al. 2009). Nonetheless, due to the increased viscosity of samples containing more than 70wt% UDMA, the movement of free radicals to functional monomer groups might have been restricted leading to decreased DC (Figure 3.4), which concurs with previous research using UDMA/TEGDMA unfilled resin systems (Sideridou et al. 2002). This restriction in radical movement also resulted in lower polymerisation rate of methacrylate double bonds and finished prior to conversion of all carbon double bonds to single bonds because of vitrification

of the resin network (Table 3.2), which concurs with previous research (Palin et al. 2003). Recently, unfilled resin systems containing UDMA/TEGDMA were found to exhibit an increased degree of polymer conversion compared with bisGMA/TEGDMA unfilled resin systems (Moszner et al. 2008). Indeed, only a relatively small increase in UDMA resulted in a significant rise in RP and DC owing to its higher reactivity compared with bisGMA using similar diluent ratios including for unfilled resin systems containing bisGMA/UDMA/TEGDMA monomers (Figures 3.4, 3.5; Tables 3.2, 3.3). Moreover, stronger hydrogen bonding conferred by the UDMA molecule and increased concentration of double bonds given by the TEGDMA molecule of unfilled resin systems containing bisGMA/UDMA/TEGDMA in the organic matrix likely led to higher values for the DC of these unfilled resin systems compared with bisGMA/TEGDMA unfilled resin systems (Figure 3.5), which concurs with previous research (Sideridou et al. 2002). However, the addition of UDMA to unfilled resin systems containing TEGDMA/bisGMA did not increase the DC compared with UDMA/TEGDMA unfilled resin systems, which might be explained by the increased viscosity and lower flexibility conferred by the bisGMA molecule to this unfilled resin system (Figures 3.4, 3.5).

When TEGDMA was incorporated into unfilled resin systems containing bisGMA the viscosity of the system decreased, which led to increased movement of free radicals and an off-set of the diffusion controlled propagation during polymerisation (Lovell et al. 1999). This also led to increased DC with increasing concentration of TEGDMA for bisGMA/TEGDMA unfilled resin systems (Figure 3.4), which concurs with previous research (Asmussen and Peutzfeldt 2002). Moreover, bisGMA/TEGDMA unfilled resin systems that contained decreased amounts of TEGDMA exhibited decreased DC (Figure 3.4) due to a more rapid on-set of auto-acceleration, which severely hindered the mobility of free radicals (Tanimoto et al. 2005). These data further

demonstrated the negative impact of bisGMA on the DC of the final polymer even when used in combination with UDMA and TEGDMA (Figure 3.5). This low conversion might have been due to the high viscosity of the bisGMA molecule (Table 3.1) conferred by the π-π interactions of the aromatic rings in its chemical structure, resulting in decreased flexibility therefore low mobility of radicals during polymerisation reaction. The low DC of unfilled resin systems containing bisGMA (Figure 3.4) might also have been due to the low mobility of radicals, which might have led the resin mixture to reach the gelation stage at lower conversion of carbon double bonds during polymerisation (Gajewski et al. 2012).

3.4.2 Mechanical properties: Vickers hardness of the unfilled resin systems

DC refers to the amount of polymer formed during the polymerisation reaction, whereas hardness refers to the ability of a material to resist wear. Indirectly, the hardness test also assess the brittleness of a material, because the harder a material, the brittle it is. The hardness of unfilled resin systems provides information about longevity (shelf life) of such systems and is influenced by the chemical structure and weight ratio of the monomers present (Ekworapoj et al. 2002).

Both the bisGMA/TEGDMA and the UDMA/TEGDMA unfilled resin systems exhibited relatively constant DC, whereas hardness values increased up to 60/40wt% bisGMA/TEGDMA or UDMA/TEGDMA followed by a decrease. The decrease in hardness values of unfilled resin systems containing >60wt% bisGMA/TEGDMA or UDMA/TEGDMA might have been due to increased viscosity of the system, decreased mobility of the free radicals and lower cross-linking density of the polymer network (Lovell et al. 2001). For unfilled resin systems containing bisGMA/UDMA/TEGDMA, the DC increased with increasing concentration of TEGDMA, whereas the hardness values increased up to a maximum amount of TEGDMA of 30wt% for unfilled resin systems containing either 50wt% bisGMA or 50wt% UDMA and up

to 20wt% TEGDMA for unfilled resin systems containing 60wt% UDMA. The lowest concentration of carbon double bonds was exhibited by the Bis-GMA molecule possibly due to its relatively stiff bisphenol A core and two pendant hydroxyl groups, which formed strong hydrogen bonds. Thus, the bisGMA/TEGDMA unfilled resin systems exhibited the lowest hardness values (Figure 3.6).

The analysis of the hardness values of both the upper and lower surface of unfilled resin systems provided information about the extent of cure of such systems. There was a >1% decrease in the hardness values for the lower surface compared with the upper surface of unfilled resin systems (Figures 3.6, 3.7). The higher hardness values observed for the upper surface compared with the lower surface of bisGMA/TEGDMA, UDMA/TEGDMA or bisGMA/UDMA/TEGDMA unfilled resin systems (Figures 3.6, 3.7) might be explained by the optical characteristics (refractive index and light transmission through depth) of the final polymer network. The larger difference between upper and lower surfaces of bisGMA/UDMA/TEGDMA unfilled resin systems compared with bisGMA/TEGDMA, UDMA/TEGDMA unfilled resin systems may be due to a more pronounced decrease in light transmission and an increase in light scattering and opacity with increasing depth of the resin, possibly because of a significant increase in refractive index during the polymerisation reaction of such unfilled resin systems.

3.4.3 Mechanical properties: flexural strength and modulus of the unfilled resin systems

Mechanical properties of dimethacrylate unfilled resin systems were influenced by the DC and the formation of a three-dimensional network of the final polymer (Gajewski et al. 2012). While hardness tests provided information about “localised, non-uniform deformation”, flexure tests provided information about the fracture of the entire specimen when subjected to loading (Hosseinalipour et al. 2010).

The increased viscosity and rigidity of the bisGMA molecule might have been responsible for the decreased strength and modulus of unfilled resins systems containing 100wt% bisGMA compared with 100wt% UDMA, or 100wt% TEGDMA (Figures 3.9, 3.10, 3.12, 3.13), because of the restriction in radical movement during the polymerisation reaction and relatively stiff polymer network formation upon light irradiation (Barszczewska-Rybarek 2009; Gajewski et al. 2012). However, the addition of TEGDMA to unfilled resin systems containing bisGMA resulted in increased FS, which might have been due to increased flexibility conferred by the TEGDMA monomer to the free radicals during the polymerisation reaction (because of decreased viscosity and increased reactivity), while still retaining the formation of a stiff polymer network (Figure 3.9). The increased FS of unfilled resin systems containing bisGMA/TEGDMA compared with resins containing only bisGMA may also be a result of the increased degree of conversion of such resins; possibly because of increased concentration of carbon double bonds available for conversion with the introduction of the TEGDMA monomer to the unfilled resin system containing bisGMA. The increase in FS for unfilled resin systems containing bisGMA/TEGDMA occurred up to 70wt% TEGDMA, with unfilled resin systems containing 20/80wt% bisGMA/TEGDMA exhibiting lower FS, which might have been due to the ability of the TEGDMA molecule to cyclise (as a result of the presence of ether linkages in its molecular structure), leading to decreased cross-linkage and network formation (Figure 3.9). BisGMA/TEGDMA unfilled resin systems exhibited lower FS and FM values compared with unfilled resin systems containing UDMA/TEGDMA (Figures 3.9, 3.12), which might have been due to increased flexibility of the UDMA molecule and higher degree of crosslinking in the polymer network of these latter unfilled resin system formulations. The significant increase in FS and FM of unfilled resin systems containing up to 70:30wt% UDMA/TEGDMA was a result of increased cross-linked networks (Figures 3.9, 3.12), which is in agreement with

previous research (Berger et al. 2009). Moreover, when UDMA was added to unfilled resin systems containing bisGMA/TEGDMA, there was a marginal increase in FS, but not FM. This observation might be attributed to the decreased DC of carbon double bonds to single bonds due to bisGMA stiff backbone and high intermolecular interactions (Figures 3.10, 3.13), which is in agreement with previous research (Gajewski et al. 2012). However, compared with 100wt% bis-GMA and 100wt% UDMA, 100wt% TEGDMA exhibited the highest FS and FM (Figures 3.9, 3.12), probably due to increased reactivity because of the presence of ether groups and cross-linkage of the polymer network (Pfeifer et al. 2009).

The degree of conversion, rate of polymerisation, hardness, flexural strength and modulus of UDMA/TEGDMA unfilled resin systems were significantly higher compared with bisGMA/TEGDMA unfilled resin systems and bisGMA/UDMA/TEGDMA unfilled resin systems. Concentrations of 50/50, 60/40 and 70/30wt% UDMA/TEGDMA exhibited the most suitable values in terms of the properties studied (degree of conversion, rate of polymerisation, hardness, flexural strength and modulus). Further studies were performed on these UDMA/TEGDMA unfilled resin systems, with the 60/40wt% UDMA/TEGDMA concentration chosen for the incorporation of bioactive glass.

3.5 Conclusions

Physical and mechanical properties of unfilled resin systems containing bisGMA, UDMA, TEGDMA are influenced by the viscosity of the system as well as the chemical structure of the individual monomers, which has an impact on the mobility of the radicals during the polymerisation reaction. Unfilled resin systems containing UDMA/TEGDMA exhibited higher physical (DC and RP) and mechanical (hardness, FS and FM) compared with bisGMA/TEGDMA or bisGMA/UDMA/TEGDMA resins. These unfilled resin systems

containing UDMA/TEGDMA can further be optimised (Chapter 4) to develop new materials that exhibit similar or higher DC, RP, FS, FM compared with conventional resin systems.

3.6 Limitations of present work and recommendations for future studies

Only resins containing the amine-diketone photo-initiator system were tested. Future studies may involve the analysis of resin systems containing novel photo-initiator systems to increase the degree of conversion and mechanical properties (flexural strength) of such resins.

References

Asmussen, S., Arenas, G., Cook, W.D., Vallo, C. 2009. Photobleaching of camphorquinone during polymerization of dimethacrylate-based resins. *Dental Materials*, 25, (12) 1603-1611

Asmussen, E., Peutzfeldt, A. 1998. Influence of UEDMA, BisGMA and TEGDMA on selected mechanical properties of experimental resin composites. *Dental Materials*, 14, (1) 51-56

Asmussen, E., Peutzfeldt, A. 2002. Influence of composition on rate of polymerization contraction of light-curing resin composites. *Acta Odontologica Scandinavica*, 60, (3) 146-150

Barszczewska-Rybarek, I.M. 2009. Structure-property relationships in dimethacrylate networks based on Bis-GMA, UDMA and TEGDMA. *Dental Materials*, 25, (9) 1082-1089

Cornelio, R.B., Wikant, A., Mjosund, H., Kopperud, H.M., Hassu,, J., Gedde, W.U., Ortengren, U. 2013. The influence of bis-EMA and bis-GMA on the degree of conversion on water soprtion and solubility of dental composite materials. *Acta Odontologica Scandinavica,* 72, (6) 440-447

Ekworapoj, P., Magaraphan, R., Martin, D.C. 2002. Heat effect on viscosity and curing of light-cured dental resin and mechanical strength of conventional dental composites. *Journal of Metals, Materials and Methods,* 12, (1) 39-50

Emami, N., Soderholm, K. 2009. Young's Modulus and Degree of Conversion of Different Combination of Light-Cure Dental Resins. *The Open Dentistry Journal*, 3, (1) 202-207

Ferracanne, J.L., Matsumoto, H., Okabe, T. 1985. Time-dependent deformation of composite resins- compositional considerations. *Journal of Dental Research,* 64, (11) 1332-1336

Floyd, C.J.E., Dickens, S.H. 2006. Network structure of bis-GMA- and UDMA-based resin systems. *Dental Materials*, 22, (12) 1143-1149

Gajewski, V.E.S., Pfeifer, C.S., Froes-Salgado, N.R.G., Boaro, L.C.C., Braga, R.R. 2012. Monomers used in resin composites: degree of conversion, mechanical properties and water sorption/solubility. *Brazilian Dental Journal*, 23, (5) 508-514

Goncalves, F., Kawano, Y., Pfeifer, C., Stansbury, J.W., Braga, R.R. 2009. Influence of BisGMA, TEGDMA, and BisEMA contents on viscosity, conversion, and flexural strength of experimental resins and composites. *European Journal of Oral Sciences*, 117, (4) 442-446

Hosseinalipour, M., Javadpour, J., Rezaie, H., Dadras, T., and Hayati, A.N. 2010. Investigation of Mechanical Properties of Experimental Bis-GMA/TEGDMA Dental Composite Resins Containing Various Mass Fractions of Silica Nanoparticles. *Journal of Prosthodontics-Implant Esthetic and Reconstructive Dentistry*, 19, (2) 112-117

Ikemura, K., Endo, T. 2010. A review of the development of radical photopolymerization initiators used for designing light-curing dental adhesives and resin composites. *Dental Materials Journal*, 29, (5) 481-501

Kalachandra, S., Sankrapandian, M., Shobha, H.K., Taylor, D.F., McGrath, J.E. 1997. Influence of hydrogen bonding on properties of bis-GMA analogues. *Journal of Materials Science: Materials in Medicine,* 8, (5) 283-286

Lovell, L.G., Lu, H., Elliott, J.E., Stansbury, J.W., Bowman, C.N. 2001. The effect of cure rate on the mechanical properties of dental resins. *Dental Materials*, 17, (6) 504-511

Lovell, L.G., Newman, S.M., Donaldson, M.M., Bowman, C.N. 2003. The effect of light intensity on double bond conversion and flexural strength of a model, unfilled dental resin. *Dental Materials*, 19, (6) 458-465

Lovell, L.G., Stansbury, J.W., Syrpes, D.C., Bowman, C.N. 1999. Effects of composition and reactivity on the reaction kinetics of dimethacrylate dimethacrylate copolymerizations. *Macromolecules*, 32, (12) 3913-3921

Moszner, N., Fischer, U.K., Angermann, J., Rheinberyer, V. 2008. A partially aromatic urethane dimethacrylate as a new substitute for Bis-GMA in restorative composites. *Dental Materials*, 24, (5) 694-699

Palin, W.M., Fleming, G.J.P., Burke, F.J.T., Marquis, P.M., Randall, R.C. 2003. Monomer conversion versus flexure strength of a novel dental composite. *Journal of Dentistry*, 31, (5) 341-351

Pfeifer, C.S., Silva, L.R., Kawano, Y., Braga, R.R. 2009. Bis-GMA co-polymerizations: Influence on conversion, flexural properties, fracture toughness and susceptibility to ethanol degradation of experimental composites. *Dental Materials*, 25, (9) 1136-1141

Sideridou, I., Tserki, V., Papanastasiou, G. 2002. Effect of chemical structure on degree of conversion in light-cured dimethacrylate-based dental resins. *Biomaterials*, 23, (8) 1819-1829

Tanimoto, Y., Hayakawa, T., and Nemoto, K. 2005. Analysis of photopolymerization behavior of UDMA/TEGDMA resin mixture and its composite by differential scanning calorimetry. *Journal of Biomedical Materials Research Part B-Applied Biomaterials*, 72B, (2) 310-315

CHAPTER 4 DEVELOPMENT OF LOW AND HIGH VISCOSITY RESIN BASED COMPOSITES AND THEIR MECHANICAL AND PHYSICAL CHARACTERISTICS

4.1 Introduction

Orthopaedic applications involve the use of metallic implants to repair fractures and bone cements (such as calcium phosphates, acrylics and composites) to stabilise the metallic implants and fill gaps in the skeleton following trauma or as a result of congenital malformations (Stadelmann et al. 2010; Chang et al. 2010; Clarkin et al. 2009). These cements, however, need to be much improved to resemble the structure and functionality of bone tissue. By combining bioactive glass with unfilled resin systems, a bone cement may be developed, which exhibits direct bond to bone, reduced exothermicity during polymerisation and mechanical properties that closer match the adjacent bone compared with existing cements. A suitable unfilled resin system may consist of 60/40wt% UDMA/TEGDMA monomers and 1wt% photo-initiator system as it was determined in Chapter 3. The addition of filler particles to this system may lead to the development of a filled resin composite (FRC) material for orthopaedic applications. The size, type, morphology, chemical structure and amount of filler particles have a direct impact on the viscosity, physical and mechanical properties of the FRC material (Begum et al. 2006; Masouras et al. 2008; Shen et al. 2004; Tanimoto et al. 2005). For chemical bonding, through the formation of covalent bonds between the organic resin matrix and the inorganic filler particles, a silane coupling agent may be added (Figure 4.1), which was, also, shown to increase the mechanical properties of the FRCs (Lin et al. 2000; Shen et al, 2004). Mechanical strength and hardness increase with an increase in the amount of filler present in the FRCs (Hosseinalipour et al. 2010; Masouras et al. 2008).

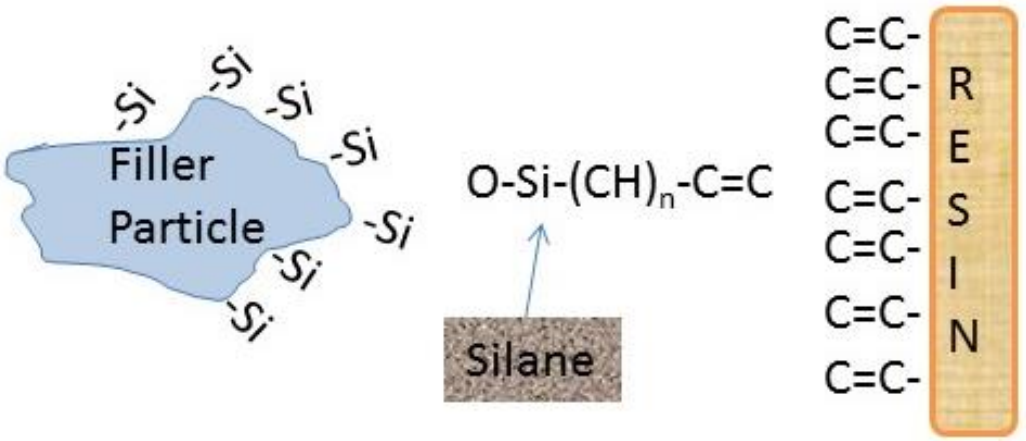

Figure 4.1 Illustration of the bonding between the silane coupling agent with the filler particles and the resin matrix in filled resin composite materials. The silane coupling agent may lead to better chemical bonding between the filler particles and the resin matrix (adapted from Ferracane, 1995).

Therefore, the aims of this chapter were to analyse different concentrations and sizes of bioactive glass and barium silicate filler added to 60/40wt% UDMA/TEGDMA and to determine the optimum FRC formulations in terms of degree of conversion (DC), flexural strength (FS) and modulus (FM) for orthopaedic applications. A low (46vol%) (suitable for injectable cements) and a high (60vol%) (suitable to be moulded in shape in situ) filler content in the final FRC was analysed in order to adapt the viscosity of the system to different orthopaedic applications.

4.2 Materials and methods

All substances were sourced from Sigma Aldrich, UK and used without modification unless otherwise stated.

For the synthesis of unfilled resin systems containing 60/40wt% UDMA/TEGDMA refer to Chapter 2, Section 2.1.

For the synthesis of bioactive glass refer to Chapter 2, Section 2.2.

For the synthesis of polymethylmethacrylate refer to Chapter 2, Section 2.4.

FRCs were synthesised containing the 60/40wt% UDMA/TEGDMA unfilled resin system, barium silicate glass and bioactive glass fillers. Barium silicate glass filler (G018-186) (Figure 4.1A) was purchased from Schott Glass (Landshut, Germany) and had the composition: $(Al_2O_3)_{10}(B_2O_3)_{10}(BaO)_{35}(SiO_2)_{45}(F)_{<2}$ with a Silane content of 6.0%. The average size of the particles was approximately 0.7μm. There were three types of bioactive glass fillers tested. There were two types of bioactive glass fillers (G018-144) purchased from Schott Glass (Landshut, Germany): silanated (silane content of 0.5%) (Type I) (Figure 4.1B) and non-silanated (Type II) (Figure 4.1C). The third bioactive glass filler (45S5) was synthesised in the laboratory and it was non-silanated (Type III) (Table 4.1).

The morphology of the commercially available bioactive glass filler particles and barium silicate filler was observed using scanning electron microscopy (SEM). Particles of each bioactive glass filler type (Type I or Type II) as well as particles of barium silicate filler were carefully placed on an aluminium specimen stub to avoid particle agglomeration (Berger et al. 2009; Lin et al, 2000; Tian et al. 2008). Each specimen was then examined using a scanning electron microscope (EVO MA10, ZEISS, Germany) operating in backscatter electron mode under high vacuum. For the commercially available bioactive glass fillers, the average particle

size was 10μm; whereas for the laboratory synthesised bioactive glass, the average particle size was of <50μm. The filament gun conditions were kept constant throughout the experiment through the control of the spot size and the operating current and maintaining the accelerating voltage at 5kV (Palin et al. 2005; Sideridou et al 2007). Representative micrographs of the particles for each condition were photographed at x1500 magnification (Figure 4.2).

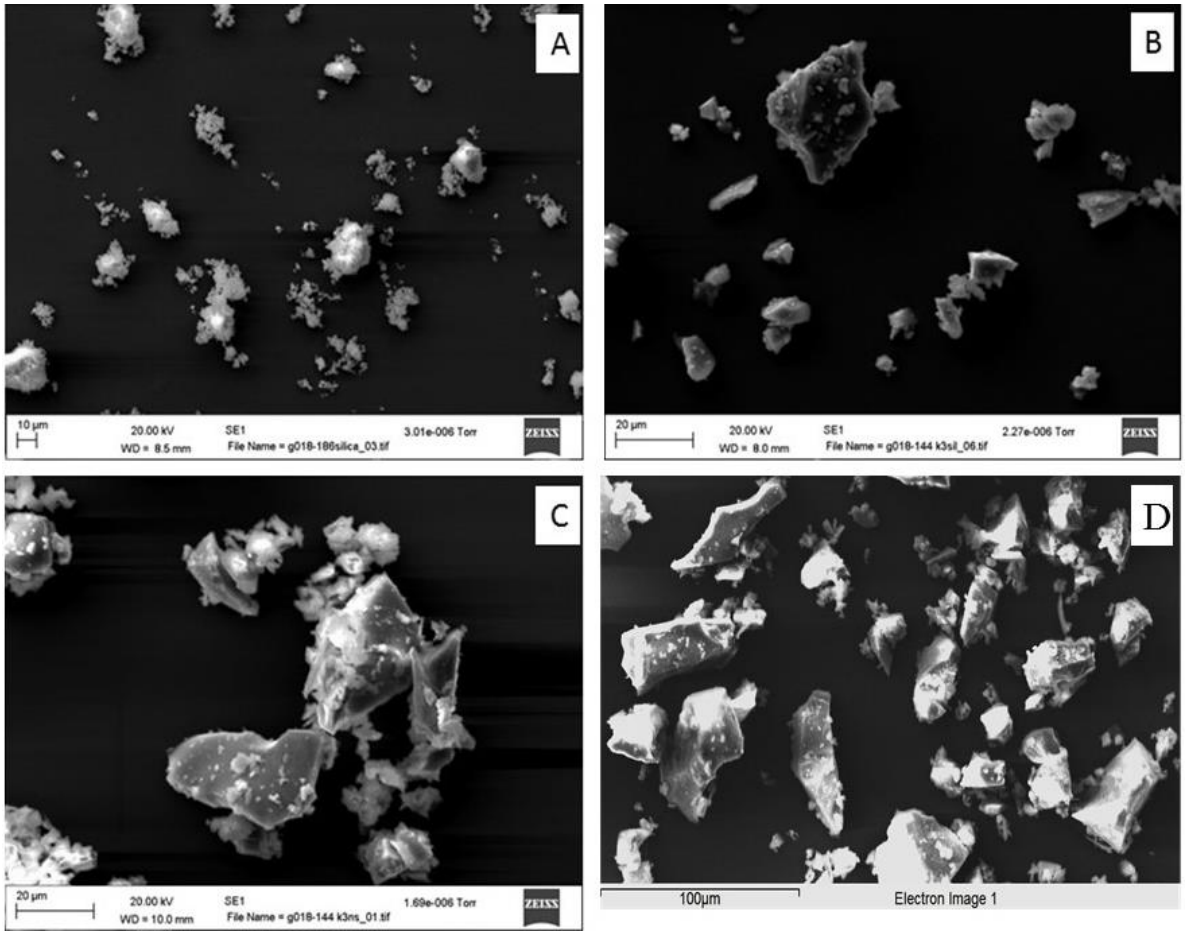

Figure 4.2 The morphology and silanisation of commercially available fillers and the filler synthesised in the laboratory. Barium silicate glass filler (A) had a silane content of 6% and had a particle size of 0.7µm.The were two types of bioactive glass fillers with an average particle size of 10µm: silanated (silane content of 0.5%) (B) and non-silanted (C). The filler synthesised in the laboratory (D) had an average particle size of <50 µm and was non-silanated.

Filled resin composite	Low filler content				High filler content			
wt%	10	20	30	40	11	23	34	45
Type I	SIL10	SIL20	SIL30	SIL40	SIL11	SIL23	SIL34	SIL45
Type II	NS10	NS20	NS30	NS40	NS11	NS23	NS34	NS45
Type III	AB10	AB20	AB30	AB40	AB11	AB23	AB34	AB45

Table 4.1 Filled resin composite compositions in wt% for both low filler (46vol% filler) and high filler (60vol% filler) content. Type I, Type II and Type III refer to the types of bioactive glass used in this study.

FRCs were synthesised to have either a low viscosity or a high viscosity filler content and consisted of 60/40wt% UDMA/TEGDMA; 10, 20, 30 or 40wt% (low filler), 11, 23, 34, 45 (high filler) bioactive glass (Type I, Type II or Type III) and barium silicate glass to a ratio of resin to filler in the final FRC of 30:70wt% (low filler) or 20:80wt% (high filler) (Table 4.2). FRCs containing 70wt% (low filler) or 80wt% (high filler) barium silicate glass filler only were used as positive control, whereas FRCs containing 70w% (low filler) or 80wt% (high filler) Type I, II or III bioactive glass fillers were used as negative controls. All the substances were measured using a balance accurate to 0.0001mg (TS400D, Ohaus, USA). The bioactive glass and barium silicate filler particles were placed in a container and gently mixed with a spatula. The unfilled resin system formulation containing 60/40wt% UDMA/TEGDMA was then added to this bioactive glass, barium silicate mixture. This formulation was then mixed in a Speed Mixer (DAC 150 FV2-K, Hauschild Engineering, Germany) for 90s at low speed (1000rpm) and 180s at high speed (3000rpm). The mixed formulations were, subsequently, stored in a lightproof container at 4°C to avoid premature photo-curing prior to further testing.

As the weight percentage calculations do not take into consideration the density of a particular substance, the wt% were transformed to volume percentage for increased accuracy, with the results shown in Table 4.2. Thus, the total filler volume used was approximately 47vol% for low content filler and 60vol% for high filler content formulations.

	Low viscosity						High viscosity						
60/40 UT	wt%	0	10	20	30	40	70	0	11.37	22.72	34.05	45.29	79.51	Bioglass
	vol%	0	7.27	14.44	21.51	28.48	48.79	0	9.36	18.33	27.27	35.82	60	
	wt%	70	60	50	40	30	0	80.31	68.65	56.97	45.40	34.02	0	Barium
	vol%	46.17	39.28	32.50	25.81	19.22	0	60	50.27	41.27	32.52	24.02	0	Silicate

Table 4.2 Filled resin composite formulations based on low and high filler content. Different concentrations of Bioglass (Type I, Type II or Type III bioactive glass) and Barium Silicate (barium silicate filler) were added to 60/40UT (60/40wt% UDMA/TEGDMA unfilled resin system mixture) in 30:70wt% (low filler) or 20:80wt% (high filler) unfilled resin system to filler ratio.

For testing of the degree of conversion of filled resin composites refer to Chapter 2, Section 2.6.1.

For the preparation and light curing of FRCs for mechanical (three point bend) testing refer to Chapter 2, section 2.5.

4.2.1 Statistical analysis

Minitab statistical software (Minitab, UK) was used to analyse the data using one-way analysis of variance (ANOVA) test. A difference of $P<0.05$ was considered statistically significant. Anderson-Darling test was used to determine whether the data followed a normal distribution. Tukey's post hoc tests were used for pair-wise comparison using a significance value of $P=0.05$.

4.3 Results

4.3.1 Physical properties: degree of conversion of filled resin systems

Type I and Type II FRCs containing 20, or 30wt% bioactive glass and Type III FRCs containing 20wt% bioactive glass exhibited the highest DC (Figure 4.3). Type I, Type II and Type III FRCs containing low filler content exhibited similar DC up to 30wt% bioactive glass filler content (Figure 4.3). Type I FRCs containing high filler content exhibited a decrease in DC with increased filler content ($p<0.001$). Type II and Type III FRCs containing high filler content exhibited an increase in DC with increased filler content up to 34wt% bioactive glass filler content (Figure 4.3); which was statistically significant for Type III FRCs (high filler content) ($p=0.001$), but not Type III FRCs ($p>0.398$, low filler content) and Type II FRCs both low and high filler content ($p>0.100$). The DC of FRCs containing bioactive glass and barium silicate filler was lower compared with the DC of PMMA cement, which exhibited a DC of 89.7 +/- 1.5 %. For analysis of significant differences between the degree of conversion values of filled resin composites refer to Appendix 2, Tables 2.1-2.9.

Due to the low DC of FRCs containing 45wt% Type III bioactive glass and 34wt% barium silicate filler (high filler) (not measurable), there was no analysis performed on filled resin composites containing 80wt% Type III bioactive glass (high filler). Due to the low DC (<30%) of FRCs containing 80wt% Type I or Type II bioactive glass filler (low and high filler content), there was no further analysis performed on these FRCs (Figure 4.3).

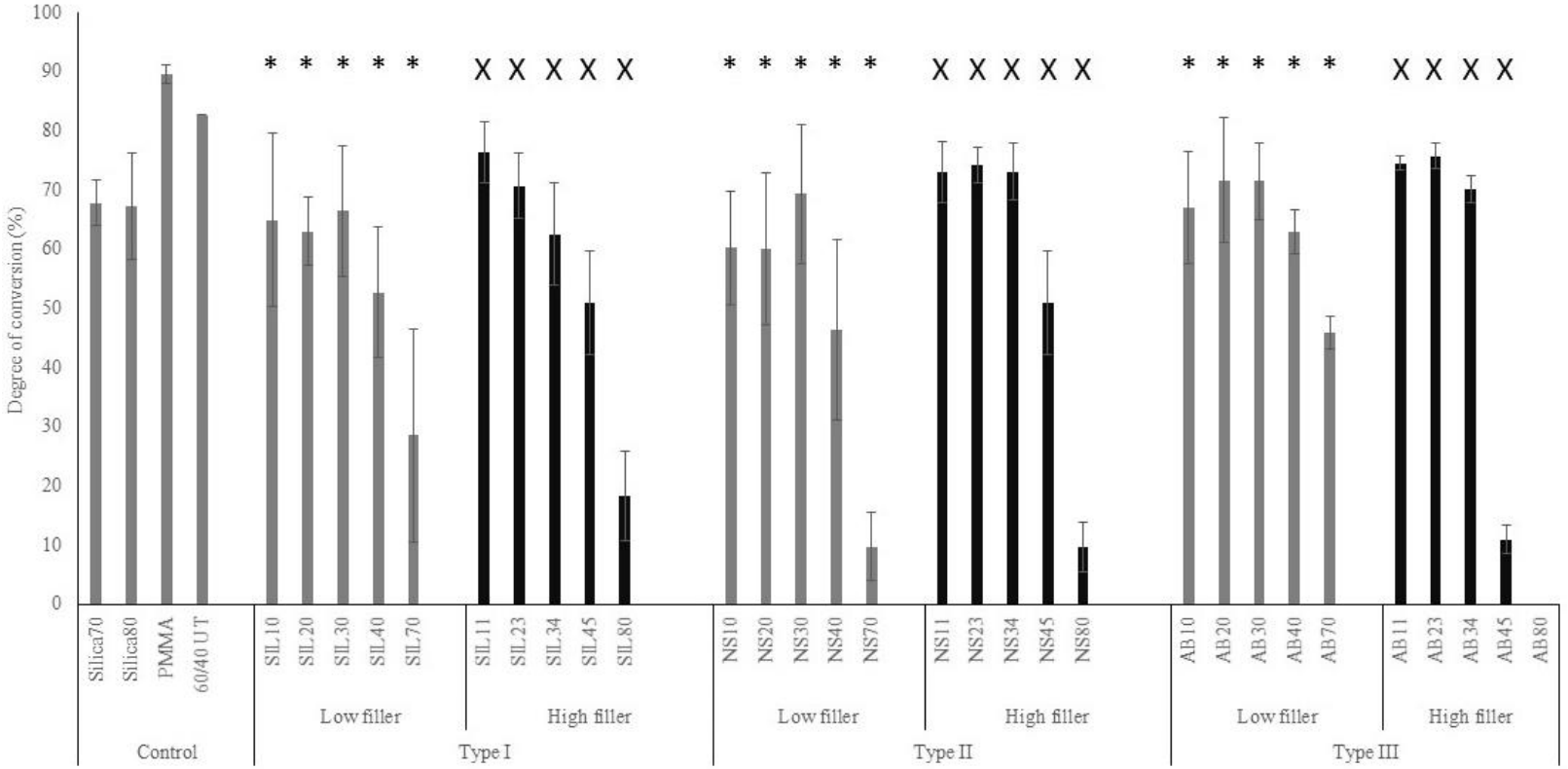

Figure 4.3 Degree of conversion of filled resin composites containing Type I, Type II or Type III bioactive glass (low and high filler content). Filled resin composite percentage inclusions are shown within bar labels. * denotes statistical differences with filled resin composites containing 70wt% barium silicate filler; X denotes statistical differences with filled resin composites containing 80wt% barium silicate filler. Type II and Type III filled resin composites containing high filler content exhibited an increase in DC with increased filler content up to 34wt% bioactive glass filler content. Error bars indicate standard deviation over mean average of 5 samples.

4.3.2 Mechanical properties: three point flexural strength and modulus analysis

Flexural strength of FRCs and PMMA

For filled resin composites containing 20, 30, or 40wt% bioactive glass (low filler) and 11wt% bioactive glass (high filler), the FS increased in the order: Type II < Type I < Type III. For filled resin composites containing 10wt% bioactive glass (low filler) and 23, 34, or 45wt% bioactive glass (high filler), the flexural strength increased in the order: Type I < Type II < Type III. The filled resin composites containing 20, 30, or 40wt% bioactive glass exhibited significantly higher flexural strength for low filler content compared with filled resin composites containing 23, 34, or 45wt% bioactive glass high filler content (Figure 4.4). For both low and high filler content, FRCs containing 20 or 23wt% bioactive glass filler exhibited higher flexural strength compared with FRCs containing 40 or 45wt%, respectively, bioactive glass filler, regardless of the type of filler (Type I, Type II or Type III) ($p<0.001$). For analysis of significant differences between the flexural strength values of filled resin composites refer to Appendix 2, Tables 2.10-2.18.

PMMA cement exhibited an FS value of 52.46±10.26MPa. The FS of filled resin composites containing 70wt% barium silicate filler was 84.3±14.3MPa (low filler) and 72.4±24.3MPa (high filler).

For analysis of correlation between the degree of conversion and flexural strength values of filled resin composites refer to Appendix 6, Tables 6.29-6.54. There was a strong positive correlation between the degree of conversion and flexural strength values of Type III filled resin composites containing 20wt% bioactive glass filler ($r=0.951$), Type III filled resin composites containing 11wt% bioactive glass filler ($r=0.610$) (Figure 4.5).

Flexural modulus of FRCs and PMMA

The lowest FM was exhibited by filled resin composites containing 40 or 45wt% bioactive glass (low and high filler content), which was significantly lower compared with the filled resin composites containing 10, 20, 30wt% (low filler content) or 11, 23, 34 (high filler content) bioactive glass ($p<0.001$) (Figure 4.6). PMMA cement exhibited a flexural modulus of 1.80±0.3MPa. Filled resin composites containing 70 or 80wt% barium silicate filler exhibited a FM value of 7.0±1.0GPa (low filler) and 7.0±1.7GPa (high filler).

The filled resin composites containing 60/40wt% UDMA/TEGDMA, 20 or 23wt% bioactive glass and 50 or 57wt% barium silicate glass exhibited the optimum DC and FS of all the filled resin composites tested (Figures 4.3, 4.4). Moreover, 40 or 45wt% bioactive glass was the highest amount that could be added to 60/40wt% UDMA/TEGDMA resins containing 30 or 34wt% barium silicate filler (low and high filler content), that resulted in a degree of conversion of >45% of the final filled resin composite (Figures 4.3, 4.4). These filled resin composites containing 40 or 45wt% bioactive glass (low and high filler) were tested for use in applications where the focus is on providing a scaffold containing bioactive glass, which promotes tissue regeneration and repair, as it may be the case for cranio-facial reconstruction surgeries. Filled resin composites containing 40 or 45wt% (low and high filler content) bioactive glass were also tested to determine whether such composites provide increased viability and proliferation of bone marrow stromal stem cells compared with filled resin composites containing 20 or 23wt% bioactive glass (low and high filler content). FRCs containing 20 or 23wt% bioactive glass filler exhibited higher flexural modulus compared with FRCs containing 40 or 45wt% bioactive glass filler, regardless of the type (Type I, Type II or Type III) or amount (low or high) of filler

($p<0.001$). For analysis of significant differences between the flexural strength values of filled resin composites refer to Appendix 2, Tables 2.19-2.27.

For analysis of correlation between the degree of conversion and flexural modulus values of filled resin composites refer to Appendix 6, Tables 6.29-6.54. There was a strong negative correlation between the degree of conversion and flexural modulus of Type II filled resin composites containing 34wt% bioactive glass filler ($r=-0.666$) and Type II filled resin composites containing 45wt% bioactive glass filler ($r=-0.663$) (Figure 4.7).

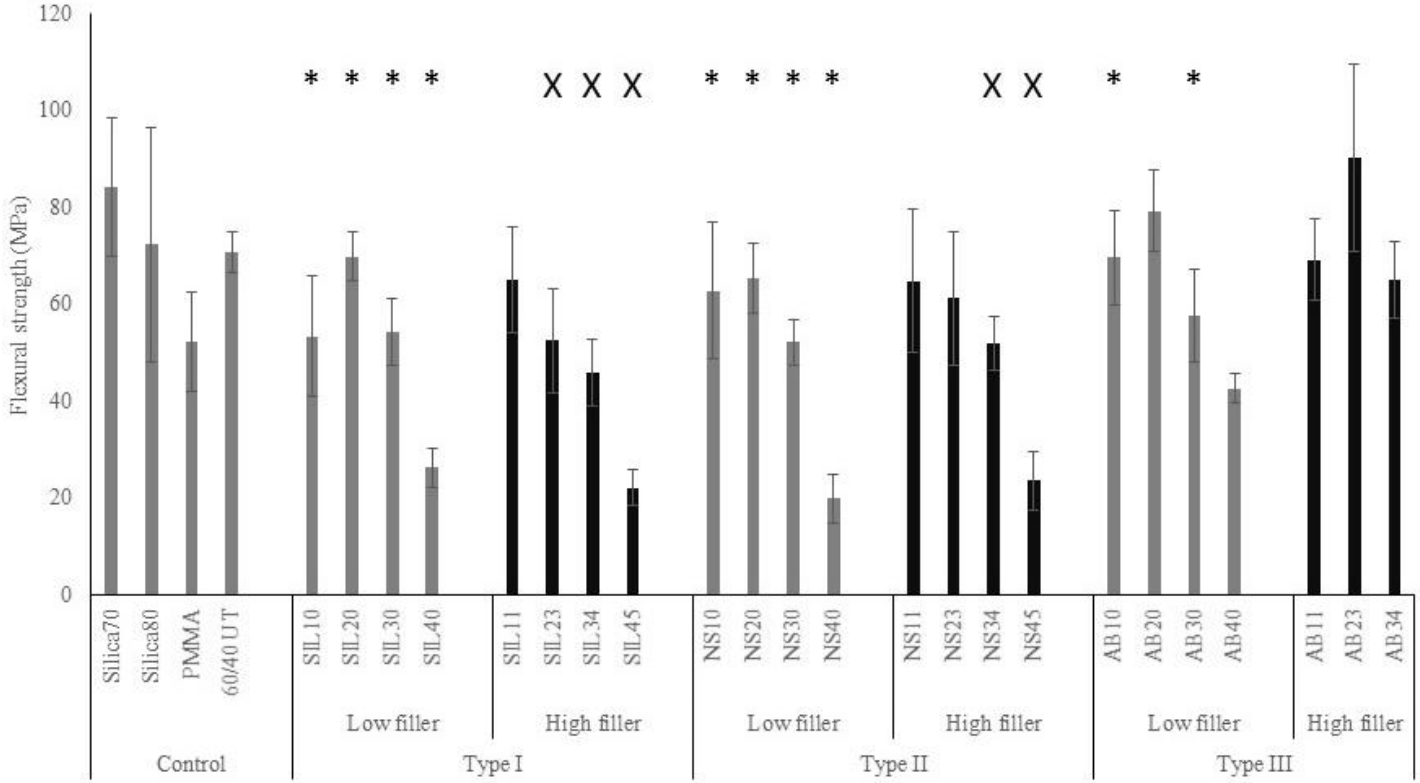

Figure 4.4 Flexural strength of filled resin composites containing low (LF) and high (HF) filler content. * denotes statistical differences with filled resin composites containing 70wt% barium silicate filler; X denotes statistical differences with filled resin composites containing 80wt% barium silicate filler. Filled resin composites containing 20wt% Type I or Type II bioactive glass exhibited higher flexural strength for low filler compared with high filler content (23wt%). Filled resin composites containing Type III bioactive glass filler exhibited the highest flexural strength of all FRCs studied. Error bars indicate standard deviation over mean average of 10 samples.

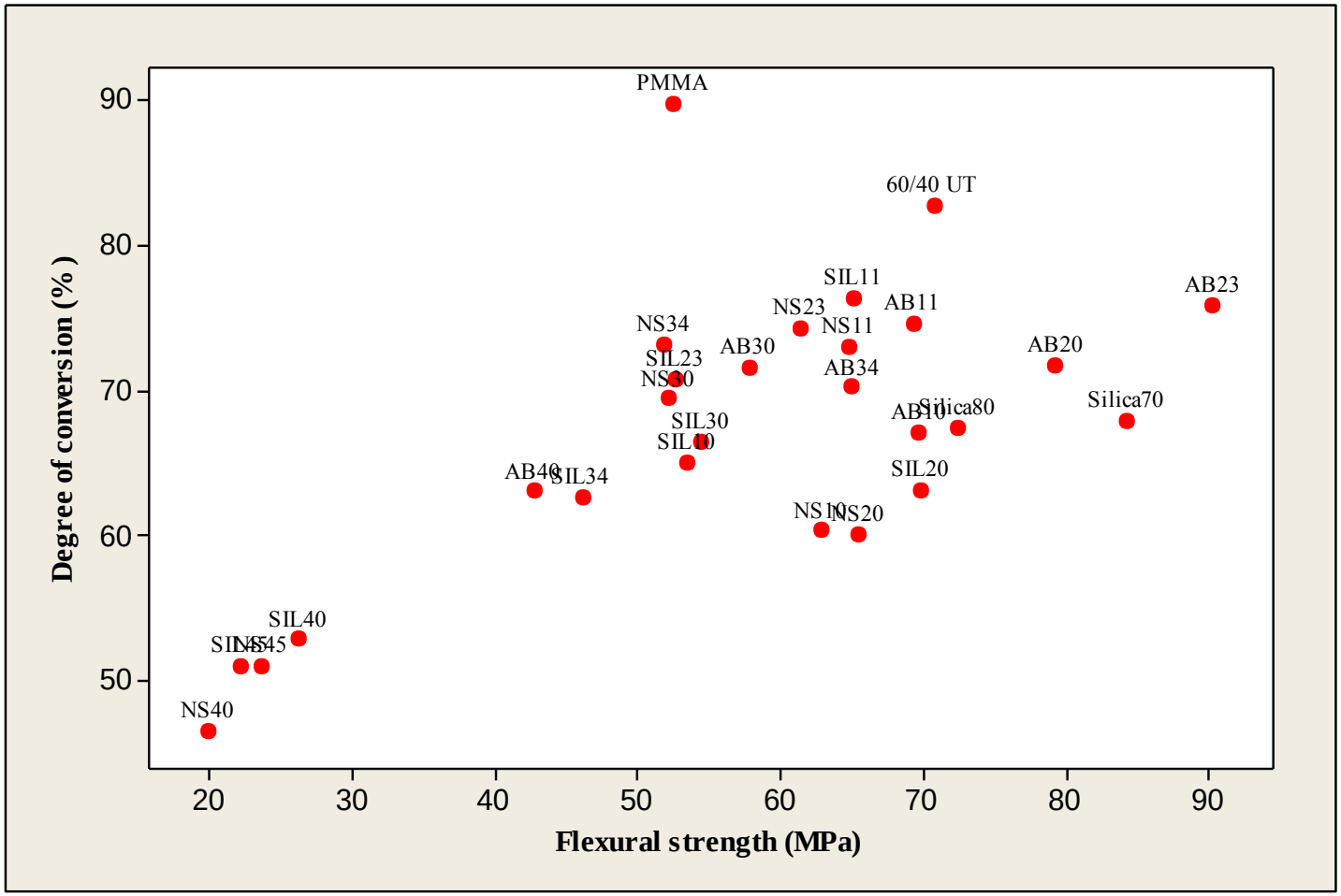

Figure 4.5 Correlation between the degree of conversion and flexural strength of filled resin composites containing Type I filler (SIL), Type II filler (NS) and Type III filler (AB). Filled resin composite percentage inclusions are shown within labels. There was a strong positive correlation between the degree of conversion and flexural strength of filled resin composites containing 20wt% Type III bioactive glass filler (r=0.951).

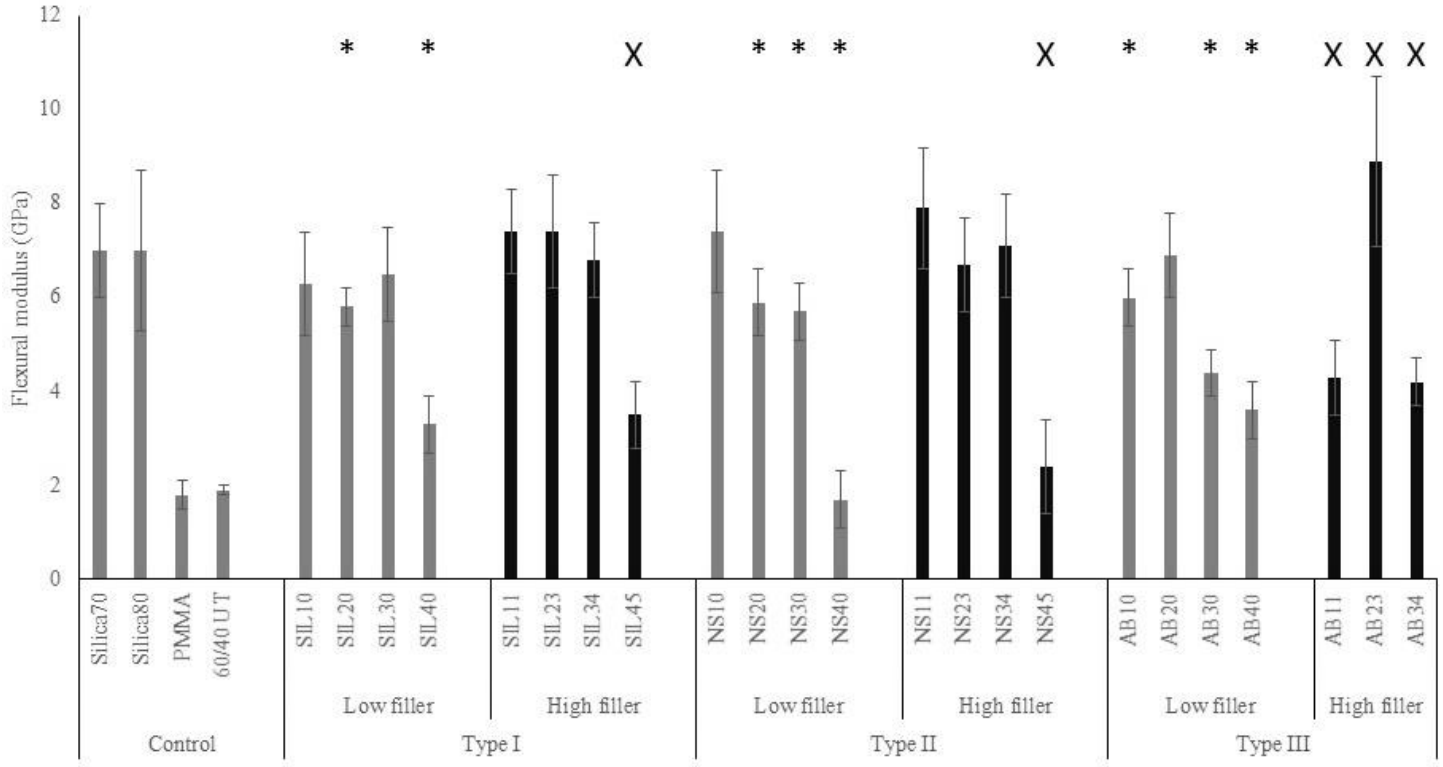

Figure 4.6 Flexural modulus of filled resin composites containing low (LF) and high (HF) filler content. * denotes statistical differences with filled resin composites containing 70wt% barium silicate filler; X denotes statistical differences with filled resin composites containing 80wt% barium silicate filler. Filled resin composites containing 23wt% Type I, Type II or Type III bioactive glass exhibited higher FM for high filler compared with low filler content (20wt%). Error bars indicate standard deviation over mean average of 10 samples.

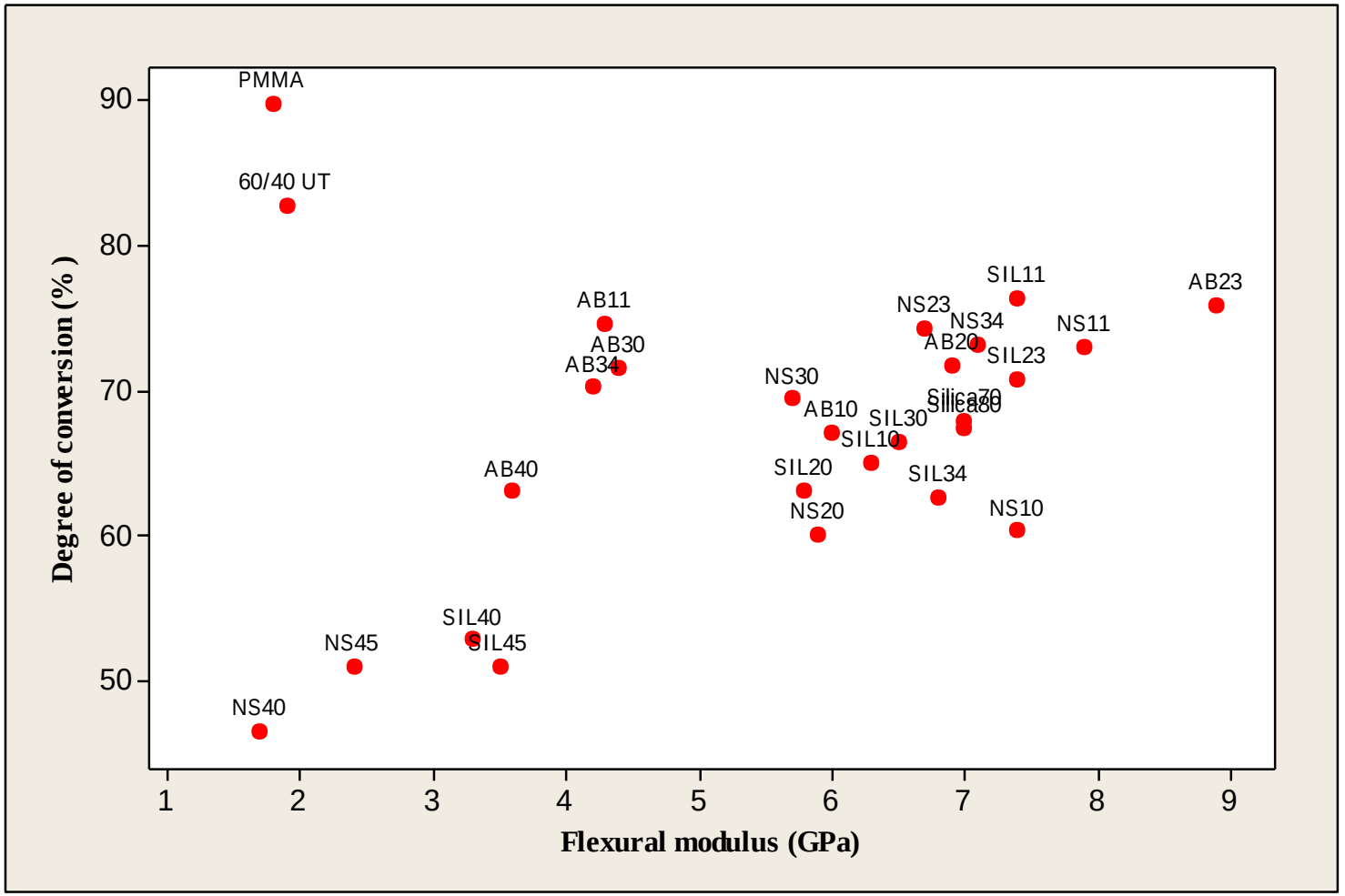

Figure 4.7 Correlation between the degree of conversion and flexural modulus of filled resin composites containing Type I filler (SIL), Type II filler (NS) and Type III filler (AB). Filled resin composite percentage inclusions are shown within labels. There was a strong negative correlation between the degree of conversion and flexural modulus of filled resin composites containing 45wt% Type II bioactive glass filler (r=-0.663).

4.4 Discussion

The physical and mechanical characteristics of a cement based on filled resin composites containing bioactive glass are influenced by the chemical structure of the monomers and the filler particles (Figure 4.2) present in the final polymer (Pfeifer et al. 2009). Dimethacrylate resins and silica fillers are usually employed in dental applications as tooth filling materials. For a dental material based on dimethacrylate resins and silica fillers to be considered as a viable option in orthopaedic applications it must not only exhibit mechanical properties similar to adjacent bone but also a high degree of conversion of the monomer to polymer; which for dental materials was deemed to be between 55-75% (higher conversion also leads to decreased amount of leachable monomer) (Ekworapoj et al. 2002).

Bioactive glass filler and barium silicate filler were added to the suitable formulation of base monomers determined to be 60/40wt% UDMA/TEGDMA (Chapter 3). Barium silicate is an inert filler usually added to reinforce the organic resin matrix, increase viscosity and make the material more manageable for the dentist. For the development of the orthopaedic cement, this inert filler was combined with two commercially available types of bioactive glass fillers or with 45S5 bioactive glass filler, which was synthesised in the laboratory (Figure 4.2). These bioactive glass fillers are known to increase viability of mesenchymal stem cells as well as their differentiation to bone cells (Rahaman et al. 2011).

There were two types of filled resin composite cements formulated depending on viscosity, referred to as low and high viscosity cements (with low or high filler content), each developed for particular orthopaedic applications. The low viscosity filled resin composite (with a low filler content) was formulated for ex situ preparation and for injectable cements, where the cement can be placed in premade moulds (for example for auditory and cranio-facial repair surgeries) to harden and then placed at the required site in the body. This will lead to a reduction

in the time and cost of the surgery due to the use of cost effective materials that can be made into the required shape before surgery. The high viscosity cement (with high filler content), on the other hand, was developed to be used and moulded in shape in situ. This cement can be employed for hand and wrist reconstruction where the command set of curing allows the surgeon the time to place the material in the desired shape and location.

4.4.1 Physical properties of the filled resin systems

The degree of conversion of filled resin composites containing dimethacrylate unfilled resin systems and fillers was reported to be between 55 and 75% (Chung and Greener, 1990; Ferracane et al. 1998; Ruyter and Oysaed, 1987; Stansbury and Dickens, 2001). In this study, for FRCs containing bioactive glass (up to 30wt%) and barium silicate filler, the lowest DC was 60.1% exhibited by the FRC containing 20wt% bioactive glass (low filler, Type II), whereas the highest DC was exhibited by the FRC containing 11wt% bioactive glass (high filler, Type I composites) (76.4%) (Figure 4.3), both values in the range of those reported for DC in literature. The higher DC in the current investigation compared with previous studies (Chung and Greener, 1990; Ferracane et al. 1998; Ruyter and Oysaed, 1987; Stansbury and Dickens, 2001) might have also been due to the use of UDMA instead of bisGMA as the base monomer. The UDMA molecule is less viscous and more flexible than the bisGMA molecule, due to the absence of aromatic rings and presence of urethane groups in the UDMA molecule, which might have led to stronger hydrogen bonding interactions between the imino group of the UDMA molecule and the carbonyl group of the co-monomer, thus higher concentration of carbon double bonds and increased mobility of free radicals in the polymerising network (Pfeifer et al. 2009).

The degree of conversion of filled resin composites containing bioactive glass and barium silicate filler was influenced by the size and amount of the filler particles, with the composition

of the resin matrix and light curing kept constant. The incorporation of filler particles in the unfilled resin system matrix results in increased viscosity of the final filled resin composite, which was influenced by the morphology, size and amount of the filler, possibly leading to decreased degree of conversion, with increasing amount of filler particles present in the polymer network.

Thus, the maximum amount of filler that could be added to the FRCs without a detrimental effect on the degree of conversion was 30wt% for low filler, Type I, 23wt% for high filler, Type I, 30 or 34wt% for low and high filler, Type II and 30 or 34wt% for low and high filler, Type III composites (Figure 4.3). The increase in filler content might, nonetheless, have led to increased insulating properties of the final FRCs, which might have resulted in a slight increase in degree of conversion (Figure 4.3), with the slight increase in temperature during the polymerisation reaction. Therefore, increased amount of bioactive glass filler could be added to the unfilled resin system matrix (up to 30 or 34wt%, low and high filler content), with the final FRC still exhibiting an increase in the degree of conversion (Figure 4.3). This might have been due to the higher flexibility and decreased viscosity of such FRCs compared with FRCs containing >30 or 34wt% (low and high filler content) bioactive glass at the beginning of the polymerisation reaction, resulting in increased conversion to a gel phase before the propagation step of the reaction, therefore increased degree of conversion (Nicolae et al. 2014).

The degree of conversion of the FRCs was also affected by the difference in refractive index between the unfilled resin system matrix and the filler particles. The filled resin composites containing Type III bioactive glass filler exhibited increased degree of conversion compared with all the FRCs studied (Figure 4.3), which might have been due to a similar refractive index between the unfilled resin system matrix and the filler particles of these FRCs, possibly because of decreased bioactive glass filler –resin matrix interfacial light scattering (Stansbury, 2000).

During the polymerisation reaction, the filler particles in the FRCs interacted with the light, leading to decreased degree of conversion with high filler content (>30 or 34wt%, low and high filler content), because of high scattering, light absorption and increased opacity (LePrince et al. 2011; Stansbury, 2000). The size of filler particles also had an impact on the DC of FRCs, possibly due to the direct impact such fillers had on the scattering of light during the polymerisation reaction of such filled resin composites (Turssi et al. 2005). Thus Type III FRCs exhibited overall higher degree of conversion compared with Type I and Type II composites (Figure 4.3), which was in agreement with previous research (Turssi et al. 2005). The low DC of FRCs containing high amount of filler particles (>30 or 34wt%. low and high filler content) might have also been due to increased viscosity during the polymerisation reaction, which negatively affected the mobility of the radicals, regardless of whether the filler particles were silanised (Du and Zheng, 2008, Nicolae et al. 2014).

The increased degree of conversion of PMMA compared with filled resin composites might be explained by its increased temperature and reactivity during the polymerisation reaction, with increased carbon double bonds converted to carbon single bonds (Ha et al. 2011). The increased degree of conversion of PMMA compared with both filled resin composites and unfilled 60/40wt% UDMA/TEGDMA unfilled resin systems might also be due to the curing time of the PMMA (600sec) compared with the unfilled resin systems and filled resin composites (40sec).

4.4.2 Mechanical properties: flexural strength and modulus of the filled resin systems

The composition and chemical structure of the unfilled resin system matrix had a direct impact on the amount of released monomer, mechanical characteristics and ability to absorb liquids of the final filled resin composite (Deb et al. 2005). Moreover, by adding fillers to the resin matrix of unfilled resin systems, the mechanical properties might be improved, depending on the type, shape, concentration and size of the filler particles (Curtis et al. 2009; Masouras et al. 2008;

Hosseinalipour et al. 20110). Silica was also added to the FRCs containing bioactive glass as a reinforcement filler to preserve proper mechanical strength for orthopaedic applications (Vakiparta et al. 2005). By applying a load to the filled resin composite specimen, an area of stress formed at the interface betweeen the unfiled resin system matrix and the filler, which ultimately resulted in the failure of the specimen, when a certain load was exceded (Du and Zheng, 2007). The failure of these specimens was also affected by the viscosity of the FRC formulation. The point where the filled resin composite specimen failed under such a constant load determined the flexural strength of the FRC material (Kim and Han, 2004). The flexural modulus of a filled resin composite depended on the amount of filler particles to resin matrix (Du and Zheng, 2007; Kim and Han 2004). Moreover, the flexural strength and modulus of FRCs were also directly influenced by the formation of a chemical bond between the organic matrix and the filler particles. Effective coupling should have enabled successful transfer of stress between the unfilled resin system matrix and the filler particles, when the filled resin composites were subjected to loading (Masouras et al. 2008). Thus, filled resin composites which had silanised filler particles in their compositions (Type I in the current study), should have exhibited a strong chemical bond between the organic and inorganic components and thus increased mechanical strength (Shirai et al. 2000). This was, however, not observed with high filler content FRCs formulations containing silanised (Type I), which exhibited lower flexural strength compared with high filler content FRCs containing non-silanised (Type II) bioactive glass fillers (Figure 4.4), which might have been due to the small amount of silane content in the Type I fillers (0.5%). The lower flexural strength of such FRCs (Figure 4.4) might also be explained by the significantly increased viscosity of the Type I FRCs formulations compared with Type II FRC formulations, which hindered the mobility of free radicals during polymerisation. However, FRCs containing silanised filler particles (Type I in this study)

exhibited a small increase in flexural strength compared with FRCs containing non-silanised filler particles (Type II and Type III) (Figure 4.4), which might have been due to the stronger chemical connection between the unfilled resin system matrix and the filler achieved through the coupling agent. Moreover, the silanised filler particles present in Type I FRCs, through the presence of a silanating agent might have led to the formation of a flexible, mechanically strong polymer network, because of the optimum stress transfer from the unfilled resin system matrix to the bioactive glass filler; whereas the absence of such a coupling agent as was the case of Type II FRCs might have led to the formation of a rigid, brittle polymer network, leading to the development of a high stress area between the resin matrix and filler particles, thus lower flexural strength (Figure 4.4), which concurs with previous research (Du and Zheng, 2007).

When the effect of filler size on the flexural strength of FRCs was analysed, it was observed that FRCs containing larger sized particles (Type III) exhibited increased flexural strength compared with FRCs containing smaller sized particles (Type I and Type II) (Figure 4.4). The incorporation of smaller sized filler particles considerably increased the viscosity of Type I and Type II FRCs compared with Type III FRCs, possibly due to the effect of increased surface area of the smaller size filler particles at equivalent volume%, which was in agreement with previous research (Masouras et al. 2008). Moreover, the smaller filler size of Type I and Type II FRCs might have resulted in increased packing of filler particles inside the resin matrix, possibly resulting in regions with increased stress area between the unfilled resin system matrix and the filler particles, leading to a decrease in the flexural strength of such FRCs compared with Type III FRCs (Figure 4.4).

Not only the size but also the amount of filler particles influenced the flexural strength of FRCs, with Type III FRCs (up to 20 or 23wt% bioactive glass, low and high filler content) exhibiting higher strength compared with Type I and Type II FRCs (Figure 4.4). For FRCs containing <20

or 23wt% bioactive glass (low and high filler content), there was no significant deterioration in flexural strength and flexural modulus observed (Figures 4.4, 4.6). Increasing the bioactive glass content for Type I, II and III FRCs (>20 or 23wt%, low and high filler content) significantly affected optical characteristics (light scattering and absorption), which led to a reduction in degree of conversion (Figure 4.3) and consequently flexural strength and flexural modulus (Figures 4.4, 4.6). Therefore, a decrease in the amount of filler present in the FRCs resulted in a lower viscosity of the polymer, thus an increase in degree of conversion as well as flexural strength for FRCs containing less than 30 or 34wt% bioactive glass for both low and high filler content. This increase in DC (Figures 4.3) might have been due to increased mobility of radical species thus increased conversion of carbon double to single bonds, which was in agreement with previous research (Tanimoto et al. 2005).

Moreover, FRCs of varying mechanical characteristics may be required for particular orthopaedic applications depending on the flexural strength and modulus of the surrounding bone (Asmussen and Peutzfeldt 1998). For example, cortical bone exhibits a flexural modulus of between 5-15GPa and a compressive strength of 100-150MPa in perpendicular direction to orientation axis of bone; whereas when tested in perpendicular direction to the long axis of bone the strength and modulus are approximately 2 times lower (Rahaman et al. 2011). Trabecular bone exhibits a compressive strength of 2-12MPa and an elastic modulus of 0.1-5GPa (Rahaman et al. 2011). Thus, bone exhibits different mechanical properties depending on the direction of load applied to it due to its oriented microstructure (known as anisotropy). Therefore, to successfully replace cortical or trabecular bone, FRCs should exhibit similar mechanical strength to the bone being replaced and similar flexural modulus (Table 4.3) to avoid high stress formation between the material and the surrounding bone which may lead to the failure of the implant when a certain load is exceeded (Giannoudis et al. 2005; Larsson

2006; Lin et al. 2005). Moreover, the optimum flexural strength for a synthetic material to be considered in orthopaedic applications should be between 50 and 125MPa (Table 4.3) (Lewis 1997). For some filler types the ideal value may be obtained at a specific filler concentration, followed by a significant decrease in the properties of the end product (Masouras et al. 2008). For the FRCs developed in this study, the maximum amount of bioactive glass filler that could be added to the resin matrix without a detrimental effect on flexural strength and modulus was 30 or 34wt%, low and high filler content. The flexural strength and flexural modulus decreased significantly in FRCs containing 40 or 45wt% bioactive glass (low and high filler content), which might have been due to the presence of bioactive glass fillers which might have resulted in decreased light absorption in during curing, increased light scattering, both having a negative impact on the degree of conversion and mechanical properties (Figures 4.4, 4.6; Tables 4.3). Flexural modulus was also higher in the developed FRCs compared with PMMA cement (1.80GPa). Due to the low modulus, the use of PMMA cement to stabilise implants in cortical bones (flexural modulus of 5 to 15GPa) might lead to the formation of a stress area between the cement and the bone, which ultimately may result in the aseptic loosening of the cement and failure of the implant. The high filler FRCs (23wt% bioactive glass) developed in this study exhibited a flexural modulus higher than 6.5GPa, which makes such cements more suitable for stabilisation of implants in cortical bone compared with PMMA, due to the absence of a stress area between the cement and the bone. Nonetheless, PMMA cement could be used to stabilise implants in trabecular bone, which has a flexural modulus of between 0.1 and 5GPa. The FRCs containing low filler content (20wt%) exhibited a flexural modulus of 5.8GPa, which is slightly higher than the flexural modulus of trabecular bone, however the slight increase in flexural modulus may provide an area with increased stress transfer from the bone to the cement, thus providing the bone with time to heal following the implant procedure.

			FS (MPa)	FM (GPa)
Cortical bone			50-125	5-15
Trabecular bone			2-12	0.1-5
PMMA			52.5 (10)	1.8 (0.3)
Silica70			84.3 (14)	7.0 (1.0)
Silica80			72.4 (24)	7.0 (1.7)
Type I	Low filler content	SIL20	69.9 (5.1)	5.8 (0.4)
		SIL40	26.3 (4.0)	3.3 (0.6)
	High filler content	SIL23	52.6 (11)	7.4 (1.2)
		SIL45	22.2 (3.6)	3.5 (0.7)
Type II	Low filler content	NS20	65.5 (7.3)	5.9 (0.7)
		NS40	19.9 (5.1)	1.7 (0.6)
	High filler content	NS23	61.4 (14)	6.7 (1.0)
		NS45	23.6 (6.0)	2.4 (1.0)
Type III	Low filler content	AB20	79.3 (8.4)	6.9 (0.9)
		AB40	42.7 (3.0)	3.6 (0.6)
	High filler content	AB23	90.3 (19)	8.9 (1.8)

Table 4.3 The flexural strength and modulus of bone and filled resin composites. PMMA refers to the commercially available bone cement; Silica70 and Silica80 refer to the filled resin composite containing 70, respectively 80wt% barium silicate filler (low and high filler content). FS refers to the flexural strength of filled resin composites tested dry. FM refers to the flexural modulus of filled resin composites tested dry. The Type I, Type II and Type III filled resin composites containing 20, respectively 23wt% bioactive glass (low and high filler content) exhibited flexural strength and flexural modulus values in the range of those of cortical bone. The Type I, Type II and Type III filled resin composites containing 40, or 45wt% bioactive glass (low and high filler content) exhibited flexural modulus values in the range of those of trabecular bone, however, higher values of flexural strengtth compared with trabecular bone.

Therefore the optimum physical and mechanical properties in terms of degree of conversion, flexural strength and flexural modulus were exhibited by FRCs containing 20 or 23wt% bioactive glass filler and 50 or 57wt% barium silicate filler (low and high filler content). The maximum amount of bioactive glass filler that could be added to the FRCs without a significant decrease in the degree of conversion, flexural strength and flexural modulus was 40 or 45wt%

(low and high filler content). To further analyse the possible application of FRCs to orthopaedic applications, the impact of water immersion was determined on these FRC formulations in Chapter 5.

4.5 Conclusion

By analyzing the effect of bioactive glass filler addition to 60/40wt% UDMA/TEGDMA resin formulations, the most suitable filled resin composites in terms of degree of conversion, flexural strength and flexural modulus were determined to be those containing 20 or 23wt% bioactive glass (low and high filler content). These characteristics of the filled resin composites (degree of conversion, flexural strength and flexural modulus) were influenced by the size (10μm and 50μm), type (silanised and non-silanised) and filler volume% added (low and high), which in turn affected the viscosity, handling and optical properties of the final composite. By changing the viscosity, while still maintaining suitable physical and mechanical properties, filled resin composites can be developed for injectable, in situ and ex situ orthopedic applications.

Therefore, a filled resin composite system was developed containing 20 or 23wt% (low and high filler content) bioactive glass (known for its advantageous effect on the viability of cells) and 50 or 57wt% (low and high filler content) barium silicate filler that still retained high degree of conversion and flexural strength. Moreover, this filled resin composite system was based on a set curing command (the composite hardened following exposure to light), thus eliminating the waiting time required for PMMA cement formulations (approximately 15min), before the operation can be closed. This is of key importance for surgeons.

4.6 Limitations of present work and recommendations for future studies

1. Only two types of bioactive glasses were analysed (limitation). By varying the size, chemical structure and amount of bioactive glasses present in the filled resin composites, these materials can be optimised for a wide range of orthopaedic applications (future studies).
2. The Type I FRCs contained bioactive glass filler particles with a silane content of 0.5%. By increasing the silane content of the bioactive glass fillers, filled resin composites may be developed with increased flexural strength for orthopaedic applications.

References

Asmussen, E. and Peutzfeldt, A. 1998. Influence of UEDMA, BisGMA and TEGDMA on selected mechanical properties of experimental resin composites. *Dental Materials*, 14, (1) 51-56

Begum, A.N., Rajendran, V., Ylanen, H. 2006. Effect of thermal treatment on physical properties of bioactive glass. *Materials Chemistry and Physics,* 96, (2-3) 409-417

Berger, S.B., Palialol, A.R.M., Cavalli, V., Giannini, M. 2009. Characterization of water sorption, solubility and filler particles of light-cured composite resins. *Brazilian Dental Journal*, 20, (4) 314-318

Chang, C.H., Liao, T.C., Hsu, Y.M., Fang, H.W., Chen, C.C., and Lin, F.H. 2010. A poly(propylene fumarate) - Calcium phosphate based angiogenic injectable bone cement for femoral head osteonecrosis. *Biomaterials*, 31, (14) 4048-4055

Chang, K.H., Greener, E.H. 1990. Correlation between degree of conversion, filler concentration and mechanical properties of posterior composite resins. *Journal of Oral Rehabilitation,* 17, (5) 487-494

Clarkin, O.M., Boyd, D., Madigan, S., Towler, M.R. 2009. Comparison of an experimental bone cement with a commercial control, Hydroset. *Journal of Materials Science-Materials in Medicine*, 20, (7) 1563-1570

Curtis, A.R., Palin, W.M., Fleming, G.J.P., Shortall, A.C.C., and Marquis, P.M. 2009. The mechanical properties of nanofilled resin-based composites: Characterizing discrete filler particles and agglomerates using a micromanipulation technique. *Dental Materials*, 25, (2) 180-187

Deb, S., Aiyathurai, L., Roether, J.A., and Luklinska, Z.B. 2005. Development of high-viscosity, two-paste bioactive bone cements. *Biomaterials*, 26, (17) 3713-3718

Du, M. and Zheng, Y. 2007. Modification of silica nanoparticles and their application in UDMA dental polymeric composites. *Polymer composites,* 28, (2) 198-207

Du, M. and Zheng, Y. 2008. Degree of conversion and mechanical properties studies of UDMA based materials for producing dental posts. *Polymer Composites,* 29, (6) 623-630

Ekworapoj, P., Magaraphan, R., Martin, D.C. 2002. Heat effect on viscosity and curing of light-cured dental resin and mechanical strength of conventional dental composites. *Journal of metals, materials and methods,* 12, (1) 39-50

Ferracane, J.L., Berge, H.X., Condon, J.R. 1998. In vitro ageing of dental composites in water-effect of degree of conversion, filler volume, and filler/matrix coupling. *Journal of Biomaterials Materials Research,* 42, (3) 465-472

Giannoudis, P.V., Dinopoulos, H., Tsiridis, E. 2005. Bone substitutes: an update. *Injury,* 36, (3) 20-27

Ha, J.Y., Kim, S.H., Kim, K.H.,Kwon, T.Y. 2011. Influence of the volumes of bis-acryl and poly(methyl methacrylate) resins on their exothermic behaviour during polymerisation. *Dental Materials,* 30, (3) 336-342

Hosseinalipour, M., Javadpour, J., Rezaie, H., Dadras, T., and Hayati, A.N. 2010. Investigation of Mechanical Properties of Experimental Bis-GMA/TEGDMA Dental Composite Resins Containing Various Mass Fractions of Silica Nanoparticles. *Journal of Prosthodontics-Implant Esthetic and Reconstructive Dentistry*, 19, (2) 112-117

Kim, O., Han, S. 2004. Effect of urethane dimethacrylate diluent on the mechanical properties of hybrid-filled polymeric dental restorative composites. *Journal of industrial and engineering chemistry,* 10, (3) 395-401

Larsson, S. 2006. Cement augmentation in fracture treatment. *Scandinavian Journal of Surgery*, 95, (2) 111-118

LePrince, J.G., Hadis, M., Shortall, A.C., Ferracane, J.L., Devaux, J., Leloup, G., Palin, W.M. 2011. Photoinitiator type and applicability of exposure reciprocity law in filled and unfilled photoactive resins. *Dental materials*, 27, (2) 157-164

Lewis, G. 1997. Properties of acrylic bone cement: State of the art review. *Journal of Biomedical Materials Research*, 38, (2) 155-182

Lin, C.C., Huang, L.C., and Shen, P.Y. 2005. Na2CaSi2O6-P2O5 based bioactive glasses. Part 1: Elasticity and structure. *Journal of Non-Crystalline Solids*, 351, (40-42) 3195-3203

Lin, C.T., Lee, S.Y., Keh, E.S., Dong, D.R., Huang, H.M., Shih, Y.H. 2000. Influence of silanisation and filler fraction on aged dental composites. *Journal of oral rehabilitation,* 27, (11) 919-926

Masouras, K., Silikas, N., Watts, D. 2008. Correlation of filler content and elastic properties of resin-composites. *Dental materials,* 24, (7) 932-939

Nicolae, C.L., Shelton. R.M., Cooper, P.R., Martin, R.A., Palin, W.M. 2013. The effect of bioglass addition on mechanical and physical properties of photoactive UDMA-TEGDMA resin composites. *Key Engineering Materials,* 587, (25) 215-221

Nicolae, C.L., Shelton. R.M., Cooper, P.R., Martin, R.A., Palin, W.M. 2014. The effect of UDMA/TEGDMA mixtures and bioglass incorporation on the mechanical and physical properties of resin and resin-based composite materials. *Conference Papers in Science*

Palin, WW.M., Fleming, G.J.P., Marquis, P.M. 2005. The reliability of standardised flexure strength testing procedures for a light-activated resin-based composite. *Dental Materials,* 21, (10) 911-919

Pfeifer, C.S., Silva, L.R., Kawano, Y., and Braga, R.R. 2009. Bis-GMA co-polymerizations: Influence on conversion, flexural properties, fracture toughness and susceptibility to ethanol degradation of experimental composites. *Dental Materials*, 25, (9) 1136-1141

Rahaman, M.N., Day, D.E., Bal, B.S., Fu, Q., Jung, S.B., Bonewald, L.F., and Tomsia, A.P. 2011. Bioactive glass in tissue engineering. *Acta Biomaterialia*, 7, (6) 2355-2373

Ruyter, I.E., Oysaed, H. 1987. Composites for use in posterior teeth: composition and conversion. *Journal of Biomedical Materials Research,* 21, (1) 11-23

Shen, C., Oh, W.S., Williams, J.R. 2004. Effect of post-silanisation drying on the bond strength of composite to ceramic. *The Journal of Prosthetic Dentistry,* 91, (5) 453-458

Shirai, K., Yoshida, Y., Nakayama, Y., Fujitani, M., Shintani, H., Wakasa, K., Okazaki, M., Snauwaert, J., Van Meerbeek, B. 2000. Assessment of decontamination methods as pretreatment of silanization of composite glass fillers. *Journal of Biomedical Materials Research*, 53, (3) 204-210

Sideridou, I.D., Karabela, M.M., Bikiaris, D.N. 2007. Ageing studies of light cured dimethacrylate-based dental resins and a resin composite in water or ethanol/water. *Dental Materials,* 23, (9) 1142-1149

Stadelmann, V.A., Bretton, E., Terrier, A., Procter, P., Pioletti, D.P. 2010. Calcium phosphate cement augmentation of cancellous bone screws can compensate for the absence of cortical fixation. *Journal of Biomechanics,* 43, (15) 2869-2874

Stansbury, J.W. 2000. Curing dental resins and composites by photopolymerization. *Journal of Eshetic Dentistry,* 12, (6) 300-308

Stansbury, J.W., Dickens, H. 2001. Determination of double bond conversion in dental resins by near infrared spectroscopy. *Dental Materials,* 17, (1) 71-79

Tanimoto, Y., Hayakawa, T., and Nemoto, K. 2005. Analysis of photopolymerization behavior of UDMA/TEGDMA resin mixture and its composite by differential scanning calorimetry. *Journal of Biomedical Materials Research Part B-Applied Biomaterials*, 72B, (2) 310-315

Tian, M., Gao, Y., Liu, Y., Liao, Y., Hedin, N.E., Fong, H. 2008. Fabrication and evaluation of Bis-GMA/TEGDMA dental resins/composites containing nano fibrillar silicate. *Dental Materials,* 24, (2) 235-243

Turssi, C.P., Ferracane, J.L. Vogel, K. 2005. Filler features and their effects on wear and degree of conversion of particulate dental resin composites. *Biomaterials,* 26, (24) 4932–4937

Vakiparta, M., Forsback AP, F.A.U., Lassila LV, F.A.U., Jokinen, M.F., Yli-Urpo AU FAU - Vallittu, and Vallittu, P.K. 2005. Biomimetic mineralization of partially bioresorbable glass

fiber reinforced composite. *Journal of materials science: materials in medicine,* 16, (9) 873-879

CHAPTER 5 WATER SORPTION AND SOLUBILITY OF FILLED RESIN COMPOSITES AND PMMA CEMENT

5.1 Introduction

Filled resin composites are formed of a hydrophobic resin matrix and a hydrophilic glass filler, with absorption of water occurring in the resin matrix and at the resin and filler interface (Ito et al. 2005). The resin matrix may undergo plasticization following water immersion, leading to the swelling of the resin matrix, which may have a detrimental impact on the mechanical characteristics of the filled resin composite. Water sorption (WS) by the filled resin composites may also lead to hygrothermal degradation following water storage, development of microcracks, weakening of the interfacial bond between the resin matrix and filler particles and scission of the polymer chain as a result of hydrolytic cleavage (Ito et al. 2005; Berger et al. 2009; Sideridou and Achilias 2005). The interface between the resin matrix and the filler has a significant impact on the ability of the filled resin composite to resist deformation under loading. Stronger bonding between the resin matrix and the filler can be achieved through silanization of the filler particles (formation of covalent bonds between the filler and the resin). However, this silane coupling agent may dissolve following water immersion leading to increased absorption of water inside the filled resin composites, leading to decreased mechanical strength (Lin et al. 2000; Podgorski, 2010). Thus, following water immersion, filled resin composites exhibit degradation and a decrease in mechanical strength, which is mainly due to sorption of water mostly in the resin matrix. The general decrease in mechanical strength of FRCs following water immersion is influenced by the amount of time in water as well as the amount and size of the filler present in the filled resin composite (Gohring et al. 2002; Musanje et al. 2001; Sideridou et al. 2003; Soderholm and Roberts, 1990)".

The aims of this particular study were to determine the solubility (SO) and water sorption of filled resin composite specimens exposed to water for up to three months to further analyse their suitability for orthopaedic applications and the impact of water immersion on the bi-axial flexural strength (BIFS) of such filled resin composites.

5.2 Materials and Methods

For synthesis of filled resin composites containing different sizes and types of bioactive glass and barium silicate filler refer to Chapter 2, Section 2.3.

For synthesis of polymethylmethacrylate refer to Chapter 2, Section 2.4.

For preparation and light curing of FRCs for water sorption, solubility and bi-axial flexure testing refer to Chapter 2, Section 2.5.

5.2.1 Water sorption and solubility of filled resin composites and PMMA cement

Water sorption and solubility of FRC and PMMA specimens were measured at 1 day, 7 days, 1 month and 3 months. The initial mass (m_0) of FRCs and PMMA for each sample condition was measured using a balance accurate to 0.0001g (TS400D, Ohaus, USA). The thickness and diameter of every specimen were also recorded for the calculation of volume (V) of each disc. The specimens were, then, placed in Petri dishes covered with aluminium foil, stored in a desiccator (Nalgene, Sigma Aldrich, UK) at room temperature (21°C) and weighed daily until a stable mass was recorded (m_1) (change of mass of ≤0.001g over 3 days). When a stable mass was reached, FRC and PMMA samples were immersed in double distilled water (10 resin specimens for each condition in 30ml water). Water was replaced every 7 days to avoid changes in pH. At each time point (1 day, 7 days, 1 month, or 3 months), samples were removed from water, dried in air for 15sec and reweighed (m_2). Specimens were then placed again in a desiccator at room temperature and weighed daily until a stable mass reading was recorded (m_3) (change of mass of ≤0.001g over 3 days). Water sorption (WS:µg/mm^3) and solubility (SL: µg/mm^3) were than calculated using the following Equations (Berger et al. 2009; Gajewski et al. 2012; Ito et al. 2005; Pearson 1979; Podgorski, 2010; Ortengren et al. 2001):

Equation 5.1 $WS=\frac{m_2-m_3}{V}$

Equation 5.2 $SL=\frac{m_1-m_2}{V}$

5.2.2 Bi-axial flexural strength of filled resin composites and PMMA cement

The disc shaped FRCs and PMMA used to determine the water sorption and solubility were also employed to determine the bi-axial flexural strength of each sample condition. The disc shaped specimens were placed centrally (the FRC specimens were placed with the cured surface in tension) on a thin sheet of rubber on a 10mm knife edge support (to avoid variations in peripheral thickness of the filled resin composites and promote uniform loading) and were loaded centrally using a 3mm ball indenter at a crosshead speed of 1mm/min on a universal tensile testing instrument (Instron Ltd, Buckinghamshire, England). The load of each filled resin composite and PMMA disc was, then, recorded at failure and the bi-axial flexural strength was calculated using Timoshenko and Woinowsky-Kreiger Equation (Timoshenko and Woinowsky-Krieger 1959):

Equation 5.3 $BiFS=\frac{P}{h^2}\left\{(1+\nu)\left[0.485x\ln\left[\frac{\alpha}{h}\right]+h\right]+0.48\right\}$, where

BiFS was the bi-axial flexural strength, P: the measured load at fracture, α: the radius of the knife edge support, h: the sample thickness and ν: the Poisson ratio for each specimen condition. The Poisson's ratio ("change in cross-linked density" (Begum et al. 2006)) of a material can be determined from the lateral contraction per unit breadth divided by the longitudinal extension per unit length and a value of 0.300 was used for FRCs and PMMA in the current study (Boyd et al. 2008; Higgs et al. 2001). The thickness of each filled resin composite and PMMA disc was measured at the point of fracture with a micrometre screw gauge (Moore and Wright, Sheffield, England) accurate to 10μm (Palin et al. 2003).

5.2.3 Statistical analysis

Minitab statistical software (Minitab, UK) was used to analyse the data using one-way analysis of variance (ANOVA) test. A difference of $P<0.05$ was considered statistically significant. Anderson-Darling test was used to determine whether the data followed a normal distribution. Tukey's post hoc tests were used for pair-wise comparison using a significance value of $P=0.05$.

5.3 Results

5.3.1 Water sorption and solubility of filled resin composites and PMMA cement

By plotting water sorption and water solubility values for each filled resin composite or PMMA sample condition against time, it was determined that the lowest water sorption occurred in Type III composites containing 20wt% bioactive glass (Figure 5.1). Filled resin composite specimens containing the highest amount of bioactive glass filler (40wt%) exhibited the highest water sorption, regardless of the type of bioactive glass particles (Type I, Type II or Type III) (Figure 5.1). For analysis of significant differences between the water sorption of filled resin composites and PMMA refer to Appendix 3, Tables 3.1-3.14.

The water sorption of filled resin composites containing low filler content increased with decreasing filler size in the order: AB40<SIL40<NS40<SIL20<NS20<AB20, with filled resin composites containing 70wt% barium silicate filler exhibiting higher water sorption compared with AB40 filled resin composites, however, these were lower compared with SIL40 filled resin composites (Figures 5.1, 5.2). For filled resin composites containing 40wt% bioactive glass, water sorption was higher with higher particle size. For filled resin composites containing 20wt% bioactive glass, water sorption was lower with increased particle size (Figure 5.1). Filled resin composites containing 20wt% bioactive glass filler exhibited an increase in water sorption at 3 months compared with 1 day, regardless of the filler type (Type I, Type II, or Type III) ($p<0.001$). However, Type I and Type II filled resin composites containing 40wt% bioactive glass filler exhibited similar values for water sorption at 3 months compared with 1 day ($p>0.060$), with the exception of Type III FRCs, which exhibited an increase in water sorption ($p<0.001$). FRCs containing 80wt% barium silicate filler exhibited a decrease ($p<0.001$) for high filler and a similar value ($p=0.146$) for low filler (70wt%) of water sorption at 3 months water immersion compared with 1 day. There was a %increase in the water sorption of filled

resin composites containing low filler content in the order: NS40<SIL40<AB40<SIL20<AB20<NS20, with water sorption increasing with decreased bioactive glass filler particle size (Figure 5.2).

For analysis of significant differences between the water solubility of filled resin composites and PMMA refer to Appendix 3, Tables 3.15-3.28. The solubility of filled resin composites containing low filler content increased with decreasing bioactive glass filler size in the order: AB40<AB20<SIL20<NS20<NS40<SIL40, with filled resin composites containing 70wt% barium silicate filler exhibiting the lowest SO (Figures 5.3, 5.4). For Type III resin composites, solubility decreased with decreasing amount of filler present in the filled resin composite. For Type I and Type II filled resin composites, solubility increased with increasing amount of filler present in the filled resin composite (Figure 5.2). There was an increase in the water solubility of filled resin composites at month 3 water immersion compared with day 1 water immersion for all types of bioactive glass filler particles (Type I, Type II, or Type III) ($p<0.002$). FRCs containing barium silicate filler only exhibited a similar value of water solubility for both low (70wt%) ($p=0.548$) and high (80wt%) ($p=0.674$) filler at 3 months water immersion compared with 1 day. There was a %increase in the water solubility of resin composites containing low filler content in the order: NS40<SIL40<AB40<AB20<SIL20<NS20, with water solubility increasing with decreased bioactive glass filler size particle (Figure 5.4).

The water sorption of filled resin composites containing high filler content increased with increasing filler size in the order: NS45<SIL45<SIL23<NS23<AB23, with filled resin composites containing 80wt% barium silicate filler exhibiting the lowest water sorption (Figure 5.5). There was a %increase in the water sorption of resin composites containing high filler content in the order: NS45<SIL45<SIL23<NS23<AB23, with water sorption increasing with decreased bioactive glass filler particle size (Figure 5.6).

The solubility of filled resin composites containing the high filler content increased with increasing amount of filler in the order: NS23<AB23<SIL23<NS45<SIL45, with filled resin composites containing 80wt% barium silicate filler exhibiting the lowest solubility. The Type I filled resin composites exhibited the highest solubility for both 23 and 45wt% bioactive glass content (Figure 5.7). There was a %increase in the water solubility of resin composites containing high filler content in the order: NS23<SIL23<SIL45<NS45<AB23.

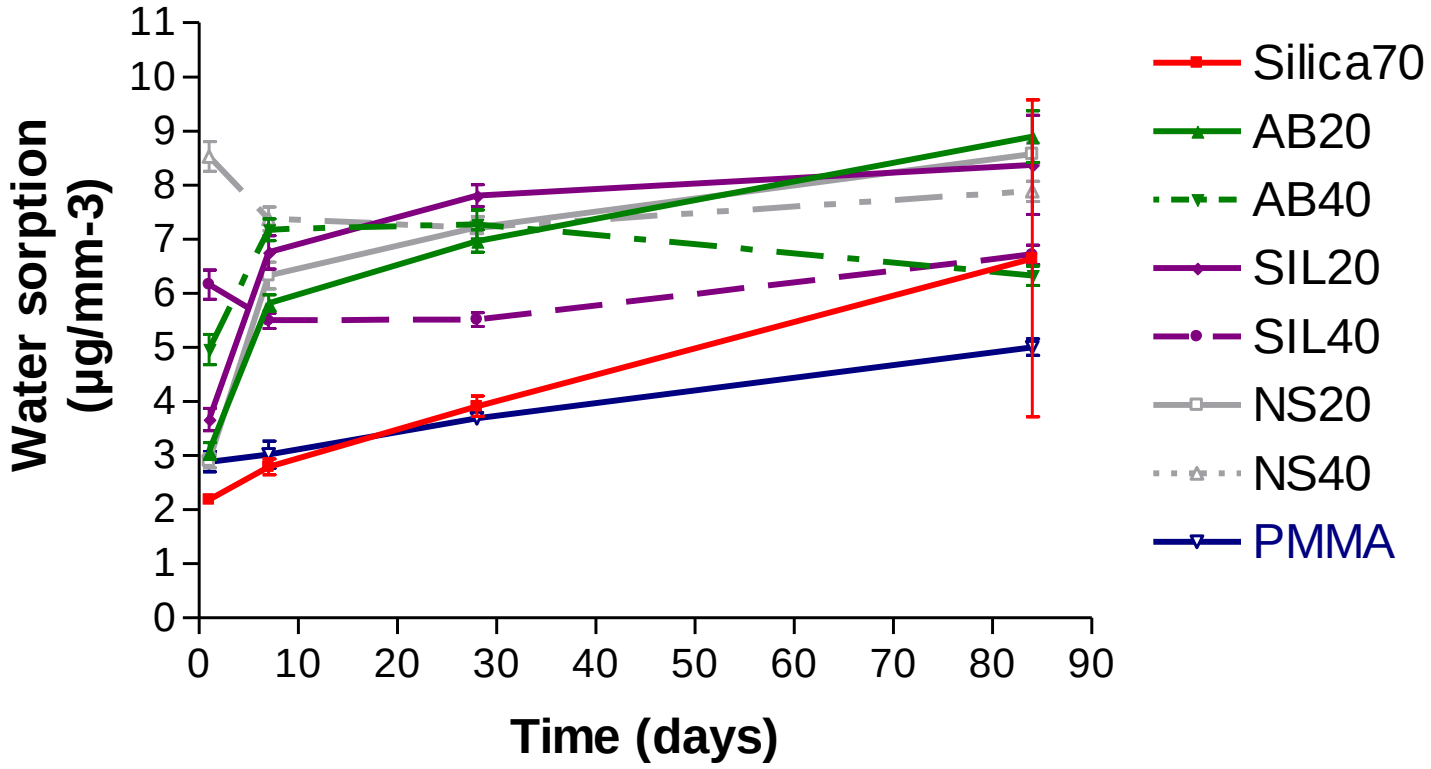

Figure 5.1 The water sorption of filled resins composites containing low filler content following wet storage for 1 day, 7 days, 1 month and 3 months. Filled resin composite percentage inclusions are shown within bar labels. Silica70 refers to filled resin composites containing 70wt% barium silicate filler. SIL20 and SIL40 refer to Type I filled resin composites. NS20 and NS40 refer to Type II filled resin composites. AB20 and AB40 refer to Type III filled resin composites. The water sorption of filled resin composites containing low filler content decreased in the order: AB40<SIL40<NS40<SIL20<NS20<AB20. Error bars indicate one standard deviation from the mean for 10 samples.

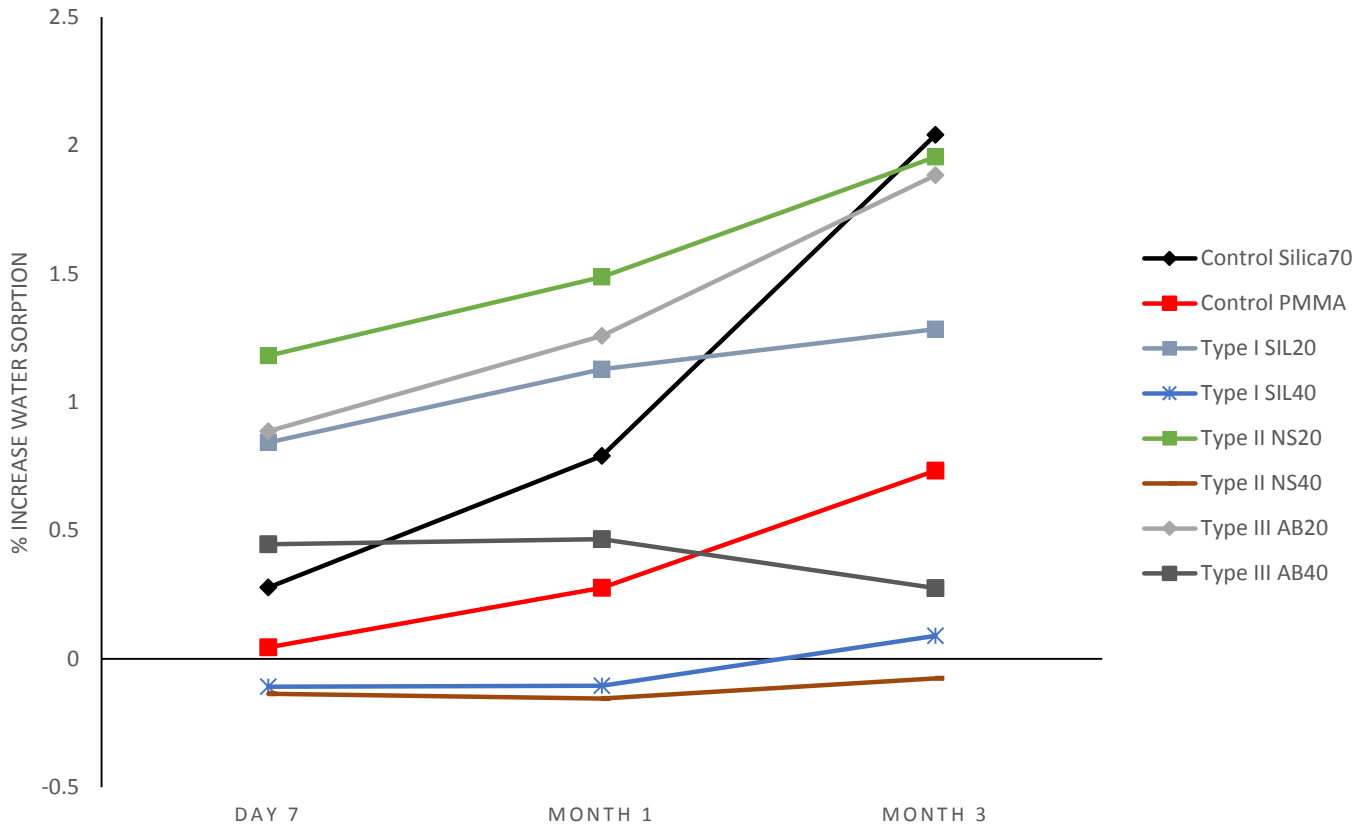

Figure 5.2 The %increase in water sorption of filled resins composites containing low filler content following wet storage for 1 day, 7 days, 1 month and 3 months. Filled resin composite percentage inclusions are shown within bar labels. Silica70 refers to filled resin composites containing 70wt% barium silicate filler. SIL20 and SIL40 refer to Type I filled resin composites. NS20 and NS40 refer to Type II filled resin composites. AB20 and AB40 refer to Type III filled resin composites. The water sorption of filled resin composites containing low filler content increased in the order: NS40<SIL40<AB40<SIL20<AB20<NS20.

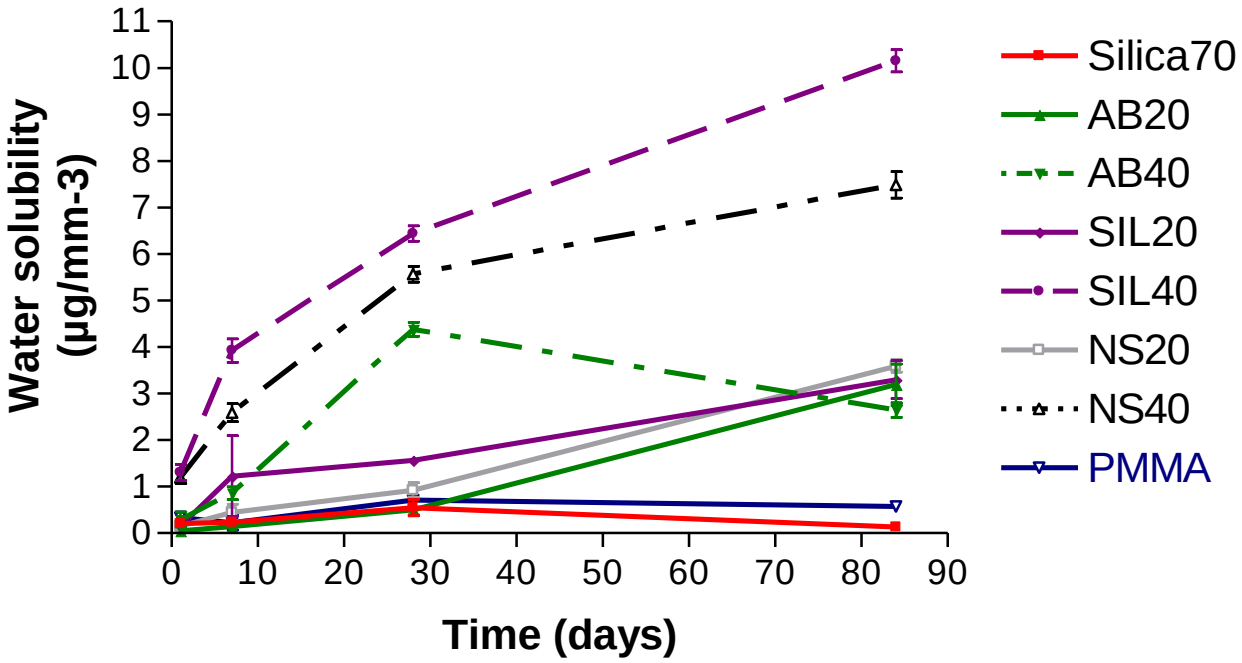

Figure 5.3 The water solubility of resins composites containing low filler content following wet storage for 1 day, 7 days, 1 month and 3 months. Filled resin composite percentage inclusions are shown within bar labels. Silica70 refers to filled resin composites containing 70wt% barium silicate filler. SIL20 and SIL40 refer to Type I filled resin composites. NS20 and NS40 refer to Type II filled resin composites. AB20 and AB40 refer to Type III filled resin composites. The water solubility of resin composites containing low filler content increased in the order: AB40<AB20<SIL20<NS20<NS40<SIL40. Error bars indicate standard deviation over a mean average of 10 samples.

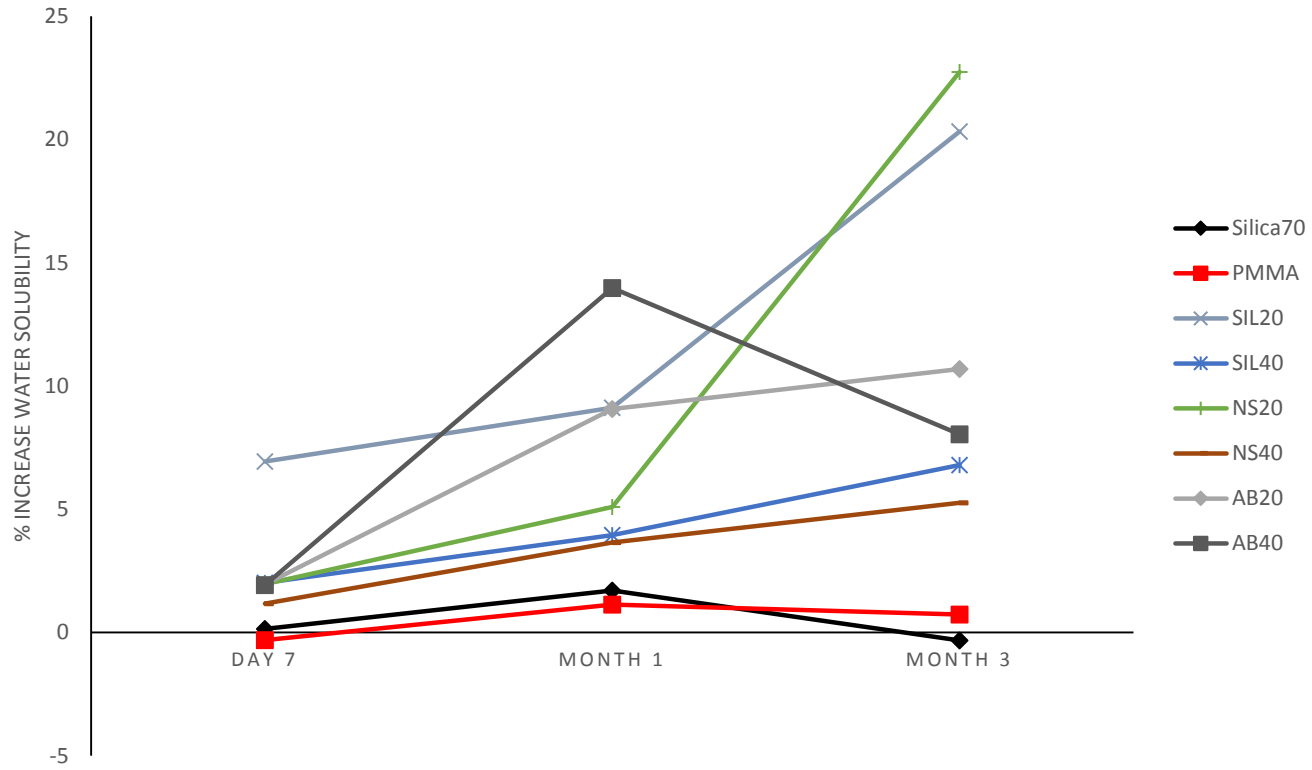

Figure 5.4 The %increase in water solubility of resins composites containing low filler content following wet storage for 1 day, 7 days, 1 month and 3 months. Filled resin composite percentage inclusions are shown within bar labels. Silica70 refers to filled resin composites containing 70wt% barium silicate filler. SIL20 and SIL40 refer to Type I filled resin composites. NS20 and NS40 refer to Type II filled resin composites. AB20 and AB40 refer to Type III filled resin composites. The water solubility of resin composites containing low filler content increased in the order: NS40<SIL40<AB40<AB20<SIL20<NS20.

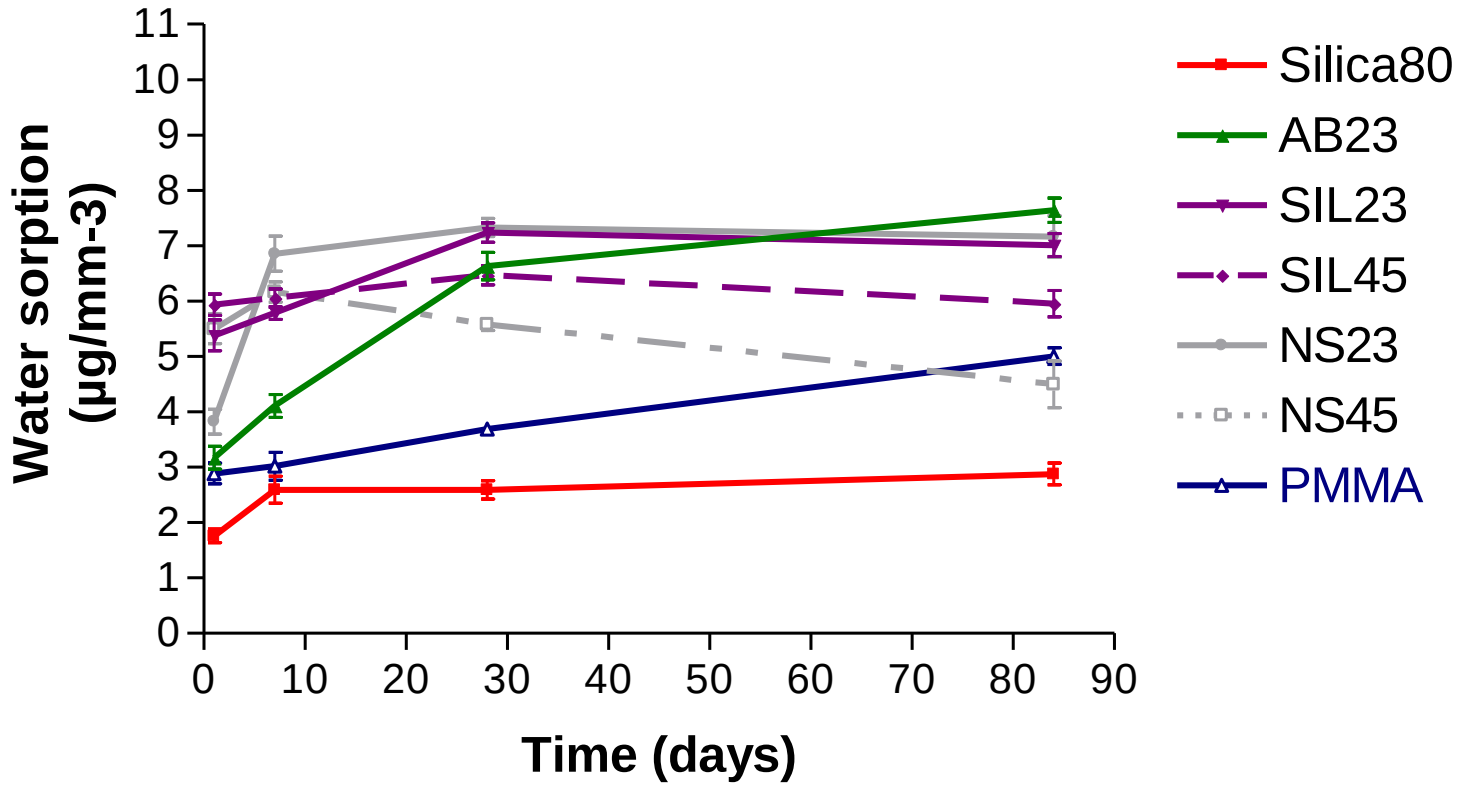

Figure 5.5 The water sorption of resins composites containing high filler content following wet storage for 1 day, 7 days, 1 month and 3 months. Filled resin composite percentage inclusions are shown within bar labels. Silica80 refers to filled resin composites containing 80wt% barium silicate filler. SIL23 and SIL45 refer to Type I filled resin composites. NS23 and NS45 refer to Type II filled resin composites. AB23 refers to Type III filled resin composites. The water sorption of resin composites containing high filler content increased in the order: NS45<SIL45<SIL23<NS23<AB23. Error bars indicate standard deviation over a mean average of 10 samples.

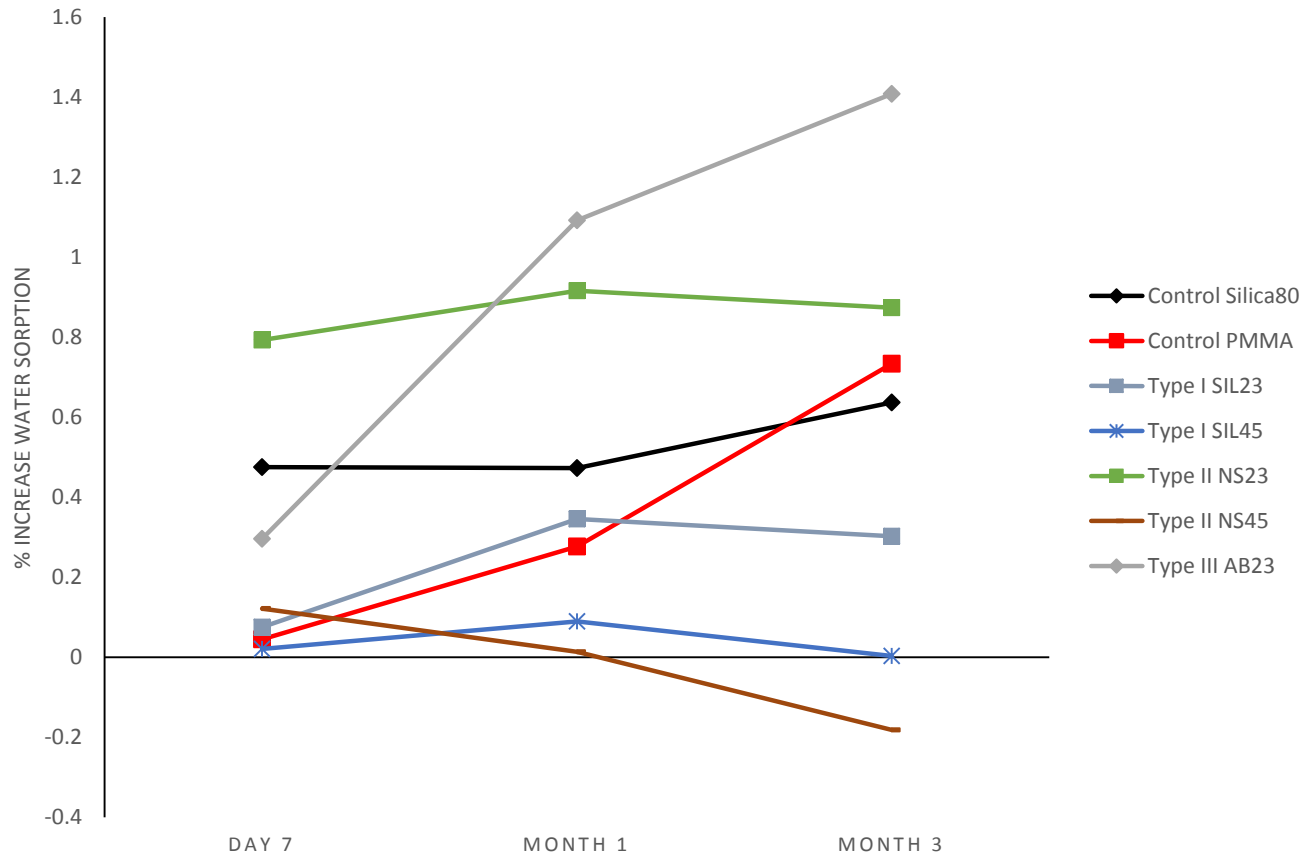

Figure 5.6 The %increase in water sorption of resins composites containing high filler content following wet storage for 1 day, 7 days, 1 month and 3 months. Filled resin composite percentage inclusions are shown within bar labels. Silica80 refers to filled resin composites containing 80wt% barium silicate filler. SIL23 and SIL45 refer to Type I filled resin composites. NS23 and NS45 refer to Type II filled resin composites. AB23 refers to Type III filled resin composites. The water sorption of resin composites containing high filler content increased in the order: NS45<SIL45<SIL23<NS23<AB23.

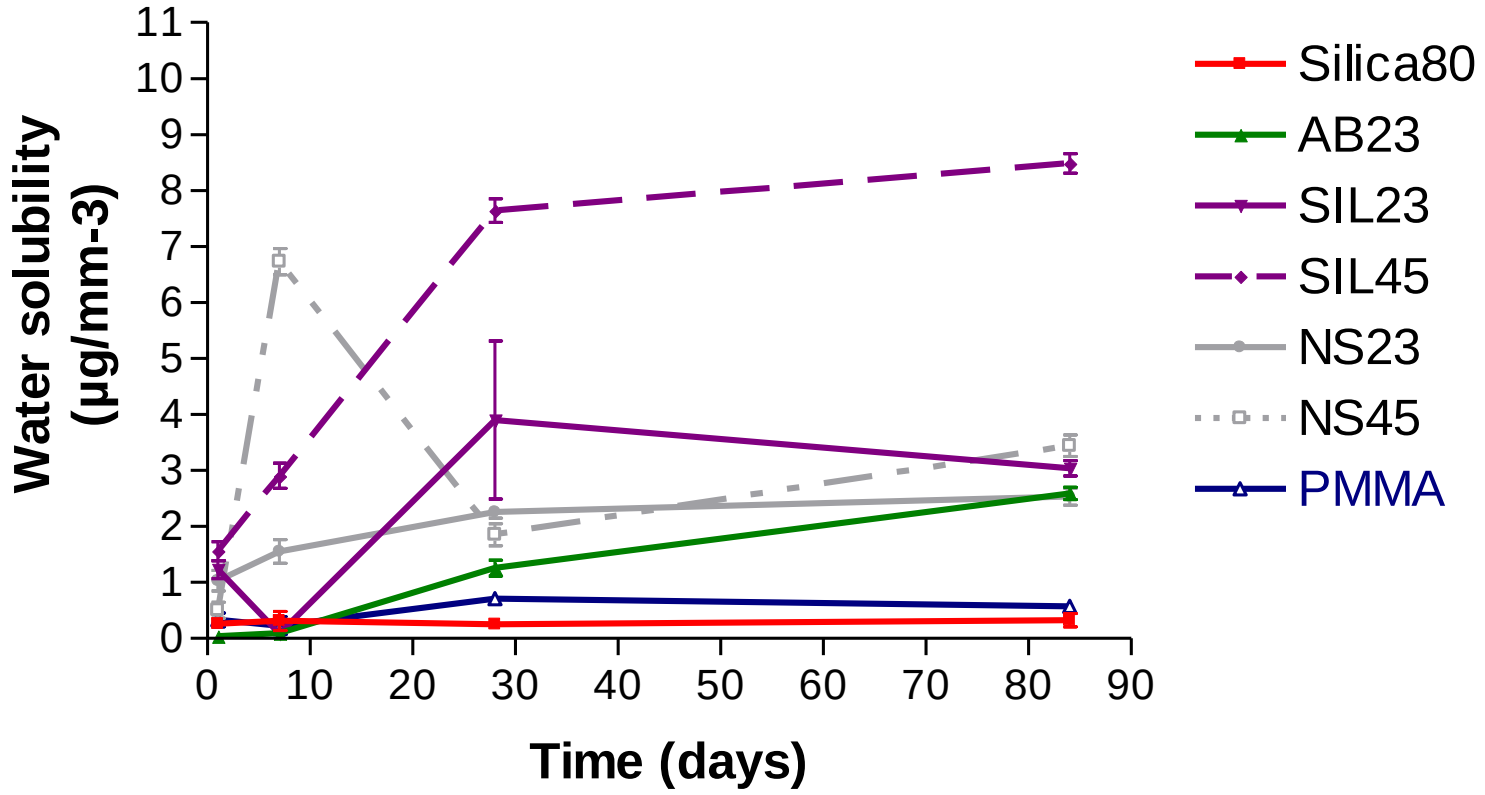

Figure 5.7 The water solubility of resins composites containing high filler content following wet storage for 1 day, 7 days, 1 month and 3 months. Filled resin composite percentage inclusions are shown within bar labels. Silica80 refers to filled resin composites containing 80wt% barium silicate filler. SIL23 and SIL45 refer to Type I filled resin composites. NS23 and NS45 refer to Type II filled resin composites. AB23 refers to Type III filled resin composites. The water solubility of resin composites containing high filler content increased in the order: NS23<AB23<SIL23<NS45<SIL45. Error bars indicate standard deviation over a mean average of 10 samples.

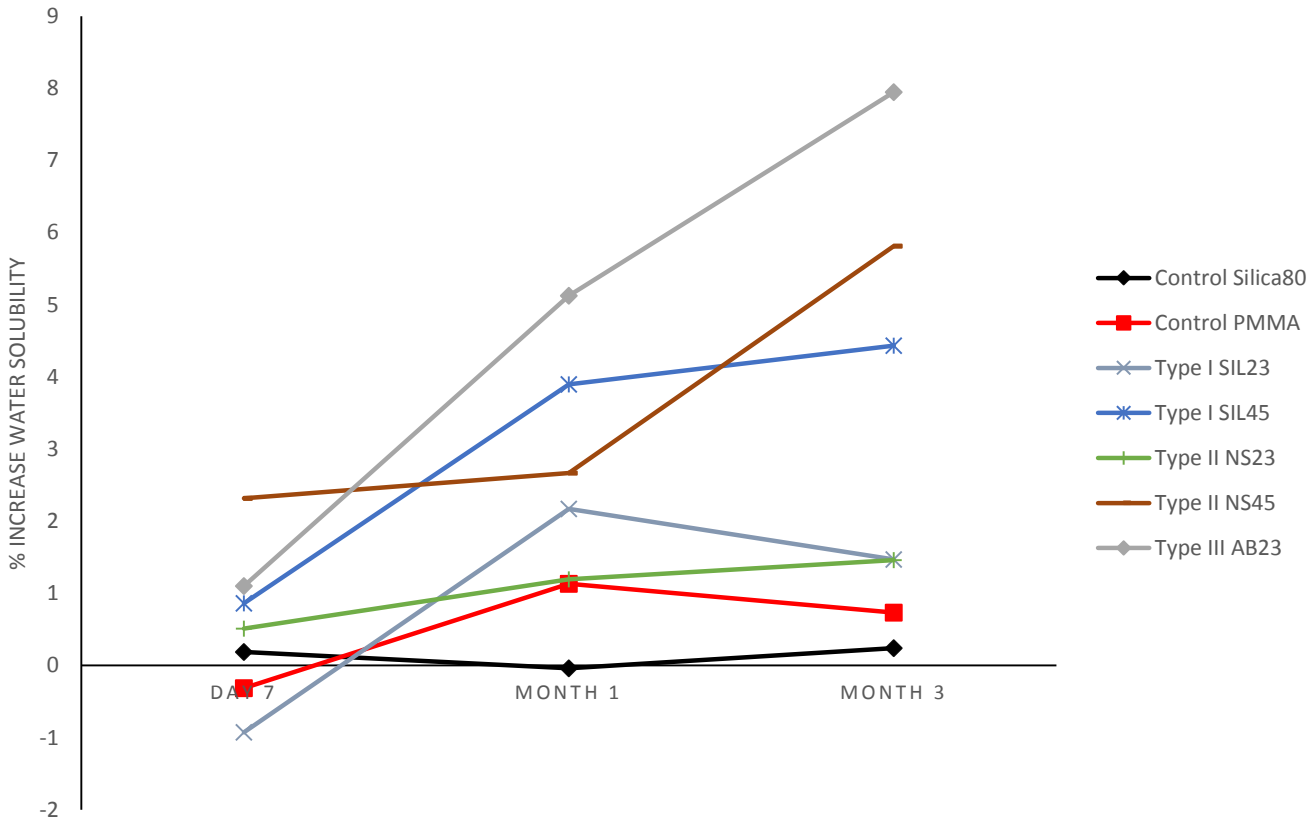

Figure 5.8 The %increase in water solubility of resins composites containing high filler content following wet storage for 1 day, 7 days, 1 month and 3 months. Filled resin composite percentage inclusions are shown within bar labels. Silica80 refers to filled resin composites containing 80wt% barium silicate filler. SIL23 and SIL45 refer to Type I filled resin composites. NS23 and NS45 refer to Type II filled resin composites. AB23 refers to Type III filled resin composites.

5.3.2 Bi-axial flexural strength of filled resin composites and PMMA cement

The BIFS of filled resin composites containing low filler content increased with decreasing filler content in the order: SIL40<NS40<AB40<SIL20<AB20<NS20 (Figure 5.9). The filled resin composites containing 70 or 80wt% barium silicate filler (low and high filler content) exhibited the highest BIFS. For filled resin composites containing 40wt% bioactive glass, the BIFS increased with increasing filler size (Figure 5.13). For filled resin composites containing either 40wt% bioactive glass, or 20wt% bioactive glass the lowest BIFS was exhibited by Type I filled resin composites (Figure 5.9). The %decrease in bi-axial flexural strength of resin composites containing low filler content increased with decreasing filler content in the order: SIL40<NS40<AB40<AB20<NS20<SIL20 (Figure 5.10).

The BIFS of filled resin composites containing high filler content increased in the order: SL45<SIL23<NS45<NS23<AB23 (or Type I < Type II < Type III filled resin composites) (Figure 5.11). The filled resin composites containing 80wt% barium silicate filler exhibited the highest BIFS. The resin composites containing bioactive glass exhibited higher BIFS with increasing filler size, thus, Type III composites exhibiting the highest BIFS. The Type I composites exhibited the lowest BIFS (Figure 5.11). The %decrease in bi-axial flexural strength of resin composites containing high filler content increased in the order: SIL45<AB23<NS23<SIL23<NS45 (Figure 5.12).

For analysis of significant differences between the bi-axial flexural strength values of filled resin composites and PMMA refer to Appendix 3, Tables 3.28-3.42. FRCs containing bioactive glass filler particles exhibited a decrease in bi-axial flexural strength values at 3 months water immersion compared with 1 day, regardless of amount (low, or high filler content), type (Type I, Type II, or Type III) and size of particles ($p<0.040$). The only exception was the low filler FRCS containing 40wt% Type I bioactive glass filler, which exhibited a similar bi-axial flexural

strength value at 3 months water immersion compared with 1 month water immersion ($p=0.190$). FRCs containing barium silicate filler only exhibited a decrease ($p=0.014$) for low filler (70wt%) and a similar value ($p=0.161$) for high filler (80wt%) of bi-axial flexural strength at 3 months water immersion compared with 1 day.

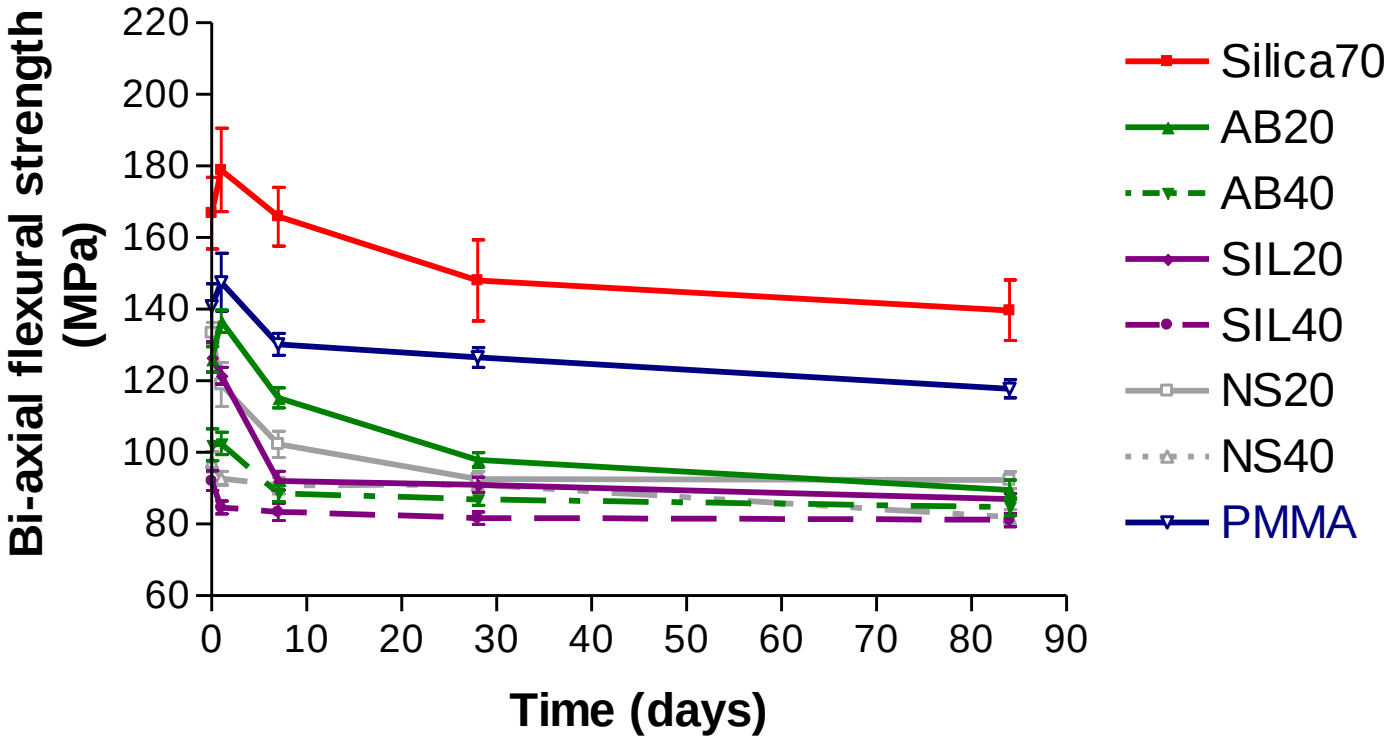

Figure 5.9 The bi-axial flexural strength of filled resins composites containing low filler content tested following water immersion for 1 day, 7 days, 1 month and 3 months. Filled resin composite percentage inclusions are shown within bar labels. Silica70 refers to filled resin composites containing 70wt% barium silicate filler. SIL20 and SIL40 refer to Type I filled resin composites. NS20 and NS40 refer to Type II filled resin composites. AB20 and AB40 refer to Type III filled resin composites. The bi-axial flexural strength of resin composites containing low filler content increased with decreasing filler content in the order: SIL40<NS40<AB40<SIL20<AB20<NS20. Error bars indicate standard deviation over a mean average of 10 samples.

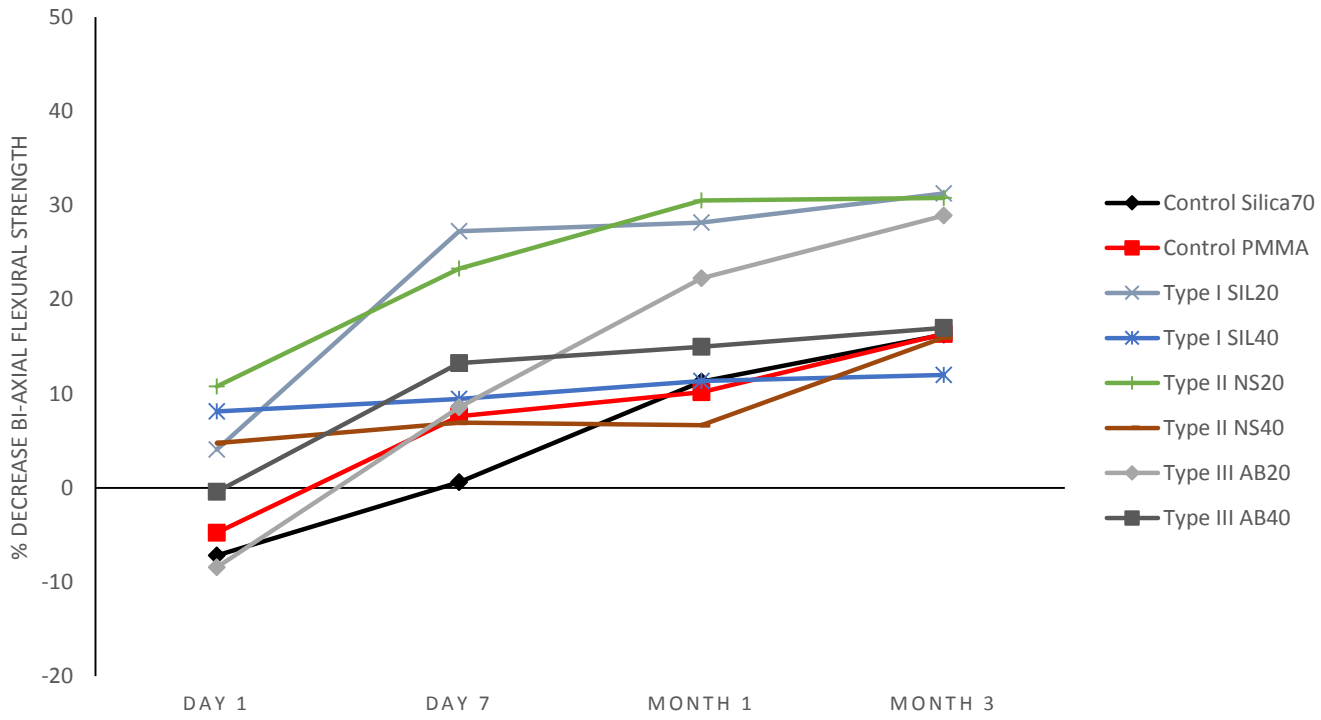

Figure 5.10 The %decrease in bi-axial flexural strength of filled resins composites containing low filler content tested following water immersion for 1 day, 7 days, 1 month and 3 months compared with specimens tested dry. Filled resin composite percentage inclusions are shown within bar labels. Negative values denote a % increase in the bi-axial flexural strength of filled resin composites containing low filler content. Silica70 refers to filled resin composites containing 70wt% barium silicate filler. SIL20 and SIL40 refer to Type I filled resin composites. NS20 and NS40 refer to Type II filled resin composites. AB20 and AB40 refer to Type III filled resin composites. The % decrease in bi-axial flexural strength of resin composites containing low filler content increased with decreasing filler content in the order: SIL40<NS40<AB40<AB20<NS20<SIL20.

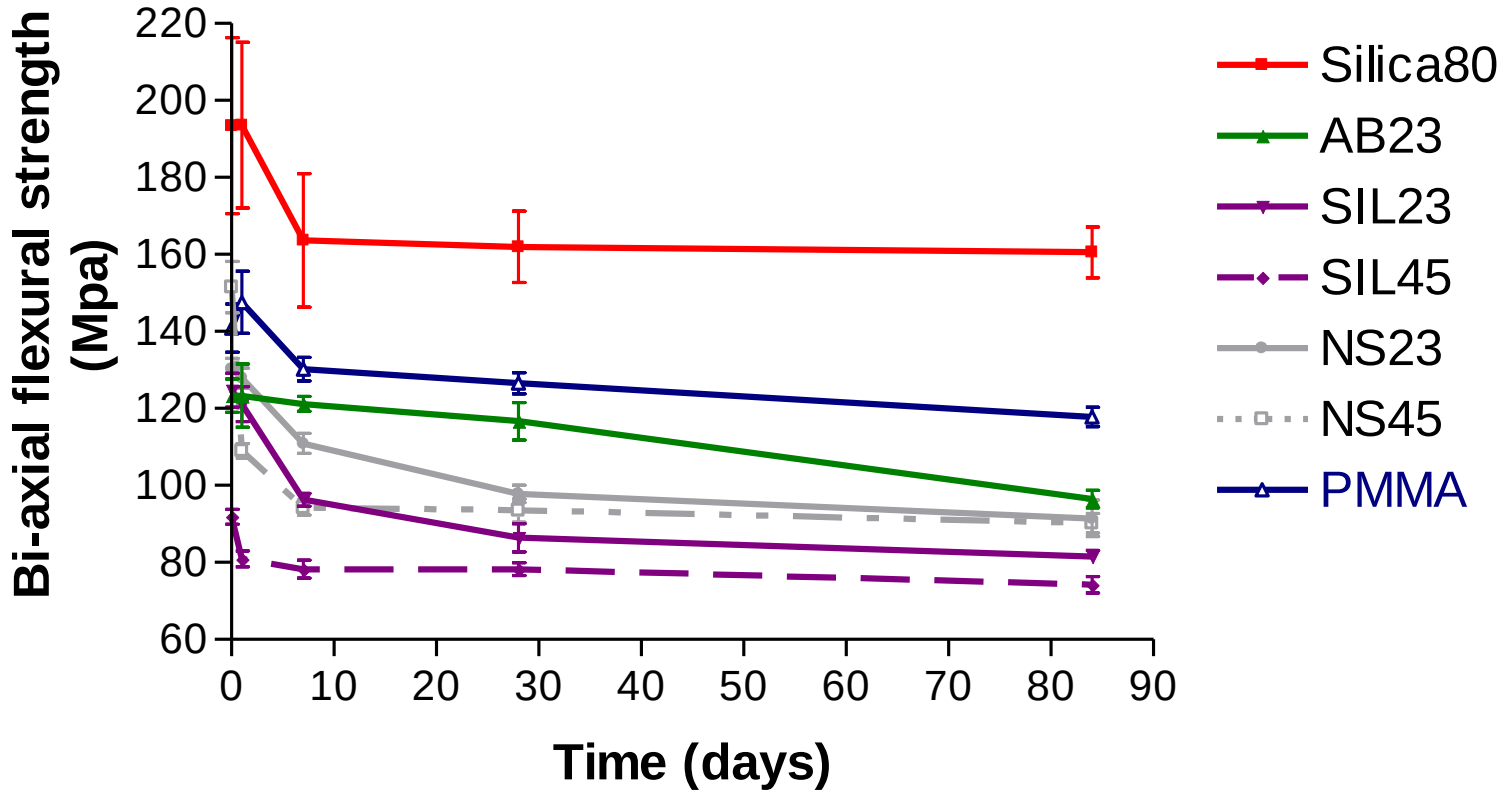

Figure 5.11 The bi-axial flexural strength of resins composites containing high filler content tested following water immersion for 1 day, 7 days, 1 month and 3 months. Filled resin composite percentage inclusions are shown within bar labels. Silica80 refers to filled resin composites containing 80wt% barium silicate filler. SIL23 and SIL45 refer to Type I filled resin composites. NS23 and NS45 refer to Type II filled resin composites. AB23 refers to Type III filled resin composites. The bi-axial flexural strength of resin composites containing high filler content increased in the order: SIL45<SIL23<NS45<NS23<AB23. Error bars indicate standard deviation over a mean average of 10 samples.

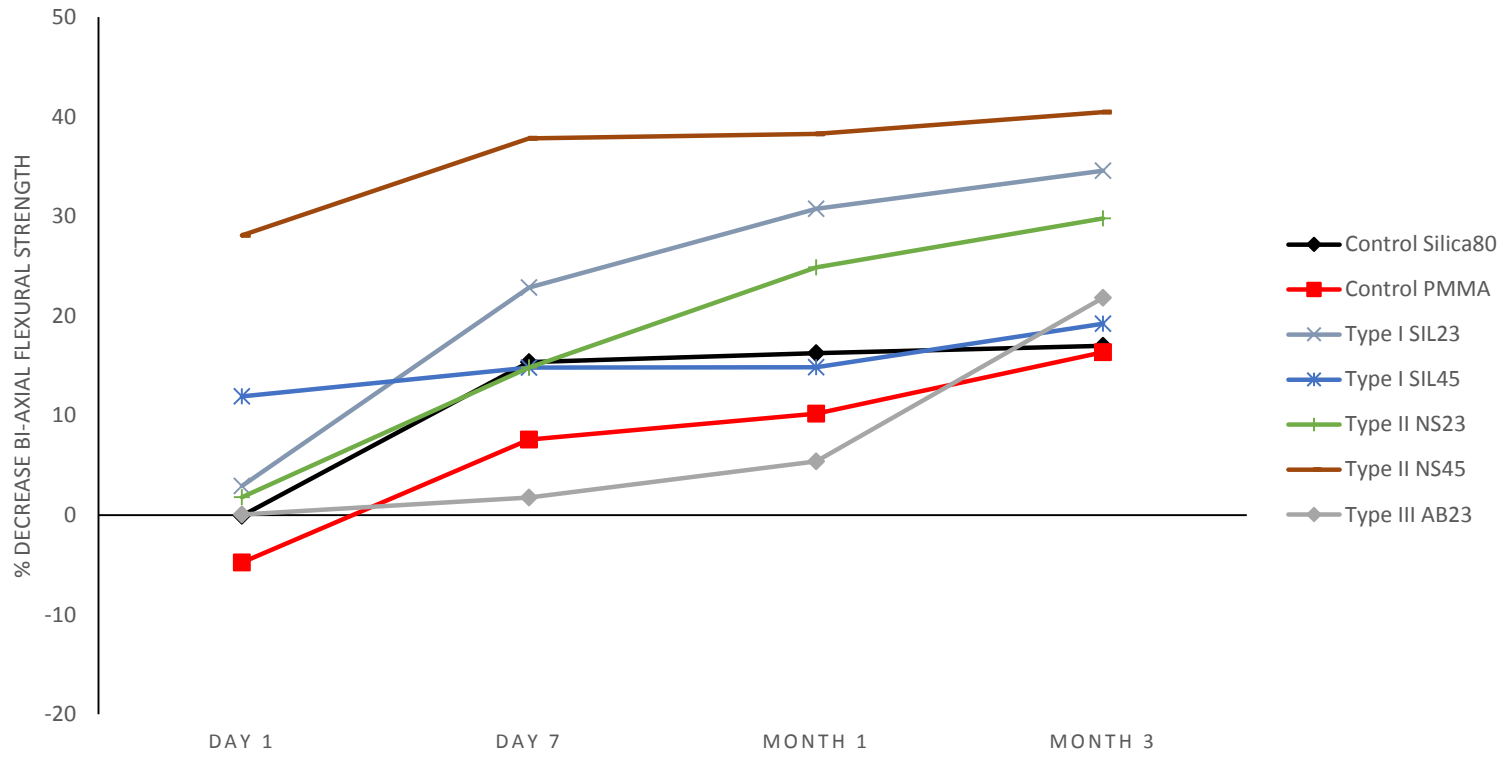

Figure 5.12 The %decrease in bi-axial flexural strength of resins composites containing high filler content tested following water immersion for 1 day, 7 days, 1 month and 3 months compared with specimens tested dry. Negative values denote a % increase in the bi-axial flexural strength of filled resin composites containing low filler content. Filled resin composite percentage inclusions are shown within bar labels. Silica80 refers to filled resin composites containing 80wt% barium silicate filler. SIL23 and SIL45 refer to Type I filled resin composites. NS23 and NS45 refer to Type II filled resin composites. AB23 refers to Type III filled resin composites. The % decrease in bi-axial flexural strength of resin composites containing high filler content increased in the order: SIL45<AB23<NS23<SIL23<NS45.

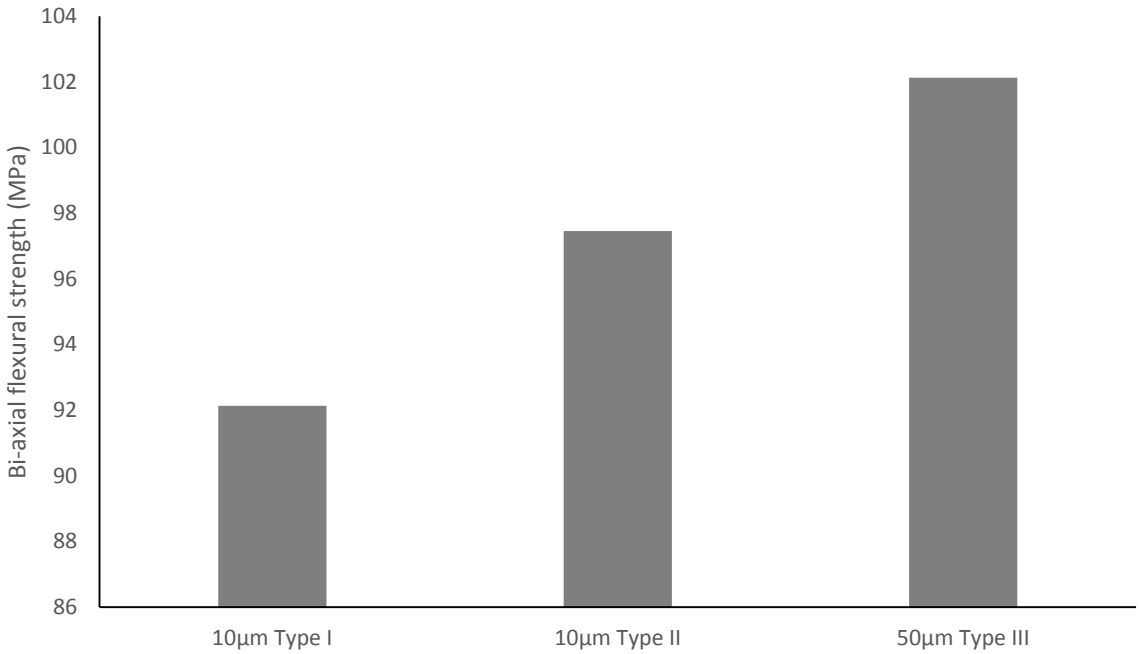

Figure 5.13 The bi-axial flexural strength increased with an increase in the filler particle size. The filled resin composites containing 10µm bioactive glass filler exhibited an increase in the bi-axial flexural strength when the filler particles were non-silanised compared with silanised particles.

5.4 Discussion

5.4.1 Water sorption and solubility of filled resin composites and PMMA cement

FRCs were composed of the organic resin matrix and the inorganic filler particles. Bioactive glass filler particles had hydrogen groups through which sorption of water might have occurred into the polymer network (Lin et al. 2000). The resin matrix in the present study consisted of hydrophobic monomers UDMA and TEGDMA, which during the polymerisation reaction formed a three dimensional polymer network, which was composed of both highly cross-linked and weakly cross-linked regions (Sauro et al. 2013). Therefore, the amount of polymer formed during the polymerising reaction, the hydrophilicity, the dimensional structure, volume of this polymer and chemical structure of the filler particles had a direct impact on the water sorption of the final filled resin composite (Berger et al. 2009; Skrtic and Antonucci 2003). The water sorption of filled resin composite materials was previously shown to be less than 1% (Skrtic and Antonucci 2003). The filled resin composites in the current investigation exhibited water sorption values of less than 10µl/mm^{-3} (Figures 5.2, 5.6), which were lower than those required by the ISO4049 standard (maximum water sorption value of 40µg/mm^{3}) (Berger et al. 2009; Sauro et al. 2013).

Water sorption increased with a decrease in the degree of conversion (for more information refer to Chapter 4, Section 4.3.1) of the FRCs and an increase in water storage time only for filled resin composites containing low filler content, whereas the filled resin composites containing high filler content became saturated after two weeks immersion time (Figures 5.1, 5.5), which was, however, in contrast with previous research (Sideridou et al. 2002). The increased water sorption with decreased degree of conversion might be explained by the increased volume of resin matrix in the FRCs, where hydrogen bonds were developed when water molecules were attracted to the polar groups found in the filled resin composites, leading

to swelling of the resin matrix and plasticisation of the polymer, with degradation of the filler/resin interface (Ito et al. 2005; Masouras et al. 2008).

Each FRC condition exhibited fast water sorption in the first 2 weeks, with the FRCs being saturated after 2 weeks water immersion (Figures 5.1, 5.2, 5.5, 5.6), as expected from a diffusion process. Thus, in the first two weeks, water was absorbed in the polymer network, filling the voids left by release of unreacted monomer between polymer chains, which were influenced by the concentration and chemical structure of the unreacted monomer (including polarity and hydrogen bonding ability), the amount of absorbed water as well as the plasticising effect of monomer and water. The barium silicate filler in the filled resin composites forms a low-solubility molecular network of silicate chains for the ions contained in the bioactive glass (Na^+, P^+, Ca^{2+}). These ions stimulate the biochemical environment surrounding the filled resin composite following immersion in a physiological environment. There is an exchange of ions between the bioactive glass from the filled resin composite and the biochemical environment of the organism, with sodium ions leaching out of the filled resin composite and hydrogen ions entering the composite (due to charge electro-neutrality) (Figure 5.14). The dissolution of these ions from the bioactive glass fillers contained in the filled resin composites has a significant role in the bonding of the composite to the surrounding bone. Immediately, after implantation, there is a rapid release of ions from the cement with the development of a polycrystalline hydroxy carbonate apatite and hydrated silica by-layer on the surface of the cement containing bioactive glass. Bonding of the filled resin composites containing bioactive glass to surrounding bone, thus, involves a series of chemical reactions taking place at the surface of the composite, resulting in the formation of a dynamic interface between the two, consisting of calcium phosphates. This interface is a result of the assimilation of calcium monoacid phosphate (formed from the transformation of calcium phosphates), which can then turn into

hydroxyapatite, thus promoting the migration of osteoblasts to the interface formed between the bone and the filled resin composite, through the recruitment of collagen, mucopolysaccharides and glycoproteins from the surrounding bone. The migration and attachment of such cells is further stimulated by the alkalinisation of the local pH as a result of ions dissolution from the bioactive glass contained in the filled resin composites. Moreover, there will be attachment of osteogenic stem cells to the surface of the cement due to the dissolution of silica ions from the cement containing bioactive glass. The formation of such a by-layer also has a crucial role in the recruitment of growth factors (such as VEGF (vascular endothelial growth factor), IGF2 (insulin like growth factor 2)); macrophages, which play a role in tissue repair and regeneration. Matrix mineralisation and osteocytes formation in a matrix formed from collagen (from the osteoblasts) and the HCA layer, then, occurs at the surface of the cement; with the resin component providing a scaffold for new bone ingrowth (Hench, 2006; Pryor et al. 2009). Therefore, filled resin composites containing bioactive glass should stimulate the migration, attachment and proliferation of mesenchymal stem cells and osteoblasts at the interface between the bone and the composite (Figure 5.14).

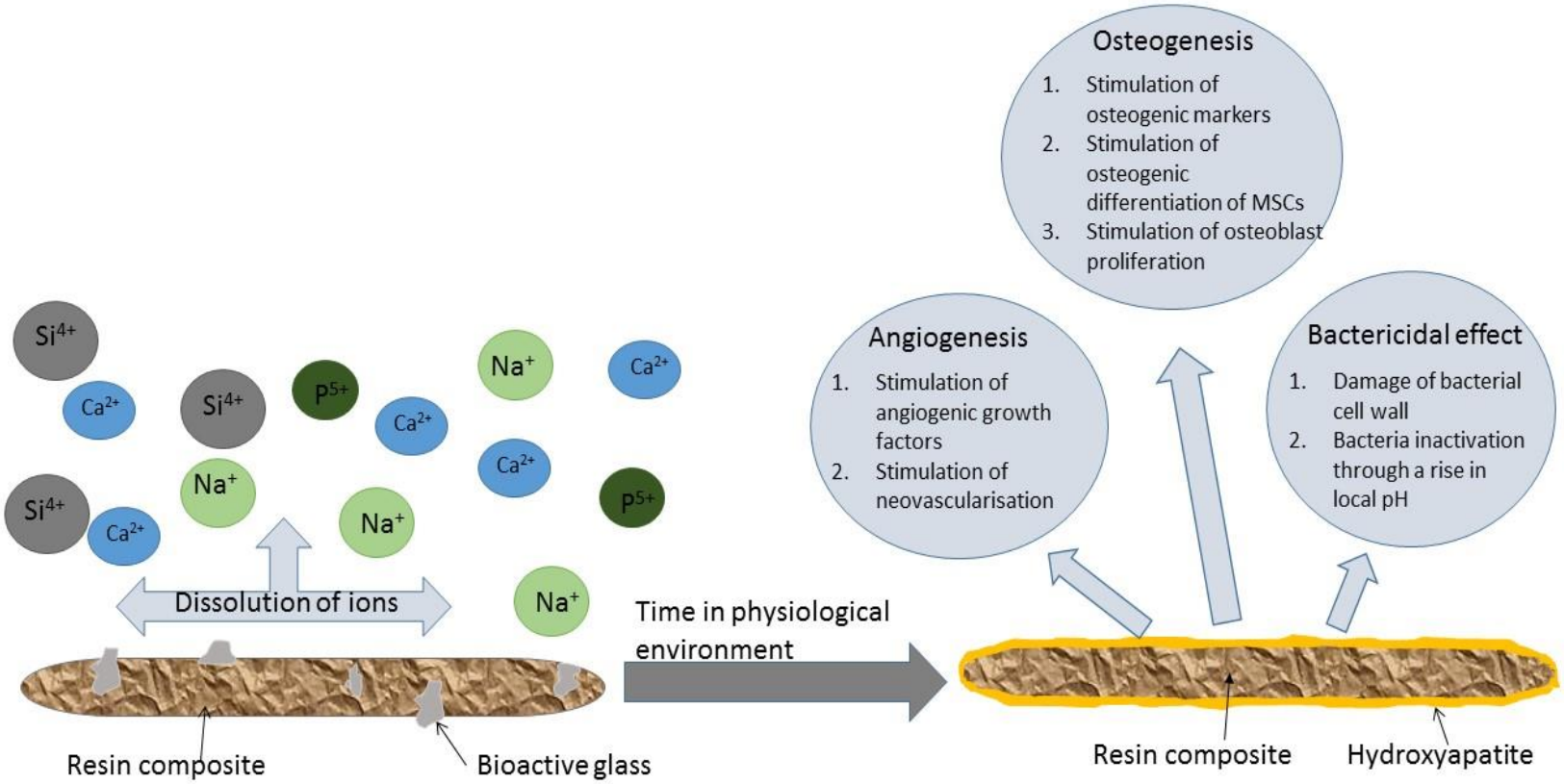

Figure 5.14 The mechanism of the potential adhesion of the developed filled resin composites containing bioactive glass to surrounding bone. There is dissolution of ions from the surface of the bioactive glass fillers contained in the filled resin composites, which with time in a physiological environment has a bactericidal effect (thus preventing infection), stimulates angiogenesis, which in turn promotes osteogenesis through the recruitment of osteogenic stem cells and osteoblasts to the interface zone formed between the filled resin composites and the surrounding bone.

The FRCs containing barium silicate filler without bioactive glass exhibited decreased water sorption compared with FRCs containing bioactive glass (Figure 5.1, 5.5), which might be explained by the presence of siloxane groups in their structure through which a strong chemical bond was formed between the methyl acrylate groups of the resin polymer and the hydroxyl groups of the filler particles (Shawkat et al. 2009, Skrtic and Antonucci 2003). However, when silanised bioactive glass filler particles were added to the FRCs containing barium silicate filler an increase in water sorption was observed (Figures 5.1, 5.5), possibly because of the dissolution of ions from the particles and chemical interaction between the water molecules and the filler particles; which might have resulted in degradation of the interface between the filler particles and the resin matrix, through breakage of the siloxane bonds (Berger et al. 2009). The degradation of the interface between the organic resin matrix and inorganic filler particles and infiltration of water inside the polymer matrix might have resulted in de-bonding of the filler particles from the resin matrix, thus increased water sorption and reduced mechanical strength as was the case with FRCs containing 40 or 45wt% (low and high filler content) bioactive glass particles (Figures 5.1, 5.2, 5.5, 5.6), which concurs with previous research (Soderholm, 1981).

The FRCs containing low filler content exhibited higher water sorption compared with FRCs containing higher filler content (Figures 5.1, 5.5), possibly because of increased amount of polymer, thus increased capacity of the FRC to absorb water, which was in accordance with previous literature (Braden and Clarke 1984; Masouras et al. 2008; Ortengren et al. 2001; Oysaed and Ruyter 1986; Schneider et al. 2010). The increased water sorption of FRCs containing low filler content compared with high filler content (Figures 5.1, 5.5) might be explained by the fact that the polymer network consisted of regions of unreacted monomers trapped inside microgel clusters, between polymer chains. When immersed in water, the polymer network swelled, thus opening up the regions between the polymer chains, with

unreacted monomers leaching out as a consequence of this diffusion process (swelling of the polymer and leaching of unreacted monomer); where the amount of water in the resin matrix was inversely proportional to the diffusion coefficient, which also resulted in less water sorption with immersion period of FRCs (Figures 5.1, 5.5), which was in agreement with previous research (Ortengren et al. 2001; Sauro et al. 2013; Schneider et al. 2010; Sideridou et al. 2007).

The amount of water sorption increased with a decrease in the size of filler particles and increase in the amount of filler as seen in FRCs containing both low and high filler content (Figures 5.1, 5.2, 5.5, 5.6), possibly because of increased surface area and volume of filler particles to the polymer, leading to increased packing of filler particles inside the resin matrix, which was in accordance with previous research (Turssi et al. 2005). Moreover, the increase in the amount of water sorption of low filler content FRCs containing small size silanised bioactive glass filler particles (Type I FRCs) (Figure 5.1) might be explained by the increased surface area of such fillers to the resin matrix, which due to their hydrophilic characteristics might have interacted with water molecules leading to the degradation of the chemical bond between the filler and the resin matrix. The increase in the amount of water sorption of low filler content Type I filled resin composites might also be due to the degradation of the silane coupling agent due to water dissolution, also resulting in increased loss of filler ass suggested by Soderholm (Soderholm, 1981). PMMA exhibited slow water sorption with time occurring through the unsaturated bonds present in the monomer molecules (Miettinen and Vallittu 1997).

The hydrophilicity and quantity of monomers present, amount, type and size of filler particles, as well as water sorption of the resin matrix influenced the solubility of the filled resin composites, resulting in a reduction in the mass weight of the filled resin composite with storage time (Ortengren et al. 2001). The filled resin composites (low and high filler content) containing 20 or23wt% bioactive glass exhibited water solubility values less than 5µg (Figures 5.3, 5.7),

which were lower compared with the maximum values stipulated by the ISO4049 standard (<7.5µg/mm^3) (Berger et al. 2009; Sauro et al. 2013). However, the filled resin composites (low and high filler content) containing 40 or 45wt'% bioactive glass exhibited water solubility values >7.5µg (Figures 5.4, 5.8), which were higher compared with the maximum values stipulated by the ISO4049 standard (<7.5µg/mm^3) (Berger et al. 2009). For filled resin composites containing low filler content, the highest solubility was exhibited by those containing Type I or Type II bioactive glass filler particles which contained the lowest size of filler particles (Figures 5.3, 5.7). The Type I filled resin composites containing silanised filler particles consisted of silane bonds due to a condensation reaction occurring between the silane coupling agent and the silanol groups of the silica particles resulting in the development of siloxane bridge bonds and covalent bonds with the resin matrix. Following water immersion, the siloxane bonds degraded to silanol groups probably through a hydrolysis reaction, possibly resulting in the high water solubility of these filled resin composites (Figures 5.3, 5.7), however, further analysis testing hydrolysis of these filled resin composites is required.

5.4.2 Bi-axial flexural strength of resin composites and PMMA cement

The bi-axial flexural testing may be more reliable than three point bend test as it eliminates the impact of intersecting planes of shear as well as edge defects from analysis, resulting in easy detection of structural differences in the integrity of the composite material (Boyd et al. 2008). Therefore, the bi-axial flexural strength was also analysed to further determine the suitability of these filled resin composites for orthopaedic applications. Following immersion in water, filled resin composites swelled, which might be advantageous by reducing the interfacial stress between the filler particles and the resin matrix formed during polymerisation. However, there is a maximum limit of filler addition into the resin matrix, which when exceeded might negatively impact on the mixing of the filler particles within the liquid resin matrix, resulting

in absorption of high amounts of water which might have a detrimental effect on the mechanical strength of the filled resin composite by decreasing the strength of the chemical bond between the resin matrix and bioactive glass particles. The bonding of the resin matrix and filler particles might have led to the formation of a matrix-filler interface, with decreased capacity for water sorption, resulting in higher bi-axial flexural strength for Type III filled resin composites instead of Type I filled resin composites, which contain silanised filler particles (Figures 5.1, 5.5, 5.9, 5.11), which was in contrast with previous research (Sauro et al. 20113). Moreover, the absorption of water into the FRCs might have led to breakdown of the intermolecular connection between the monomer molecules and the filler particles, with increasing bioactive glass content resulting in reduced BIFS values for FRCs containing 40wt% bioactive glass filler (Figure 5.10). The possible breakdown of the filler/resin interface due to water sorption might also explain the decreased BIFS of FRCs with increased immersion period (Figures 5.10, 5.12). The reduced BIFS for such FRCs might be explained by the hydrophilic characteristics of and dissolution of sodium and calcium ions from the bioactive glass filler particles present in the FRC. Immediately after immersion in water of the filled resin composites containing bioactive glass fillers, there is a fast exchange of sodium and potassium ions from the bioactive glass filler particles with hydrogen and hydronium ions from the surrounding water. This ion exchange resulted in a dissolution of the structure of the bioactive glass filler particles, with the leaching out of sodium, calcium, phosphorus and silicon ions (Jones, 2013; Valimaki and Aro, 2006). A silica rich surface layer was formed on the bioactive glass filler particles (which were in contact with water) “through polycondensation of the hydrated silica groups” (Valimaki and Aro, 2006). Therefore, higher dissolution of ions from bioactive glass filler particles of the filled resin composites might have resulted in increased water sorption and decreased BIFS.

5.5 Conclusions

The amount, size and type of bioactive glass filler had a significant impact on the water sorption, solubility and BIFS of filled resin composites. The water sorption and solubility increased with an increase in the amount of bioactive glass filler present. The bi-axial flexural strength increased with decreased amount and increased size of bioactive glass filler present. Therefore by varying the type, size or amount of bioactive glass filler particles, filled resin composites with a wide range of sorption and solubility values (which are less than 40µl/mm^3 (water sorption) and 7.5µl/mm^3 (water solubility)) can be developed for specific orthopaedic applications, for use either as pre-made, injectable or *in situ* materials for bone regeneration and repair.

5.6 Limitations of present work and recommendations for future studies

1. Only the water sorption and solubility of two concentrations of bioactive glass filler in the filled resin composites (20, 40wt% (low filler content) and 23, 45wt% (high filler content)) were analysed (limitation). Future studies may involve the analysis of water sorption and solubility of filled resin composites containing bioactive glass fillers with different chemical structures. By changing the chemical structure of the bioactive glass fillers, dissolution of ions, sorption and solubility values can be varied, which may lead to increased bone regeneration and repair compared with current materials.
2. The water sorption and solubility of only resin composites containing micron-sized bioactive glass filler particles were tested (limitation). Future studies may analyse the water sorption and solubility of filled resin composites containing either nanoscale sized bioactive particles or a mixture of microscopic and nano-sized particles. The use of such particles may increase the filler volume to resin matrix of such composites, possibly

leading to an increase the viability of bone cells in contact with these filled resin composites.

References

Begum, A.N., Rajendran, V., Ylanen, H. 2006. Effect of thermal treatment on physical properties of bioactive glass. *Materials Chemistry and Physics,* 96, (2-3) 409-417

Berger, S.B., Palialol, A.R.M., Cavalli, V., Giannini, M. 2009. Characterization of water sorption, solubility and filler particles of light-cured composite resins. *Brazilian Dental Journal*, 20, (4) 314-318

Boyd, D., Towler, M.R., Wren, A., Clarkin, O.M. 2008. Comparison of an experimental bone cement with surgical Simplex P, Spineplex and Cortoss. *Journal of Materials Science: Materials in Medicine,* 19, (4) 1745-1752

Braden, M., Clarke, R.L. 1984. Water absorption characteristics of dental microfine composite filling materials. Proprietary materials. *Biomaterials,* 5, (6) 369-372

Gajewski, V.E.S., Pfeifer, C.S., Froes-Salgado, N.R.G., Boaro, L.C.C., Braga, R.R. 2012. Monomers used in resin composites: degree of conversion, mechanical properties and water sorption/solubility. *Brazilian Dental Journal*, 23, (5) 508-514

Gohring, T.N., Besek, M.J., Schmidlin, P.R. 2002. Attritional wear and abrasive surface alterations of composite resin materials in vitro. *Journal of Dentistry,* 30, (2-3) 119-127

Higgs, W.A.J., Lucksanasombool, P. 2001. A simple method of determining the modulus of orthopaedic bone cement. *Journal of Biomedical Materials Research (Applied Biomaterials),* 58, (2) 188-195

International Standard Organisation: ISO 4049, Dentistry-Polymer-Based Filling, Restorative and Luting Materials (ed 3). Geneva, ISO, 2000, pp. 15-18

Ito, S., Hashimoto, M., Wadgaonkar, B., Svizero, N., Carvalho, R.M., Yiu, C., Rueggeberg, F.A., Foulger, S., Saito. T., Nishitani, Y., Yoshiyama, M., Tay, F.R., Pashley, D.H. 2005. Effects of resin hydrophilicity on water sorption and changes in modulus of elasticity. *Biomaterials,* 26, (33) 6449-6459

Jones, J.R. 2013. Review of bioactive glass: From Hench to hybrids. *Acta Biomaterialia,* 9, (1) 4457-4486

Lin, C.T., Lee, S.Y., Keh, E.S., Dong, D.R., Huang, H.M., Shih, Y.H. 2000. Influence of silanisation and filler fraction on aged dental composites. *Journal of Oral Rehabilitation,* 27, (11) 919-926

Masouras, K., Silikas, N., Watts, D. 2008. Correlation of filler content and elastic properties of resin-composites. *Dental Materials,* 24, (7) 932-939

Miettinen, V.M., Vallittu, P.K. 1997. Water sorption and solubility of glass fiber-reinforced denture polymethyl methacrylate resin. *The Journal of Prosthetic Dentistry,* 77, (5) 531-534

Musanje, L., Shu, M., Darvell, B.W. 2001. Water sorption and mechanical behaviour of cosmetic direct restorative materials in artificial saliva. *Dental Materials,* 17, (5) 394-401

Ortengren, U., Wellendorf, H., Karlsson, S., Ruyter, I.E. 2001. Water sorption and solubility of dental composites and identification of monomers released in an aqueous environment. *Journal of Oral Rehabilitation,* 28, (12) 1106-1115

Oysaed, H., Ruyter, L.E. 1986. Water sorption and filler characteristics of composites for use in posterior teeth. *Journal of Dental Research,* 65, (11) 1315

Palin, W.M., Fleming, G.J.P., Burke, F.J.T., Marquis, P.M., Randall, R.C. 2003. Monomer conversion versus flexure strength of a novel dental composite. *Journal of Dentistry*, 31, (5) 341-351

Pearson, G.J. 1979. Long term water sorption and solubility of composite filling materials. *Journal of Dentistry,* 7, (1) 64-68

Podgorski, M. 2010. Synthesis and characterisation of novel dimethacrylates of different chain lengths as possible dental resins. *Dental Materials,* 26, (6) e188-e194

Sauro, S., Osorio, R., Fulgencio, R., Watson, T.F., Cama, G., Thompson, I., Toledano, M. 2013. Remineralisation properties of innovative light-curable resin-based dental materials containing bioactive micro-fillers (vol 1, pg 2624, 2013). *Journal of Materials Chemistry B*, 1, (48) 6670

Schneider, O.D., Stepuk, A.F., Mohn, D.F., Luechinger NA FAU - Feldman, K., Feldman, K.F., Stark, W.J. 2010. Light-curable polymer/calcium phosphate nanocomposite glue for bone defect treatment. *Acta Biomaterialia,* 6, (7) 2704-2710

Shawkat, E.S., Shortall, A.C., Addison, O., Palin, W.M. 2009. Oxygen inhibition and incremental layer bond strengths of resin composites. *Dental Materials,* 25, (11) 1338-1346

Sideridou, I.D., Achilias, D.S. 2005. Elution study of unreacted bisGMA, TEGDMA, UDMA, and bisEMA from light-cured dental resins and resin composites using HPLC. *Journal of Biomedical Materials Research Part B: Applied Biomaterials,* 74, (1) 617-626

Sideridou, I.D., Karabela, M.M., Bikiaris, D.N. 2007. Ageing studies of light cured dimethacrylate-based dental resins and a resin composite in water or ethanol/water. *Dental Materials,* 23, (9) 1142-1149

Sideridou, I., Tserki, V., Papanastasiou, G. 2002. Effect of chemical structure on degree of conversion in light-cured dimethacrylate-based dental resins. *Biomaterials*, 23, (8) 1819-1829

Sideridou, I., Tserki, V., Papanastasiou, G. 2003. Study of water sorption, solubility and modulus of elasticity of light-cured dimethacrylate-based dental resins. *Biomaterials,* 24, (4) 655-665

Skrtic, D., Antonucci, J.M. 2003. Effect of bifunctional comonomers on mechanical strength and water sorption of amorphous calcium phosphate- and silanized glass-filled bisGMA-based composites. *Biomaterials,* 24, (17) 2881-2888

Soderholm, K.J. 1981. Degradation of glass filler in experimental composite. *Journal of Dental Research,* 60, (11) 1867-1875

Soderholm, K.J., Roberts, M.J. 1990. Influence of water exposure on the tensile strength of composites. *Journal of Dental Research,* 69, (12) 1812-1816

Timoshenko, S., Woinowsky-Kreiger, S. 1959. Symetricl bending of circular plates. Theory of plates and shells. 2nd ed. New York: McGraw-Hill; 87-121

Turssi, C.P., Ferracane, J.L. Vogel, K. 2005. Filler features and their effects on wear and degree of conversion of particulate dental resin composites. *Biomaterials,* 26, (24) 4932–4937

Valimaki, V.V. Aro, H.T. 2006. Molecular basis for action of bioactive glasses as bone graft substitute. *Scandinavian Journal of Surgery*, 95, (2) 95-102

CHAPTER 6 AGEING OF FILLED RESIN COMPOSITES AND PMMA CEMENT

6.1 Introduction

Filled resin composites (FRCs) consisting of a polymerisable resin matrix and filler particles of different sizes, structure and bioactive behaviour may be developed as suitable materials (biocompatible) for specific orthopaedic applications. Such orthopaedic applications may include cranio-facial bone repair surgeries as a result of trauma or disease, bone void fillings and fixation of metallic prosthesis due to their set command cure and low exothermicity during polymerisation (Shirai et al. 2000). Suitable FRCs may contain 60/40wt% UDMA/TEGDMA, 20wt% bioactive glass and 50wt% barium silicate filler (low filler content) or 60/40wt% UDMA/TEGDMA, 23wt% bioactive glass and 57wt% barium silicate filler (high filler content) as was shown in Chapter 4 and Chapter 5. These FRCs exhibited the highest flexural strength and a suitable flexural modulus compared with bone. Therefore FRCs containing 23wt% bioactive glass (high filler content) exhibited slightly lower values of flexural modulus (6.7-8.9GPa) (Chapter 4, Section 4.3.2, Table 4.4) compared with cortical bone (10-20GPa) (An, 2000; Ling et al. 2009; Rahaman et al. 2011; Rho et al. 1995); whereas FRCs containing 40 or 45wt% bioactive glass (both low and high filler content) exhibited suitable flexural modulus (1.7-3.6GPa) (Chapter 4, Section 4.3.2, Table 4.4) for trabecular bone (0.1-5GPa) (An, 2000; Ling et al. 2009; Rahaman et al. 2011; Rho et al. 1995). FRCs containing 20wt% bioactive glass (low filler content) exhibited slightly higher values of flexural modulus (5.8-6.9GPa) (Chapter 4, Section 4.3.2, Table 4.4) compared with trabecular bone (0.1-5GPa) (An, 2000; Ling et al. 2009; Rahaman et al. 2011; Rho et al. 1995). These FRCs can, thus, possibly be used in repairing bone tissue and restoring function as such FRCs exhibit flexural modulus values that are similar to the flexural modulus of bone. Therefore, such FRCs may provide increased resilience and limit stress shielding in the adjacent bone.

Moreover, bioactive glass filler was shown to increase the attachment, viability, proliferation and differentiation of osteogenic cells to osteoblasts (Pryor et al. 2009; Rahaman et al. 2011, Soundrapandian et al. 2010). Thus, FRCs containing 60/40wt% UDMA/TEGDMA, 40wt% bioactive glass and 30wt% barium silicate filler (low filler content) or 60/40wt% UDMA/TEGDMA, 45wt% bioactive glass and 34wt% barium silicate filler (high filler content) may provide enhanced biocompatibility to surrounding hard and soft tissue, due to increased bioactive glass content. However, increasing the content of bioactive glass in the FRCs may have a detrimental impact on the mechanical properties of the FRCs, when exposed to an aqueous solution as encountered in the body. Therefore, following assessment of the water sorption and solubility of these FRCs (Chapter 5), the impact of aqueous solution compared with dry environment on the mechanical behaviour of the FRCs was analysed to determine any significant differences in strength and modulus of these filled resin composites. The size, amount and type of filler particles as well as the mass of resin present in the FRCs have an impact on the amount of liquid absorbed from an aqueous environment as it was shown in Chapter 5. Following immersion or exposure to a liquid environment the strength of FRCs commonly decreases in association with the absorption of water into the material (Gohring et al. 2002; Musanje et al. 2001; Podgorski, 2010; Sideridou et al. 2003; Soderholm and Roberts, 1990).

The aims of this chapter were to determine the impact of short, medium and long water immersion periods on the flexural strength and flexural modulus of the most suitable developed FRCs formulations as well as those containing the highest amount of bioactive glass: 60/40wt% UDMA/TEGDMA, 20wt% bioactive glass and 50wt% barium silicate glass or 60/40wt% UDMA/TEGDMA, 40wt% bioactive glass and 30wt% barium silicate glass (low filler content) or 60/40wt% UDMA/TEGDMA, 23wt% bioactive glass and 57wt% barium silicate glass or

60/40wt% UDMA/TEGDMA, 45wt% bioactive glass and 34wt% barium silicate glass (high filler content).

6.2 Materials and methods

For the synthesis of FRCs containing bioactive glass and barium silicate filler refer to Chapter 2, Section 2.3.

For synthesis of PMMA cement, refer to Chapter 2, section 2.4.

For the preparation and light curing of specimens for mechanical (three point bend) testing refer to Chapter 2, Section 2.5.

6.2.1 Water immersion of filled resin composites and PMMA cement

FRCs and PMMA rectangular bar specimens were wet aged for 12 months (time periods: 1 day, 7 days, 1 month, 3 months, 6 months, 9 months and 12 months) at 37°C. For each sample condition, there were 10 rectangular bars made, which were placed in Petri dishes covered with aluminium foil. Each Petri dish contained 30ml of double distilled water (changed every 7days) and the analysis was performed on wet specimens.

For the mechanical (three point bend) testing of FRCs and PMMA refer to Chapter 2, Section 2.7.

6.2.2 Fracture surface of filled resin composite specimens

Scanning electron microscopy (SEM) may be used to determine the mechanism of failure of RBCs subjected to load following three point bend testing (Du and Zheng, 2008). Thus, SEM was used to analyse the fracture surface of FRCs following each water immersion period: 1 day, 7 days, 1, 3, 6, 9, or 12 months. Each FRC specimen was mounted on an aluminium specimen stub and sputter coated with a gold layer for 2min to minimise charge accumulation during testing using a sputter coater (Emitech K55OX, Quorum Technologies Ltd, UK) (Berger et al. 2009; Lin et al. 2000; Tian et al. 2008). Each FRC specimen was examined using a scanning electron microscope (EVO MA10, ZEISS, Germany) operating in backscatter electron

mode under high vacuum. The filament gun conditions were kept constant throughout the experiment through the control of the spot size and the operating current and maintaining the accelerating voltage at 5kV (Palin et al. 2005; Sideridou et al 2007). Representative sections of fracture surfaces of each FRC sample condition were photographed at x1500 magnification**.**

6.2.3 Statistical analysis

Minitab statistical software (Minitab, UK) was used to analyse the data using one-way analysis of variance (ANOVA) test. A difference of $P<0.05$ was considered statistically significant. The Anderson-Darling test was used to determine whether the data followed a normal distribution. Tukey's post hoc tests were used for pair-wise comparison using a significance value of $P=0.05$.

6.3 Results

6.3.1 The impact of wet ageing on the flexural strength and modulus of PMMA and filled resin composites

FRCs and PMMA were subjected to three point bend test to assess the FS and FM values of each condition following water immersion for 1 day, 7 days, 1 month, 3 months, 6 months, 9 months and 12 months.

For analysis of significant differences between the flexural strength values of filled resin composites and PMMA refer to Appendix 4, Tables 4.1-4.14. There was a general decrease in the FS of FRCs following water immersion for 12 months (maximum immersion period) compared with 1 day (Figure 6.2, 6.6). The low filler content FRCs containing 20wt% Type II, or 40wt% Type III bioactive glass filler exhibited similar FRCs at 1 day compared with 12 months wet ageing ($p>0.052$) (Figure 6.1, 6.2). The high filler content FRCs containing 23wt% Type I bioactive glass filler also exhibited a similar FS value at 1 day compared with 12 months wet ageing ($p=0.078$) (Figure 6.5, 6.6). All the other FRCs containing bioactive glass filler exhibited a decrease in FS value at 12 months compared with 1 day wet ageing ($p<0.030$). Low filler FRCs containing 70wt% barium silicate filler exhibited an increase in FS value at 1 day compared with 12 months wet ageing ($p=0.025$). High filler FRCs containing 80wt% barium silicate filler exhibited similar FS value at 1 day compared with 12 months wet ageing ($p=0.827$) (Figure 6.5, 6.6). The %decrease in flexural strength of filled resin composites containing low filler content increased with a decrease in the filler size in the order: NS40<SIL40<AB40<NS20<SIL20<AB20 (Figure 6.2).

The FS of filled resin composites (low filler content) containing bioactive glass and barium silicate filler increased in the order: Type II composite (40wt%)< Type I composite (40wt%)<

Type III composite (40wt%)< Type I composite (20wt%)< Type II composite (20wt%)< Type III composite (20wt%)< Control, following water immersion at 37°C for 12 months (Figure 6.1). The filled resin composites (low filler) containing bioactive glass and barium silicate filler exhibited an increase in FM in the order: Type II composites (40wt%)< Type III composites (40wt%)< Type I composites (40wt%)< Type III composites (20wt%)< Type I composites (20wt%)< Type II composites (20wt%)< Control, following water immersion at 37°C for 12 months (Figure 6.3).

The FS of resin composites (high filler content) increased in the order: Type II composites (45wt%)< Type I composites (45wt%)< Type I composites (23wt%)< Type III composites (23wt%)< Type II composites (23wt%)< Control following water immersion at 37°C for 12 months (Figure 6.5). The %decrease in flexural strength of filled resin composites containing high filler content increased with increasing filler size in the order: SIL45<SIL23<NS23<NS45<AB23 (Figure 6.6).

For analysis of significant differences between the flexural modulus values of filled resin composites and PMMA refer to Appendix 4, Tables 4.14-4.28. There was a general increase in the FM value of FRCs containing bioactive glass filler at 12 months compared with 1 day wet ageing. However, FRCs containing low filler Type III 20wt% bioactive glass and FRCs containing high filler 23wt% (Type I and Type III) and 40wt% Type II exhibited a decrease in FM values at 12 months compared with 1 day wet ageing ($p<0.004$). The FRCs containing low filler Type II (20 and 40wt%) bioactive glass filler exhibited similar FM value at 12 months compared with 1 day wet ageing ($p=0.595$, $p=0.8804$, respectively). The %decrease in the flexural modulus of filled resin composites containing low filler content increased with increasing filler size in the order: NS40<SIL40<NS20<SIL0<AB40<AB20 (Figure 6.4).

The filled resin composites (high filler) containing bioactive glass and barium silicate filler exhibited an increase in FM in the order: Type II composites (45wt%)< Type I composites (45wt%)< Type I composites (23wt%)< Type II composites (23wt%)< Type III composites (23wt%)< Control following water immersion at 37°C for 12 months (Figure 6.7). The %decrease in the flexural modulus of filled resin composites containing high filler content increased with decreasing filler content in the order: NS45<SIL45<NS23<AB23<SIL23 (Figure 6.8).

The specimens containing the highest amount of bioactive glass filler (40 or 45wt% (low and high filler content)) exhibited lower FS compared with filled resin composites containing 20 or 23wt% bioactive glass (low and high filler content).

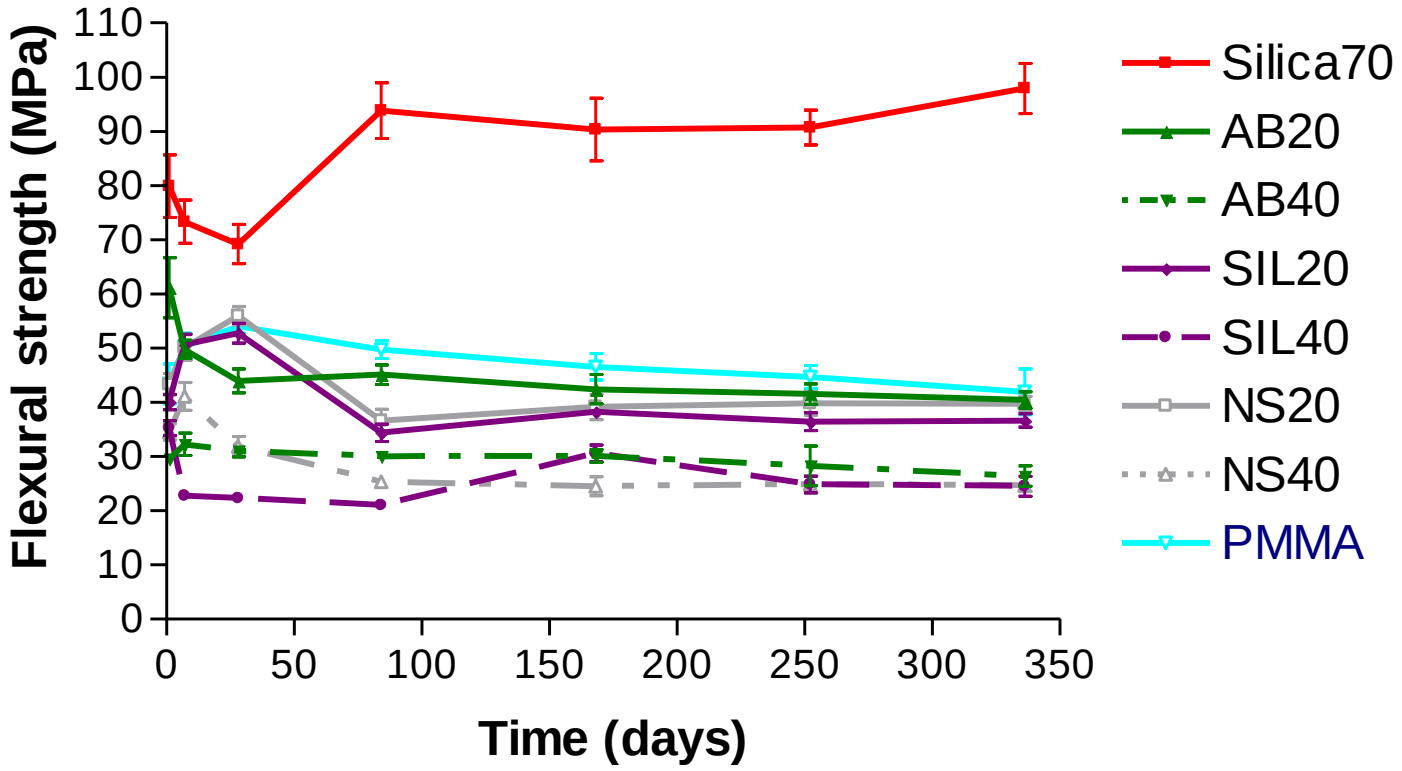

Figure 6.1 Flexural strength of filled resin composites (low filler content) tested following wet ageing for 1 day, 7 days, 1 month, 3 months, 6 months, 9 months and 12 months. Filled resin composite percentage inclusions are shown within bar labels. Silica70 refers to filled resin composites containing 70wt% barium silicate filler. SIL20 and SIL40 refer to Type I filled resin composites. NS20 and NS40 refer to Type II filled resin composites. AB20 and AB40 refer to Type III filled resin composites. The filled resin composites containing 20wt% bioactive glass exhibited higher flexural strength compared with the filled resin composites containing 40wt% bioactive glass.

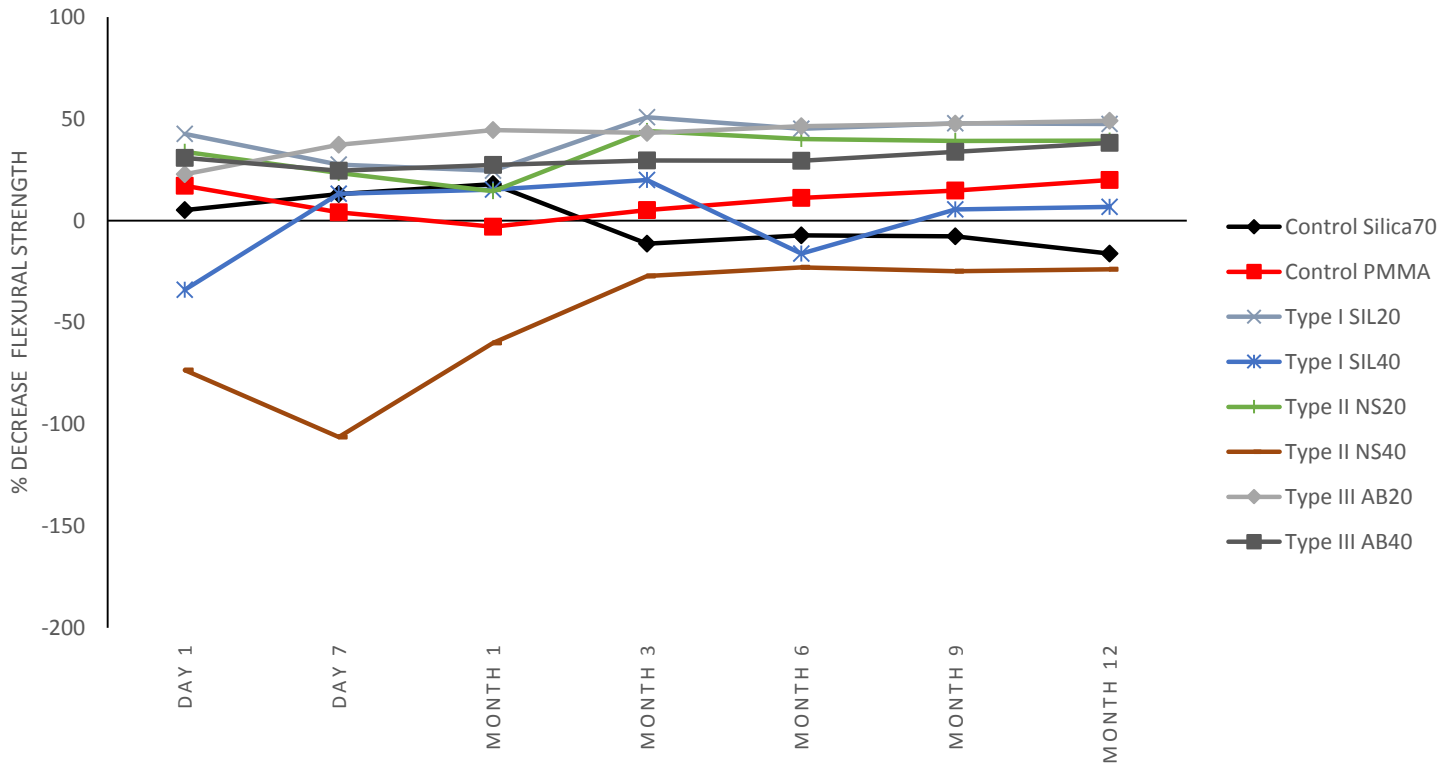

Figure 6.2 The %decrease in flexural strength of filled resin composites (low filler content) tested following wet ageing for 1 day, 7 days, 1 month, 3 months, 6 months, 9 months and 12 months compared with specimens tested dry. Negative values denote a % increase in the flexural strength of such filled resin composites. Filled resin composite percentage inclusions are shown within bar labels. Silica70 refers to filled resin composites containing 70wt% barium silicate filler. SIL20 and SIL40 refer to Type I filled resin composites. NS20 and NS40 refer to Type II filled resin composites. AB20 and AB40 refer to Type III filled resin composites. The %decrease in flexural strength of filled resin composites containing low filler content increased with a decrease in the filler size in the order: NS40<SIL40<AB40<NS20<SIL20<AB20.

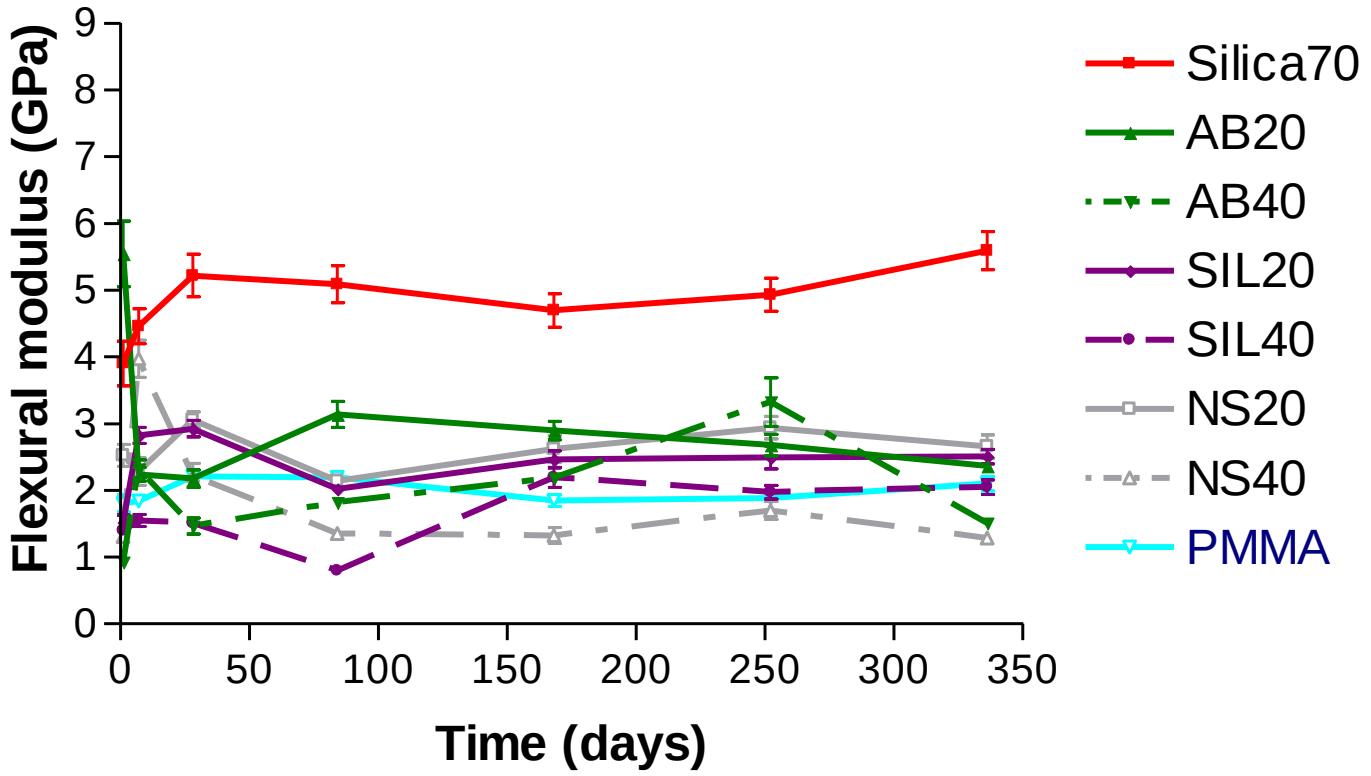

Figure 6.3 Flexural modulus of filled resin composites (low filler content) tested following wet ageing for 1 day, 7 days, 1 month, 3 months, 6 months, 9 months and 12 months. Filled resin composite percentage inclusions are shown within bar labels. Silica70 refers to filled resin composites containing 70wt% barium silicate filler. SIL20 and SIL40 refer to Type I filled resin composites. NS20 and NS40 refer to Type II filled resin composites. AB20 and AB40 refer to Type III filled resin composites. The filled resin composites containing 20wt% bioactive glass exhibited higher flexural modulus compared with filled resin composites containing 40wt% bioactive glass.

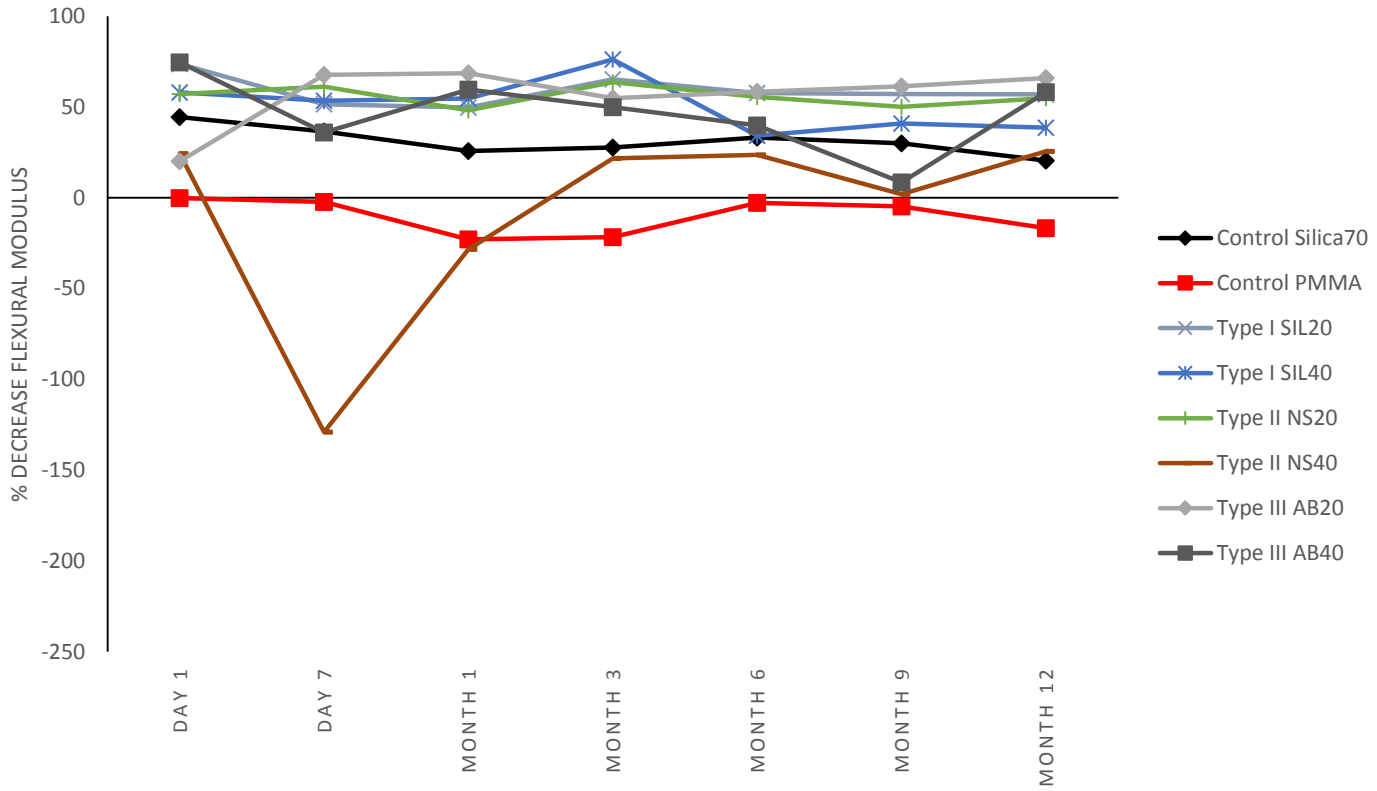

Figure 6.4 The %decrease in the flexural modulus of filled resin composites (low filler content) tested following wet ageing for 1 day, 7 days, 1 month, 3 months, 6 months, 9 months and 12 months compared with specimens tested dry. Negative values denote a % increase in the flexural modulus of such filled resin composites. Filled resin composite percentage inclusions are shown within bar labels. Silica70 refers to filled resin composites containing 70wt% barium silicate filler. SIL20 and SIL40 refer to Type I filled resin composites. NS20 and NS40 refer to Type II filled resin composites. AB20 and AB40 refer to Type III filled resin composites. The %decrease in the flexural modulus of filled resin composites containing low filler content increased with increasing filler size in the order: NS40<SIL40<NS20<SIL0<AB40<AB20.

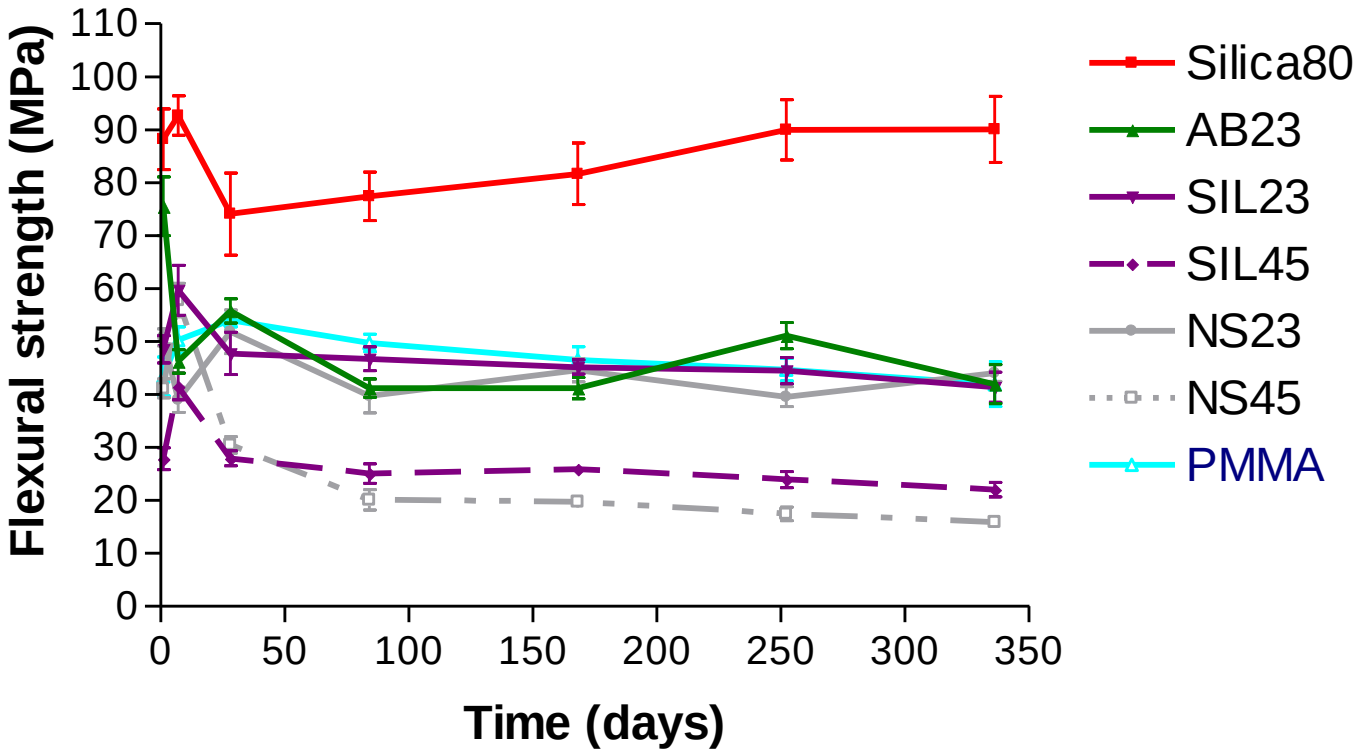

Figure 6.5 Flexural strength of filled resin composites (high filler content) tested following wet ageing for 1 day, 7 days, 1 month, 3 months, 6 months, 9 months and 12 months. Filled resin composite percentage inclusions are shown within bar labels. Silica80 refers to filled resin composites containing 80wt% barium silicate filler. SIL23 and SIL45 refer to Type I filled resin composites. NS23 and NS45 refer to Type II filled resin composites. AB23 refers to Type III filled resin composites. The filled resin composites containing 23wt% bioactive glass exhibited higher flexural strength and flexural modulus compared with filled resin composites containing 45wt% bioactive glass.

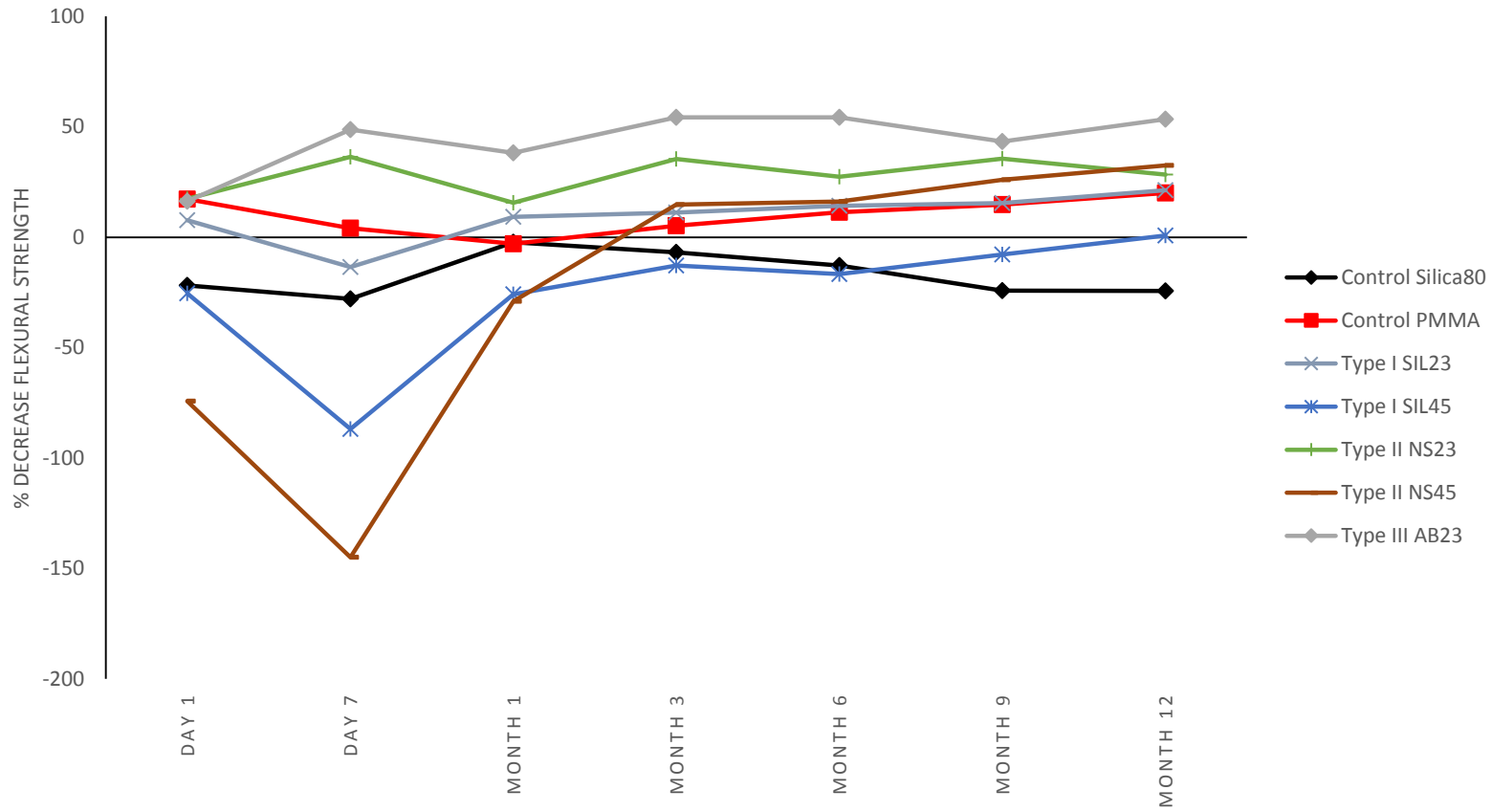

Figure 6.6 The %decrease in the flexural strength of filled resin composites (high filler content) tested following wet ageing for 1 day, 7 days, 1 month, 3 months, 6 months, 9 months and 12 months compared with specimens tested dry. Negative values denote a % increase in the flexural strength of such filled resin composites. Filled resin composite percentage inclusions are shown within bar labels. Silica80 refers to filled resin composites containing 80wt% barium silicate filler. SIL23 and SIL45 refer to Type I filled resin composites. NS23 and NS45 refer to Type II filled resin composites. AB23 refers to Type III filled resin composites. The %decrease in flexural strength of filled resin composites containing high filler content increased with increasing filler size in the order: SIL45<SIL23<NS23<NS45<AB23.

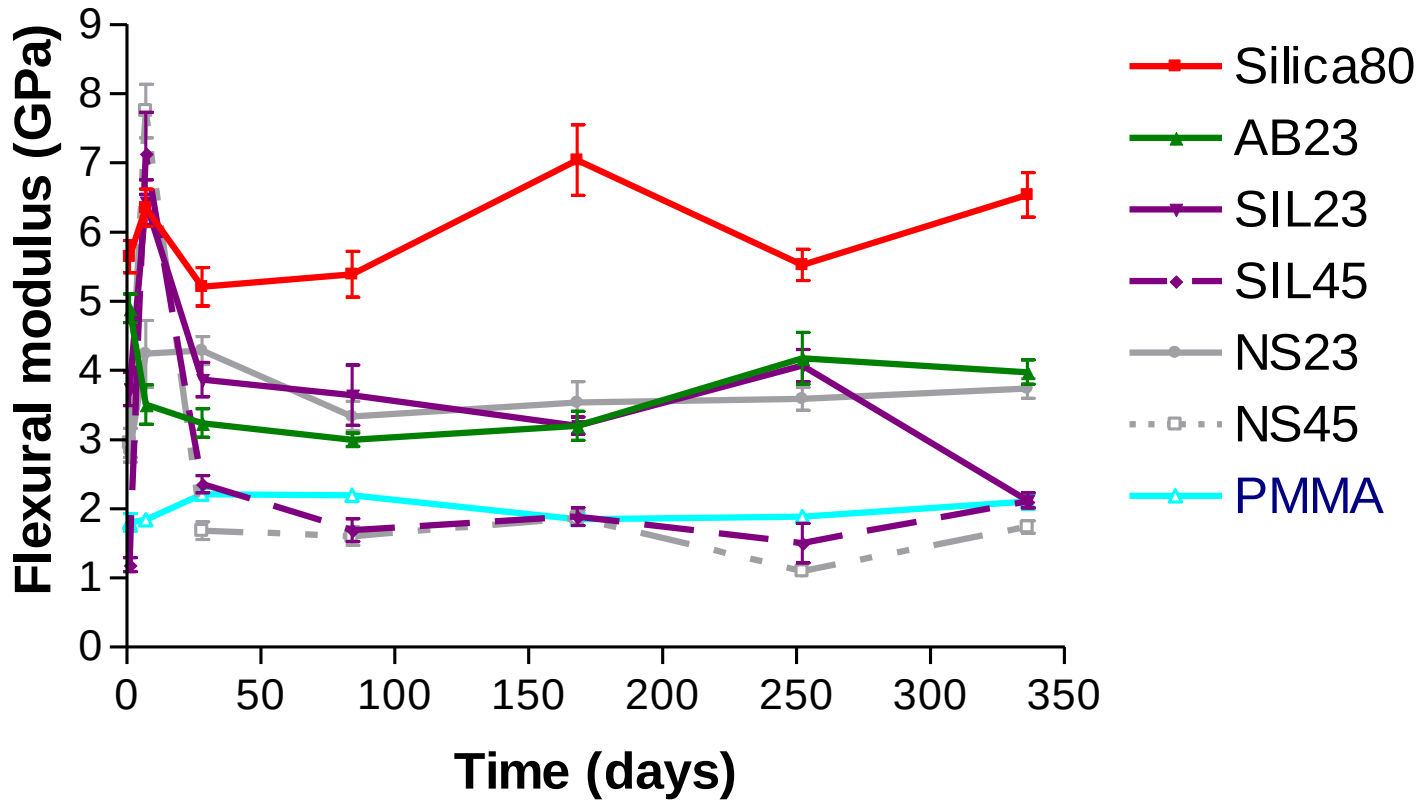

Figure 6.7 Flexural modulus of filled resin composites (high filler content) tested following wet ageing for 1 day, 7 days, 1 month, 3 months, 6 months, 9 months and 12 months. Filled resin composite percentage inclusions are shown within bar labels. Silica80 refers to filled resin composites containing 80wt% barium silicate filler. SIL23 and SIL45 refer to Type I filled resin composites. NS23 and NS45 refer to Type II filled resin composites. AB23 refers to Type III filled resin composites. The Type II resin composites containing 23wt% bioactive glass exhibited higher flexural modulus compared with Type I and Type III filled resin composites.

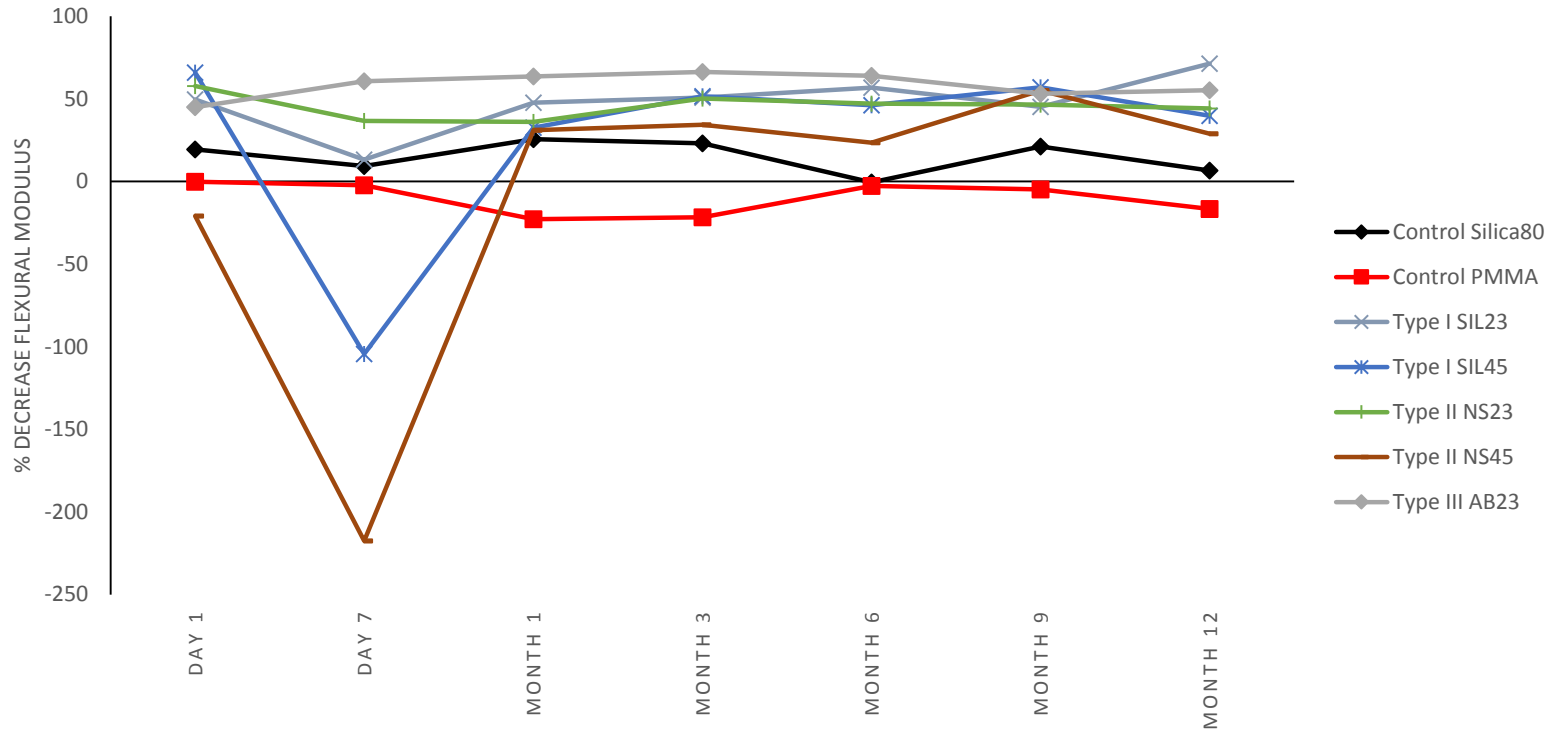

Figure 6.8 The %decrease in the flexural modulus of filled resin composites (high filler content) tested following wet ageing for 1 day, 7 days, 1 month, 3 months, 6 months, 9 months and 12 months compared with specimens tested dry. Negative values denote a % increase in the flexural strength of such filled resin composites. Filled resin composite percentage inclusions are shown within bar labels. Silica80 refers to filled resin composites containing 80wt% barium silicate filler. SIL23 and SIL45 refer to Type I filled resin composites. NS23 and NS45 refer to Type II filled resin composites. AB23 refers to Type III filled resin composites. The %decrease in the flexural modulus of filled resin composites containing high filler content increased with decreasing filler content in the order: NS45<SIL45<NS23<AB23<SIL23.

6.3.3 Fracture surface of filled resin composites

The fracture surface of filled resin composites containing 70 or 80wt% barium silicate filler (low and high filler content) exhibited a smooth surface, with evidence of fracture lines (Figure 6.9). However, the filled resin composites containing bioactive glass exhibited an irregular surface, with evidence of filler "plucking" (de-bonding of filler from the resin matrix, with a void, or gap left behind), filler "shearing" (fracture of filler particle) and de-bonding of the filler particles from the resin (fracture of the interfacial surface between the resin matrix and the filler particles) (Figure 6.9).

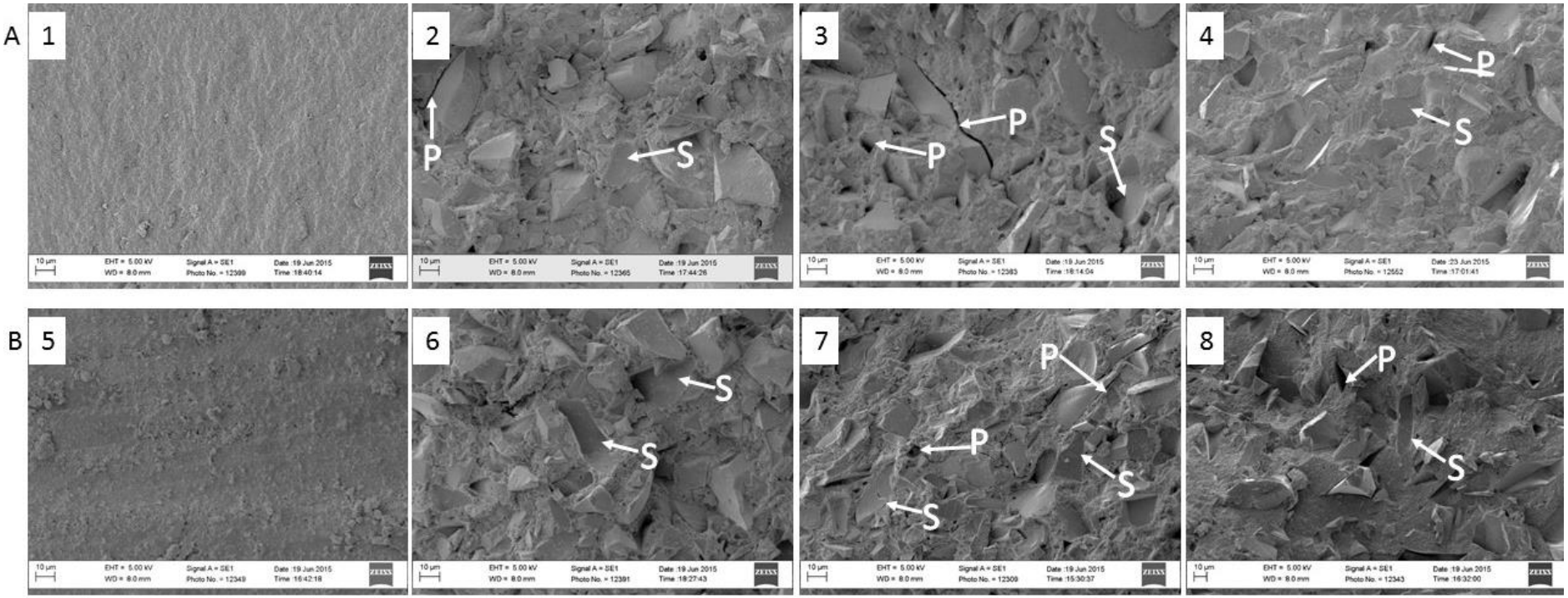

Figure 6.9 Representative SEM micrographs of the fracture morphology of filled resin composites subjected to three point bend test following water immersion for 12 months. The fractured surface was visualised using an SEM. The morphology of the fractured surface of (low (A) and high (B) filler content) FRCs containing Type I (2, 6), Type II (3, 7), or Type III (4, 8) bioactive glass filler as well as of FRCs containing 70wt% barium silicate filler (1, 5) is shown. The FRCs containing bioactive glass filler exhibited an irregular surface, with evidence of filler "plucking" (P) and filler "shearing" (S). The FRCs containing 70wt% barium silicate filler exhibited a smooth surface, with strong chemical affinity between the filler particles and the resin matrix.

6.4 Discussion

6.4.1 The impact of wet ageing on the mechanical properties of FRCs and PMMA

A key property of a material to be successfully used in orthopaedic applications with low rates of failure is a similar mechanical strength to the surrounding cortical or cancellous bone tissue as well as flexural modulus that closely matches the flexural modulus of bone in order to allow transfer of stress from the cement to the bone, when load is applied (Giannoudis et al. 2005; Lin et al. 2005; Liu et al. 2011). The maximum stress that a filled resin composite can resist before failure when subjected to load is referred to as flexural strength (FS). The FS, thus, involves the analysis of tensile strength on the lower surface of the specimen with compressive strength on the upper surface of the specimen and shear strength in parallel direction to load (Sideridou et al. 2007; Kim and Han 2004; Khaled et al. 2011). Flexural testing is probably the most precise analysis of strength of a material due to the fact that a material can only fail through separation of the planes of atoms (tensile failure), or through slipping of the planes of atoms (shear failure) (Sideridou et al. 2007). The analysis of the flexural strength and modulus of the commercial PMMA cement showed that this cement exhibited higher modulus compared with trabecular vertebral bone, thus when used in vertebroplasty, it might lead to an increase in the stiffness of the bone. The increase in the stiffness of the bone results in a transfer of stress from the treated vertebrae to neighbouring ones, ultimately leading to failure of the PMMA cement implant in the body (Boyd et al. 2008). FRCs containing bioactive glass and barium silicate fillers might provide a suitable alternative with a flexural modulus and flexural strength closer to that of the surrounding bone compared with PMMA for orthopaedic applications. The polymerisation of such filled resin composites results in the formation of a three dimensional, heterogeneous network, where barium silicate filler was added as a reinforcement filler to

maintain appropriate mechanical characteristics for orthopaedic applications as specified by Vakiparta and colleagues (Vakiparta et al. 2005). The filled resin composites contained UDMA molecules in the resin matrix, which could have influenced the viscosity and degree of conversion of the final filled resin composite material (Cornelio et al. 2014; Pfeifer et al. 2009). However, during the polymerisation process, the carbon double bonds were converted to carbon single bonds resulting in the growth of the polymer chain and formation of a highly cross-linked three dimensional polymer matrix. However, due to the decrease in the mobility of free radicals during the polymerisation process, unreacted monomer molecules and functional groups were still present in the polymer network (Cornelio et al. 2014; Floyd and Dickens 2006; Pfeifer et al. 2009). Moreover, the organic matrix had a direct impact on the mechanical characteristics and the amount of water absorption of the final composite (Deb et al. 2005). The heterogeneity of the filled resin composite containing bioactive glass filler particles and barium silicate filler might mean that there is an increased microscopic space between the polymer clusters and the filler particles resulting in the possibility of increased water infiltration in the polymer network as it was shown in Chapter 5, Section 5.3.1, which concurs with studies performed on a similar system (Sideridou et al. 2003).

			FS1 (MPa)	FS2 (MPa)	FM1 (GPa)	FM2 (GPa)
Cortical bone			50-125	-	5-15	-
Trabecular bone			2-12	-	0.1-5	-
PMMA			52.5 (10)	42.0 (13)	1.8 (0.3)	2.1 (0.3)
Silica70			84.3 (14)	97.9 (15)	7.0 (1.0)	5.6 (0.9)
Silica80			72.4 (24)	90.0 (18)	7.0 (1.7)	6.5 (1.0)
Type I	Low filler content	SIL20	69.9 (5.1)	36.6 (3.9)	5.8 (0.4)	2.5 (0.3)
		SIL40	26.3 (4.0)	24.5 (5.5)	3.3 (0.6)	2.0 (0.3)
	High filler content	SIL23	52.6 (11)	41.4 (8.9)	7.4 (1.2)	2.1 (0.3)
		SIL45	22.2 (3.6)	22.0 (4.4)	3.5 (0.7)	2.1 (0.3)
Type II	Low filler content	NS20	65.5 (7.3)	39.7 (4.6)	5.9 (0.7)	2.7 (0.5)
		NS40	19.9 (5.1)	24.7 (3.3)	1.7 (0.6)	1.3 (0.2)
	High filler content	NS23	61.4 (14)	44.0 (5.0)	6.7 (1.0)	3.7 (0.4)
		NS45	23.6 (6.0)	15.9 (3.2)	2.4 (1.0)	1.7 (0.3)
Type III	Low filler content	AB20	79.3 (8.4)	40.4 (4.8)	6.9 (0.9)	2.4 (0.2)
		AB40	42.7 (3.0)	26.4 (5.6)	3.6 (0.6)	1.5 (0.2)
	High filler content	AB23	90.3 (19)	41.9 (11)	8.9 (1.8)	4.0 (0.5)

Table 6.1 Flexural strength and modulus of bone and filled resin composites. PMMA refers to the commercially available cement; Silica70 and Silica80 refer to filled resin composites containing 70, or 80wt% barium silicate filler (low and high filler content). FS1 refers to the flexural strength of dry specimens, whereas FS2 refers to the flexural strength of specimens tested wet following 12 months water immersion. FM1 refers to the flexural modulus of dry specimens, whereas FM2 refers to the flexural modulus of specimens tested wet following 12 months water immersion. Type I, Type II and Type III filled resin composites containing 20, or 23wt% bioactive glass (low and high filler content) exhibited flexural strength values lower compared with the values for the flexural strength of cortical bone. Type I, Type II and Type III filled resin composites containing 20, 40wt% (low filler content) or 23, 45wt% (filler content) bioactive glass exhibited flexural modulus in the range of the values for the flexural modulus of both trabecular and cortical bone.

The flexural strength and flexural modulus of filled resin composites tested following water immersion was influenced by the type (silanised or non-silanised) and concentration (20 or 40wt% (low filler content) and 23 or 45wt% (high filler content)) of bioactive glass filler in the polymer network (Figures 6.1-6.8), which concurs with previous research in a similar system (Skrtic and Antonucci 2003; Kim and Han, 2004). The FRCs containing 20 or 23wt% bioactive glass filler particles (low and high filler content) exhibited higher FS compared with FRCs

containing 40 or 45wt% bioactive glass (low and high filler content) following water immersion (Figures 6.1, 6.2, 6.5, 6.6), which might have been due to stronger chemical affinity between the resin matrix and the filler particles and lower viscosity during polymerisation allowing increased conversion, which might have also resulted in decreased absorption of water, which was also indicated by Sauro, Turssi and colleagues in a similar system (Sauro et al. 2013; Turssi et al. 2005). By increasing the amount of bioactive glass filler particles from 20 to 40wt% (low filler content) or from 23 to 45wt% (high filler content) present in the FRCs, a decrease was observed in the flexural strength of such filled resin composites (Figure 6.2, 6.6), which might have been due to increased viscosity of the FRC formulation, which hindered the mobility of free radicals during polymerisation leading to the formation of a three dimensional polymer network with lower cross-linked density, which concurs with previous research in a similar system (Kim and Han, 2004; Sideridou et al. 2007). Following water immersion, the high modulus of FRCs containing 20 or 23wt% bioactive glass (low and high filler content) (Figures 6.2, 6.4) compared with dry specimens (Chapter 4, Figure 4.6) might be explained by the ability of UDMA to form hydrogen bonds and the flexibility of TEGDMA as indicated in a similar system (Emami and Soderholm 2009). Thus, FS and FM were influenced by the compatibility between the chemical structure of the resin matrix and filler particles, which had a direct impact on the transfer of stress between the resin matrix and the filler particles (Du and Zheng 2007; Khaled et al. 2011).

6.4.2 Morphology of the fractured surface of filled resin composites and PMMA

When subjected to load, the FRCs fracture through the propagation of cracks under tensile stresses (Hosseinalipour et al. 2009). Griffith's law stipulates that any flaw or defect (such as poor interfacial bonding between the filler particles and the resin matrix) occurring in the microscopic structure of the material might act as a crack (Palin et al. 2005). Following flexural

loading, a stress area forms at the interface between the filler particles and resin matrix, with failure of the filled resin composite specimen occurring when the applied load exceeds a specific point, which was greater than the ability of the filled resin composite specimen to transfer the stress between the resin matrix and the filler particles (Du and Zheng 2007). Therefore, failure of a filled resin composite specimen under a constant load might be due to the viscoelasticity of the resin matrix, the length or mechanism of the propagating crack tip (Ekworapoj et al. 2002). The fractured surface of FRCs (tested following water immersion for specified periods of time) was observed by scanning electron microscopy (SEM), which could provide information about the mechanism and location of fracture (Figure 6.9). The fracture surface of the filled resin composites showed different mechanisms of failure: adhesive, cohesive and brittle fracture (Figure 6.9), which concurs with previous research on a similar system (Sideridou et al. 2007).

Adhesive fracture involved the "plucking" of filler particles from the resin matrix, with fracture occurring at the interface between the resin matrix and filler particles. Therefore, the Type II and Type III filled resin composites exhibited adhesive fracture, which might have been due to the absence of the silanating agent, which might have decreased the bonding strength between the filler particles and the resin matrix (Figure 6.9), which concurs with previous research in a similar system (Oh et al. 1967).

Cohesive fracture involved "shearing" of filler particles because of scission of the polymer chain through hydrolytic cleavage, where the fracture occurred through the filler particle (Dewaele et al. 2005; Ito et al. 2005; Shen et al. 2004; Shirai et al. 2000). The resin matrix stretches under a constant load, whereas the filler particles are solid, which might have resulted in the start of the propagation of the crack tip at the resin filler interface, followed by propagation through the soft resin matrix, instead of through the filler particles (Curtis et al.

2009b; Ekworapoj et al. 2002; Pfeifer et al. 2009;). Thus, the filled resin composites containing only barium silicate filler exhibited a smooth, brittle surface, with oriented fracture lines with the propagating crack tip, requiring little energy for failure of specimen to occur (Figure 6.9), which concurs with previous research in a similar system (Ekworapoj et al. 2002; Kenny and Buggy 2003; Tian et al. 2008). Moreover, the FRCs containing barium silicate filler and no bioactive glass filler exhibited a fractured surface with no distinguishable interface between the resin matrix and the filler particles (Figure 6.9), which might have been related to the strong chemical affinity between the barium silicate filler and the resin matrix (Lin et al. 2000). Type I, Type II and Type III filled resin composites exhibited cohesive fracture which might have been due to the absorption of stress under flexural loading by the softer resin matrix, which was then transferred from the resin matrix to the stronger filler particles, resulting in breaking of the filler particles, which was in agreement with previous research on a similar system (Khaled et al. 2011; Shen et al. 2004; Sideridou et al. 2007).

Moreover, the filled resin composites containing both barium silicate filler and bioactive glass had a rough, heterogeneous fracture surface due to the presence of irregular filler particles with no clear crack propagation initiation site or distinguishable fracture lines (Figure 6.9), which was in agreement with previous research in a similar system (Tian et al. 2008). Thus, the propagating crack tip might have experienced the irregular filler particles as obstacles, with more energy required to break the specimen.

FRCs containing non-silanised bioactive glass fillers exhibited a fractured surface with protrusion and “plucking” (de-bonding) of particles from the resin matrix (Figure 6.9), which might have been due to the weaker chemical affinity between the organic resin matrix and inorganic filler particles because of the absence of the silanasing agent (Liu et al. 2011).

On the other hand, the irregular filler particles might have failed to dissipate or deflect the energy required for the propagation of the crack tip resulting in lower mechanical strength following water immersion in filled resin composites containing 40 or 45wt% bioactive glass (low and high filler content), which might have been due to a weaker chemical bond between the resin matrix and the filler particles (Figure 6.9). However, the propagation of the crack tip, following flexural load application, could be significantly reduced, by water infiltrating in the polymer network, due to plasticisation of the resin matrix, which decreased the amount of stress present as well as dissipated the crack (Curtis et al. 2009a). Moreover, different sizes of filler particles might have had a direct influence on the geometry of the packing of filler particles in the resin matrix (Turssi et al. 2005). Therefore, a decrease in the amount of bioactive filler particles from 40 to 20wt% (low filler content) or from 45 to 23wt% (high filler content) present in Type I, Type II and Type III filled resin composites might have led to different propagation of cracks following load application on specimens, which might have also resulted in the blunting of the progressing crack tip and higher flexural strength (Figures 6.1, 6.5, 6.9), which was in agreement with previous research on a similar system (Curtis et al. 2009a).

Moreover, the irregular filler particles also had a direct impact on the amount of filler present in the polymer network, as well as the orientation and distribution of the particles in the resin matrix (Figure 6.9), which was in agreement with previous research in a similar system (Curtis et al. 2009a). Thus, the larger size of filler particles present in the Type III compared with Type I and Type II filled resin composites might have had a detrimental effect on the surface area to volume ratio of the particles present in the resin matrix and might have also extended further through the polymer network, which might have resulted in early "filler plucking" (pull out of the filler glass particles from the resin matrix, with gaps left behind), when a load was applied to the filled resin composites specimen (Figure 6.9), which was in agreement with previous

research (Tian et al. 2008, Turssi et al. 2005). Moreover, the larger, irregular size of the particles present in Type III filled resin composites might have led to the formation of a defect area at the interface between the filler particle and the resin matrix, thereby increased the stress transfer between the filler and the resin matrix leading to stress induced damage (Figure 6.9), which was in agreement with previous research in a similar system (Curtis et al. 2009b). When the filled resin composites were tested wet at specific periods of times, it was previously noticed (Curtis et al. 2009a; Turssi et al. 2005) that for filled resin composites containing 20wt% bioactive glass filler, the water in the polymer network might have resulted in decreased area of stress between the filler particles and resin matrix due to plasticisation of the resin matrix, which might have reduced the propagation of the crack tip leading to higher mechanical strength in such filled resin composites (Figure 6.1, 6.5).

The failure of the PMMA cement under flexural loading, might have started with the crack tip propagating through the resin surface, ultimately resulting in the formation of a single, continuous crack tip (Lewis 1997; Nguyen et al. 1997). The propagation of the crack tip in the PMMA cement might have first developed in micro-defect zones (which could have been produced during mixing), which might have extended and resulted in unstable growth of the crack tip resulting in failure of the cement and thus the implant, with the fracture surface exhibiting an irregular surface on several planes (Hosseinalipour et al. 2009; Lewis 1997a; Nguyen et al. 1997). Nonetheless, the propagation of the crack tip might be stopped by the presence of pores in the polymer network, which might have led to higher mechanical strength and longevity of the final PMMA as indicated by Lewis and colleagues (Lewis 1997a, Lewis et al. 1997b).

The type, amount and size of bioactive glass filler particles influenced water sorption and solubility of filled resin composites as it was showed in Chapter 5, which in turn had an impact

on the flexural strength and modulus of these filled resin composites tested following water immersion. As these FRCs also contain bioactive glass filler particles in their composition, the effect on bone marrow stromal cells of such FRCs will be analysed (Chapter 7).

6.5 Conclusions

The filled resin composites containing 20 or 23wt% bioactive glass (low and high filler content) exhibited increased flexural strength following water immersion compared with filled resin composites containing 40 or 45wt% bioactive glass (low and high filler content), regardless of the type, size or amount of particles. The flexural modulus of these filled resins composites better matched the flexural modulus of bone compared with PMMA cement, which might make these filled resin composites containing bioactive glass a suitable alternative to PMMA cement.

6.6 Limitations of present work and recommendations for future studies

1. Only the flexural strength and modulus were analysed for these filled resin composites following water immersion. A more suitable test may involve assessing the fracture toughness of these filled resin composites following water immersion as this test assesses the ability of the FRC containing a pre-made crack to resist fracture, whereas the three point test performed in this study assess the stress and strain behaviour of the FRCs.

2. The surface composition of the filled resin composites tested following water immersion for 12 months was not analysed (limitation). Testing of the surface composition may determine the FRCs' ability to bond to bone and the mechanism through which such bonding occurs.

References

An, Y.H., Draughn, R.A., Mechanical testing of bone and the bone-implant interface. CRC Press; Boca Raton, FL:2000, p.51

Berger, S.B., Palialol, A.R.M., Cavalli, V., Giannini, M. 2009. Characterization of water sorption, solubility and filler particles of light-cured composite resins. *Brazilian Dental Journal*, 20, (4) 314-318

Boyd, D., Towler, M.R., Wren, A., Clarkin, O.M. 2008. Comparison of an experimental bone cement with surgical Simplex P, Spineplex and Cortoss. *Journal of Materials Science: Materials in Medicine,* 19, (4) 1745-1752

Cornelio, R.B., Wikant, A., Mjosund, H., Kopperud, H.M., Haasum, J., Gedde, U.W., Ortengren, U.T. 2014. The influence of bis-EMA vs bis GMA on the degree of conversion and water susceptibility of experimental composite materials. *Acta Odontologica Scandinavica,* 72, (6) 440-447

Curtis, A.R., Palin, W.M., Fleming, G.J.P., Shortall, A.C.C., Marquis, P.M. 2009a. The mechanical properties of nanofilled resin-based composites: Characterizing discrete filler particles and agglomerates using a micromanipulation technique. *Dental Materials*, 25, (2) 180-187

Curtis, A.R., Palin, W.M., Fleming, G.J.P., Shortall, A.C.C., Marquis, P.M. 2009b. The mechanical properties of nanofilled resin-based composites: The impact of dry and wet cyclic pre-loading on bi-axial flexure strength. *Dental Materials*, 25, (2) 188-197

Deb, S., Aiyathurai, L., Roether, J.A., Luklinska, Z.B. 2005. Development of high-viscosity, two-paste bioactive bone cements. *Biomaterials*, 26, (17) 3713-3718

Dewaele, M., Truffier-Boutry, D., Devaux, J., Leloup, G. 2006. Volume contraction in photocured dental resins: The shrinkage-conversion relationship revisited. *Dental Materials*, 22, (4) 359-365

Du, M. and Zheng, Y. 2007. Modification of silica nanoparticles and their application in UDMA dental polymeric composites. *Polymer Composites,* 28, (2) 198-207

Du, M. and Zheng, Y. 2008. Degree of conversion and mechanical properties studies of UDMA based materials for producing dental posts. *Polymer Composites,* 29, (6) 623-630

Emami, N., Soderholm, K. 2009. Young's Modulus and Degree of Conversion of Different Combination of Light-Cure Dental Resins. *The Open Dentistry Journal*, 3, 202-207

Ekworapoj, P., Magaraphan, R., Martin, D.C. 2002. Heat effect on viscosity and curing of light-cured dental resin and mechanical strength of conventional dental composites. *Journal of Metals, Materials and Methods,* 12, (1) 39-50

Floyd, C.J.E., Dickens, S.H. 2006. Network structure of bis-GMA- and UDMA-based resin systems. *Dental Materials*, 22, (12) 1143-1149

Gohring, T.N., Besek, M.J., Schmidlin, P.R. 2002. Attritional wear and abrasive surface alterations of composite resin materials in vitro. *Journal of Dentistry,* 30, (2-3) 119-127

Giannoudis, P.V., Dinopoulos, H., Tsiridis, E. 2005. Bone substitutes: an update. *Injury,* 36S, (3) S20-S27

Hosseinalipour, M., Javadpour, J., Rezaie, H., Dadras, T., Hayati, A.N. 2010. Investigation of Mechanical Properties of Experimental Bis-GMA/TEGDMA Dental Composite Resins

Containing Various Mass Fractions of Silica Nanoparticles. *Journal of Prosthodontics-Implant Esthetic and Reconstructive Dentistry*, 19, (2) 112-117

Ito, S., Hashimoto, M., Wadgaonkar, B., Svizero, N., Carvalho, R.M., Yiu, C., Rueggeberg, F.A., Foulger, S., Saito. T., Nishitani, Y., Yoshiyama, M., Tay, F.R., Pashley, D.H. 2005. Effects of resin hydrophilicity on water sorption and changes in modulus of elasticity. *Biomaterials,* 26, (33) 6449-6459

Kenny, S.M., Buggy, M. 2003. Bone cements and fillers: a review. *Journal of Materials Science: Materials in Medicine,* 14, (11) 923-938

Khaled, S.M.Z., Charpentier, P.A., Rizkalla, A.S. 2011. Physical and Mechanical Properties of PMMA Bone Cement Reinforced with Nano-sized Titania Fibers. *Journal of Biomaterials Applications*, 25, (6) 515-537

Kim, O., Han, S. 2004. Effect of urethane dimethacrylate diluent on the mechanical properties of hybrid-filled polymeric dental restorative composites. *Journal of Industrial and Engineering Chemistry,* 10, (3) 395-401

Lewis, G. 1997a. Properties of acrylic bone cement: State of the art review. *Journal of Biomedical Materials Research*, 38, (2) 155-182

Lewis, G., Nyman, J.S., Trieu, H.H. 1997b. Effect of mixing method on selected properties of acrylic bone cement. *Journal of Biomedical Materials Research*, 38, (3) 221-228

Lin, C.C., Huang, L.C., Shen, P.Y. 2005. Na2CaSi2O6-P2O5 based bioactive glasses. Part 1: Elasticity and structure. *Journal of Non-Crystalline Solids*, 351, (40-42) 3195-3203

Lin, C.T., Lee, S.Y., Keh, E.S., Dong, D.R., Huang, H.M., Shih, Y.H. 2000. Influence of silanisation and filler fraction on aged dental composites. *Journal of Oral Rehabilitation,* 27, (11) 919-926

Ling, L., Xu, X., Choi, G.Y., Billodeaux, D., Guo, G., Diwan, R.M. 2009. Novel F-releasing Composite with Improved Mechanical Properties. *Journal of Dental Research*, 88, (1) 83-88

Liu, X., Rahaman, M.N., Fu, Q.A. 2011. Oriented bioactive glass (13-93) scaffolds with controllable pore size by unidirectional freezing of camphene-based suspensions: Microstructure and mechanical response. *Acta Biomaterialia*, 7, (1) 406-416

Musanje, L., Shu, M., Darvell, B.W. 2001. Water sorption and mechanical behaviour of cosmetic direct restorative materials in artificial saliva. *Dental Materials,* 17, (5) 394-401

Nguyen, N.C., Maloney, W.J., Dauskardt, R.H. 1997. Reliability of PMMA bone cement fixation: fracture and fatigue crack-growth behaviour. *Journal of Materials Science: Materials in Medicine,* 8, (8) 473-483

Oh, W.S., Shen, C. 2003. Effect of surface topography on the bond strength of a composite to three different types of ceramic. *Journal of Prosthetic Dentistry,* 90, (3) 241-246

Palin, W.M., Fleming, G.J.P., Burke, F.J.T., Marquis, P.M., Randall, R.C. 2005. The influence of short and medium-term water immersion on the hydrolytic stability of novel low-shrink dental composites. *Dental Materials*, 21, (9) 852-863

Pfeifer, C.S., Silva, L.R., Kawano, Y., Braga, R.R. 2009. Bis-GMA co-polymerizations: Influence on conversion, flexural properties, fracture toughness and susceptibility to ethanol degradation of experimental composites. *Dental Materials*, 25, (9) 1136-1141

Podgorski, M. 2010. Synthesis and characterisation of novel dimethacrylates of different chain lengths as possible dental resins. *Dental Materials,* 26, (6) e188-e194

Pryor, L.S., Gage, E., Langevin, C.J., Herrera, F., Breithaupt, A.D., Gordon, C.R., Afifi, A.M., Zins, J.E., Meltzer, H., Gosman, A., Cohen, S.R., Holmes, R. 2009. Review of bone substitutes. *Craniomaxillofacial Trauma and Reconstruction*, 2, (3) 151-160

Rahaman, M.N., Day, D.E., Bal, B.S., Fu, Q., Jung, S.B., Bonewald, L.F., Tomsia, A.P. 2011. Bioactive glass in tissue engineering. *Acta Biomaterialia*, 7, (6) 2355-237

Rho, J.Y., Hobatho, M.C., Ashman, R.B. 1995. Relations of densitty and CT numbers to mechanical properties for human cortical and cancellous bone. *Medical Engineering and Physics*, 17, (5) 347-355

Sauro, S., Osorio, R., Fulgencio, R., Watson, T.F., Cama, G., Thompson, I., Toledano, M. 2013. Remineralisation properties of innovative light-curable resin-based dental materials containing bioactive micro-fillers (vol 1, pg 2624, 2013). *Journal of Materials Chemistry B*, 1, (48) 6670

Shen, C., Oh, W., Williams, J.R. 2004. Effect of post-silanisation drying on the bond strength of composite to ceramic. *The Journal of Prosthetic Dentistry,* 91, (5) 453-458

Shirai, K., Yoshida, Y., Nakayama, Y., Fujitani, M., Shintani, H., Wakasa, K., Okazaki, M., Snauwaert, J., Van Meerbeek, B. 2000. Assessment of decontamination methods as pretreatment of silanization of composite glass fillers. *Journal of Biomedical Materials Research*, 53, (3) 204-210

Sideridou, I.D., Karabela, M.M., Bikiaris, D.N. 2007. Ageing studies of light cured dimethacrylate-based dental resins and a resin composite in water or ethanol/water. *Dental Materials,* 23, (9) 1142-1149

Sideridou, I., Tserki, V., Papanastasiou, G. 2002. Effect of chemical structure on degree of conversion in light-cured dimethacrylate-based dental resins. *Biomaterials*, 23, (8) 1819-1829

Sideridou, I., Tserki, V., Papanastasiou, G. 2003. Study of water sorption, solubility and modulus of elasticity of light-cured dimethacrylate-based dental resins. *Biomaterials*, 24, (4) 655-665

Skrtic, D., Antonucci, J.M. 2003. Effect of bifunctional comonomers on mechanical strength and water sorption of amorphous calcium phosphate- and silanized glass-filled bisGMA-based composites. *Biomaterials,* 24, (17) 2881-2888

Soderholm, K.J., Roberts, M.J. 1990. Influence of water exposure on the tensile strength of composites. *Journal of Dental Research,* 69, (12) 1812-1816

Soundrapandian, C., Datta, S., Kundu, B., Basu, D., Sa, B. 2010. Porous Bioactive Glass Scaffolds for Local Drug Delivery in Osteomyelitis: Development and In Vitro Characterization. *Aaps Pharmscitech*, 11, (4) 1675-1683

Tian, M., Gao, Y., Liu, Y., Liao, Y., Hedin, N,E., Fong, H. 2008. Fabrication and evaluation of bisGMA/TEGDMA dental resins/composites containing nano fibrillary silicate. *Dental Materials,* 24, (2) 235-243

Turssi, C.P., Ferracane, J.L. Vogel, K. 2005. Filler features and their effects on wear and degree of conversion of particulate dental resin composites. *Biomaterials,* 26, (24) 4932–4937

Vakiparta, M., Forsback AP, F.A.U., Lassila LV, F.A.U., Jokinen, M.F., Yli-Urpo AU FAU - Vallittu, Vallittu, P.K. 2005. Biomimetic mineralization of partially bioresorbable glass fiber reinforced composite. *Journal of Materials Science: Materials in Medicine,* 16, (9) 873-879

CHAPTER 7 THE IMPACT OF RESIN-BASED SYSTEMS ON THE VIABILITY OF BONE MARROW STROMAL CELLS VIABILITY

7.1 Introduction

The use of PMMA cement in orthopaedic applications often leads to the formation of a fibrous capsule at the interface of the cement with the surrounding bone as well as tissue necrosis as a result of the heat released during the polymerisation reaction. These events can contribute to implant failure (Aita et al. 2010, Anselmetti et al. 2009). Moreover, the culture of primary osteoblasts in the presence of PMMA cement results in cell death, decreased expression of osteoblast phenotypic markers and increased expression of inflammatory cytokines (Aita et al. 2010). By developing alternative materials based on bioactive glass, the viability of cells and differentiation of mesenchymal stem cells down the osteoblast lineage may be enhanced, which may lead to local bone regeneration and repair. Bioactive glass is part of a specific group of bioceramics, which are able to promote the attachment, growth, proliferation and differentiation of progenitor cells into osteoblasts enabling the formation of new bone at the interface between the implant and living tissue. One postulated mechanism for this effect is the dissolution of calcium ions, which may stimulate osteogenic cells to form new bone matrix (Jones 2013; Pamula et al. 2011; Pryor et al. 2009; Rahaman et al. 2011; Soundrapandian et al. 2010). The ability of bioactive glass to bond with bone is further enhanced reportedly through the specific concentration of silica (45wt%) in its composition (Cacciotti et al. 2012; Hench 2006; Martin et al. 2009). The dissolution of calcium ions from the bioactive glass when exposed to an aqueous environment is understood to initiate the formation of a layer of hydroxyl calcium apatite on its surface, due to the exchange of calcium cations with hydrogen ions with the tissue fluid (Martin et al. 2009). Thus, bioactive glass may form an interfacial bond with the

surrounding soft and hard tissue through the formation of a surface layer comprised of carbonate-containing hydroxyapatite. This may be due to its decreased SiO_2 concentration, the increased amount of Na_2O and increased CaO/P_2O_5 ratio, which subsequently may enable collagen secretion directly onto the surface of the bioactive glass when exposed to culture media (Brauer et al. 2010; Jones 2013; Lusvardi et al. 2009; Pamula et al. 2011; Pryor et al. 2009; Rahaman et al. 2011; Soundrapandian et al. 2010). Due to their potential to increase the pH, bioactive glasses may also exhibit antimicrobial characteristics, reducing the risk of post-operative infection (Sauro et al. 2013). However, a significant increase in pH may also have a detrimental effect on the viability and proliferation of cells surrounding the implant such as blood cells.

By culturing osteoblasts in the presence of FRCs containing bioactive glass, their increased attachment and proliferation was noted, furthermore differentiation of mesenchymal stem cells into osteoblast-like cells has also been reported in a similar system (Cacciotti et al. 2012; Wang et al. 2011). These cellular events were attributed to increased expression of alkaline phosphatase, osteocalcin and Type I collagen, which ultimately lead to bone regeneration and repair and were postulated to be mediated by the release of calcium and silicon ions from the material (Cacciotti et al. 2012; Wang et al. 2011). Indeed, following immersion in culture media, FRCs containing bioactive glass exhibit dissolution of calcium and sodium ions and formation of a polycrystalline hydroxy carbonate apatite and hydrated silica on their surface. The formation of this bilayer reportedly leads to recruitment of the growth factor IGFII (insulin growth factor II) and initiation of repair of tissue surrounding the implant, through the promotion of attachment, proliferation and differentiation of osteoblasts; a process that takes 6 to 12 days to complete (Hench 2006).

The aims of this study were to analyse the viability of bone marrow stromal cells containing mesenchymal stem cells cultured in direct contact with resin-based composites and PMMA cement and the impact such composites and PMMA have on the acidity of the culture media.

7.2 Materials and methods

7.2.1 Culture and transport media

All culture media and its components were purchased from Sigma Aldrich (UK), unless otherwise stated. All culture media were generated under aseptic conditions within a laminar flow hood and stored under sterile conditions at 4^0C.

α-MEM (minimum essential medium eagle, Alpha modification) was synthesised using 9.6g/L α-MEM, 2.2g/L sodium bicarbonate to which double distilled water was added to make up 1L of solution to a final pH of 7.3 prior to filter sterilisation by filtration using a nitrocellulose 0.2µm filter.

Transport medium comprised of 20ml α-MEM, 2ml Penicillin/Streptomycin (penicillin/100units/ml, streptomycin/100units/ml), 500µl HEPES (2-[4-(2-hydroxyethyl)piperazin-1-yl]ethansulfonic acid) (1M) and 200µl Amphotericin (250µl/ml) (Invitrogen, USA).

Culture medium for bone marrow stromal cells (BMSCs) was made using 60ml α-MEM, 600µl Penicillin/Streptomycin, 600µl L-Glutamine, 1500µl HEPES (1M) and 9ml Foetal Calf Serum.

All media changes (every two days) were performed in the laminar flow hood. The culture medium was removed using a pipette, and replaced with fresh 12ml culture medium. Cultures were also checked visually for bacterial or fungal contamination using a phase contrast microscope (Fluovert FS, Leitz Leica, Germany).

7.2.2 Isolation of bone marrow stromal cells

Bone marrow stromal cells (BMSCs) were extracted from the femora of 250g male, Albino-Wistar rats ( ). An incision running from the angle of the knee

and a lateral, relieving incision were made, to expose the soft tissue. The femur was cleaned of external soft tissues, using a scalpel (Swann Morton, Sheffield, England) and subsequently placed in the transport medium. Femora were then placed in a petri dish, and the distal and proximal ends removed using bone cutters. A syringe containing 10ml of culture medium was used to irrigate the femur at both ends and the resulting liquid containing cells was collected into a fresh universal container. This mixture was centrifuged (Durafuge 100, Thermo electron corporation) for 3min at 1200rpm to pellet the collected cells. The supernatant was removed, and the cells were re-suspended in 5ml culture medium immediately prior to seeding in a T75 flask (Thermo Scientific, USA) containing a further 10ml culture medium. The BMSCs were allowed to adhere to the bottom of the flask, by incubating the culture at 37°C and 5% CO_2 (Panasonic Healthcare Co. Ltd; CO_2 Incubator MCO-18 AC, Japan) for 48h prior to changing the medium every 2 days. When BMSCs reached confluence, were detached from the substrate using 5ml of 0.25% Trypsin/EDTA and seeded on the top surface of disc specimens at a ratio of $5x10^3$ cells/disk.

For the preparation and light curing of unfilled resin systems and FRCs for bone marrow stromal cell viability analysis refer to Chapter 2, Section 2.5.

7.2.3 Experimental design of viability analysis of BMSCs seeded in contact with unfilled resin systems, FRCs and PMMA discs specimens

The discs corresponding to each sample condition were disinfected by immersion in 70% ethanol for 2 minutes and allowed to air dry in the laminar flow hood prior to transferring to 24 well culture plates (Figure 3.1). 300µl of 1wt% Agarose gel (used to maintain the composite disc in a fixed position) was placed into each well and a sample disc added. Cells grown in 24 well plates containing 300µl of 1wt% Agarose gel, in the absence of composite discs were used as negative controls, cells grown in the presence of composite discs containing 70 or 80wt%

barium silicate filler (low and high filler content) and cells grown in the presence of the unfilled resin system containing 60/40wt% UDMA/TEGDMA were used as positive controls. 5,000cells/well were seeded onto the cured surface (the curing light was applied to this side of the discs) of each composite disc for viability analysis and 2ml of culture medium was added to each well. Culture plates were then incubated at 37°C and 5% CO_2 (Panasonic Healthcare Co. Ltd; CO_2 Incubator MCO-18 AC, Japan) prior to cell viability analysis at 1, 3, 5, 7 and 12 days (n=3).

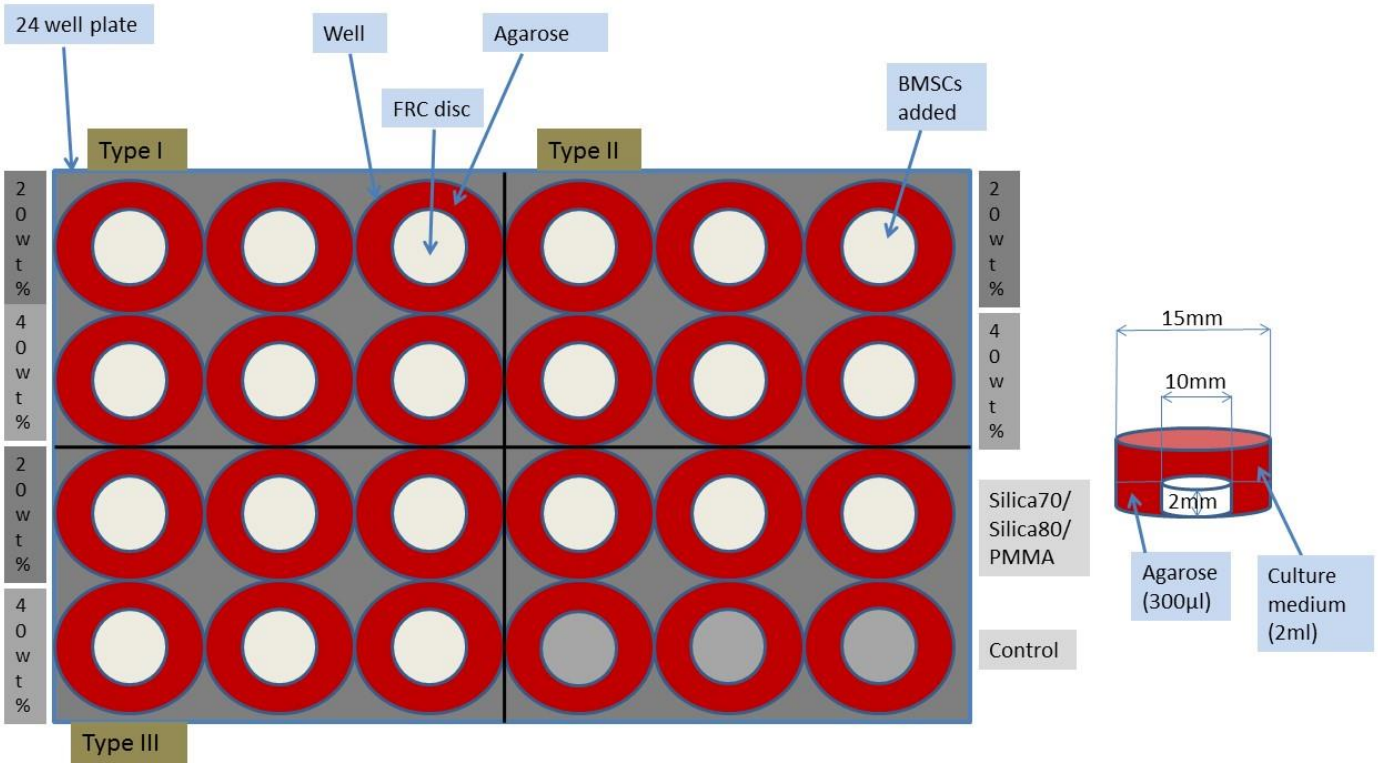

Figure 7.1 Experimental set-up for viability analysis of BMSCs seeded in direct contact on unfilled resin systems, FRCs or PMMA specimen discs. The viability of BMSCs was determined in the presence of low and high filler content FRCs containing either Type I (SIL20, SIL40, SIL23, SIL45), Type II (NS20, NS40, NS23, NS45), or Type III (AB20, AB40, AB23, AB45) bioactive glass and barium silicate filler. The viability of BMSCs in the presence of FRCs containing 70wt% barium silicate filler (Silica70) or 80wt% barium silicate filler (Silica80), PMMA, or in the absence of disc specimens (BMSCs were seeded in the space of a removed specimen disc) were used as controls. Each specimen disc was fixed to the bottom of the well with 300µl Agarose (1wt%). BMSCs ($5x10^3$) were seeded on the top surface of each disc specimen and 2ml culture medium added.

7.2.4 Viability analysis: Trypan blue staining

Cell viability was determined using Trypan blue which was used to stain non-viable cells blue, whilst viable cells remained unstained. To determine the number of viable cells found on the disk specimens at each time point (1 day, 3 days, 5 days, 7 days and 12 days), each disc was transferred to a sterile 24 well plate. Cultured cells were detached from the substrate using 1ml of 0.25% Trypsin/EDTA for each well and after cell detachment the trypsin was neutralised with 1ml of culture medium. The number of viable cells was determined by staining with 0.4% Trypan blue added to an equal volume of cell suspension. Viable cells were counted using a Neubauer-haemocytometer (Sigma Aldrich, UK) and a phase contrast microscope (Fluovert FS, Leitz Leica, Germany). The haemocytometer and the cover slips were cleaned using 70% ethanol and the cleaned cover slip was moistened with exhaled breath in order to affix it on the haemocytometer. Approximately 10µl of cell suspension/trypan blue stain was pipetted at one edge of the cover slip, to enable its uptake into the assembly by capillary action. The haemocytometer grid was then visualised using phase contrast microscopy ((Fluovert FS, Leitz Leica, Germany), where the viable cells appeared bright and colourless, whereas the dead cells appeared blue. Both viable and dead cells were counted in the 4 large, corner squares of the grid and an average value determined. The total number of viable cells in 1ml was, then, calculated:

Equation 7.1 $TC = x/4 * 2 * 10^4$;

Where TC was the number of total viable cells in 1ml; x was the average of the cell counts from the squares of the haemocytometer grid, 2 was the dilution factor (1:1 dilution of cell suspension and trypan blue stain) and 10^4 represented the volume overlying the large corner square relative to 1ml.

7.2.5 Acidity measurements

The impact of the FRCs and PMMA specimen disks on the acidity (pH) of the culture media was determined using a pH meter (Mettler-Toledo, Leicester, UK), which was calibrated prior to each experiment using pH buffer solutions (4.00±0.002 and 7.00±00,002) (Fisher Scientific, UK). The pH of the culture medium was measured at 37°C, at 1, 3, 5, 7, 12 days following BMSCs culture.

7.2.5 Statistical analysis

Minitab statistical software (Minitab, UK) was used to analyse the data using one-way analysis of variance (ANOVA) test. A difference of $P<0.05$ was considered statistically significant. Anderson-Darling test was used to determine whether the data followed a normal distribution. Tukey's post hoc tests were used for pair-wise comparison using a significance value of $P=0.05$.

7.3 Results

7.3.1 The effect of PMMA and filled resin composite discs on the acidity (pH) of culture media

The pH value at day 0 for all culture media was 7.3. For analysis of significant differences between the pH of culture media following immersion of filled resin composites and PMMA refer to Appendix 5, Tables 5.1-5.16. The pH values of the culture media following immersion of filled resin composites containing bioactive glass exhibited a marked increase in the first day ($p<0.003$) and reached a relatively constant value after day 3 up to the end of the pH measurements (which lasted 12 days). The pH of culture media following immersion of filled resin composite discs containing Type III bioactive glass filler (20 or 23wt%, low and high filler content) was ~7.6. The pH of culture media in the absence of filled resin composite discs or composite discs containing 70 or 80wt% barium silicate filler (low and high filler content) was ~7.3 and this value remained constant up to day 12. The culture media following immersion of discs containing Type II filled resin composites exhibited a pH value in excess of 7.9 (Figures 7.2, 7.3).

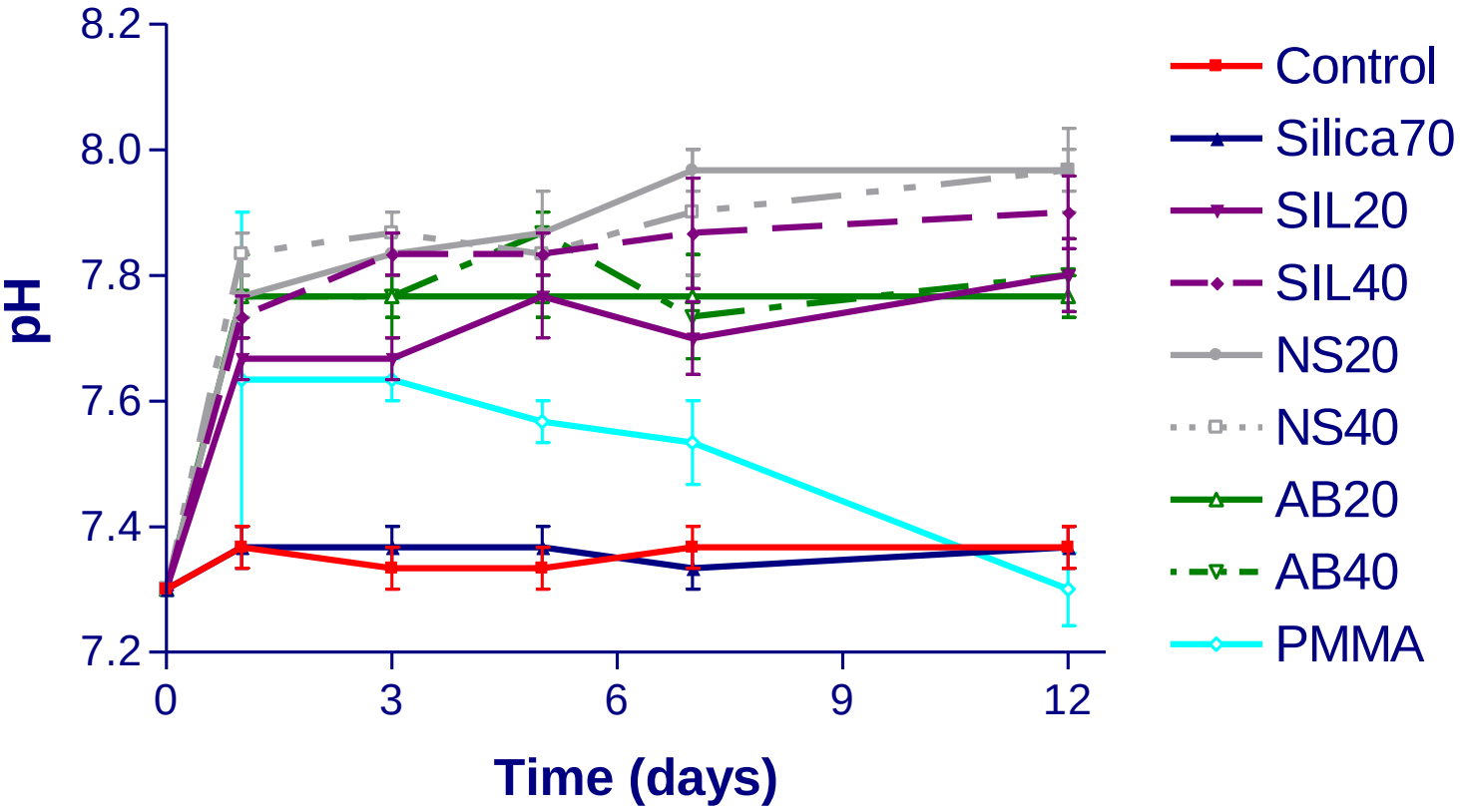

Figure 7.2 The pH of culture media following immersion of composite discs containing PMMA; Type I (SIL20, SIL40), Type II (NS20, NS40) or Type III (AB20, AB40) (low filler content) bioactive glass or 70wt% barium silicate filler (Silica70) compared with pH in the absence of composite discs (Control) in the presence of bone marrow stromal cells. The culture media following immersion of composite discs containing bioactive glass exhibited an increase in pH in the first two days, then remained at constant value for the experimental period.

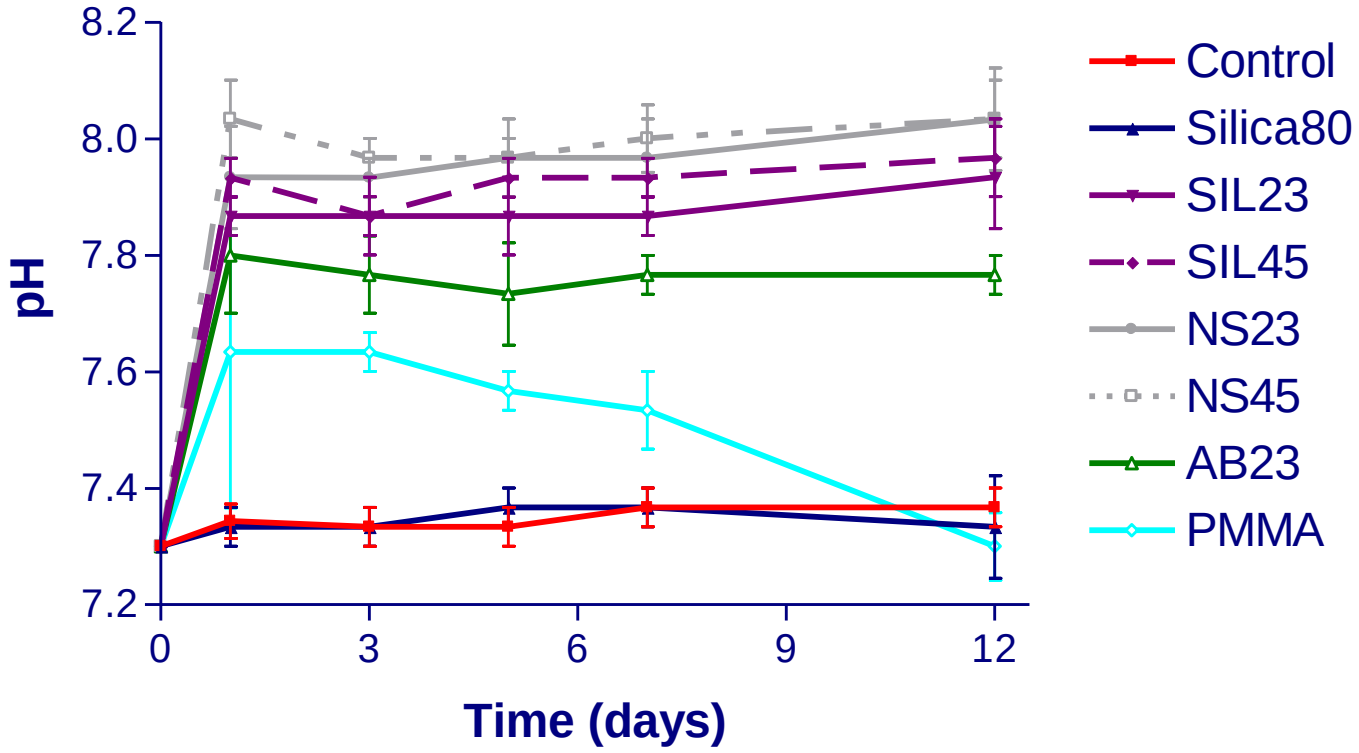

Figure 7.3 The pH of culture media following immersion of composite discs containing PMMA; Type I (SIL23, SIL45), Type II (NS23, NS45) or Type III (AB23, AB45) (high filler content) bioactive glass or 80wt% barium silicate filler (Silica80) compared with pH in the absence of composite discs (Control) in the presence of bone marrow stromal cells. The culture media following immersion of composite discs containing bioactive glass exhibited a significant increase in pH in the first two days, then reaching a relatively constant value for the remainder of the experimental period.

7.3.2 Viability of bone marrow stromal cells in the presence of unfilled resin systems, filled resin composites and PMMA cement

For analysis of significant differences between the viability values of bone marrow stromal cells seeded in the presence of unfilled resin systems, filled resin systems and PMMA refer to Appendix 5, Tables 5.17-5.34. Bone marrow stromal cells cultured in the presence of discs containing 60/40wt% UDMA/TEGDMA exhibited the lowest viability values of all sample conditions studied. There was a marked decrease in the number of viable bone marrow stromal cells seeded in direct contact on discs containing 60/40wt% UDMA/TEGDMA at day 12 compared with day 1 ($p=0.002$). There was a marked increase in the number of viable bone marrow stromal cells seeded in direct contact on discs containing filled resin composites and PMMA at day 12 compared with day 1 ($p<0.001$), with the exception of cells seeded in direct contact on filled resin composites containing 70wt% barium silicate filler ($p=0.237$).

Low filler content filled resin composites

The viability ranking of bone marrow stromal cells cultured in direct contact on composite discs containing bioactive glass was in the order: Type II, 40wt% (NS40)<Type III, 40wt% (AB40)<Type II, 20wt% (NS20)<Type III, 20wt% (AB20)<Type I, 20wt% (SIL20)<Type I, 40wt% (SIL40). Bone marrow stromal cells cultured in the absence of composite discs exhibited the highest viability, whereas when cells were cultured in the presence of composite discs containing 70wt% barium silicate filler exhibited the lowest viability. Bone marrow stromal cells cultured in the presence of composite discs containing PMMA cement exhibited similar viability compared with cells cultured in the presence of discs containing 40wt% Type II filled resin composites (Figure 7.4).

The number of non-viable bone marrow stromal cells was calculated in order to determine the total number of cells on the unfilled resin systems, filled resin composites and PMMA. For analysis of significant differences between the values for non-viable bone marrow stromal cells seeded in the presence of unfilled resin systems, filled resin systems and PMMA refer to Appendix 5, Tables 5.35-5.51. The number of non-viable bone marrow stromal cells when cultured in the presence of composite discs containing bioactive glass was in the order: (lowest to highest) Type III, 20wt% (AB20)<Type II, 20wt% (NS20)<Type I, 20wt% (SIL20)<Type II, 40wt% (NS40)<Type III, 40wt% (AB40)<Type I, 40wt% (SIL40). The number of non-viable bone marrow stromal cells cultured in the presence of resin composite discs containing 20wt% Type III bioactive glass was similar with cells cultured in the absence of composite discs. Bone marrow stromal cells cultured in the presence of composite discs containing 70wt% barium silicate filler exhibited higher non-viability compared with cells cultured in the presence of composite discs containing bioactive glass filler. The highest non-viability was exhibited by bone marrow stromal cells cultured in the presence of composite discs containing PMMA cement (Figure 7.5).

<u>High filler content filled resin composites</u>

When cells were cultured in the presence of filled resin composite discs with high filler content, the lowest viability occurred in the presence of composite discs containing barium silicate filler. The viability of bone marrow stromal cells in the presence of composite discs containing PMMA cement was lower compared with those cultured in the presence of composite discs containing bioactive glass filler. The viability of bone marrow stromal cells cultured in the presence of composite discs containing bioactive glass filler increased in the order: Type I, 23wt% (SIL23)<Type I, 45wt% (SIL45)<Type III, 23wt% (AB23)<Type II, 23wt%

(NS23)<Type II, 45wt% (NS45). Bone marrow stromal cells cultured in the absence of composite discs exhibited the highest viability (Figure 7.6).

For analysis of significant differences between the values for non-viable bone marrow stromal cells seeded in the presence of unfilled resin systems, filled resin systems and PMMA refer to Appendix 5, Tables 5.35-5.51. There was a marked increase in the number of non-viable bone marrow stromal cells seeded in direct contact on discs containing PMMA or high filler content filled resin composites containing 80wt% barium silicate filler at day 12 compared with day 1 ($p<0.001$, $p=0.006$, respectively) of all conditions studied (Figure 7.7). The number of non-viable bone marrow stromal cells, when cultured in the presence of filled resin composite discs containing bioactive glass increased in the order: Type III, 23wt% (AB23)<Type I, 23wt% (SIL23)<Type II, 45wt% (NS45)<Type I, 45wt% (SIL45)<Type II, 23wt% (NS23). Bone marrow stromal cells cultured in the presence of Type III filled resin composite discs containing 23wt% bioactive glass filler exhibited slightly lower non-viability rates than cells cultured in the absence of filled resin composite discs. Whereas the non-viability rates were higher for cells cultured in the presence of discs containing 45wt% compared with 23wt% silanated bioactive glass filler, the converse was true for non-silanated glass filler (cells exhibited higher non-viability rates in the presence of 23wt% compared with 45wt% non-silanated bioactive glass filler). The bone marrow stromal cells cultured in the presence of discs containing PMMA cement exhibited the highest non-viability (Figure 7.7).

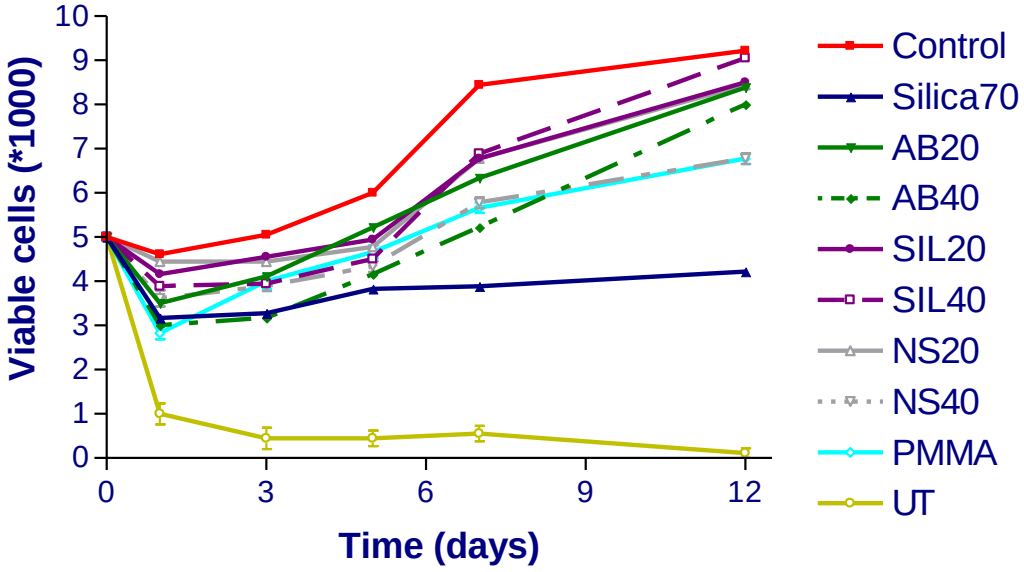

Figure 7.4 The number of viable bone marrow stromal cells cultured in direct contact on discs with low filler content. Cells seeded in the absence of disk, cells seeded in direct contact on unfilled resin systems containing 60/40wt% UDMA/TEGDMA (UT) and cells seeded in direct contact on PMMA discs were used as controls. Cells were seeded on discs containing SIL20 or SIL40 (Type I filled resin composites); NS20 or NS40 (Type II filled resin composites); AB20 or AB40 (Type III filled resin composites). Cells cultured in direct contact on discs containing 70wt% barium silicate filler (Silica70) exhibited the lowest viability. Bone marrow stromal cells cultured in the presence of discs containing 40wt% non-silanised bioactive glass filler (NS40) exhibited values for viability similar to those cultured in the absence of discs (control). The culture media was changed every 2-days. Error bars indicate standard deviation over a mean average for 3 biological samples.

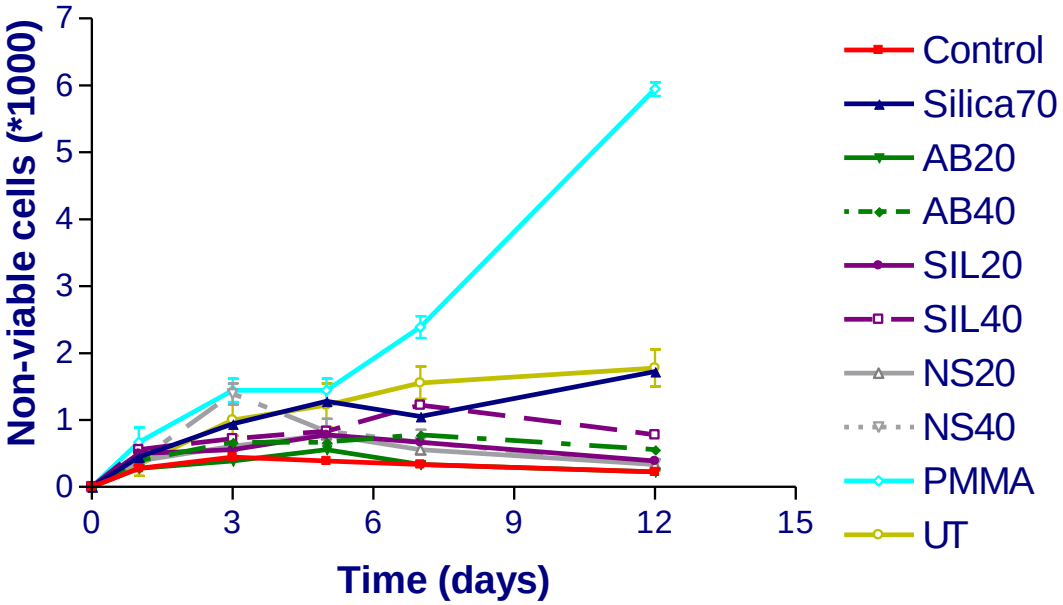

Figure 7.5 The number of non-viable cells in cultures which were in direct contact on discs with low filler content. Cells seeded in the absence of disk, cells seeded in direct contact on unfilled resin systems containing 60/40wt% UDMA/TEGDMA (UT) and cells seeded in direct contact on PMMA discs were used as controls. Cells were seeded on discs containing SIL20 or SIL40 (Type I filled resin composites); NS20 or NS40 (Type II filled resin composites); AB20 or AB40 (Type III filled resin composites). Cells cultured in the presence of discs containing 70wt% barium silicate filler (Silica70) exhibited the highest non-viability. However, cells cultured in the presence of discs containing 20wt% 45S5 bioactive glass filler (AB20) exhibited values for non-viability similar to that for cells cultured in the absence of discs (control). The culture media was replaced every 2-days. Error bars indicate standard deviation over a mean average of 3 biological samples.

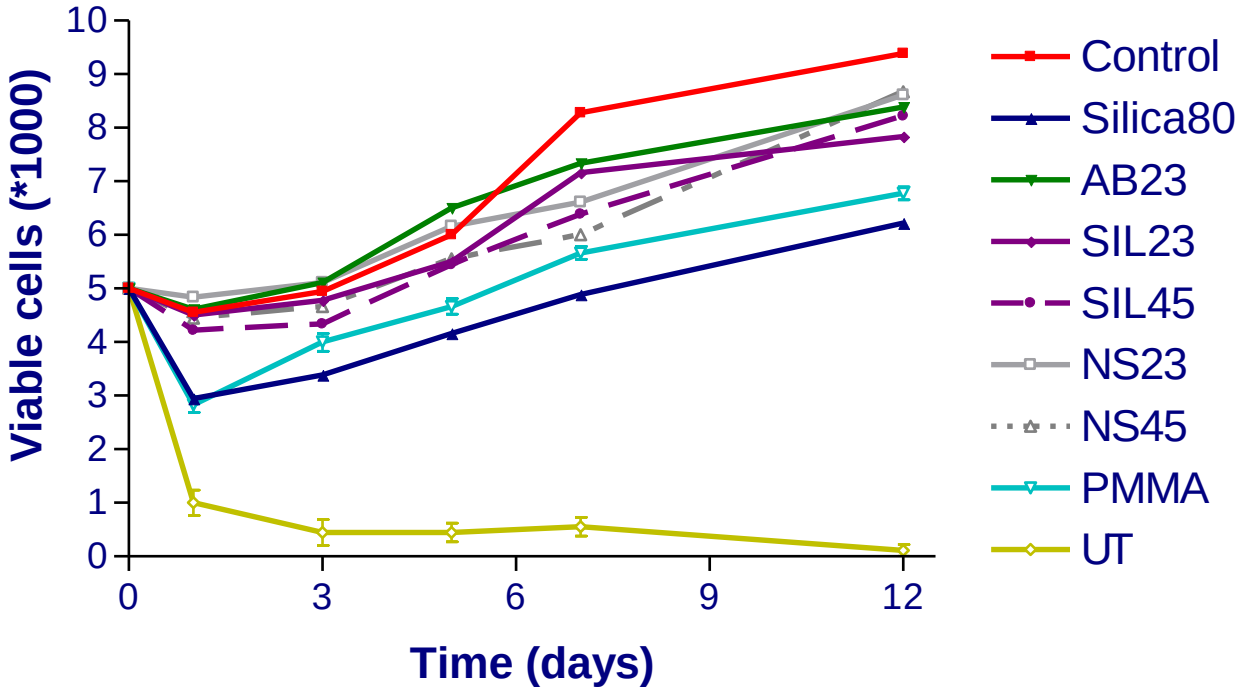

Figure 7.6 The number of viable cells in the presence of discs containing high filler content. Cells seeded in the absence of disk, cells seeded in direct contact on unfilled resin systems containing 60/40wt% UDMA/TEGDMA (UT) and cells seeded in direct contact on PMMA discs were used as controls. Cells were seeded on discs containing SIL23 or SIL45 (Type I filled resin composites); NS23 or NS45 (Type II filled resin composites); AB23 (Type III filled resin composites). Cells cultured in the presence of discs containing 80wt% barium silicate filler (Silica80) exhibited the lowest viability. However, cells cultured in the presence of discs containing 23wt% 45S5 bioactive glass filler (AB23), 23wt% non-silanated bioactive glass filler (NS23) and 455wt% non-silanated bioactive glass filler (NS45) exhibited the highest viability of cells cultured in the presence of composite discs. The cell culture medium was exchanged every 2-days. Error bars indicate standard deviation over a mean average of 3 biological samples, with some exhibiting insignificant differences.

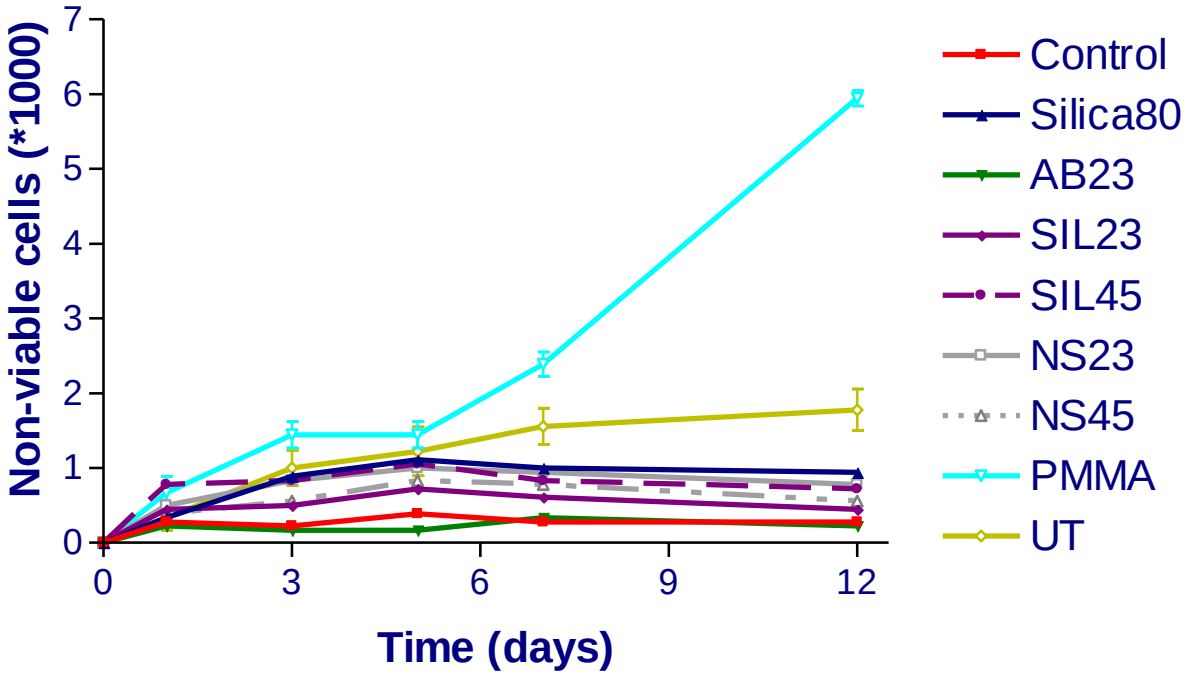

Figure 7.7 The number of non-viable cells in the presence of discs containing 60vol% filler (high filler content). Cells seeded in the absence of disk, cells seeded in direct contact on unfilled resin systems containing 60/40wt% UDMA/TEGDMA (UT) and cells seeded in direct contact on PMMA discs were used as controls. Cells were seeded on discs containing SIL23 or SIL45 (Type I filled resin composites); NS23 or NS45 (Type II filled resin composites); AB23 (Type III filled resin composites). Cells cultured in the presence of discs containing 80wt% barium silicate filler (Silica80) exhibited the lowest viability. However, the lowest number of non-viable cells occurred in the presence of discs containing 23wt% 45S5 bioactive glass filler (AB23) compared with cells cultured in the presence of composite discs; which was lower than the cells cultured in the absence of composite discs (Control). The culture media was replaced every 2-days. Error bars indicate standard deviation over a mean average of 3 biological samples.

All the cells cultured in the presence of filled resin composite discs containing bioactive glass filler exhibited higher viability compared with cells cultured in the presence of filled resin composite discs containing only barium silicate filler. The cells cultured in the presence of filled resin composite discs containing 20wt% bioactive glass filler exhibited higher viability than cells cultured in the presence of filled resin composite discs containing 40wt% bioactive glass filler with the exception of 20wt% silanated bioactive glass filler, which was lower than the 40wt%. The cells cultured in the presence of filled resin composite discs containing 40wt% non-silanated bioactive glass filler exhibited the lowest viability of all cells cultured in the presence of filled resin composite discs containing bioactive glass filler.

7.4 Discussion

Marked cell death was observed when cells were cultured in the presence of unfilled resin systems most likely due to toxic monomer leaching into the culture media, which also increased the acidity of the culture media compared with viability of cells cultured in the presence of filled resin composites. However, when cells were exposed to filled resin composites containing bioactive glass filler particles their viability was significantly increased (Figures 7.4, 7.6) compared with cells cultured in the presence of the unfilled resin system; which might have been due to the alkalinisation of the culture media. The increased cell viability when seeded in the presence of filled resin composite discs containing bioactive glass (Figures 7.4, 7.6) might have been due to the release of calcium, sodium and silica ions from the bioactive glass present in the filled resin composite discs as suggested previously on a similar system, where dissolution of these ions decreased with increasing time in culture media (Cacciotti et al. 2012; Rahaman et al. 2011; Wang et al. 2014). The low viability of bone marrow stromal cells cultured in the presence of Type I and Type II filled resin composite discs containing 40wt% bioactive glass (Figure 7.4) might have been due to a high release of phosphorous ions (>30ppm) as was suggested previously on a similar system (Goel et al. 2011). Low viability of bone marrow stromal cells, however, did not occur in the presence of Type filled resin composite discs containing 40wt% bioactive glass (Figure 7.4), which might be explained by the presence of a coupling agent between the bioactive glass and the resin matrix. The high viability of bone marrow stromal cells in the presence of filled resin composite discs containing 20 or 23wt% bioactive glass (low and high filler content) (Figure 7.4) might have been due the release of phosphorous ions from such composites in the culture media in a concentration less than 30ppm as suggested previously on a similar system (Goel et al. 2011).

Moreover, previous research had proposed that when exposed to an aqueous environment such as culture media, filled resin composite discs containing bioactive glass might have released silicon, calcium and sodium ions and might have absorbed ions of hydrogen from the water present in the culture media leading to an increase in pH, thus alkalinisation of the culture media (Brauer et al. 2010; Cacciotti et al. 2012; Cerutti et al. 2005; Sauro et al. 2013; Silver et al. 2001), which was in agreement with the current study (Figures 7.2, 7.3). The calcium ions from the filled resin composites containing bioactive glass particles reacted with the phosphate from the culture media, leading to the formation of hydroxyapatite, resulting in an increase in pH of the culture media (Huang et al. 2006). The alkalinisation of the culture media might have had a positive impact on bone cell metabolism and proliferation of osteoblasts as was suggested in previous research (Silver et al. 2001; Xynos et al. 2000). As previously suggested, the formation of collagen and hydroxyapatite required for bonding of the filled resin composite with the surrounding bone and thus for promotion of bone regeneration and repair also necessitated an alkaline pH (Silver et al. 2001; Soundrapandian et al. 2010). The compatibility of the filled resin composites containing bioactive glass filler particles might have also depended on the maintenance of a constant pH of 7.8 in the environment (in this case the culture media) (Figures 7.2, 7.3). This constant pH was suggested previously to be optimum for osteoblast viability and growth, with minimum variations in pH (Bellucci et al. 2011). The higher viability of bone marrow stromal cells cultured in the presence of filled resin composite discs containing smaller filler particle size (Type I and Type II fillers) compared with filled resin composite discs containing the larger filler particle size (Type III) might have been due to the larger surface area exhibited by the smaller particles, which might have resulted in increased cell viability (Figures 7.4-7.7), because more bioactive glass particles were exposed on the surface of the filled resin composite upon immersion in culture media, which was also shown previously on a similar

system Mousa et al. 2000). The increased viability of bone marrow stromal cells in the presence of filled resin composites containing small size filler particles (Figure 7.4) might have also been due to a rapid ion dissolution and precipitation of phosphate and calcium ions as suggested in a previous study (Wang et al. 2014).

The initial decrease observed at day 1 in bone marrow stromal cell viability in the presence of filled resin composites and PMMA (Figures 7.4, 7.6) might have been due to the fact that not all cells seeded attached on the specimen discs. Bone marrow stromal cells cultured in the presence of PMMA disks exhibited decreased viability compared with cells cultured in the presence of filled resin composite disks containing bioactive glass (Figures 7.4, 7.6). Moreover, the highest number of non-viable cells occurred in the presence of PMMA disks (Figures 7.5, 7.7), which might be explained by the significant decrease in pH (Figure 7.2), which might have had a detrimental effect on cellular metabolism.

Interestingly, the increased concentration of alkali ions in the surrounding environment from filled resin composites containing bioactive glass might also have had an antibacterial effect reducing the risk of infection as previously suggested (Sauro et al. 2013).

7.5 Conclusions

Bone marrow stromal cells cultured in the presence of filled resin composite discs containing bioactive glass exhibited significantly higher viability compared with cells cultured in the presence of unfilled resin systems containing 60/40wt% UDMA/TEGDMA, or PMMA cement. The addition of bioactive glass to filled resin composites also leads to the alkalinisation of the culture media to a pH, which was determined to be optimum for the differentiation of bone marrow stromal cells into osteoblasts and for the regeneration and repair of hard tissues.

These finding have potential applications for tissue engineering where 3D bioactive glass ceramic substrates could be used as scaffolds for in vitro production of bioengineered bone.

7.6 Limitations of present work and recommendations for future studies

1. Viability of bone marrow stromal cells was tested in direct contact on disks containing unfilled resin system, filled resin composites or PMMA in a two dimensional environment (limitation). Testing the viability of bone marrow stromal cells in a three dimensional environment (for example when seeded in hydrogel scaffolds) while in contact with the disk specimens will resemble more closely the in vivo conditions (future studies).
2. Only the pH of the culture media was determined (limitation). By testing the pH changes in the culture media and the specific ion dissolution products the molecular mechanism of bone marrow stromal cell viability in the presence of filled resin composites containing bioactive glass may be determined (future studies).

References

Aita, H., Tsukimura, N., Yamada, M., Hori, N., Kubo, K., Sato, N., Maeda, H., Kimoto, K., Ogawa, T. 2010. N-Acetyl cysteine prevents polymethyl methacrylate bone cement extract-induced cell death and functional suppression of rat primary osteoblasts. *Journal of Biomedical Materials Research Part A*, 92A, (1) 285-296

Anselmetti, G.C., Manca, A., Kanika, K., Murphy, K., Eminefendic, H., Masala, S., Regge, D. 2009. Temperature Measurement During Polymerization of Bone Cement in Percutaneous Vertebroplasty: An In Vivo Study in Humans. *Cardiovascular and Interventional Radiology*, 32, (3) 491-498

Bellucci, D., Cannillo, V., Sola, A., Chiellini, F., Gazzarri, M., Migone, C. 2011. Macroporous bioglass-derived scaffolds for bone tissue regeneration. *Ceramics international,* 37, (5) 1575-1585

Brauer, D.S., Karpukhina, N., O'Donnell, M.D., Law, R.V., Hill, R.G. 2010. Fluoride-containing bioactive glasses: Effect of glass design and structure on degradation, pH and apatite formation in simulated body fluid. *Acta Biomaterialia*, 6, (8) 3275-3282

Cacciotti, I., Lombardi, M., Bianco, A., Ravaglioli, A., Montanaro, L. 2012. Sol-gel derived 45S5 bioglass: synthesis, microstructural evolution and thermal behaviour. *Journal of Materials Sciences: Materials in Medicine,* 23, (8) 1849-1866

Cerruti, M., Greenspan, D., Powers, K. 2005. Effect of pH and ionic strength on the reactivity of Bioglass((R)) 45S5. *Biomaterials*, 26, (14) 1665-1674

Goel, A., Rajagopal RR FAU - Ferreira, J., Ferreira, J.M. 2011. Influence of strontium on structure, sintering and biodegradation behaviour of CaO-MgO-SrO-SiO(2)-P(2)O(5)-CaF(2) glasses. *Acta Biomaterialia,* 7, (11) 4071-4080

Hench, L.L. 2006. The story of Bioglass (R). *Journal of Materials Science-Materials in Medicine*, 17, (11) 967-978

Huang, W., Day, D.E., Kittiratanapiboon, K., Rahaman, M.N. 2006. Kinetics and mechanisms of the conversion of silicate (45S5), borate and borosilicate glasses to hydroxyapatite in dilute phosphate solutions. *Journal of Materials Science: Materials in Medicine,* 17, (7) 583-596

Jones, J.R. 2013. Review of bioactive glass: From Hench to hybrids. *Acta Biomaterialia,* 9, (1) 4457-4486

Lusvardi, G., Malavasi, G., Menabue, L., Aina, V., Morterra, C. 2009. Fluoride-containing bioactive glasses: Surface reactivity in simulated body fluids solutions. *Acta Biomaterialia,* 5, (9) 3548-3562

Martin, R.A., Twyman, H., Qiu, D., Knowles, J.C., Newport, R.J. 2009. A study of the formation of amorphous calcium phosphate and hydroxyapatite on melt quenched Bioglass(A (R)) using surface sensitive shallow angle X-ray diffraction. *Journal of Materials Science-Materials in Medicine*, 20, (4) 883-888

Mousa, W.F., Kobayashi, M., Shinzato, S., Kamimura, M., Neo, M., Yoshihara, S., Nakamura, T. 2000. Biological and mechanical properties of PMMA-based bioactive bone cements. *Biomaterials*, 21, (21) 2137-2146

Pamula, E., Kokoszka, J., Cholewa-Kowalska, K., Laczka, M., Kantor, L., Niedzwiedzki, L., Reilly, G.C., Filipowska, J., Madej, W., Kolodziejczyk, M., Tylko, G., Osyczka, A.M. 2011.

Degradation, Bioactivity, and Osteogenic Potential of Composites Made of PLGA and Two Different Sol-Gel Bioactive Glasses. *Annals of Biomedical Engineering*, 39, (8) 2114-2129

Pryor, L.S., Gage, E., Langevin, C.J., Herrera, F., Breithaupt, A.D., Gordon, C.R., Afifi, A.M., Zins, J.E., Meltzer, H., Gosman, A., Cohen, S.R., Holmes, R. 2009. Review of bone substitutes. *Craniomaxillofacial Trauma and Reconstruction*, 2, (3) 151-160

Rahaman, M.N., Day, D.E., Bal, B.S., Fu, Q., Jung, S.B., Bonewald, L.F., Tomsia, A.P. 2011. Bioactive glass in tissue engineering. *Acta Biomaterialia*, 7, (6) 2355-2373

Sauro, S., Osorio, R., Fulgencio, R., Watson, T.F., Cama, G., Thompson, I., Toledano, M. 2013. Remineralisation properties of innovative light-curable resin-based dental materials containing bioactive micro-fillers (vol 1, pg 2624, 2013). *Journal of Materials Chemistry B*, 1, (48) 6670

Silver, I.A., Deas, J., Erecinska, M. 2001. Interactions of bioactive glass with osteoblasts in vitro: effects of 45S5 Bioglass, and 58S and 77S bioactive glasses on metabolsim, intracellular ion concentrations and cell viability. *Biomaterials,* 22, (2) 175-185

Soundrapandian, C., Datta, S., Kundu, B., Basu, D., Sa, B. 2010. Porous Bioactive Glass Scaffolds for Local Drug Delivery in Osteomyelitis: Development and In Vitro Characterization. *Aaps Pharmscitech*, 11, (4) 1675-1683

Wang, G.C., Lu, Z.F., Liu, X.Y., Zhou, X.M., Ding, C.X., Zreiqat, H. 2011. Nanostructured glass-ceramic coatings for orthopaedic applications. *Journal of the Royal Society Interface*, 8, (61) 1192-1203

Wang, C., Xie, Y., Li, A., Shen, H., Wu, D., Qiu, D. 2014. Bioactive nanoparticle through postmodification of colloidal silica. *Applied Materials and Interfaces,* 6, (7) 4935-4939.

Xynos, I.D., Hukkanen, M.V.J., Batten, J.J., Buttery, L.D., Hench, L.L., Polak, J.M. 2000. Bioglass (R) 45S5 stimulates osteoblast turnover and enhances bone formation in vitro: Implications and applications for bone tissue engineering. *Calcified Tissue International*, 67, (4) 321-329

8. FINAL CONCLUSIONS

The majority of biomaterials used to cement artificial joints or for bone augmentation consist of PMMA based materials. PMMA based biomaterials have been used in orthopeadic applications for more then 60 years and provided a reasonable service history. However, the use of PMMA has many limitations including: a volatile liquid monomer component, which requires mixing in surgery, long working time, high setting temperature and inability to bond to bone, leading to the formation of a fibrous capsule surrounding the implant leading to adverse inflammatory responses. There have been numerous attempts to use alternative material types either by adapting existing PMMA formulations or by using new material types such as bisGMA based cements, which also suffer from adverse inflammatory responses. Therefore, in numerous orthopeadic applications including bone void filling and fixation of metallic implants there is a need for cements that are bio-compatible with surrounding hard and soft tissues and also capable of forming a bond to bone. Filled resin composites consisting of a polymerisable resin matrix and bioactive filler particles may be developed as such bio-compatible cements with surrounding soft and hard tissues for these specific orthopeadic applications.

Unfilled resin systems containing monomers with different chemical structures, thus viscosities and reactivities may be used as the base for such filled resin systems for orthopeadic applications. By testing resin formulations containing different concentrations of bisGMA, UDMA and TEGDMA, the optimum one in terms of physical and mechanical characteristics was determined to be 60/40wt% UDMA/TEGDMA. This formulation was used as the base unfilled resin system for the development of filled resin composites for orthopeadic applications. There were two types of filled resin composite cements formulated depending on viscosity referred to as low and high viscosity cement formulations (with low or high filler

content), each developed for particluar orthopeadic applications. The low viscosity cement (low filler content) was formulated for ex situ preparation, where the cement can be placed in premade molds (for example for auditory and cranio-facial repair surgeries) to harden and then placed at the required site in the body. The low viscosity cement (low filler content) may also be used as an injectable cement. This will also lead to a reduction in time and cost of the surgery due to the use of cost effective materials that are made into the required shape before surgery. The high viscosity cement (high filler content) was developed to be used and molded in shape in situ (for example for vertebroplasty surgeries, or for hand and wrist reconstruction). Changing the concentration of filler particles to the resin matrix had a crucial impact on the physical and mechanical properties of the final filled resin composite. The optimum formulation for the possible development of a material for use in orthopeadic applications was determined to be 60/40wt% UDMA/TEGDMA containing 20wt% bioactive glass filler and 50wt% barium silicate filler (low filler content) or 60/40wt% UDMA/TEGDMA containing 23wt% bioactive glass filler and 57wt% barium silicate filler (high filler content). By increasing the concentration of bioactive glass to 40 or 45wt% (low and high filler content) in filled resin composites did not result in an increase in viability of bone marrow stromal cells compared with filled resin composites containing 20 or 23w% (low and high filler content) bioactive glass. Moreover, filled resin composites containing 40 or 45wt% (low and high filler content) exhibited a decrease in flexural strength and modulus, with an increase in water sorption following wet ageing compared with filled resin composites containing 20 or 23wt% (low and high filler content) bioactive glass, regardless of the viscosity of the filled resin composites. Both low and high filler content cements, due to the presence of bioactive glass particles, were also shown to enhance proliferation of bone marrow stromal cells compared with existing PMMA cement.

Conclusively, it was shown for the first time that by incorporating bioactive glass to filled resin composites containing UDMA and TEGDMA as the base monomers, new materials can be developed for orthopeadic applications that exhibit increased bio-compatibility with surrounding soft and hard tissues while maintaining comparable physical and mechanical properties with current cement formulations.

Appendix 1 Statistical analysis of unfilled resin systems

Degree of conversion of unfilled resin systems

	20/80 BT	30/70 BT	40/60 BT	50/50 BT	60/40 BT	70/30 BT	80/20 BT	bisGMA
TEGDMA	**<0.001**	**<0.001**	**<0.001**	**<0.001**	**<0.001**	**<0.001**	**<0.001**	**<0.001**
20/80 BT		**<0.001**	**<0.001**	**<0.001**	**0.005**	0.012	0.071	**<0.001**
30/70 BT			0.552	0.639	0.034	0.013	**<0.001**	**<0.001**
40/60 BT				0.264	0.115	0.048	**<0.001**	**<0.001**
50/50 BT					0.006	**0.002**	**<0.001**	**<0.001**
60/40 BT						0.692	**<0.001**	**<0.001**
70/30 BT							**<0.001**	**<0.001**
80/20 BT								**<0.001**

Table 1.3 Significant differences between the degree of conversion of bisGMA/TEGDMA (BT) unfilled resin systems (One-way ANOVA, n=3). The numbers represent the p value, with the numbers in **bold** showing significant difference between sample conditions. Unfilled resin system percentage inclusions are shown within bar labels.

	20/80 UT	30/70 UT	40/60 UT	50/50 UT	60/40 UT	70/30 UT	80/20 UT	TEGDMA
UDMA	0.651	0.394	**0.015**	**0.034**	0.063	**<0.001**	**0.005**	**<0.001**
20/80 UT		0.268	**0.015**	**0.030**	0.053	**0.001**	**0.007**	**<0.001**
30/70 UT			0.174	0.296	0.456	**0.031**	0.138	**<0.001**
40/60 UT				0.720	0.459	0.480	0.974	**<0.001**
50/50 UT					0.708	0.263	0.712	**<0.001**
60/40 UT						0.113	0.419	**<0.001**
70/30 UT							0.401	**<0.001**
80/20 UT								**<0.001**

Table 1.4 Significant differences between the degree of conversion of UDMA/TEGDMA (UT) unfilled resins systems (One-way ANOVA, n=3). The numbers represent the p value, with the numbers in **bold** showing significant difference between sample conditions. Unfilled resin system percentage inclusions are shown within bar labels.

BUT	20/60/20	10/60/30	40/50/10	30/50/20	20/50/30	10/50/40	50/40/10	50/30/20	50/20/30	50/10/40
30/60/10	**<0.001**	**<0.001**	**0.009**	**0.002**	**<0.001**	**<0.001**	**0.001**	0.084	0.117	**0.011**
20/60/20		**<0.001**	**<0.001**	**<0.001**	**0.006**	**<0.001**	**<0.001**	**<0.001**	**<0.001**	**0.001**
10/60/30			**<0.001**	**<0.001**	**0.005**	**0.004**	**<0.001**	**<0.001**	**<0.001**	**<0.001**
40/50/10				**<0.001**	**<0.001**	**<0.001**	**0.001**	**0.006**	**0.001**	**<0.001**
30/50/20					**<0.001**	**<0.001**	**<0.001**	**<0.001**	**0.001**	**0.034**
20/50/30						**<0.001**	**<0.001**	**<0.001**	**<0.001**	**<0.001**
10/50/40							**<0.001**	**<0.001**	**<0.001**	**<0.001**
50/40/10								**<0.001**	**<0.001**	**<0.001**
50/30/20									**0.002**	**<0.001**
50/20/30										**0.024**

Table 1.5 Significant differences between the degree of conversion of bisGMA/UDMA/TEGDMA (TBU) unfilled resin systems (One-way ANOVA, n=3). The numbers represent the p value, with the numbers in **bold** showing significant difference between sample conditions. Unfilled resin system percentage inclusions are shown within bar labels.

Rate of polymerisation of unfilled resin systems

	20/80 BT	30/70 BT	40/60 BT	50/50 BT	60/40 BT	70/30 BT	80/20 BT	bisGMA
TEGDMA	**<0.001**	**<0.001**	**<0.001**	**<0.001**	**<0.001**	**<0.001**	**<0.001**	**<0.001**
20/80 BT		**<0.001**	**<0.001**	**<0.001**	**<0.001**	**<0.001**	0.146	**<0.001**
30/70 BT			0.648	0.166	0.884	0.903	**0.003**	**<0.001**
40/60 BT				0.371	0.563	0.580	**0.001**	**<0.001**
50/50 BT					0.142	0.150	**<0.001**	**<0.001**
60/40 BT						0.982	0.008	**<0.001**
70/30 BT							0.007	**<0.001**
80/20 BT								**<0.001**

Table 1.6 Significant differences between the rate of polymerisation of bisGMA/TEGDMA (BT) unfilled resin systems (One-way ANOVA, n=3). The numbers represent the p value, with the numbers in **bold** showing significant difference between sample conditions. Unfilled resin system percentage inclusions are shown within bar labels.

	20/80 UT	30/70 UT	40/60 UT	50/50 UT	60/40 UT	70/30 UT	80/20 UT	TEGDMA
UDMA	**<0.001**	**0.007**	0.233	0.334	**<0.001**	0.400	0.319	**<0.001**
20/80 UT		0.094	**0.001**	**<0.001**	0.375	**<0.001**	**<0.001**	**<0.001**
3070 UT			0.078	**0.046**	0.415	**<0.001**	**<0.001**	**<0.001**
40/60 UT				0.800	**0.009**	**0.029**	**0.022**	**<0.001**
50/50 UT					**0.005**	0.052	**0.039**	**<0.001**
60/40 UT						**<0.001**	**<0.001**	**<0.001**
70/30 UT							0.849	**<0.001**
80/20 UT								**<0.001**

Table 1.7 Significant differences between the rate of polymerisation of UDMA/TEGDMA (UT) unfilled resin systems (One-way ANOVA, n=3). The numbers represent the p value, with the numbers in **bold** showing significant difference between sample conditions. Unfilled resin system percentage inclusions are shown within bar labels.

BUT	20/60/20	10/60/30	40/50/10	30/50/20	20/50/30	10/50/40	50/40/10	50/30/20	50/20/30	50/10/40
30/60/10	**0.009**	**0.002**	**0.003**	**0.027**	0.060	0.599	**<0.001**	**<0.001**	**0.003**	**<0.001**
20/60/20		0.862	**0.001**	**0.029**	0.221	**0.006**	**<0.001**	**<0.001**	**0.001**	**<0.001**
10/60/30			**<0.001**	**<0.001**	0.116	**<0.001**	**<0.001**	**<0.001**	**0.001**	**<0.001**
40/50/10				**<0.001**	**0.002**	**0.001**	**0.001**	**0.007**	**0.032**	**0.002**
30/50/20					0.398	**<0.001**	**<0.001**	**<0.001**	**0.002**	**<0.001**
20/50/30						0.056	**<0.001**	**<0.001**	**0.002**	**<0.001**
10/50/40							**<0.001**	**<0.001**	**0.002**	**<0.001**
50/40/10								**0.001**	0.692	**0.028**
50/30/20									0.188	**0.004**
50/20/30										0.063

Table 1.8 Significant differences between the rate of polymerisation of bisGMA/UDMA/TEGDMA (BUT) unfilled resin systems (One-way ANOVA, n=3). The numbers represent the p value, with the numbers in **bold** showing significant difference between sample conditions. Unfilled resin system percentage inclusions are shown within bar labels.

Hardness of unfilled resin systems

	20/80 BT	30/70 BT	40/60 BT	50/50 BT	60/40 BT	70/30 BT	80/20 BT	bisGMA
TEGDMA	**<0.001**	**<0.001**	**<0.001**	**<0.001**	**<0.001**	**<0.001**	**<0.001**	**<0.001**
20/80 BT		**<0.001**	**<0.001**	**<0.001**	**<0.001**	**<0.001**	**<0.001**	**<0.001**
30/70 BT			**<0.001**	**<0.001**	**<0.001**	**<0.001**	**<0.001**	**<0.001**
40/60 BT				**<0.001**	**<0.001**	**<0.001**	**<0.001**	**<0.001**
50/50 BT					**<0.001**	**<0.001**	**<0.001**	**<0.001**
60/40 BT						**<0.001**	**<0.001**	**<0.001**
70/30 BT							**<0.001**	**<0.001**
80/20 BT								**<0.001**

Table 1.9 Significant differences between the upper surface (specimen was cured on this surface), hardness values of bisGMA/TEGDMA (BT) unfilled resin systems (1-way ANOVA, n=9). The numbers represent the p value, with the numbers in **bold** showing significant difference between sample conditions. Unfilled resin system percentage inclusions are shown within bar labels.

	20/80 BT	30/70 BT	40/60 BT	50/50 BT	60/40 BT	70/30 BT	80/20 BT	bisGMA
TEGDMA	**<0.001**	**<0.001**	**<0.001**	**<0.001**	**<0.001**	**<0.001**	**<0.001**	**<0.001**
20/80 BT		**<0.001**	**<0.001**	**<0.001**	**<0.001**	**<0.001**	**<0.001**	**<0.001**
30/70 BT			0.042	**<0.001**	**<0.001**	**<0.001**	**<0.001**	**<0.001**
40/60 BT				**<0.001**	**<0.001**	**<0.001**	**<0.001**	**<0.001**
50/50 BT					**<0.001**	**<0.001**	**<0.001**	**<0.001**
60/40 BT						**<0.001**	**<0.001**	**<0.001**
70/30 BT							**<0.001**	**<0.001**
80/20 BT								**<0.001**

Table 1.10 Significant differences between the lower surface hardness values of bisGMA/TEGDMA (BT) unfilled resin systems (1-way ANOVA, n=9). The numbers represent the p value, with the numbers in **bold** showing significant difference between sample conditions. Unfilled resin system percentage inclusions are shown within bar labels.

	TEGDMA	20/80 BT	30/70 BT	40/60 BT	50/50 BT	60/40 BT	70/30 BT	80/20 BT	bisGMA
Upper/Lower Surface	**<0.001**	**<0.001**	**<0.001**	**<0.001**	**<0.001**	**<0.001**	**0.001**	0.008	**<0.001**

Table 1.11 Significant differences between the upper (specimen was cured on this surface) and lower surface of each bisGMA/TEGDMA (BT) unfilled resin systems (1-way ANOVA, n=9). The numbers represent the p value, with the numbers in bold showing significant difference between sample conditions. Unfilled resin system percentage inclusions are shown within bar labels.

	20/80 UT	30/70 UT	40/60 UT	50/50 UT	60/40 UT	70/30 UT	80/20 UT	TEGDMA
UDMA	0.818	**<0.001**	**<0.001**	**<0.001**	**<0.001**	**<0.001**	**<0.001**	**<0.001**
20/80 UT		**<0.001**	**<0.001**	**<0.001**	**<0.001**	**<0.001**	**<0.001**	**<0.001**
30/70 UT			**<0.001**	**<0.001**	**<0.001**	**<0.001**	**<0.001**	**<0.001**
40/60 UT				**<0.001**	**<0.001**	**<0.001**	**<0.001**	**<0.001**
50/50 UT					**<0.001**	**<0.001**	**<0.001**	**<0.001**
60/40 UT						**<0.001**	**<0.001**	**<0.001**
70/30 UT							**<0.001**	**<0.001**
80/20 U/T								**<0.001**

Table 1.12 Significant differences between the upper surface (specimen was cured on this surface), hardness values of UDMA/TEGDMA (UT) unfilled resin systems (1-way ANOVA, n=9). The numbers represent the p value, with the numbers in **bold** showing significant difference between sample conditions. Unfilled resin system percentage inclusions are shown within bar labels.

	20/80 UT	30/70 UT	40/60 UT	50/50 UT	60/40 UT	70/30 UT	80/20 UT	TEGDMA
UDMA	**0.002**	**<0.001**	**<0.001**	**<0.001**	**<0.001**	**<0.001**	**<0.001**	0.150
20/80 UT		**<0.001**	**<0.001**	**<0.001**	**<0.001**	**<0.001**	**<0.001**	**<0.001**
30/70 UT			**<0.001**	**<0.001**	**<0.001**	**<0.001**	**<0.001**	**<0.001**
40/60 UT				**<0.001**	**<0.001**	**<0.001**	**<0.001**	**<0.001**
50/50 UT					0.051	**0.032**	**<0.001**	**<0.001**
60/40 UT						0.532	**<0.001**	**<0.001**
70/30 UT							**<0.001**	**<0.001**
80/20 UT								**<0.001**

Table 1.13 Significant differences between the lower surface hardness values of UDMA/TEGDMA (UT) unfilled resin systems (1-way ANOVA, n=9). The numbers represent the p value, with the numbers in **bold** showing significant difference between sample conditions. Unfilled resin system percentage inclusions are shown within bar labels.

	UDMA	20/80 UT	30/70 UT	40/60 UT	50/50 UT	60/40 UT	70/30 UT	80/20 UT	TEGDMA
CURED/ UNCURED	**<0.001**	**<0.001**	**<0.001**	**<0.001**	**<0.001**	**<0.001**	**<0.001**	**<0.001**	**<0.001**

Table 1.14 Significant differences between the upper (specimen was cured on this surface) and lower surface of each UDMA/TEGDMA resins (1-way ANOVA, n=9). The numbers represent the p value, with the numbers in **bold** showing significant difference between sample conditions. Unfilled resin system percentage inclusions are shown within bar labels.

	20/60/20	10/60/30	40/50/10	30/50/20	20/50/30	10/50/40	50/40/10	50/30/20	50/20/30	50/10/40
30/60/10	**<0.001**	**<0.001**	**<0.001**	0.454	**<0.001**	**<0.001**	**<0.001**	0.550	**<0.001**	**<0.001**
20/60/20		0.525	**<0.001**	**<0.001**	**<0.001**	**<0.001**	**<0.001**	**<0.001**	0.072	**<0.001**
10/60/30			**<0.001**	**<0.001**	**<0.001**	**<0.001**	**<0.001**	**<0.001**	**0.023**	**<0.001**
40/50/10				**<0.001**	**<0.001**	**<0.001**	**0.014**	**<0.001**	**<0.001**	**<0.001**
30/50/20					**<0.001**	**<0.001**	**<0.001**	0.246	**<0.001**	**<0.001**
20/50/30						**0.004**	**<0.001**	**<0.001**	**<0.001**	**0.001**
10/50/40							**<0.001**	**<0.001**	**<0.001**	**<0.001**
50/40/10								**<0.001**	**<0.001**	**<0.001**
50/30/20									**<0.001**	**<0.001**
50/20/30										**<0.001**

Table 1.15 Significant differences between the upper surface (specimen was cured on this surface) hardness values of bisGMA/UDMATEGDMA (BUT) unfilled resin systems (1-way ANOVA, n=9). The numbers represent the p value, with the numbers in **bold** showing significant difference between sample conditions. Unfilled resin system percentage inclusions are shown within bar labels.

	20/60/20	10/60/30	40/50/10	30/50/20	20/50/30	10/50/40	50/40/10	50/30/20	50/20/30	50/10/40
30/60/10	**<0.001**	**<0.001**	**<0.001**	**0.001**	**<0.001**	**<0.001**	**<0.001**	**0.030**	**<0.001**	**<0.001**
20/60/20		**<0.001**	**<0.001**	**<0.001**	**<0.001**	**<0.001**	**<0.001**	**<0.001**	**<0.001**	**<0.001**
10/60/30			**<0.001**	**<0.001**	0.081	**0.011**	**<0.001**	**<0.001**	**<0.001**	**0.037**
40/50/10				**<0.001**	**<0.001**	**<0.001**	**<0.001**	**<0.001**	**<0.001**	**<0.001**
30/50/20					**<0.001**	**0.007**	**<0.001**	0.101	**<0.001**	**<0.001**
20/50/30						**0.039**	**<0.001**	**<0.001**	**<0.001**	0.373
10/50/40							**<0.001**	**0.002**	**<0.001**	0.098
50/40/10								**<0.001**	**<0.001**	**<0.001**
50/30/20									**<0.001**	**<0.001**
50/20/30										**<0.001**

Table 1.16 Significant differences between the lower surface hardness values of bisGMA/UDMA/TEGDMA unfilled resin systems (1-way ANOVA, n=9). The numbers represent the p value, with the numbers in **bold** showing significant difference between sample conditions. Unfilled resin system percentage inclusions are shown within bar labels.

BUT	**20/60/20**	**10/60/30**	**40/50/10**	**30/50/20**	**20/50/30**	**10/50/40**	**50/40/10**	**50/30/20**	**50/20/30**	**50/10/40**	**20/60/20**
HV	**<0.001**	**<0.001**	**<0.001**	**<0.001**	**<0.001**	**<0.001**	**0.011**	**<0.001**	**<0.001**	**<0.001**	**<0.001**

Table 1.17 Significant differences between the upper (specimen was cured on this surface) and lower surface hardness values of bisGMA/UDMA/TEGDMA unfilled resin systems (1-way ANOVA, n=10). The numbers represent the p value, with the numbers in **bold** showing significant difference between sample conditions. Unfilled resin system percentage inclusions are shown within bar labels.

Flexural strength of unfilled resin systems

	20/80 BT	30/70 BT	40/60 BT	50/50 BT	60/40 BT	70/30 BT	80/20 BT	bisGMA
TEGDMA	0.378	0.028	**0.005**	**<0.001**	**0.001**	**0.001**	0.077	**<0.001**
20/80 BT		0.031	**<0.001**	**<0.001**	**<0.001**	**<0.001**	0.081	**<0.001**
30/70 BT			0.664	0.070	0.144	0.074	0.252	**<0.001**
40/60 BT				0.028	0.093	0.058	0.021	**<0.001**
50/50 BT					0.442	0.687	**<0.001**	**<0.001**
60/40 BT						0.375	**<0.001**	**<0.001**
70/30 BT							**0.001**	**<0.001**
80/20 BT								**<0.001**

Table 1.18 Significant differences between the flexural strength of UDMA/TEGDMA (UT) unfilled resin systems (1-way ANOVA, n=10). The numbers represent the p value, with the numbers in **bold** showing significant difference between sample conditions. Unfilled resin system percentage inclusions are shown within bar labels.

	20/80 UT	30/70 UT	40/60 UT	50/50 UT	60/40 UT	70/30 UT	80/20 UT	TEGDMA
UDMA	**<0.001**	**<0.001**	**<0.001**	**<0.001**	**<0.001**	**<0.001**	0.561	0.913
20/80 UT		0.143	0.360	**0.012**	0.429	0.101	**<0.001**	**<0.001**
30/70 UT			0.356	0.381	0.056	**0.005**	**<0.001**	**<0.001**
40/60 UT				**0.023**	0.122	**0.005**	**<0.001**	**<0.001**
50/50 UT					**0.007**	**<0.001**	**<0.001**	**<0.001**
60/40 UT						0.602	**<0.001**	**0.003**
70/30 UT							**<0.001**	**0.002**
80/20 UT								0.615

Table 1.19 Significant differences between the flexural strength of UDMA/TEGDMA (UT) unfilled resin systems (1-way ANOVA, n=10). The numbers represent the p value, with the numbers in **bold** showing significant difference between sample conditions. Unfilled resin system percentage inclusions are shown within bar labels.

UT	20/60/20	10/60/30	40/50/10	30/50/20	20/50/30	10/50/40	50/40/10	50/30/20	50/20/30	50/10/40
30/60/10	**0.002**	**0.047**	**0.003**	**0.001**	0.116	0.146	**<0.001**	0.611	0.393	0.088
20/60/20		**<0.001**	**<0.001**	0.902	0.108	0.188	**<0.001**	**0.001**	**<0.001**	**<0.001**
10/60/30			0.120	**<0.001**	**0.003**	**0.006**	**0.007**	0.137	0.203	0.601
40/50/10				**<0.001**	**<0.001**	**0.001**	0.521	**0.010**	**0.014**	**0.045**
30/50/20					0.071	0.143	**<0.001**	**<0.001**	**<0.001**	**<0.001**
20/50/30						0.921	**<0.001**	0.053	**0.025**	**0.004**
10/50/40							**<0.001**	0.076	**0.042**	**0.010**
50/40/10								**<0.001**	**<0.001**	**0.001**
50/30/20									0.754	0.253
50/20/30										0.378

Table 1.20 Significant differences between the flexural strength of bisGMA/UDDMA/TEGDMA (BUT) unfilled resin systems (1-way ANOVA, n=10). The numbers represent the p value, with the numbers in **bold** showing significant difference between sample conditions. Unfilled resin system percentage inclusions are shown within bar labels.

Flexural modulus of unfilled resin systems

	20/80 BT	30/70 BT	40/60 BT	50/50 BT	60/40 BT	70/30 BT	80/20 BT	bisGMA
TEGDMA	0.222	**0.004**	**0.002**	**<0.001**	**0.001**	**0.003**	0.145	**<0.001**
20/80 BT		**0.005**	**<0.001**	**<0.001**	**<0.001**	**0.001**	0.498	**<0.001**
30/70 BT			0.592	0.505	0.675	0.630	0.022	**<0.001**
40/60 BT				0.080	0.812	0.972	0.007	**<0.001**
50/50 BT					0.088	0.125	**<0.001**	**<0.001**
60/40 BT						0.870	**0.002**	**<0.001**
70/30 BT							0.013	**<0.001**
80/20 BT								**<0.001**

Table 1.21 Significant differences between the flexural modulus of bisGMA/TEGDMA (BT) unfilled resin systems (1-way ANOVA, n=10). The numbers represent the p value, with the numbers in **bold** showing significant difference between sample conditions. Unfilled resin system percentage inclusions are shown within bar labels.

	20/80 UT	30/70 UT	40/60 UT	50/50 UT	60/40 UT	70/30 UT	80/20 UT	TEGDMA
UDMA	**<0.001**	**<0.001**	**<0.001**	**<0.001**	**0.001**	**0.003**	0.511	0.714
20/80 UT		**0.029**	**0.015**	**0.006**	0.701	0.066	**<0.001**	**0.001**
30/70 UT			0.369	0.904	**0.031**	**0.002**	**<0.001**	**<0.001**
40/60 UT				0.224	**0.033**	**<0.001**	**<0.001**	**<0.001**
50/50 UT					**0.012**	**<0.001**	**<0.001**	**<0.001**
60/40 UT						0.246	**<0.001**	**0.007**
70/30 UT							**0.001**	**0.032**
80/20 UT								0.387

Table 1.22 Significant differences between the flexural modulus of UDMA/TEGDMA unfilled resin systems (1-way ANOVA, n=10). The numbers represent the p value, with the numbers in **bold** showing significant difference between sample conditions. Unfilled resin system percentage inclusions are shown within bar labels.

	20/60/20	10/60/30	40/50/10	30/50/20	20/50/30	10/50/40	50/40/10	50/30/20	50/20/30	50/10/40
30/60/10	**0.002**	0.955	**0.045**	**0.003**	**0.009**	0.053	**0.008**	0.217	0.583	0.832
20/60/20		**0.004**	**<0.001**	0.252	0.240	0.423	**<0.001**	**<0.001**	**0.006**	**0.002**
10/60/30			0.093	**0.010**	**0.020**	0.066	**0.023**	0.355	0.597	0.811
40/50/10				**<0.001**	**<0.001**	**0.002**	0.407	0.256	**0.013**	**0.016**
30/50/20					0.869	0.997	**<0.001**	**<0.001**	**0.012**	**0.002**
20/50/30						0.925	**<0.001**	**<0.001**	**0.030**	**0.007**
10/50/40							**0.001**	**0.007**	0.108	0.057
50/40/10								**0.044**	**0.002**	**0.002**
50/30/20									0.069	0.098
50/20/30										0.690

Table 1.23 Significant differences between the flexural modulus of bisGMA/UDMA/TEGDMA (BUT) unfilled resin systems (1-way ANOVA, n=10). The numbers represent the p value, with the numbers in **bold** showing significant difference between sample conditions. Unfilled resin system percentage inclusions are shown within bar labels.

Appendix 2 Statistical analysis of filled resin composites and PMMA

Degree of conversion of filled resin composites

	SIL20	SIL30	SIL40	SIL70	Silica70
SIL10	0.695	0.403	**0.017**	0.087	**<0.001**
SIL20		0.321	**0.012**	0.383	**<0.001**
SIL30			0.081	**0.003**	**<0.001**
SIL40				0.082	**<0.001**
SIL70					**<0.001**

Table 2.1 Significant differences between the degree of conversion of low filler content Type I filled resin composites (1-way ANOVA, n=10). Filled resin composite percentage inclusions are shown within bar labels. The numbers represent the p value, with the numbers in **bold** showing significant difference between sample conditions.

	SIL23	SIL34	SIL45	SIL80	Silica80
SIL11	**<0.001**	**0.003**	0.603	**<0.001**	**<0.001**
SIL23		**0.032**	**<0.001**	0.071	**<0.001**
SIL34			**0.022**	**0.001**	**<0.001**
SIL45				**<0.001**	**<0.001**
SIL80					**<0.001**

Table 2.2 Significant differences between the degree of conversion of high filler content Type I filled resin composites (1-way ANOVA, n=10). Filled resin composite percentage inclusions are shown within bar labels. The numbers represent the p value, with the numbers in **bold** showing significant difference between sample conditions.

	SIL10/ SIL11	SIL20/ SIL23	SIL30/ SIL34	SIL40/ SIL45	Silica70/ Silica80
Low/High filler	0.418	**<0.001**	0.288	**0.040**	**0.037**

Table 2.3 Significant differences between the degree of conversion of low versus high filler content Type I filled resin composites (1-way ANOVA, n=10). Filled resin composite percentage inclusions are shown within bar labels. The numbers represent the p value, with the numbers in **bold** showing significant difference between sample conditions.

	NS20	NS30	NS40	NS70	Silica70
NS10	0.126	0.108	**0.045**	**<0.001**	**<0.001**
NS20		0.986	**0.001**	**<0.001**	**<0.001**
NS30			**0.002**	**<0.001**	**0.010**
NS40				**<0.001**	**<0.001**
NS70					**<0.001**

Table 2.24 Significant differences between the degree of conversion of low filler content Type II filled resin composites (1-way ANOVA, n=10). Filled resin composite percentage inclusions are shown within bar labels. The numbers represent the p value, with the numbers in **bold** showing significant difference between sample conditions.

	NS23	NS34	NS45	NS80	Silica80
NS11	0.498	0.930	**<0.001**	**<0.001**	**<0.001**
NS23		0.457	**<0.001**	**<0.001**	**<0.001**
NS34			**<0.001**	**<0.001**	**<0.001**
NS45				**<0.001**	**<0.001**
Silica80					**<0.001**

Table 2.25 Significant differences between the degree of conversion of high filler content Type II filled resin composites (1-way ANOVA, n=10). Filled resin composite percentage inclusions are shown within bar labels. The numbers represent the p value, with the numbers in **bold** showing significant difference between sample conditions.

	NS10/NS11	NS20/NS23	NS30/NS34	NS40/NS45	Silica70/Silica80
Low/High filler	**0.002**	**0.007**	0.355	0.429	0.963

Table 2.26 Significant differences between the degree of conversion of low versus high filler content Type II filled resin composites (1-way ANOVA, n=10). Filled resin composite percentage inclusions are shown within bar labels. The numbers represent the p value, with the numbers in **bold** showing significant difference between sample conditions.

	AB20	AB30	AB40	AB70	Silica70
AB10	0.465	0.399	0.392	**<0.001**	**<0.001**
AB20		0.973	0.123	**<0.001**	**<0.001**
AB30			**0.034**	**<0.001**	**<0.001**
AB40				**<0.001**	**<0.001**
AB70					**<0.001**

Table 2.27 Significant differences between the degree of conversion of low filler content Type III filled resin composites (1-way ANOVA, n=10). Filled resin composite percentage inclusions are shown within bar labels. The numbers represent the p value, with the numbers in **bold** showing significant difference between sample conditions.

	AB23	AB34	AB45	Silica80
AB11	0.209	**0.001**	**<0.001**	**<0.001**
AB23		**0.001**	**<0.001**	**<0.001**
AB34			**<0.001**	**<0.001**
AB45				**<0.001**

Table 2.28 Significant differences between the degree of conversion of high filler content Type III filled resin composites (1-way ANOVA, n=10). Filled resin composite percentage inclusions are shown within bar labels. The numbers represent the p value, with the numbers in **bold** showing significant difference between sample conditions.

	AB10/AB11	AB20/AB23	AB30/AB34	AB40/AB45	Silica70/Silica80
Low/High filler	0.083	0.376	0.637	**<0.001**	0.874

Table 2.29 Significant differences between the degree of conversion of low versus high filler content Type III filled resin composites (1-way ANOVA, n=10). Filled resin composite percentage inclusions are shown within bar labels. The numbers represent the p value, with the numbers in **bold** showing significant difference between sample conditions.

Flexural strength of filled resin composites

	SIL20	SIL30	SIL40	Silica70
SILl10	**0.002**	0.848	**<0.001**	**<0.001**
SIL20		**<0.001**	**<0.001**	**0.011**
SIL30			**<0.001**	**<0.001**
SIL40				**<0.001**

Table 2.30 Significant differences between the flexural strength of low filler content Type I filled resin composites (One-way ANOVA, n=10). Filled resin composite percentage inclusions are shown within bar labels. The numbers represent the p value, with the numbers in **bold** showing significant difference between sample conditions.

	SIL23	SIL34	SIL45	Silica80
SIL11	**0.021**	**<0.001**	**<0.001**	0.409
SIL23		0.134	**<0.001**	**0.040**
SIL34			**<0.001**	**0.004**
SIL45				**<0.001**

Table 2.31 Significant differences between the flexural strength of high filler content Type I filled resin composites (One-way ANOVA, n=10). Filled resin composite percentage inclusions are shown within bar labels. The numbers represent the p value, with the numbers in **bold** showing significant difference between sample conditions.

	SIL10/SIL11	SIL20/SIL23	SIL30/SIL34	SIL40/SIL45	Silica70/Silica80
Low/High filler	**0.038**	**0.001**	**0.018**	**0.026**	0.206

Table 2.32 Significant differences between the flexural strength of low versus high filler content Type I filled resin composites (1-way ANOVA, n=10). Filled resin composite percentage inclusions are shown within bar labels. The numbers represent the p value, with the numbers in **bold** showing significant difference between sample conditions.

	NS20	NS30	NS40	Silica70
NS10	0.630	**0.042**	**<0.001**	**0.003**
NS20		**<0.001**	**<0.001**	**0.002**
NS30			**<0.001**	**<0.001**
NS40				**<0.001**

Table 2.33 Significant differences between the flexural strength of low filler content Type II filled resin composites (1-way ANOVA, n=10). Filled resin composite percentage inclusions are shown within bar labels. The numbers represent the p value, with the numbers in **bold** showing significant difference between sample conditions.

	NS23	NS34	NS45	Silica80
NS11	0.594	**0.017**	**<0.001**	0.419
NS23		0.057	**<0.001**	0.236
NS34			**<0.001**	**0.019**
NS45				**<0.001**

Table 2.34 Significant differences between the flexural strength of high filler content Type II filled resin composites (1-way ANOVA, n=10). Filled resin composite percentage inclusions are shown within bar labels. The numbers represent the p value, with the numbers in **bold** showing significant difference between sample conditions.

	NS10/NS11	NS20/NS23	NS30/NS34	NS40/NS45	Silica70/Silica80
Low/High filler	0.762	0.443	0.899	0.157	0.206

Table 2.35 Significant differences between the flexural strength of low versus high filler content Type II filled resin composites (1-way ANOVA, n=10). Filled resin composite percentage inclusions are shown within bar labels. The numbers represent the p value, with the numbers in **bold** showing significant difference between sample conditions.

	AB20	AB30	AB40	Silica70
AB10	**0.034**	**0.030**	**<0.001**	**0.020**
AB20		**<0.001**	**<0.001**	0.357
AB30			**<0.001**	**<0.001**
AB40				<0.001

Table 2.36 Significant differences between the flexural strength of low filler content Type III filled resin composites (1-way ANOVA, n=10). Filled resin composite percentage inclusions are shown within bar labels. The numbers represent the p value, with the numbers in **bold** showing significant difference between sample conditions.

	AB23	AB34	Silica80
AB11	**0.006**	0.255	0.704
AB23		**0.001**	0.093
AB34			0.373

Table 2.37 Significant differences between the flexural strength of high filler content Type III filled resin composites (1-way ANOVA, n=10). Filled resin composite percentage inclusions are shown within bar labels. The numbers represent the p value, with the numbers in **bold** showing significant difference between sample conditions.

	AB10/AB11	AB20/AB23	AB30/AB34	Silica70/Silica80
Low/High filler	0.921	0.119	0.152	0.206

Table 2.38 Significant differences between the flexural strength of low versus high filler content Type III filled resin composites (1-way ANOVA, n=10). Filled resin composite percentage inclusions are shown within bar labels. The numbers represent the p value, with the numbers in **bold** showing significant difference between sample conditions.

Flexural modulus of filled resin composites

	SIL20	SIL30	SIL40	Silica70
SIL10	0.227	0.793	**<0.001**	0.148
SIL20		0.088	**<0.001**	**0.002**
SIL30			**<0.001**	0.206
SIL40				**<0.001**

Table 2.39 Significant differences between the flexural modulus of low filler content Type I filled resin composites (1-way ANOVA, n=10). Filled resin composite percentage inclusions are shown within bar labels. The numbers represent the p value, with the numbers in **bold** showing significant difference between sample conditions.

	SIL23	SIL34	SIL45	Silica80
SIL11	0.978	0.145	**<0.001**	0.546
SIL23		0.204	**<0.001**	0.575
SIL34			**<0.001**	0.734
SIL45				**<0.001**

Table 2.40 Significant differences between the flexural modulus of high filler content Type I filled resin composites (1-way ANOVA, n=10). Filled resin composite percentage inclusions are shown within bar labels. The numbers represent the p value, with the numbers in **bold** showing significant difference between sample conditions.

	SIL10/SIL11	SIL20/SIL23	SIL30/SIL34	SIL40/SIL45	Silica70/Silica80
Low/High filler	**0.034**	**0.002**	0.416	0.609	0.967

Table 2.41 Significant differences between the flexural modulus of low versus high filler content Type I filled resin composites (1-way ANOVA, n=10). Filled resin composite percentage inclusions are shown within bar labels. The numbers represent the p value, with the numbers in **bold** showing significant difference between sample conditions.

	NS20	NS30	NS40	Silica70
NS10	**0.005**	**0.002**	**<0.001**	0.438
NS20		0.556	**<0.001**	**0.009**
NS30			**<0.001**	**0.002**
NS40				**<0.001**

Table 2.42 Significant differences between the flexural modulus of low filler content Type II filled resin composites (1-way ANOVA, n=10). Filled resin composite percentage inclusions are shown within bar labels. The numbers represent the p value, with the numbers in **bold** showing significant difference between sample conditions.

	NS23	NS34	NS45	Silica80
NS11	**0.037**	0.150	**<0.001**	0.222
NS23		0.437	**<0.001**	0.643
NS34			**<0.001**	0.909
NS45				**<0.001**

Table 2.43 Significant differences between the flexural modulus of high filler content Type II filled resin composites (1-way ANOVA, n=10). Filled resin composite percentage inclusions are shown within bar labels. The numbers represent the p value, with the numbers in **bold** showing significant difference between sample conditions.

	NS10/NS11	NS20/NS23	NS30/NS34	NS40/NS45	Silica70/Silica80
Low/High filler	0.428	0.069	**0.004**	0.082	0.967

Table 2.44 Significant differences between the flexural modulus of low versus high filler content Type II filled resin composites (1-way ANOVA, n=10). Filled resin composite percentage inclusions are shown within bar labels. The numbers represent the p value, with the numbers in **bold** showing significant difference between sample conditions.

	AB20	AB30	AB40	Silica70
AB10	**0.024**	**<0.001**	**<0.001**	**0.016**
AB20		**<0.001**	**<0.001**	0.839
AB30			**0.001**	**<0.001**
AB40				**<0.001**

Table 2.45 Significant differences between the flexural modulus of low filler content Type III filled resin composites (1-way ANOVA, n=10). Filled resin composite percentage inclusions are shown within bar labels. The numbers represent the p value, with the numbers in **bold** showing significant difference between sample conditions.

	AB23	AB34	Silica80
AB11	**<0.001**	0.772	**<0.001**
AB23		**<0.001**	**0.036**
AB34			**<0.001**

Table 2.46 Significant differences between the flexural modulus of high filler content Type III filled resin composites containing high amount of filler (One-way ANOVA, n=9). Filled resin composite percentage inclusions are shown within bar labels. The numbers represent the p value, with the numbers in **bold** showing significant difference between sample conditions.

	AB10/AB11	AB20/AB23	AB30/AB34	Silica70/Silica80
Low/High filler	**<0.001**	**0.008**	0.186	0.967

Table 2.47 Significant differences between the flexural modulus of low versus high filler content Type III filled resin composites (1-way ANOVA, n=10). Filled resin composite percentage inclusions are shown within bar labels. The numbers represent the p value, with the numbers in **bold** showing significant difference between sample conditions.

Appendix 3 Statistical analysis of water sorption, water solubility and bi-axial flexural strength values of filled resin composites and PMMA following wet ageing

Statistical data of water sorption values of filled resin composites and PMMA

	Day 7	Month 1	Month 3
Day 1	**0.002**	**<0.001**	0.146
Day 7		**<0.001**	0.206
Month 1			0.364

Table 3.1 Significant differences between the water sorption of low filler content filled resin composites containing 70wt% barium silicate filler following water immersion for 1 day, 7 days, 1 month and 3 months (1-way ANOVA, n=10). The numbers represent the p value, with the numbers in **bold** showing significant difference between sample conditions.

	Day 7	Month 1	Month 3
Day 1	**<0.001**	**<0.001**	**<0.001**
Day 7		**0.011**	0.112
Month 1			0.551

Table 3.2 Significant differences between the water sorption of low filler content Type I filled resin composites containing 20wt% bioactive glass following water immersion for 1 day, 7 days, 1 month and 3 months (1-way ANOVA, n=10). The numbers represent the p value, with the numbers in **bold** showing significant difference between sample conditions.

	Day 7	Month 1	Month 3
Day 1	**0.042**	**0.045**	0.106
Day 7		0.892	**<0.001**
Month 1			**<0.001**

Table 3.3 Significant differences between the water sorption of low filler content Type I filled resin composites containing 40wt% bioactive glass following water immersion for 1 day, 7 days, 1 month and 3 months (1-way ANOVA, n=10). The numbers represent the p value, with the numbers in **bold** showing significant difference between sample conditions.

	Day 7	Month 1	Month 3
Day 1	**<0.001**	**<0.001**	**<0.001**
Day 7		**0.013**	**<0.001**
Month 1			**<0.001**

Table 3.4 Significant differences between the water sorption of low filler content Type II filled resin composites containing 20wt% bioactive glass following water immersion for 1 day, 7 days, 1 month and 3 months (1-way ANOVA, n=10). The numbers represent the p value, with the numbers in **bold** showing significant difference between sample conditions.

	Day 7	Month 1	Month 3
Day 1	**0.004**	**0.001**	0.068
Day 7		0.583	0.093
Month 1			**0.024**

Table 3.5 Significant differences between the water sorption of low filler content Type II filled resin composites containing 40wt% bioactive glass following water immersion for 1 day, 7 days, 1 month and 3 months (1-way ANOVA, n=10). The numbers represent the p value, with the numbers in **bold** showing significant difference between sample conditions.

	Day 7	Month 1	Month 3
Day 1	**<0.001**	**<0.001**	**<0.001**
Day 7		**<0.001**	**<0.001**
Month 1			**0.002**

Table 3.6 Significant differences between the water sorption of low filler content Type III filled resin composites containing 20wt% bioactive glass following water immersion for 1 day, 7 days, 1 month and 3 months (1-way ANOVA, n=10). The numbers represent the p value, with the numbers in **bold** showing significant difference between sample conditions.

	Day 7	Month 1	Month 3
Day 1	**0.016**	**<0.001**	**<0.001**
Day 7		**<0.001**	**<0.001**
Month 1			**<0.001**

Table 3.7 Significant differences between the water sorption of low filler content Type III filled resin composites containing 40wt% bioactive glass (1-way ANOVA, n=10). The numbers represent the p value, with the numbers in **bold** showing significant difference between sample conditions.

	Day 7	Month 1	Month 3
Day 1	**0.006**	**0.001**	**<0.001**
Day 7		0.986	0.373
Month 1			0.275

Table 3.8 Significant differences between the water sorption of high filler content filled resin composites containing 80wt% barium silicate filler following water immersion for 1 day, 7 days, 1 month and 3 months (1-way ANOVA, n=10). The numbers represent the p value, with the numbers in **bold** showing significant difference between sample conditions.

	Day 7	Month 1	Month 3
Day 1	0.200	**<0.001**	**<0.001**
Day 7		**<0.001**	**<0.001**
Month 1			0.409

Table 3.9 Significant differences between the water sorption of high filler content Type I filled resin composites containing 23wt% bioactive glass following water immersion for 1 day, 7 days, 1 month and 3 months (1-way ANOVA, n=10). The numbers represent the p value, with the numbers in **bold** showing significant difference between sample conditions.

	Day 7	Month 1	Month 3
Day 1	0.637	0.055	0.954
Day 7		0.109	0.729
Month 1			0.103

Table 3.10 Significant differences between the water sorption of high filler content Type I filled resin composites containing 45wt% bioactive glass following water immersion for 1 day, 7 days, 1 month and 3 months (1-way ANOVA, n=10). The numbers represent the p value, with the numbers in **bold** showing significant difference between sample conditions.

	Day 7	Month 1	Month 3
Day 1	**<0.001**	**<0.001**	**<0.001**
Day 7		0.204	0.541
Month 1			0.696

Table 3.11 Significant differences between the water sorption of high filler content Type II filled resin composites containing 23wt% bioactive glass following water immersion for 1 day, 7 days, 1 month and 3 months (1-way ANOVA, n=10). The numbers represent the p value, with the numbers in **bold** showing significant difference between sample conditions.

	Day 7	Month 1	Month 3
Day 1	0.056	0.798	0.062
Day 7		**0.013**	**0.002**
Month 1			**0.024**

Table 3.12 Significant differences between the water sorption of high filler content Type II filled resin composites containing 45wt% bioactive glass following water immersion for 1 day, 7 days, 1 month and 3 months (1-way ANOVA, n=10). The numbers represent the p value, with the numbers in **bold** showing significant difference between sample conditions.

	Day 7	Month 1	Month 3
Day 1	**0.005**	**<0.001**	**<0.001**
Day 7		**<0.001**	**<0.001**
Month 1			**0.007**

Table 3.13 Significant differences between the water sorption of high filler content Type III filled resin composites containing 23wt% bioactive glass following water immersion for 1 day, 7 days, 1 month and 3 months (1-way ANOVA, n=10). The numbers represent the p value, with the numbers in **bold** showing significant difference between sample conditions.

	Day 7	Month 1	Month 3
Day 1	0.683	**0.001**	**<0.001**
Day 7		**0.022**	**<0.001**
Month 1			**<0.001**

Table 3.14 Significant differences between the water sorption of PMMA following water immersion for 1 day, 7 days, 1 month and 3 months (1-way ANOVA, n=10). The numbers represent the p value, with the numbers in **bold** showing significant difference between sample conditions.

Statistical data of water solubility values of filled resin composites and PMMA

	Day 7	Month 1	Month 3
Day 1	0.794	0.093	0.548
Day 7		0.119	0.369
Month 1			**0.043**

Table 3.15 Significant differences between the water solubility of low filler content filled resin composites containing 70wt% barium silicate filler following water immersion for 1 day, 7 days, 1 month and 3 months (1-way ANOVA, n=10). The numbers represent the p value, with the numbers in **bold** showing significant difference between sample conditions.

	Day 7	Month 1	Month 3
Day 1	0.233	**<0.001**	**<0.001**
Day 7		0.703	**0.044**
Month 1			**0.001**

Table 3.16 Significant differences between the water solubility of low filler content Type I filled resin composites containing 20wt% bioactive glass following water immersion for 1 day, 7 days, 1 month and 3 months (1-way ANOVA, n=10). The numbers represent the p value, with the numbers in **bold** showing significant difference between sample conditions.

	Day 7	Month 1	Month 3
Day 1	**<0.001**	**<0.001**	**<0.001**
Day 7		**<0.001**	**<0.001**
Month 1			**<0.001**

Table 3.17 Significant differences between water solubility of low filler content Type I filled resin composites containing 40wt% bioactive glass following water immersion for 1 day, 7 days, 1 month and 3 months (1-way ANOVA, n=10). The numbers represent the p value, with the numbers in **bold** showing significant difference between sample conditions.

	Day 7	Month 1	Month 3
Day 1	0.165	**0..001**	**<0.001**
Day 7		0.060	**<0.001**
Month 1			**<0.001**

Table 3.18 Significant differences between the water solubility of low filler content Type II filled resin composites containing 20wt% bioactive glass following water immersion for 1 day, 7 days, 1 month and 3 months (1-way ANOVA, n=10). The numbers represent the p value, with the numbers in **bold** showing significant difference between sample conditions.

	Day 7	Month 1	Month 3
Day 1	**<0.001**	**<0.001**	**<0.001**
Day 7		**<0.001**	**<0.001**
Month 1			**<0.001**

Table 319 Significant differences between the water solubility of low filler content Type II filled resin composites containing 40wt% bioactive glass following water immersion for 1 day, 7 days, 1 month and 3 months (1-way ANOVA, n=10). The numbers represent the p value, with the numbers in **bold** showing significant difference between sample conditions.

	Day 7	Month 1	Month 3
Day 1	0.295	**0.001**	**<0.001**
Day 7		**0.013**	**<0.001**
Month 1			**<0.001**

Table 3.20 Significant differences between the water solubility of low filler content Type III filled resin composites containing 20wt% bioactive glass following water immersion for 1 day, 7 days, 1 month and 3 months (1-way ANOVA, n=10). The numbers represent the p value, with the numbers in **bold** showing significant difference between sample conditions.

	Day 7	Month 1	Month 3
Day 1	**<0.001**	**<0.001**	**0.001**
Day 7		0.784	**0.006**
Month 1			**0.010**

Table 3.21 Significant differences between the water solubility of low filler content Type III filled resin composites containing 40wt% bioactive glass following water immersion for 1 day, 7 days, 1 month and 3 months (1-way ANOVA, n=10). The numbers represent the p value, with the numbers in **bold** showing significant difference between sample conditions.

	Day 7	Month 1	Month 3
Day 1	0.800	0.933	0.674
Day 7		0.757	0.945
Month 1			0.618

Table 3.22 Significant differences between the water solubility of high filler content filled resin composites containing 80wt% barium silicate filler following water immersion for 1 day, 7 days, 1 month and 3 months (1-way ANOVA, n=10). The numbers represent the p value, with the numbers in **bold** showing significant difference between sample conditions.

	Day 7	Month 1	Month 3
Day 1	**<0.001**	0.076	**<0.001**
Day 7		**0.015**	**<0.001**
Month 1			0.552

Table 3.23 Significant differences between the water solubility of high filler content Type I filled resin composites containing 23wt% bioactive glass following water immersion for 1 day, 7 days, 1 month and 3 months (1-way ANOVA, n=10). The numbers represent the p value, with the numbers in **bold** showing significant difference between sample conditions.

	Day 7	Month 1	Month 3
Day 1	**<0.001**	**<0.001**	**<0.001**
Day 7		**<0.001**	**<0.001**
Month 1			**0.007**

Table 3.24 Significant differences between the water solubility of high filler content Type I filled resin composites containing 45wt% bioactive glass following water immersion for 1 day, 7 days, 1 month and 3 months (1-way ANOVA, n=10. The numbers represent the p value, with the numbers in **bold** showing significant difference between sample conditions.

	Day 7	Month 1	Month 3
Day 1	0.078	**<0.001**	**<0.001**
Day 7		**0.009**	**0.002**
Month 1			0.157

Table 3.25 Significant differences between the water solubility of high filler content Type II filled resin composites containing 23wt% bioactive glass following water immersion for 1 day, 7 days, 1 month and 3 months (1-way ANOVA, n=10). The numbers represent the p value, with the numbers in **bold** showing significant difference between sample conditions.

	Day 7	Month 1	Month 3
Day 1	**<0.001**	**<0.001**	**<0.001**
Day 7		**<0.001**	**<0.001**
Month 1			**<0.001**

Table 3.26 Significant differences between the water solubility of high filler content Type II filed resin composites containing 45wt% bioactive glass following water immersion for 1 day, 7 days, 1 month and 3 months (1-way ANOVA, n=10). The numbers represent the p value, with the numbers in **bold** showing significant difference between sample conditions.

	Day 7	Month 1	Month 3
Day 1	0.532	**<0.001**	**<0.001**
Day 7		**<0.001**	**<0.001**
Month 1			**<0.001**

Table 3.27 Significant differences between the water solubility of high filler content Type III filled resin composites containing 23wt% bioactive glass following water immersion for 1 day, 7 days, 1 month and 3 months (1-way ANOVA, n=10). The numbers represent the p value, with the numbers in **bold** showing significant difference between sample conditions.

	Day 7	Month 1	Month 3
Day 1	0.612	**0.021**	0.144
Day 7		**0.016**	0.083
Month 1			0.324

Table 3.28 Significant differences between the water solubility of PMMA following water immersion for 1 day, 7 days, 1 month and 3 months (1-way ANOVA, n=10). The numbers represent the p value, with the numbers in **bold** showing significant difference between sample conditions.

Statistical data of bi-axial flexural strength values of filled resin composites and PMMA

	Day 1	Day 7	Week 4	Month 3
Dry	0.445	0.939	0.229	0.053
Day 1		0.375	0.075	**0.014**
Day 7			0.220	**0.040**
Week 4				0.563

Table 3.29 Significant differences between the bi-axial flexural strength of low filler content filled resin composites containing 70wt% barium silicate filler dry and following water immersion for 1 day, 7 days, 1 month and 3 months (1-way ANOVA, n=10). The numbers represent the p value, with the numbers in **bold** showing significant difference between sample conditions.

	Day 1	Day 7	Week 4	Month 3
Dry	0.298	**<0.001**	**<0.001**	**<0.001**
Day 1		**<0.001**	**<0.001**	**<0.001**
Day 7			0.732	0.104
Week 4				0.153

Table 3.30 Significant differences between the bi-axial flexural strength of low filler content Type I filled resin composites containing 20wt% bioactive glass dry and following water immersion for 1 day, 7 days, 1 month and 3 months (1-way ANOVA, n=10). The numbers represent the p value, with the numbers in **bold** showing significant difference between sample conditions.

	Day 1	Day 7	Week 4	Month 3
Dry	**0.035**	**0.028**	**0.004**	**0.004**
Day 1		0.691	0.248	0.190
Day 7			0.555	0.450
Week 4				0.822

Table 3.31 Significant differences between the bi-axial flexural strength of low filler content Type I filled resin composites containing 40wt% bioactive glass dry and following water immersion for 1 day, 7 days, 1 month and 3 months (1-way ANOVA, n=10). The numbers represent the p value, with the numbers in **bold** showing significant difference between sample conditions.

	Day 1	Day 7	Week 4	Month 3
Dry	**0.051**	**<0.001**	**<0.001**	**<0.001**
Day 1		**0.032**	**0.001**	**0.001**
Day 7			**0.036**	**0.035**
Week 4				0.911

Table 3.32 Significant differences between the bi-axial flexural strength of low filler content Type II filled resin composites containing 20wt% bioactive glass dry and following water immersion for 1 day, 7 days, 1 month and 3 months (1-way ANOVA, n=10). The numbers represent the p value, with the numbers in **bold** showing significant difference between sample conditions.

	Day 1	Day 7	Week 4	Month 3
Dry	0.188	0.076	**0.045**	**<0.001**
Day 1		0.487	0.420	**0.002**
Day 7			0.919	**0.012**
Week 4				**0.002**

Table 3.33 Significant differences between the bi-axial flexural strength of low filler content Type II filled resin composites containing 40wt% bioactive glass dry and following water immersion for 1 day, 7 days, 1 month and 3 months (1-way ANOVA, n=10). The numbers represent the p value, with the numbers in **bold** showing significant difference between sample conditions.

	Day 1	Day 7	Week 4	Month 3
Dry	**0.039**	**0.030**	**<0.001**	**<0.001**
Day 1		**<0.001**	**<0.001**	**<0.001**
Day 7			**<0.001**	**<0.001**
Week 4				**0.004**

Table 3.34 Significant differences between the bi-axial flexural strength of low filler content Type III filled resin composites containing 20wt% bioactive glass dry and following water immersion for 1 day, 7 days, 1 month and 3 months (1-way ANOVA, n=10). The numbers represent the p value, with the numbers in **bold** showing significant difference between sample conditions.

	Day 1	Day 7	Week 4	Month 3
Dry	0.943	**0.014**	**0.005**	**0.003**
Day 1		**0.002**	**<0.001**	**<0.001**
Day 7			0.523	0.263
Week 4				0.491

Table 3.35 Significant differences between the bi-axial flexural strength of low filler content Type III filled resin composites containing 40wt% bioactive glass dry and following water immersion for 1 day, 7 days, 1 month and 3 months (1-way ANOVA, n=10). The numbers represent the p value, with the numbers in **bold** showing significant difference between sample conditions.

	Day 1	Day 7	Week 4	Month 3
Dry	0.997	0.313	0.217	0.183
Day 1		0.295	0.195	0.161
Day 7			0.931	0.867
Week 4				0.902

Table 3.36 Significant differences between the bi-axial flexural strength of high filler content filled resin composites containing 80wt% barium silicate filler dry and following water immersion for 1 day, 7 days, 1 month and 3 months following water immersion for 1 day, 7 days, 1 month and 3 months (1-way ANOVA, n=10). The numbers represent the p value, with the numbers in **bold** showing significant difference between sample conditions.

	Day 1	Day 7	Week 4	Month 3
Dry	0.568	**<0.001**	**<0.001**	**<0.001**
Day 1		**<0.001**	**<0.001**	**<0.001**
Day 7			**0.024**	**<0.001**
Week 4				0.243

Table 3.37 Significant differences between the bi-axial flexural strength of high filler content Type I filled resin composites containing 23wt% bioactive glass dry and following water immersion for 1 day, 7 days, 1 month and 3 months (1-way ANOVA, n=10). The numbers represent the p value, with the numbers in **bold** showing significant difference between sample conditions.

	Day 1	Day 7	Week 4	Month 3
Dry	**0.001**	**<0.001**	**<0.001**	**<0.001**
Day 1		0.405	0.332	**0.039**
Day 7			**0.039**	0.158
Week 4				0.157

Table 3.38 Significant differences between the bi-axial flexural strength of high filler content Type I filled resin composites containing 45wt% bioactive glass dry and following water immersion for 1 day, 7 days, 1 month and 3 months (1-way ANOVA, n=10). The numbers represent the p value, with the numbers in **bold** showing significant difference between sample conditions.

	Day 1	Day 7	Week 4	Month 3
Dry	0.546	**<0.001**	**<0.001**	**<0.001**
Day 1		**<0.001**	**<0.001**	**<0.001**
Day 7			**0.001**	**0.002**
Week 4				0.241

Table 3.39 Significant differences between the bi-axial flexural strength of high filler content Type II filled resin composites containing 23wt% bioactive glass dry and following water immersion for 1 day, 7 days, 1 month and 3 months (1-way ANOVA, n=10). The numbers represent the p value, with the numbers in **bold** showing significant difference between sample conditions.

	Day 1	Day 7	Week 4	Month 3
Dry	**<0.001**	**<0.001**	**<0.001**	**<0.001**
Day 1		**<0.001**	**<0.001**	**<0.001**
Day 7			0.845	0.221
Week 4				0.410

Table 3.40 Significant differences between the bi-axial flexural strength of high filler content Type II filled resin composites containing 45wt% bioactive glass dry and following water immersion for 1 day, 7 days, 1 month and 3 months (1-way ANOVA, n=10). The numbers represent the p value, with the numbers in **bold** showing significant difference between sample conditions.

	Day 1	Day 7	Week 4	Month 3
Dry	**<0.001**	0.650	0.322	**<0.001**
Day 1		**<0.001**	**<0.001**	**<0.001**
Day 7			0.408	**<0.001**
Week 4				**0.001**

Table 3.41 Significant differences between the bi-axial flexural strength of high filler content Type III filled resin composites containing 23wt% bioactive glass dry and following water immersion for 1 day, 7 days, 1 month and 3 months (1-way ANOVA, n=10). The numbers represent the p value, with the numbers in **bold** showing significant difference between sample conditions.

	Day 1	Day 7	Week 4	Month 3
Dry	**0.522**	0.146	0.053	**0.003**
Day 1		**0.060**	**0.024**	**0.003**
Day 7			0.396	**0.006**
Week 4				**0.033**

Table 3.42 Significant differences between the bi-axial flexural strength of PMMA dry and following water immersion for 1 day, 7 days, 1 month and 3 months (1-way ANOVA, n=10). The numbers represent the p value, with the numbers in **bold** showing significant difference between sample conditions.

Appendix 4 Statistical analysis of flexural strength and flexural modulus values of filled resin composites and PMMA tested following wet ageing

Flexural strength following wet ageing of filled resin composites

	Day 1	Day 7	Week 4	Month 3	Month 6	Month 9	Month 12
Dry	0.553	**<0.001**	**0.002**	0.180	0.418	0.265	**0.049**
Day 1		0.359	**0.043**	0.087	0.214	0.118	**0.025**
Day 7			0.445	**0.005**	**0.026**	**0.003**	**0.001**
Week 4				**<0.001**	**0.006**	**<0.001**	**<0.001**
Month 3					0.659	0.608	0.561
Month 6						0.964	0.321
Month 9							0.214

Table 4.1 Significant differences between the flexural strength of low filler content filled resin composites containing 70wt% barium silicate filler dry and following wet ageing for 1 day, 7 days, 4 weeks, 3 months, 6 months, 9 months and 12 months (1-way ANOVA, n=10). The numbers represent the p value, with the numbers in **bold** showing significant difference between sample conditions.

	Day 1	Day 7	Week 4	Month 3	Month 6	Month 9	Month 12
Dry	0.271	**0.021**	**0.003**	**0.006**	0.063	**0.027**	**0.021**
Day 1		**<0.001**	**<0.001**	**0.017**	0.305	0.107	0.082
Day 7			0.440	**<0.001**	**<0.001**	**<0.001**	**<0.001**
Week 4				**<0.001**	**<0.001**	**<0.001**	**<0.001**
Month 3					0.058	0.387	0.288
Month 6						0.351	0.319
Month 9							0.924

Table 4.2 Significant differences between the flexural strength of low filler content Type I filled resin composites containing 20wt% bioactive glass dry and following wet ageing for 1 day, 7 days, 4 weeks, 3 months, 6 months, 9 months and 12 months (1-way ANOVA, n=10). The numbers represent the p value, with the numbers in **bold** showing significant difference between sample conditions.

	Day 1	Day 7	Week 4	Month 3	Month 6	Month 9	Month 12
Dry	**<0.001**	**0.023**	**0.020**	**0.002**	**0.048**	0.470	0.422
Day 1		**<0.001**	**<0.001**	**<0.001**	**0.039**	**<0.001**	**<0.001**
Day 7			0.650	0.086	**<0.001**	0.229	0.370
Week 4				0.323	**<0.001**	0.168	0.280
Month 3					**<0.001**	**0.036**	0.085
Month 6						**0.017**	**0.022**
Month 9							0.887

Table 4.3 Significant differences between the flexural strength of low filler content Type I filled resin composites containing 40wt% bioactive glass dry and following wet ageing for 1 day, 7 days, 4 weeks, 3 months, 6 months, 9 months and 12 months (1-way ANOVA, n=10). The numbers represent the p value, with the numbers in **bold** showing significant difference between sample conditions.

	Day 1	Day 7	Week 4	Month 3	Month 6	Month 9	Month 12
Dry	**0.044**	**0.001**	**<0.001**	0.902	0.508	0.376	0.312
Day 1		**0.041**	**<0.001**	**0.034**	0.189	0.240	0.156
Day 7			0.058	**0.001**	**0.004**	**0.005**	**0.001**
Week 4				**<0.001**	**<0.001**	**<0.001**	**<0.001**
Month 3					0.439	0.315	0.241
Month 6						0.847	0.843
Month 9							0.979

Table 4.4 Significant differences between the flexural strength of low filler content Type II filled resin composites containing 20wt% bioactive glass dry and following wet ageing for 1 day, 7 days, 4 weeks, 3 months, 6 months, 9 months and 12 months (1-way ANOVA, n=10). The numbers represent the p value, with the numbers in **bold** showing significant difference between sample conditions.

	Day 1	Day 7	Week 4	Month 3	Month 6	Month 9	Month 12
Dry	**<0.001**	**<0.001**	**<0.001**	**0.007**	0.071	**0.043**	**0.024**
Day 1		**0.039**	0.278	**<0.001**	**<0.001**	**<0.001**	**<0.001**
Day 7			**0.008**	**<0.001**	**<0.001**	**<0.001**	**<0.001**
Week 4				**0.004**	**0.009**	**0.009**	**0.003**
Month 3					0.655	0.789	0.609
Month 6						0.873	0.926
Month 9							0.922

Table 4.5 Significant differences between the flexural strength of low filler content Type II filled resin composites containing 40wt% bioactive glass dry and following wet ageing for 1 day, 7 days, 4 weeks, 3 months, 6 months, 9 months and 12 months (1-way ANOVA, n=10). The numbers represent the p value, with the numbers in **bold** showing significant difference between sample conditions.

	Day 1	Day 7	Week 4	Month 3	Month 6	Month 9	Month 12
Dry	**0.008**	**<0.001**	**<0.001**	**<0.001**	**<0.001**	**<0.001**	**<0.001**
Day 1		0.064	**0.010**	**0.013**	**0.007**	**0.005**	**0.002**
Day 7			**0.050**	0.071	**0.032**	**0.005**	**0.001**
Week 4				0.686	0.670	0.426	0.208
Month 3					0.416	0.187	0.061
Month 6						0.791	0.524
Month 9							0.657

Table 4.6 Significant differences between the flexural strength of low filler content Type III filled resin composites containing 20wt% bioactive glass dry and following wet ageing for 1 day, 7 days, 4 weeks, 3 months, 6 months, 9 months and 12 months (1-way ANOVA, n=10). The numbers represent the p value, with the numbers in **bold** showing significant difference between sample conditions.

	Day 1	Day 7	Week 4	Month 3	Month 6	Month 9	Month 12
Dry	**<0.001**	**<0.001**	**<0.001**	**<0.001**	**<0.001**	**0.001**	**<0.001**
Day 1		0.131	0.222	0.652	0.651	0.650	0.053
Day 7			0.604	0.344	0.386	0.355	0.053
Week 4				0.494	0.581	0.478	**0.041**
Month 3					0.965	0.638	0.084
Month 6						0.633	0.103
Month 9							0.662

Table 4.7 Significant differences between the flexural strength of low filler content Type III filled resin composites containing 40wt% bioactive glass dry and following wet ageing for 1 day, 7 days, 4 weeks, 3 months, 6 months, 9 months and 12 months (1-way ANOVA, n=10). The numbers represent the p value, with the numbers in **bold** showing significant difference between sample conditions.

	Day 1	Day 7	Week 4	Month 3	Month 6	Month 9	Month 12
Dry	0.124	**0.031**	0.885	0.592	0.360	**0.006**	0.104
Day 1		0.520	0.158	0.157	0.433	0.829	0.827
Day 7			**0.043**	**0.018**	0.128	0.691	0.719
Week 4				0.716	0.442	0.122	0.130
Month 3					0.571	0.100	0.115
Month 6						0.323	0.337
Month 9							0.991

Table 4.8 Significant differences between the flexural strength of high filler content filled resin composites containing 80wt% barium silicate filler dry and following wet ageing for 1 day, 7 days, 4 weeks, 3 months, 6 months, 9 months and 12 months (1-way ANOVA, n=10). The numbers represent the p value, with the numbers in **bold** showing significant difference between sample conditions.

	Day 1	Day 7	Week 4	Month 3	Month 6	Month 9	Month 12
Dry	0.364	0.257	0.383	0.184	**0.059**	0.075	**0.024**
Day 1		0.053	0.871	0.611	**0.263**	0.275	0.078
Day 7			0.069	**0.029**	**0.008**	**0.011**	**0.004**
Week 4				0.834	0.547	0.498	0.210
Month 3					0.540	0.512	0.159
Month 6						0.816	0.240
Month 9							0.415

Table 4.9 Significant differences between the flexural strength of high filler content Type I filled resin composites containing 23wt% bioactive glass dry and following wet ageing for 1 day, 7 days, 4 weeks, 3 months, 6 months, 9 months and 12 months (1-way ANOVA, n=10). The numbers represent the p value, with the numbers in **bold** showing significant difference between sample conditions.

	Day 1	Day 7	Week 4	Month 3	Month 6	Month 9	Month 12
Dry	**0.023**	**<0.001**	**0.005**	0.732	**0.018**	0.367	0.925
Day 1		**0.001**	0.970	0.186	0.370	0.145	**0.029**
Day 7			**<0.001**	**<0.001**	**<0.001**	**<0.001**	**<0.001**
Week 4				0.128	0.229	0.072	**0.008**
Month 3					0.315	0.801	0.699
Month 6						0.263	**0.029**
Month 9							0.368

Table 4 Significant differences between the flexural strength of high filler content Type I filled resin composites containing 45wt% bioactive glass dry and following wet ageing for 1 day, 7 days, 4 weeks, 3 months, 6 months, 9 months and 12 months (One-way ANOVA, n=10). The numbers represent the p value, with the numbers in **bold** showing significant difference between sample conditions.

	Day 1	Day 7	Week 4	Month 3	Month 6	Month 9	Month 12
Dry	**0.033**	**<0.001**	0.128	**0.001**	**0.003**	**<0.001**	**0.001**
Day 1		**0.001**	0.810	**0.006**	**0.035**	**<0.001**	**0.008**
Day 7			**0.016**	0.868	0.104	0.857	0.098
Week 4				**0.033**	0.140	**0.015**	0.095
Month 3					0.225	0.975	0.241
Month 6						0.102	0.839
Month 9							0.088

Table 4.11 Significant differences between the flexural strength of high filler content Type II filled resin composites containing 23wt% bioactive glass dry and following wet ageing for 1 day, 7 days, 4 weeks, 3 months, 6 months, 9 months and 12 months (1-way ANOVA, n=10). The numbers represent the p value, with the numbers in **bold** showing significant difference between sample conditions.

	Day 1	Day 7	Week 4	Month 3	Month 6	Month 9	Month 12
Dry	**<0.001**	**<0.001**	**0.014**	0.215	0.087	**0.016**	**0.002**
Day 1		**<0.001**	**<0.001**	**<0.001**	**<0.001**	**<0.001**	**<0.001**
Day 7			**<0.001**	**<0.001**	**<0.001**	**<0.001**	**<0.001**
Week 4				**0.001**	**<0.001**	**<0.001**	**<0.001**
Month 3					0.875	0.265	0.069
Month 6						0.157	**0.010**
Month 9							0.366

Table 4.12 Significant differences between the flexural strength of high filler content Type II filled resin composites containing 45wt% bioactive glass dry and following wet ageing for 1 day, 7 days, 4 weeks, 3 months, 6 months, 9 months and 12 months (1-way ANOVA, n=10). The numbers represent the p value, with the numbers in **bold** showing significant difference between sample conditions.

	Day 1	Day 7	Week 4	Month 3	Month 6	Month 9	Month 12
Dry	0.091	**<0.001**	**<0.001**	**<0.001**	**<0.001**	**<0.001**	**<0.001**
Day 1		**<0.001**	**0.004**	**<0.001**	**<0.001**	**0.001**	**<0.001**
Day 7			**0.007**	0.091	0.110	0.158	0.332
Week 4				**<0.001**	**<0.001**	0.180	**0.005**
Month 3					0.994	**0.005**	0.861
Month 6						**0.007**	0.868
Month 9							0.061

Table 4.13 Significant differences between the flexural strength of high filler content Type III filled resin composites containing 23wt% bioactive glass dry and following wet ageing for 1 day, 7 days, 4 weeks, 3 months, 6 months, 9 months and 12 months (1-way ANOVA, n=10). The numbers represent the p value, with the numbers in **bold** showing significant difference between sample conditions.

	Day 1	Day 7	Week 4	Month 3	Month 6	Month 9	Month 12
Dry	0.081	0.602	**0.660**	**0.461**	**0.161**	**0.060**	**0.064**
Day 1		**0.136**	**0.013**	**0.133**	**0.483**	0.767	**0.796**
Day 7			0.193	0.847	0.290	0.101	0.105
Week 4				0.051	0.013	**0.001**	**0.013**
Month 3					0.291	**0.077**	**0.103**
Month 6						**0.568**	**0.356**
Month 9							0.570

Table 4.14 Significant differences between the flexural strength of PMMA dry and following wet ageing for 1 day, 7 days, 4 weeks, 3 months, 6 months, 9 months and 12 months (1-way ANOVA, n=10). The numbers represent the p value, with the numbers in **bold** showing significant difference between sample conditions.

Flexural modulus of filled resin composites following wet ageing

	Day 1	Day 7	Week 4	Month 3	Month 6	Month 9	Month 12
Dry	**<0.001**	**<0.001**	**0.001**	**<0.001**	**<0.001**	**<0.001**	**0.003**
Day 1		0.204	**0.010**	**0.013**	0.072	**0.023**	**0.001**
Day 7			0.083	0.116	0.524	0.211	**0.009**
Week 4				0.765	0.212	0.483	0.391
Month 3					0.303	0.670	0.221
Month 6						0.514	**0.029**
Month 9							0.095

Table 4.15 Significant differences between the flexural modulus of low filler content filled resin composites containing 70wt% barium silicate filler dry and following wet ageing for 1 day, 7 days, 4 weeks, 3 months, 6 months, 9 months and 12 months (1-way ANOVA, n=10). The numbers represent the p value, with the numbers in **bold** showing significant difference between sample conditions.

	Day 1	Day 7	Week 4	Month 3	Month 6	Month 9	Month 12
Dry	**<0.001**	**<0.001**	**<0.001**	**<0.001**	**<0.001**	**<0.001**	**<0.001**
Day 1		**<0.001**	**<0.001**	**0.001**	**<0.001**	**<0.001**	**<0.001**
Day 7			0.558	**<0.001**	0.054	0.137	0.066
Week 4				**<0.001**	**0.018**	0.059	**0.020**
Month 3					**0.006**	**0.021**	**0.001**
Month 6						0.888	0.795
Month 9							0.950

Table 4.1648 Significant differences between the flexural modulus of low filler content Type I filled resin composites containing 20wt% bioactive glass dry and following wet ageing for 1 day, 7 days, 4 weeks, 3 months, 6 months, 9 months and 12 months (1-way ANOVA, n=10). The numbers represent the p value, with the numbers in **bold** showing significant difference between sample conditions.

	Day 1	Day 7	Week 4	Month 3	Month 6	Month 9	Month 12
Dry	**<0.001**	**<0.001**	**<0.001**	**<0.001**	**<0.001**	**<0.001**	**<0.001**
Day 1		0.237	0.353	**<0.001**	**<0.001**	**<0.001**	**<0.001**
Day 7			0.758	**<0.001**	**0.002**	**0.006**	**0.002**
Week 4				**<0.001**	**0.001**	**0.002**	**0.001**
Month 3					**<0.001**	**<0.001**	**<0.001**
Month 6						0.232	0.443
Month 9							0.614

Table 4.17 Significant differences between the flexural modulus of low filler content Type I filled resin composites containing 40wt% bioactive glass dry and following wet ageing for 1 day, 7 days, 4 weeks, 3 months, 6 months, 9 months and 12 months (1-way ANOVA, n=10). The numbers represent the p value, with the numbers in **bold** showing significant difference between sample conditions.

	Day 1	Day 7	Week 4	Month 3	Month 6	Month 9	Month 12
Dry	**<0.001**	**<0.001**	**0.002**	**<0.001**	**<0.001**	**0.002**	**<0.001**
Day 1		0.367	**0.019**	**0.049**	0.728	0.099	0.595
Day 7			**0.005**	0.538	0.262	**0.025**	0.185
Week 4				**<0.001**	0.085	0.583	0.080
Month 3					**0.047**	**0.001**	**0.016**
Month 6						**0.247**	**0.892**
Month 9							**0.265**

Table 4.18 Significant differences between the flexural modulus of low filler content Type II filled resin composites containing 20wt% bioactive glass dry and following wet ageing for 1 day, 7 days, 4 weeks, 3 months, 6 months, 9 months and 12 months (1-way ANOVA, n=10). The numbers represent the p value, with the numbers in **bold** showing significant difference between sample conditions.

	Day 1	Day 7	Week 4	Month 3	Month 6	Month 9	Month 12
Dry	**0.049**	**<0.001**	0.079	0.090	0.092	0.891	**0.047**
Day 1		**<0.001**	**<0.001**	0.603	0.913	**0.013**	0.804
Day 7			**<0.001**	**<0.001**	**<0.001**	**<0.001**	**<0.001**
Week 4				**<0.001**	**0.001**	**0.029**	**<0.001**
Month 3					0.822	**0.039**	0.525
Month 6						0.051	0.804
Month 9							**0.014**

Table 4.19 Significant differences between the flexural modulus of low filler content Type II filled resin composites containing 40wt% bioactive glass dry and following wet ageing for 1 day, 7 days, 4 weeks, 3 months, 6 months, 9 months and 12 months (1-way ANOVA, n=10). The numbers represent the p value, with the numbers in **bold** showing significant difference between sample conditions.

	Day 1	Day 7	Week 4	Month 3	Month 6	Month 9	Month 12
Dry	**0.025**	**<0.001**	**<0.001**	**<0.001**	**<0.001**	**<0.001**	**<0.001**
Day 1		**<0.001**	**<0.001**	**<0.001**	**<0.001**	**<0.001**	**<0.001**
Day 7			0.716	**0.001**	**0.001**	**0.031**	0.340
Week 4				**0.001**	**0.001**	**0.026**	0.232
Month 3					0.324	0.091	**0.002**
Month 6						0.316	**0.003**
Month 9							0.089

Table 4.20 Significant differences between the flexural modulus of low filler content Type III filled resin composites containing 20wt% bioactive glass dry and following wet ageing for 1 day, 7 days, 4 weeks, 3 months, 6 months, 9 months and 12 months (1-way ANOVA, n=10). The numbers represent the p value, with the numbers in **bold** showing significant difference between sample conditions.

	Day 1	Day 7	Week 4	Month 3	Month 6	Month 9	Month 12
Dry	**<0.001**	**<0.001**	**<0.001**	**<0.001**	**<0.001**	0.464	**<0.001**
Day 1		**<0.001**	**<0.001**	**<0.001**	**<0.001**	**<0.001**	**<0.001**
Day 7			**<0.001**	**0.005**	0.381	**0.019**	**<0.001**
Week 4				**0.024**	**<0.001**	**<0.001**	0.726
Month 3					**0.004**	**0.001**	**0.010**
Month 6						**0.007**	**<0.001**
Month 9							**<0.001**

Table 4.21 Significant differences between the flexural modulus of low filler content Type III filled resin composites containing 40wt% bioactive glass dry and following wet ageing for 1 day, 7 days, 4 weeks, 3 months, 6 months, 9 months and 12 months (1-way ANOVA, n=10). The numbers represent the p value, with the numbers in **bold** showing significant difference between sample conditions.

	Day 1	Day 7	Week 4	Month 3	Month 6	Month 9	Month 12
Dry	**0.037**	0.303	**0.010**	**0.024**	0.963	**0.030**	0.489
Day 1		0.064	0.246	0.540	**0.023**	0.714	**0.036**
Day 7			**0.008**	**0.037**	0.245	**0.032**	0.660
Week 4				0.681	**0.005**	0.398	**0.006**
Month 3					**0.014**	0.752	**0.024**
Month 6						**0.018**	0.425
Month 9							**0.020**

Table 4.22 Significant differences between the flexural modulus of high filler content filled resin composites containing 80wt% barium silicate filler dry and following wet ageing for 1 day, 7 days, 4 weeks, 3 months, 6 months, 9 months and 12 months (1-way ANOVA, n=10). The numbers represent the p value, with the numbers in **bold** showing significant difference between sample conditions.

	Day 1	Day 7	Week 4	Month 3	Month 6	Month 9	Month 12
Dry	**<0.001**	0.071	**<0.001**	**<0.001**	**<0.001**	**<0.001**	**<0.001**
Day 1		**<0.001**	0.693	0.852	0.066	0.329	**<0.001**
Day 7			**<0.001**	**<0.001**	**<0.001**	**<0.001**	**<0.001**
Week 4				0.644	**0.026**	0.566	**<0.001**
Month 3					0.326	0.385	**0.002**
Month 6						**0.004**	**<0.001**
Month 9							**<0.001**

Table 4.23 Significant differences between the flexural modulus of high filler content Type I filled resin composites containing 23wt% bioactive glass dry and following wet ageing for 1 day, 7 days, 4 weeks, 3 months, 6 months, 9 months and 12 months (1-way ANOVA, n=10). The numbers represent the p value, with the numbers in **bold** showing significant difference between sample conditions.

	Day 1	Day 7	Week 4	Month 3	Month 6	Month 9	Month 12
Dry	**<0.001**	**<0.001**	**0.001**	**<0.001**	**<0.001**	**<0.001**	**<0.001**
Day 1		**<0.001**	**<0.001**	**0.024**	**0.001**	0.340	**<0.001**
Day 7			**<0.001**	**<0.001**	**<0.001**	**<0.001**	**<0.001**
Week 4				**0.005**	**0.017**	**0.014**	0.107
Month 3					0.368	0.567	**0.036**
Month 6						0.220	0.170
Month 9							**0.048**

Table 4.24 Significant differences between the flexural modulus of high filler content Type I filled resin composites containing 45wt% bioactive glass dry and following wet ageing for 1 day, 7 days, 4 weeks, 3 months, 6 months, 9 months and 12 months (1-way ANOVA, n=10). The numbers represent the p value, with the numbers in **bold** showing significant difference between sample conditions.

	Day 1	Day 7	Week 4	Month 3	Month 6	Month 9	Month 12
Dry	**<0.001**	**0.001**	**<0.001**	**<0.001**	**<0.001**	**<0.001**	**<0.001**
Day 1		**0.012**	**<0.001**	0.067	**0.047**	**0.003**	**<0.001**
Day 7			0.931	0.106	0.233	0.218	0.334
Week 4				**0.005**	0.053	**0.015**	**0.039**
Month 3					0.591	0.366	0.135
Month 6						0.886	0.549
Month 9							0.490

Table 4.25 Significant differences between the flexural modulus of high filler content Type II filled resin composites containing 23wt% bioactive glass dry and following wet ageing for 1 day, 7 days, 4 weeks, 3 months, 6 months, 9 months and 12 months (1-way ANOVA, n=10). The numbers represent the p value, with the numbers in **bold** showing significant difference between sample conditions.

	Day 1	Day 7	Week 4	Month 3	Month 6	Month 9	Month 12
Dry	0.209	**<0.001**	0.057	**0.030**	0.116	**0.001**	0.055
Day 1		**<0.001**	**<0.001**	**<0.001**	**<0.001**	**<0.001**	**<0.001**
Day 7			**<0.001**	**<0.001**	**<0.001**	**<0.001**	**<0.001**
Week 4				0.662	0.283	**0.001**	0.740
Month 3					0.137	**0.003**	0.416
Month 6						**<0.001**	0.363
Month 9							**<0.001**

Table 4.26 Significant differences between the flexural modulus of high filler content Type II filled resin composites containing 45wt% bioactive glass dry and following wet ageing for 1 day, 7 days, 4 weeks, 3 months, 6 months, 9 months and 12 months (1-way ANOVA, n=10). The numbers represent the p value, with the numbers in **bold** showing significant difference between sample conditions.

	Day 1	Day 7	Week 4	Month 3	Month 6	Month 9	Month 12
Dry	**<0.001**	**<0.001**	**<0.001**	**<0.001**	**<0.001**	**<0.001**	**<0.001**
Day 1		**0.001**	**<0.001**	**<0.001**	**<0.001**	0.098	**0.003**
Day 7			0.460	0.122	0.405	0.166	0.175
Week 4				0.319	0.890	**0.038**	**0.014**
Month 3					0.392	**0.007**	**<0.001**
Month 6						**0.036**	**0.011**
Month 9							0.624

Table 4.27 Significant differences between the flexural modulus of high filler content Type III filled resin composites containing 23wt% bioactive glass dry and following wet ageing for 1 day, 7 days, 4 weeks, 3 months, 6 months, 9 months and 12 months (1-way ANOVA, n=10). The numbers represent the p value, with the numbers in **bold** showing significant difference between sample conditions.

	Day 1	Day 7	Week 4	Month 3	Month 6	Month 9	Month 12
Dry	0.988	0.759	**0.009**	**0.009**	**0.727**	**0.474**	**0.065**
Day 1		**0.794**	**0.015**	**0.017**	**0.760**	0.535	**0.087**
Day 7			0.004	0.004	0.936	0.058	0.859
Week 4				0.859	0.009	**0.003**	**0.426**
Month 3					0.009	**0.003**	**0.426**
Month 6						**0.717**	**0.088**
Month 9							0.080

Table 4.28 Significant differences between the flexural modulus of PMMA dry and following wet ageing for 1 day, 7 days, 4 weeks, 3 months, 6 months, 9 months and 12 months (1-way ANOVA, n=10). The numbers represent the p value, with the numbers in **bold** showing significant difference between sample conditions.

Appendix 5 Statistical analysis of culture media acidity values; viable and non-viable bone marrow stromal cells data in the presence of unfilled resin systems, filled resin composites and PMMA

Statistical data of pH change of culture media in the absence/presence of filled resin composites and PMMA

	Day 1	Day 3	Day 5	Day 7	Day 12
Day 0	0.116	0.374	**0.008**	0.116	0.116
Day 1		0.519	**0.018**	>0.999	>0.999
Day 3			**0.013**	0.519	0.519
Day 5				**0.018**	**0.018**
Day 7					>0.999

Table 5.1 Significant differences between the pH of culture media in the absence of filled composite discs (1-way ANOVA, n=9). The numbers represent the p value, with the numbers in **bold** showing significant difference between sample conditions.

	Day 1	Day 3	Day 5	Day 7	Day 12
Day 0	0.116	0.116	0.116	0.374	0.116
Day 1		>0.999	>0.999	0.519	>0.999
Day 3			>0.999	0.519	>0.999
Day 5				0.519	>0.999
Day 7					0.519

Table 5.2 Significant differences between the pH of culture media following immersion of low viscosity filled resin composite discs containing 70wt% barium silicate filler (1-way ANOVA, n=9). The numbers represent the p value, with the numbers in **bold** showing significant difference between sample conditions.

	Day 1	Day 3	Day 5	Day 7	Day 12
Day 0	**<0.001**	**<0.001**	**0.002**	**0.002**	**0.001**
Day 1		>0.999	0.251	0.643	0.116
Day 3			0.251	0.643	0.116
Day 5				0.492	0.725
Day 7					0.288

Table 5.3 Significant differences between the pH of culture media following immersion of low viscosity Type I filled resin composite discs containing 20wt% bioactive glass (1-way ANOVA, n=9). The numbers represent the p value, with the numbers in **bold** showing significant difference between sample conditions.

	Day 1	Day 3	Day 5	Day 7	Day 12
Day 0	**<0.001**	**<0.001**	**<0.001**	**0.003**	**<0.001**
Day 1		0.101	0.101	0.230	0.067
Day 3			>0.999	0.742	0.374
Day 5				0.742	0.374
Day 7					0.768

Table 5.4 Significant differences between the pH of culture media following immersion of low viscosity Type I filled resin composite discs containing 40wt% bioactive glass (1-way ANOVA, n=9). The numbers represent the p value, with the numbers in **bold** showing significant difference between sample conditions.

	Day 1	Day 3	Day 5	Day 7	Day 12
Day 0	**<0.001**	**<0.001**	**0.001**	**<0.001**	**0.001**
Day 1		0.230	0.251	**0.013**	0.055
Day 3			0.678	**0.047**	0.148
Day 5				0.251	0.349
Day 7					>0.999

Table 5.5 Significant differences between the pH of culture media following immersion of low viscosity Type II filled resin composite discs containing 20wt% bioactive glass (1-way ANOVA, n=9). The numbers represent the p value, with the numbers in **bold** showing significant difference between sample conditions.

	Day 1	Day 3	Day 5	Day 7	Day 12
Day 0	**<0.001**	**<0.001**	**<0.001**	**0.004**	**<0.001**
Day 1		0.519	>0.999	0.561	**0.047**
Day 3			0.519	0.768	0.101
Day 5				0.561	**0.047**
Day 7					0.561

Table 5.6 Significant differences between the pH of culture media following immersion of low viscosity Type II filled resin composite discs containing 40wt% bioactive glass (1-way ANOVA, n=9). The numbers represent the p value, with the numbers in **bold** showing significant difference between sample conditions.

	Day 1	Day 3	Day 5	Day 7	Day 12
Day 0	**<0.001**	**0.002**	**<0.001**	**0.002**	**<0.001**
Day 1		>0.999	>0.999	>0.999	>0.999
Day 3			>0.999	>0.999	>0.999
Day 5				>0.999	>0.999
Day 7					>0.999

Table 5.7 Significant differences between the pH of culture media following immersion of low viscosity Type III filled resin composite discs containing 20wt% bioactive glass (1-way ANOVA, n=9). The numbers represent the p value, with the numbers in **bold** showing significant difference between sample conditions.

	Day 1	Day 3	Day 5	Day 7	Day 12
Day 0	**0.002**	**<0.001**	**<0.001**	**0.003**	**0.001**
Day 1		>0.999	0.251	0.742	0.725
Day 3			0.101	0.678	0.643
Day 5				0.148	0.374
Day 7					0.492

Table 5.8 Significant differences between the pH of culture media following immersion of low viscosity Type III filled resin composite discs containing 40wt% bioactive glass (1-way ANOVA, n=9). The numbers represent the p value, with the numbers in **bold** showing significant difference between sample conditions.

	Day 1	Day 3	Day 5	Day 7	Day 12
Day 0	0.217	0.374	0.374	0.116	0.116
Day 1		0.834	0.834	0.628	0.628
Day 3			>0.999	0.519	0.519
Day 5				0.519	0.519
Day 7					>0.999

Table 5.9 Significant differences between the pH of culture media in the absence of filled composite discs (1-way ANOVA, n=9). The numbers represent the p value, with the numbers in **bold** showing significant difference between sample conditions.

	Day 1	Day 3	Day 5	Day 7	Day 12
Day 0	0.374	0.374	0.116	0.116	0.725
Day 1		>0.999	0.519	0.519	>0.999
Day 3			0.519	0.519	>0.999
Day 5				>0.999	0.742
Day 7					0.742

Table 5.10 Significant differences between the pH of culture media following immersion of high viscosity filled resin composite discs containing 70wt% barium silicate filler (1-way ANOVA, n=9). The numbers represent the p value, with the numbers in **bold** showing significant difference between sample conditions.

	Day 1	Day 3	Day 5	Day 7	Day 12
Day 0	**<0.001**	**<0.001**	**0.001**	**<0.001**	**0.002**
Day 1		>0.999	>0.999	>0.999	0.519
Day 3			>0.999	>0.999	0.519
Day 5				>0.999	0.579
Day 7					0.519

Table 5.11 Significant differences between the pH of culture media following immersion of high viscosity Type I filled resin composite discs containing 20wt% bioactive glass (1-way ANOVA, n=9). The numbers represent the p value, with the numbers in **bold** showing significant difference between sample conditions.

	Day 1	Day 3	Day 5	Day 7	Day 12
Day 0	**<0.001**	**0.001**	**<0.001**	**<0.001**	**0.001**
Day 1		0.422	>0.999	>0.999	0.678
Day 3			0.422	0.422	0.349
Day 5				>0.999	0.678
Day 7					0.678

Table 5.12 Significant differences between the pH of culture media following immersion of high viscosity Type I filled resin composite discs containing 40wt% bioactive glass (1-way ANOVA, n=9). The numbers represent the p value, with the numbers in **bold** showing significant difference between sample conditions.

	Day 1	Day 3	Day 5	Day 7	Day 12
Day 0	**0.002**	**<0.001**	**<0.001**	**0.001**	**0.001**
Day 1		>0.999	0.742	0.778	0.468
Day 3			0.519	0.678	0.349
Day 5				>0.999	0.519
Day 7					0.579

Table 5.13 Significant differences between the pH of culture media following immersion of high viscosity Type II filled resin composite discs containing 20wt% bioactive glass (1-way ANOVA, n=9). The numbers represent the p value, with the numbers in **bold** showing significant difference between sample conditions.

	Day 1	Day 3	Day 5	Day 7	Day 12
Day 0	**<0.001**	**<0.001**	**0.001**	**<0.001**	**<0.001**
Day 1		0.422	0.519	0.725	>0.999
Day 3			>0.999	0.643	0.422
Day 5				0.725	0.519
Day 7					0.725

Table 5.14 Significant differences between the pH of culture media following immersion of high viscosity Type II filled resin composite discs containing 40wt% bioactive glass (1-way ANOVA, n=9). The numbers represent the p value, with the numbers in **bold** showing significant difference between sample conditions.

	Day 1	Day 3	Day 5	Day 7	Day 12
Day 0	**0.007**	**0.002**	**0.008**	**<0.001**	**<0.001**
Day 1		0.795	0.643	0.768	0.768
Day 3			0.778	>0.999	>0.999
Day 5				0.742	0.742
Day 7					>0.999

Table 5.15 Significant differences between the pH of culture media following immersion of high viscosity Type III filled resin composite discs containing 20wt% bioactive glass (1-way ANOVA, n=9). The numbers represent the p value, with the numbers in **bold** showing significant difference between sample conditions.

	Day 1	Day 3	Day 5	Day 7	Day 12
Day 0	0.279	**0.001**	**0.001**	**0.025**	>0.999
Day 1		>0.999	0.816	0.734	0.289
Day 3			0.230	0.251	**0.007**
Day 5				0.678	**0.016**
Day 12					**0.057**

Table 5.16 Significant differences between the pH of culture media following immersion of PMMA discs containing (1-way ANOVA, n=9). The numbers represent the p value, with the numbers in **bold** showing significant difference between sample conditions.

Statistical data of viability values of bone marrow stromal cells seeded in the absence/presence of filled resin composites, unfilled resin systems and PMMA

	Day 1	Day 3	Day 5	Day 7	Day 12
Day 0	**<0.001**	**<0.001**	**<0.001**	**<0.001**	**<0.001**
Day 1		>0.999	0.363	**0.018**	**0.002**
Day 3			0.504	0.099	**0.024**
Day 5				0.270	0.063
Day 7					0.332

Table 5.17 Significant differences between viable bone marrow stromal cells following culture in direct contact on unfilled resin system discs containing 60/40wt% UDMA/TEGDMA for 1 day, 3 days, 5 days, 7 days and 12 days (1-way ANOVA, n=3 biological replicates). The culture media was replaced every 2-days.The numbers represent the p value, with the numbers in **bold** showing significant difference between sample conditions.

	Day 1	Day 3	Day 5	Day 7	Day 12
Day 0	**<0.001**	**<0.001**	**0.035**	**<0.001**	**<0.001**
Day 1		**<0.001**	**<0.001**	**<0.001**	**<0.001**
Day 3			**0.008**	**<0.001**	**<0.001**
Day 5				**<0.001**	**<0.001**
Day 7					**<0.001**

Table 5.18 Significant differences between viable bone marrow stromal cells following culture in direct contact on discs containing PMMA for 1 day, 3 days, 5 days, 7 days and 12 days (1-way ANOVA, n=3 biological replicates). The culture media was replaced every 2-days. The numbers represent the p value, with the numbers in **bold** showing significant difference between sample conditions.

	Day 1	Day 3	Day 5	Day 7	Day 12
Day 0	0.114	0.779	**<0.001**	**<0.001**	**<0.001**
Day 1		0.162	**<0.001**	**<0.001**	**<0.001**
Day 3			**0.004**	**<0.001**	**<0.001**
Day 5				**<0.001**	**<0.001**
Day 7					**0.011**

Table 5.19 Significant differences between the viability of bone marrow stromal cells following culture in the absence of filled resin composite discs for 1 day, 3 days, 5 days, 7 days and 12 days (1-way ANOVA, n=3 biological replicates). The culture media was replaced every 2-days. The numbers represent the p value, with the numbers in **bold** showing significant difference between sample conditions.

	Day 1	Day 3	Day 5	Day 7	Day 12
Day 0	**0.001**	**<0.001**	**<0.001**	**0.022**	0.313
Day 1		0.882	0.143	0.255	0.237
Day 3			**0.042**	0.239	0.245
Day 5				0.903	0.611
Day 7					0.705

Table 5.20 Significant differences between the viability of bone marrow stromal cells following culture in direct contact on low viscosity filled resin composite discs containing 70wt% barium silicate filler for 1 day, 3 days, 5 days, 7 days and 12 days (1-way ANOVA, n=3 biological replicates). The culture media was replaced every 2-days. The

numbers represent the p value, with the numbers in **bold** showing significant difference between sample conditions.

	Day 1	Day 3	Day 5	Day 7	Day 12
Day 0	**0.002**	**<0.001**	0.675	**0.003**	**<0.001**
Day 1		0.128	**0.008**	**<0.001**	**<0.001**
Day 3			**0.031**	**0.001**	**<0.001**
Day 5				**0.003**	**<0.001**
Day 7					**0.009**

Table 5.21 Significant differences between the viability of bone marrow stromal cells following culture in direct contact on low viscosity Type I filled resin composite discs containing 20wt% bioactive glass for 1 day, 3 days, 5 days, 7 days and 12 days (1-way ANOVA, n=3 biological replicates). The culture media was replaced every 2-days. The numbers represent the p value, with the numbers in **bold** showing significant difference between sample conditions.

	Day 1	Day 3	Day 5	Day 7	Day 12
Day 0	**<0.001**	**<0.001**	**0.008**	**<0.001**	**<0.001**
Day 1		0.774	**0.008**	**<0.001**	**<0.001**
Day 3			**0.027**	**<0.001**	**<0.001**
Day 5				**<0.001**	**<0.001**
Day 7					**<0.001**

Table 5.22 Significant differences between the viability of bone marrow stromal cells following culture in direct contact on low viscosity Type I filled resin composite discs containing 40wt% bioactive glass for 1 day, 3 days, 5 days, 7 days and 12 days (1-way ANOVA, n=3 biological replicates). The culture media was replaced every 2-days. The numbers represent the p value, with the numbers in **bold** showing significant difference between sample conditions.

	Day 1	Day 3	Day 5	Day 7	Day 12
Day 0	**<0.001**	**0.001**	0.390	**<0.001**	**<0.001**
Day 1		>0.999	0.236	**<0.001**	**<0.001**
Day 3			0.257	**<0.001**	**<0.001**
Day 5				**<0.001**	**<0.001**
Day 7					**0.001**

Table 5.23 Significant differences between the viability of bone marrow stromal cells following culture in direct contact on low viscosity Type II filled resin composite discs containing 20wt% bioactive glass for 1 day, 3 days, 5 days, 7 days and 12 days (1-way ANOVA, n=3 biological replicates). The culture media was replaced every 2-days. The numbers represent the p value, with the numbers in **bold** showing significant difference between sample conditions.

	Day 1	Day 3	Day 5	Day 7	Day 12
Day 0	**<0.001**	**<0.001**	**<0.001**	**<0.001**	**<0.001**
Day 1		0.211	**0.004**	**<0.001**	**<0.001**
Day 3			**0.014**	**<0.001**	**<0.001**
Day 5				**<0.001**	**<0.001**
Day 7					**<0.001**

Table 5.24 Significant differences between the viability of bone marrow stromal cells following culture in direct contact on low viscosity Type II filled resin composite discs containing 40wt% bioactive glass for 1 day, 3 days, 5

days, 7 days and 12 days (1-way ANOVA, n=3 biological replicates). The culture media was replaced every 2-days. The numbers represent the p value, with the numbers in **bold** showing significant difference between sample conditions.

	Day 1	Day 3	Day 5	Day 7	Day 12
Day 0	**<0.001**	**0.077**	0.595	**<0.001**	**<0.001**
Day 1		0.238	**0.001**	**<0.001**	**<0.001**
Day 3			0.093	**0.001**	**<0.001**
Day 5				**0.039**	**<0.001**
Day 7					**<0.001**

Table 5.25 Significant differences between the viability of bone marrow stromal cells following culture in direct contact on low viscosity Type III filled resin composite discs containing 20wt% bioactive glass for 1 day, 3 days, 5 days, 7 days and 12 days (1-way ANOVA, n=3 biological replicates). The culture media was replaced every 2-days. The numbers represent the p value, with the numbers in **bold** showing significant difference between sample conditions.

	Day 1	Day 3	Day 5	Day 7	Day 12
Day 0	**<0.001**	**<0.001**	**0.044**	0.414	**<0.001**
Day 1		0.700	**0.018**	**<0.001**	**<0.001**
Day 3			0.076	**<0.001**	**<0.001**
Day 5				**0.037**	**<0.001**
Day 7					**<0.001**

Table 5.26 Significant differences between the viability of bone marrow stromal cells following culture in direct contact on low viscosity Type III filled resin composite discs containing 40wt% bioactive glass for 1 day, 3 days, 5 days, 7 days and 12 days (1-way ANOVA, n=3 biological replicates). The culture media was replaced every 2-days. The numbers represent the p value, with the numbers in **bold** showing significant difference between sample conditions.

	Day 1	Day 3	Day 5	Day 7	Day 12
Day 0	**0.022**	0.675	**<0.001**	**<0.001**	**<0.001**
Day 1		0.094	**<0.001**	**<0.001**	**<0.001**
Day 3			**<0.001**	**<0.001**	**<0.001**
Day 5				**<0.001**	**<0.001**
Day 7					**<0.001**

Table 5.27 Significant differences between the viability of bone marrow stromal cells following culture in the absence of filled composite discs for 1 day, 3 days, 5 days, 7 days and 12 days (1-way ANOVA, n=3 biological replicates). The culture media was replaced every 2-days. (1-way ANOVA, n=3 biological replicates). The numbers represent the p value, with the numbers in **bold** showing significant difference between sample conditions.

	Day 1	Day 3	Day 5	Day 7	Day 12
Day 0	**<0.001**	**<0.001**	**<0.001**	0.332	**<0.001**
Day 1		**0.020**	**<0.001**	**<0.001**	**<0.001**
Day 3			**<0.001**	**<0.001**	**<0.001**
Day 5				**<0.001**	**<0.001**
Day 7					**<0.001**

Table 5.28 Significant differences between the viability of bone marrow stromal cells following culture in in direct contact on high viscosity filled resin composite discs containing 70wt% barium silicate filler for 1 day, 3 days, 5

days, 7 days and 12 days (1-way ANOVA, n=3 biological replicates). The culture media was replaced every 2-days. The numbers represent the p value, with the numbers in **bold** showing significant difference between sample conditions.

	Day 1	Day 3	Day 5	Day 7	Day 12
Day 0	**0.001**	0.150	**0.003**	**<0.001**	**<0.001**
Day 1		0.160	**<0.001**	**<0.001**	**<0.001**
Day 3			**0.003**	**<0.001**	**<0.001**
Day 5				**<0.001**	**<0.001**
Day 7					**0.002**

Table 5.29 Significant differences between the viability of bone marrow stromal cells following culture in in direct contact on high viscosity Type I filled resin composite discs containing 20wt% bioactive glass for 1 day, 3 days, 5 days, 7 days and 12 days (1-way ANOVA, n=3 biological replicates). The culture media was replaced every 2-days. The numbers represent the p value, with the numbers in **bold** showing significant difference between sample conditions.

	Day 1	Day 3	Day 5	Day 7	Day 12
Day 0	**0.001**	**<0.001**	**0.004**	**<0.001**	**<0.001**
Day 1		0.624	**<0.001**	**<0.001**	**<0.001**
Day 3			**<0.001**	**<0.001**	**<0.001**
Day 5				**<0.001**	**<0.001**
Day 7					**<0.001**

Table 5.30 Significant differences between the viability of bone marrow stromal cells following culture in in direct contact on high viscosity Type I filled resin composite discs containing 40wt% bioactive glass for 1 day, 3 days, 5 days, 7 days and 12 days (1-way ANOVA, n=3 biological replicates). The culture media was replaced every 2-days. The numbers represent the p value, with the numbers in **bold** showing significant difference between sample conditions.

	Day 1	Day 3	Day 5	Day 7	Day 12
Day 0	0.265	0.435	**<0.001**	**<0.001**	**<0.001**
Day 1		0.185	**<0.001**	**<0.001**	**<0.001**
Day 3			**0.001**	**<0.001**	**<0.001**
Day 5				0.074	**<0.001**
Day 7					**<0.001**

Table 5.31 Significant differences between the viability of bone marrow stromal cells following culture in direct contact on high viscosity Type II filled resin composite discs containing 20wt% bioactive glass for 1 day, 3 days, 5 days, 7 days and 12 days (1-way ANOVA, n=3 biological replicates). The culture media was replaced every 2-days. The numbers represent the p value, with the numbers in **bold** showing significant difference between sample conditions.

	Day 1	Day 3	Day 5	Day 7	Day 12
Day 0	**0.001**	**0.012**	**0.011**	**<0.001**	**<0.001**
Day 1		0.224	**<0.001**	**<0.001**	**<0.001**
Day 3			**0.001**	**<0.001**	**<0.001**
Day 5				0.102	**<0.001**
Day 7					**<0.001**

Table 5.32 Significant differences between the viability of bone marrow stromal cells following culture in direct contact on high viscosity Type II filled resin composite discs containing 40wt% bioactive glass for 1 day, 3 days, 5 days, 7 days and 12 days (1-way ANOVA, n=3 biological replicates). The culture media was replaced every 2-days. The numbers represent the p value, with the numbers in **bold** showing significant difference between sample conditions.

	Day 1	Day 3	Day 5	Day 7	Day 12
Day 0	**0.013**	0.332	**<0.001**	**<0.001**	**<0.001**
Day 1		**0.013**	**<0.001**	**<0.001**	**<0.001**
Day 3			**<0.001**	**<0.001**	**<0.001**
Day 5				**0.001**	**<0.001**
Day 7					**<0.001**

Table 5.34 Significant differences between the viability of bone marrow stromal cells following culture in in direct contact on high viscosity Type III filled resin composite discs containing 20wt% bioactive glass for 1 day, 3 days, 5 days, 7 days and 12 days (1-way ANOVA, n=3 biological replicates). The culture media was replaced every 2-days. The numbers represent the p value, with the numbers in **bold** showing significant difference between sample conditions.

Statistical data of values for non-viable bone marrow stromal cells seeded in the absence/presence of filled resin composites, unfilled resin systems and PMMA

	Day 1	Day 3	Day 5	Day 7	Day 12
Day 0	**0.006**	**0.004**	**0.013**	**0.012**	**0.022**
Day 1		0.305	0.509	0.710	0.661
Day 3			0.774	0.536	0.176
Day 5				0.764	0.326
Day 7					0.461

Table 5.35 Significant differences between non-viable bone marrow stromal cells following culture in the absence of filled resin composite discs for 1 day, 3 days, 5 days, 7 days and 12 days (1-way ANOVA, n=3 biological replicates). The culture media was replaced every 2-days. The numbers represent the p value, with the numbers in **bold** showing significant difference between sample conditions.

	Day 1	Day 3	Day 5	Day 7	Day 12
Day 0	**<0.001**	**<0.001**	**<0.001**	**<0.001**	**<0.001**
Day 1		**0.014**	**0.014**	**<0.001**	**<0.001**
Day 3			>0.999	**0.001**	**<0.001**
Day 5				**0.001**	**<0.001**
Day 7					**<0.001**

Table 5.36 Significant differences between non-viable bone marrow stromal cells following culture in direct contact on discs containing PMMA for 1 day, 3 days, 5 days, 7 days and 12 days (1-way ANOVA, n=3 biological replicates). The culture media was replaced every 2-days. The numbers represent the p value, with the numbers in **bold** showing significant difference between sample conditions.

	Day 1	Day 3	Day 5	Day 7	Day 12
Day 0	**0.004**	**<0.001**	**<0.001**	**<0.001**	**<0.001**

Day 1		0.015	0.005	0.004	<0.001
Day 3			0.214	0.555	0.001
Day 5				0.401	0.115
Day 7					0.004

Table 5.37 Significant differences between non-viable bone marrow stromal cells following culture in direct contact on low viscosity filled resin composite discs containing 70wt% barium silicate filler for 1 day, 3 days, 5 days, 7 days and 12 days (1-way ANOVA, n=3 biological replicates). The culture media was replaced every 2-days. The numbers represent the p value, with the numbers in **bold** showing significant difference between sample conditions.

	Day 1	Day 3	Day 5	Day 7	Day 12
Day 0	<0.001	<0.001	0.001	<0.001	<0.001
Day 1		<0.001	<0.001	<0.001	<0.001
Day 3			0.016	<0.001	<0.001
Day 5				<0.001	<0.001
Day 7					0.040

Table 5.38 Significant differences between non-viable bone marrow stromal cells following culture in direct contact on unfilled resin system discs containing 60/40wt% UDMA/TEGDMA for 1 day, 3 days, 5 days, 7 days and 12 days (1-way ANOVA, n=3 biological replicates). The culture media was replaced every 2-days.The numbers represent the p value, with the numbers in **bold** showing significant difference between sample conditions.

	Day 1	Day 3	Day 5	Day 7	Day 12
Day 0	0.001	0.001	<0.001	<0.001	0.013
Day 1		0.756	0.077	0.265	0.550
Day 3			0.176	0.483	0.394
Day 5				0.372	0.031
Day 7					0.106

Table 5.39 Significant differences between non-viable bone marrow stromal cells following culture in direct contact on low viscosity Type I filled resin composite discs containing 20wt% bioactive glass for 1 day, 3 days, 5 days, 7 days and 12 days (1-way ANOVA, n=3 biological replicates). The culture media was replaced every 2-days. The numbers represent the p value, with the numbers in **bold** showing significant difference between sample conditions.

	Day 1	Day 3	Day 5	Day 7	Day 12
Day 0	0.001	<0.001	<0.001	<0.001	<0.001
Day 1		0.305	0.133	0.004	0.229
Day 3			0.461	0.010	0.715
Day 5				0.056	0.747
Day 7					0.033

Table 5.40 Significant differences between non-viable bone marrow stromal cells following culture in direct contact on low viscosity Type I filled resin composite discs containing 40wt% bioactive glass for 1 day, 3 days, 5 days, 7 days and 12 days (1-way ANOVA, n=3 biological replicates). The culture media was replaced every 2-days. The numbers represent the p value, with the numbers in **bold** showing significant difference between sample conditions.

	Day 1	Day 3	Day 5	Day 7	Day 12
Day 0	0.003	<0.001	<0.001	0.001	0.001

Day 1		**0.176**	0.051	0.345	0.694
Day 3			0.379	0.750	0.063
Day 5				0.275	**0.018**
Day 7					0.170

Table 5.41 Significant differences between non-viable bone marrow stromal cells following culture in direct contact on low viscosity Type II filled resin composite discs containing 20wt% bioactive glass for 1 day, 3 days, 5 days, 7 days and 12 days (1-way ANOVA, n=3 biological replicates). The culture media was replaced every 2-days. The numbers represent the p value, with the numbers in **bold** showing significant difference between sample conditions.

	Day 1	Day 3	Day 5	Day 7	Day 12
Day 0	**0.003**	**<0.001**	**<0.001**	**0.003**	**0.001**
Day 1		**<0.001**	0.057	0.219	0.694
Day 3			**0.039**	**0.010**	**<0.001**
Day 5				0.536	**0.026**
Day 7					0.122

Table 5.42 Significant differences between non-viable bone marrow stromal cells following culture in direct contact on low viscosity Type II filled resin composite discs containing 40wt% bioactive glass for 1 day, 3 days, 5 days, 7 days and 12 days (1-way ANOVA, n=3 biological replicates). The culture media was replaced every 2-days. The numbers represent the p value, with the numbers in **bold** showing significant difference between sample conditions.

	Day 1	Day 3	Day 5	Day 7	Day 12
Day 0	**0.006**	**0.003**	**0.002**	**0.012**	**0.022**
Day 1		0.444	0.138	0.710	0.661
Day 3			0.394	0.736	0.257
Day 5				0.270	0.079
Day 7					0.461

Table 5.43 Significant differences between non-viable bone marrow stromal cells following culture in direct contact on low viscosity Type III filled resin composite discs containing 20wt% bioactive glass for 1 day, 3 days, 5 days, 7 days and 12 days (1-way ANOVA, n=3 biological replicates). The culture media was replaced every 2-days. The numbers represent the p value, with the numbers in **bold** showing significant difference between sample conditions.

	Day 1	Day 3	Day 5	Day 7	Day 12
Day 0	**0.003**	**<0.001**	**<0.001**	**<0.001**	**0.001**
Day 1		0.106	0.147	**0.014**	0.345
Day 3			>0.999	0.461	0.536
Day 5				0.520	0.576
Day 7					0.176

Table 5.44 Significant differences between non-viable bone marrow stromal cells following culture in direct contact on low viscosity Type III filled resin composite discs containing 40wt% bioactive glass for 1 day, 3 days, 5 days, 7 days and 12 days (1-way ANOVA, n=3 biological replicates). The culture media was replaced every 2-days. The numbers represent the p value, with the numbers in **bold** showing significant difference between sample conditions.

	Day 1	Day 3	Day 5	Day 7	Day 12

Day 0	0.006	0.022	0.013	0.006	0.006
Day 1		0.661	0.509	>0.999	>0.999
Day 3			0.326	0.661	0.661
Day 5				0.509	0.509
Day 7					>0.999

Table 5.45 Significant differences between non-viable bone marrow stromal cells following culture in the absence of filled resin composite discs for 1 day, 3 days, 5 days, 7 days and 12 days (1-way ANOVA, n=3 biological replicates). The culture media was replaced every 2-days. The numbers represent the p value, with the numbers in **bold** showing significant difference between sample conditions.

	Day 1	Day 3	Day 5	Day 7	Day 12
Day 0	0.001	<0.001	<0.001	<0.001	<0.001
Day 1		0.014	0.001	0.008	0.006
Day 3			0.375	0.609	0.829
Day 5				0.675	0.496
Day 7					0.839

Table 5.46 Significant differences between non-viable bone marrow stromal cells following culture in direct contact on high viscosity filled resin composite discs containing 70wt% barium silicate filler for 1 day, 3 days, 5 days, 7 days and 12 days (1-way ANOVA, n=3 biological replicates). The culture media was replaced every 2-days. The numbers represent the p value, with the numbers in **bold** showing significant difference between sample conditions.

	Day 1	Day 3	Day 5	Day 7	Day 12
Day 0	0.022	0.003	<0.001	<0.001	0.004
Day 1		0.810	0.211	0.434	>0.999
Day 3			0.255	0.550	0.779
Day 5				0.509	0.138
Day 7					0.345

Table 5.47 Significant differences between non-viable bone marrow stromal cells following culture in direct contact on high viscosity Type I filled resin composite discs containing 20wt% bioactive glass for 1 day, 3 days, 5 days, 7 days and 12 days (1-way ANOVA, n=3 biological replicates). The culture media was replaced every 2-days. The numbers represent the p value, with the numbers in **bold** showing significant difference between sample conditions.

	Day 1	Day 3	Day 5	Day 7	Day 12
Day 0	<0.001	<0.001	<0.001	<0.001	0.001
Day 1		0.772	0.211	0.747	0.793
Day 3			0.343	>0.999	0.624
Day 5				0.309	0.190
Day 7					0.597

Table 5.48 Significant differences between non-viable bone marrow stromal cells following culture in direct contact on high viscosity Type I filled resin composite discs containing 40wt% bioactive glass for 1 day, 3 days, 5 days, 7 days and 12 days (1-way ANOVA, n=3 biological replicates). The culture media was replaced every 2-days. The numbers represent the p value, with the numbers in **bold** showing significant difference between sample conditions.

	Day 1	Day 3	Day 5	Day 7	Day 12
Day 0	**0.001**	**<0.001**	**<0.001**	**<0.001**	**<0.001**
Day 1		0.063	**0.050**	**0.022**	0.120
Day 3			0.490	0.536	0.747
Day 5				0.821	0.363
Day 7					0.363

Table 5.49 Significant differences between non-viable bone marrow stromal cells following culture in direct contact on high viscosity Type II filled resin composite discs containing 20wt% bioactive glass for 1 day, 3 days, 5 days, 7 days and 12 days (1-way ANOVA, n=3 biological replicates). The culture media was replaced every 2-days. The numbers represent the p value, with the numbers in **bold** showing significant difference between sample conditions.

	Day 1	Day 3	Day 5	Day 7	Day 12
Day 0	**0.003**	**0.002**	**<0.001**	**<0.001**	**0.001**
Day 1		0.394	**0.014**	0.072	0.345
Day 3			0.172	0.346	>0.999
Day 5				0.791	0.133
Day 7					0.313

Table 5.50 Significant differences between non-viable bone marrow stromal cells following culture in direct contact on high viscosity Type II filled resin composite discs containing 40wt% bioactive glass for 1 day, 3 days, 5 days, 7 days and 12 days (1-way ANOVA, n=3 biological replicates). The culture media was replaced every 2-days. The numbers represent the p value, with the numbers in **bold** showing significant difference between sample conditions.

	Day 1	Day 3	Day 5	Day 7	Day 12
Day 0	0.085	0.063	0.063	**0.001**	**0.022**
Day 1		0.710	0.710	0.461	>0.999
Day 3			>0.999	0.176	0.653
Day 5				0.176	0.653
Day 7					0.372

Table 5.51 Significant differences between non-viable bone marrow stromal cells following culture in direct contact on high viscosity Type III filled resin composite discs containing 20wt% bioactive glass for 1 day, 3 days, 5 days, 7 days and 12 days (1-way ANOVA, n=3 biological replicates). The culture media was replaced every 2-days. The numbers represent the p value, with the numbers in **bold** showing significant difference between sample conditions.

Appendix 5 Statistical analysis of culture media acidity values; viable and non-viable bone marrow stromal cells data in the presence of unfilled resin systems, filled resin composites and PMMA

Statistical data of pH change of culture media in the absence/presence of filled resin composites and PMMA

	Day 1	Day 3	Day 5	Day 7	Day 12
Day 0	0.116	0.374	**0.008**	0.116	0.116
Day 1		0.519	**0.018**	>0.999	>0.999
Day 3			**0.013**	0.519	0.519
Day 5				**0.018**	**0.018**
Day 7					>0.999

Table 5.1 Significant differences between the pH of culture media in the absence of filled resin composite discs (1-way ANOVA, n=9). The numbers represent the p value, with the numbers in **bold** showing significant difference between sample conditions.

	Day 1	Day 3	Day 5	Day 7	Day 12
Day 0	0.116	0.116	0.116	0.374	0.116
Day 1		>0.999	>0.999	0.519	>0.999
Day 3			>0.999	0.519	>0.999
Day 5				0.519	>0.999
Day 7					0.519

Table 5.2 Significant differences between the pH of culture media following immersion of low viscosity filled resin composite discs containing 70wt% barium silicate filler (1-way ANOVA, n=9). The numbers represent the p value, with the numbers in **bold** showing significant difference between sample conditions.

	Day 1	Day 3	Day 5	Day 7	Day 12
Day 0	**<0.001**	**<0.001**	**0.002**	**0.002**	**0.001**
Day 1		>0.999	0.251	0.643	0.116
Day 3			0.251	0.643	0.116
Day 5				0.492	0.725
Day 7					0.288

Table 5.3 Significant differences between the pH of culture media following immersion of low viscosity Type I filled resin composite discs containing 20wt% bioactive glass (1-way ANOVA, n=9). The numbers represent the p value, with the numbers in **bold** showing significant difference between sample conditions.

	Day 1	Day 3	Day 5	Day 7	Day 12
Day 0	**<0.001**	**<0.001**	**<0.001**	**0.003**	**<0.001**
Day 1		0.101	0.101	0.230	0.067
Day 3			>0.999	0.742	0.374
Day 5				0.742	0.374
Day 7					0.768

Table 5.4 Significant differences between the pH of culture media following immersion of low viscosity Type I filled resin composite discs containing 40wt% bioactive glass (1-way ANOVA, n=9). The numbers represent the p value, with the numbers in **bold** showing significant difference between sample conditions.

	Day 1	Day 3	Day 5	Day 7	Day 12
Day 0	**<0.001**	**<0.001**	**0.001**	**<0.001**	**0.001**
Day 1		0.230	0.251	**0.013**	0.055
Day 3			0.678	**0.047**	0.148
Day 5				0.251	0.349
Day 7					>0.999

Table 5.5 Significant differences between the pH of culture media following immersion of low viscosity Type II filled resin composite discs containing 20wt% bioactive glass (1-way ANOVA, n=9). The numbers represent the p value, with the numbers in **bold** showing significant difference between sample conditions.

	Day 1	Day 3	Day 5	Day 7	Day 12
Day 0	**<0.001**	**<0.001**	**<0.001**	**0.004**	**<0.001**
Day 1		0.519	>0.999	0.561	**0.047**
Day 3			0.519	0.768	0.101
Day 5				0.561	**0.047**
Day 7					0.561

Table 5.6 Significant differences between the pH of culture media following immersion of low viscosity Type II filled resin composite discs containing 40wt% bioactive glass (1-way ANOVA, n=9). The numbers represent the p value, with the numbers in **bold** showing significant difference between sample conditions.

	Day 1	Day 3	Day 5	Day 7	Day 12
Day 0	**<0.001**	**0.002**	**<0.001**	**0.002**	**<0.001**
Day 1		>0.999	>0.999	>0.999	>0.999
Day 3			>0.999	>0.999	>0.999
Day 5				>0.999	>0.999
Day 7					>0.999

Table 5.7 Significant differences between the pH of culture media following immersion of low viscosity Type III filled resin composite discs containing 20wt% bioactive glass (1-way ANOVA, n=9). The numbers represent the p value, with the numbers in **bold** showing significant difference between sample conditions.

	Day 1	Day 3	Day 5	Day 7	Day 12
Day 0	**0.002**	**<0.001**	**<0.001**	**0.003**	**0.001**
Day 1		>0.999	0.251	0.742	0.725
Day 3			0.101	0.678	0.643
Day 5				0.148	0.374
Day 7					0.492

Table 5.8 Significant differences between the pH of culture media following immersion of low viscosity Type III filled resin composite discs containing 40wt% bioactive glass (1-way ANOVA, n=9). The numbers represent the p value, with the numbers in **bold** showing significant difference between sample conditions.

	Day 1	Day 3	Day 5	Day 7	Day 12
Day 0	0.217	0.374	0.374	0.116	0.116
Day 1		0.834	0.834	0.628	0.628
Day 3			>0.999	0.519	0.519
Day 5				0.519	0.519
Day 7					>0.999

Table 5.9 Significant differences between the pH of culture media in the absence of filled composite discs (1-way ANOVA, n=9). The numbers represent the p value, with the numbers in **bold** showing significant difference between sample conditions.

	Day 1	Day 3	Day 5	Day 7	Day 12
Day 0	0.374	0.374	0.116	0.116	0.725
Day 1		>0.999	0.519	0.519	>0.999
Day 3			0.519	0.519	>0.999
Day 5				>0.999	0.742
Day 7					0.742

Table 5.10 Significant differences between the pH of culture media following immersion of high viscosity filled resin composite discs containing 80wt% barium silicate filler (1-way ANOVA, n=9). The numbers represent the p value, with the numbers in **bold** showing significant difference between sample conditions.

	Day 1	Day 3	Day 5	Day 7	Day 12
Day 0	**<0.001**	**<0.001**	**0.001**	**<0.001**	**0.002**
Day 1		>0.999	>0.999	>0.999	0.519
Day 3			>0.999	>0.999	0.519
Day 5				>0.999	0.579
Day 7					0.519

Table 5.11 Significant differences between the pH of culture media following immersion of high viscosity Type I filled resin composite discs containing 23wt% bioactive glass (1-way ANOVA, n=9). The numbers represent the p value, with the numbers in **bold** showing significant difference between sample conditions.

	Day 1	Day 3	Day 5	Day 7	Day 12
Day 0	**<0.001**	**0.001**	**<0.001**	**<0.001**	**0.001**
Day 1		0.422	>0.999	>0.999	0.678
Day 3			0.422	0.422	0.349
Day 5				>0.999	0.678
Day 7					0.678

Table 5.12 Significant differences between the pH of culture media following immersion of high viscosity Type I filled resin composite discs containing 45wt% bioactive glass (1-way ANOVA, n=9). The numbers represent the p value, with the numbers in **bold** showing significant difference between sample conditions.

	Day 1	Day 3	Day 5	Day 7	Day 12
Day 0	**0.002**	**<0.001**	**<0.001**	**0.001**	**0.001**
Day 1		>0.999	0.742	0.778	0.468
Day 3			0.519	0.678	0.349
Day 5				>0.999	0.519
Day 7					0.579

Table 5.13 Significant differences between the pH of culture media following immersion of high viscosity Type II filled resin composite discs containing 23wt% bioactive glass (1-way ANOVA, n=9). The numbers represent the p value, with the numbers in **bold** showing significant difference between sample conditions.

	Day 1	Day 3	Day 5	Day 7	Day 12
Day 0	**<0.001**	**<0.001**	**0.001**	**<0.001**	**<0.001**
Day 1		0.422	0.519	0.725	>0.999
Day 3			>0.999	0.643	0.422
Day 5				0.725	0.519
Day 7					0.725

Table 5.14 Significant differences between the pH of culture media following immersion of high viscosity Type II filled resin composite discs containing 45wt% bioactive glass (1-way ANOVA, n=9). The numbers represent the p value, with the numbers in **bold** showing significant difference between sample conditions.

	Day 1	Day 3	Day 5	Day 7	Day 12
Day 0	**0.007**	**0.002**	**0.008**	**<0.001**	**<0.001**
Day 1		0.795	0.643	0.768	0.768
Day 3			0.778	>0.999	>0.999
Day 5				0.742	0.742
Day 7					>0.999

Table 5.15 Significant differences between the pH of culture media following immersion of high viscosity Type III filled resin composite discs containing 20wt% bioactive glass (1-way ANOVA, n=9). The numbers represent the p value, with the numbers in **bold** showing significant difference between sample conditions.

	Day 1	Day 3	Day 5	Day 7	Day 12
Day 0	0.279	**0.001**	**0.001**	**0.025**	>0.999
Day 1		>0.999	0.816	0.734	0.289
Day 3			0.230	0.251	**0.007**
Day 5				0.678	**0.016**
Day 12					**0.057**

Table 5.16 Significant differences between the pH of culture media following immersion of PMMA discs containing (1-way ANOVA, n=9). The numbers represent the p value, with the numbers in **bold** showing significant difference between sample conditions.

Statistical data of viability values of bone marrow stromal cells seeded in the absence/presence of filled resin composites, unfilled resin systems and PMMA

	Day 1	Day 3	Day 5	Day 7	Day 12
Day 0	**<0.001**	**<0.001**	**<0.001**	**<0.001**	**<0.001**
Day 1		>0.999	0.363	**0.018**	**0.002**
Day 3			0.504	0.099	**0.024**
Day 5				0.270	0.063
Day 7					0.332

Table 5.17 Significant differences between viable bone marrow stromal cells following culture in direct contact on unfilled resin system discs containing 60/40wt% UDMA/TEGDMA for 1 day, 3 days, 5 days, 7 days and 12 days (1-way ANOVA, n=3 biological replicates). The culture media was replaced every 2-days.The numbers represent the p value, with the numbers in **bold** showing significant difference between sample conditions.

	Day 1	Day 3	Day 5	Day 7	Day 12
Day 0	**<0.001**	**<0.001**	**0.035**	**<0.001**	**<0.001**
Day 1		**<0.001**	**<0.001**	**<0.001**	**<0.001**
Day 3			**0.008**	**<0.001**	**<0.001**
Day 5				**<0.001**	**<0.001**
Day 7					**<0.001**

Table 5.18 Significant differences between viable bone marrow stromal cells following culture in direct contact on discs containing PMMA for 1 day, 3 days, 5 days, 7 days and 12 days (1-way ANOVA, n=3 biological replicates). The culture media was replaced every 2-days. The numbers represent the p value, with the numbers in **bold** showing significant difference between sample conditions.

	Day 1	Day 3	Day 5	Day 7	Day 12
Day 0	0.114	0.779	**<0.001**	**<0.001**	**<0.001**
Day 1		0.162	**<0.001**	**<0.001**	**<0.001**
Day 3			**0.004**	**<0.001**	**<0.001**
Day 5				**<0.001**	**<0.001**
Day 7					**0.011**

Table 5.19 Significant differences between the viability of bone marrow stromal cells following culture in the absence of filled resin composite discs for 1 day, 3 days, 5 days, 7 days and 12 days (1-way ANOVA, n=3 biological replicates). The culture media was replaced every 2-days. The numbers represent the p value, with the numbers in **bold** showing significant difference between sample conditions.

	Day 1	Day 3	Day 5	Day 7	Day 12
Day 0	**0.001**	**<0.001**	**<0.001**	**0.022**	0.313
Day 1		0.882	0.143	0.255	0.237
Day 3			**0.042**	0.239	0.245
Day 5				0.903	0.611
Day 7					0.705

Table 5.20 Significant differences between the viability of bone marrow stromal cells following culture in direct contact on low viscosity filled resin composite discs containing 70wt% barium silicate filler for 1 day, 3 days, 5 days, 7 days and 12 days (1-way ANOVA, n=3 biological replicates). The culture media was replaced every 2-days. The numbers represent the p value, with the numbers in **bold** showing significant difference between sample conditions.

	Day 1	Day 3	Day 5	Day 7	Day 12
Day 0	**0.002**	**<0.001**	0.675	**0.003**	**<0.001**
Day 1		0.128	**0.008**	**<0.001**	**<0.001**
Day 3			**0.031**	**0.001**	**<0.001**
Day 5				**0.003**	**<0.001**
Day 7					**0.009**

Table 5.21 Significant differences between the viability of bone marrow stromal cells following culture in direct contact on low viscosity Type I filled resin composite discs containing 20wt% bioactive glass for 1 day, 3 days, 5 days, 7 days and 12 days (1-way ANOVA, n=3 biological replicates). The culture media was replaced every 2-days. The numbers represent the p value, with the numbers in **bold** showing significant difference between sample conditions.

	Day 1	Day 3	Day 5	Day 7	Day 12
Day 0	**<0.001**	**<0.001**	**0.008**	**<0.001**	**<0.001**
Day 1		0.774	**0.008**	**<0.001**	**<0.001**
Day 3			**0.027**	**<0.001**	**<0.001**
Day 5				**<0.001**	**<0.001**
Day 7					**<0.001**

Table 5.22 Significant differences between the viability of bone marrow stromal cells following culture in direct contact on low viscosity Type I filled resin composite discs containing 40wt% bioactive glass for 1 day, 3 days, 5 days, 7 days and 12 days (1-way ANOVA, n=3 biological replicates). The culture media was replaced every 2-days. The numbers represent the p value, with the numbers in **bold** showing significant difference between sample conditions.

	Day 1	Day 3	Day 5	Day 7	Day 12
Day 0	**<0.001**	**0.001**	0.390	**<0.001**	**<0.001**
Day 1		>0.999	0.236	**<0.001**	**<0.001**
Day 3			0.257	**<0.001**	**<0.001**
Day 5				**<0.001**	**<0.001**
Day 7					**0.001**

Table 5.23 Significant differences between the viability of bone marrow stromal cells following culture in direct contact on low viscosity Type II filled resin composite discs containing 20wt% bioactive glass for 1 day, 3 days, 5 days, 7 days and 12 days (1-way ANOVA, n=3 biological replicates). The culture media was replaced every 2-days. The numbers represent the p value, with the numbers in **bold** showing significant difference between sample conditions.

	Day 1	Day 3	Day 5	Day 7	Day 12
Day 0	**<0.001**	**<0.001**	**<0.001**	**<0.001**	**<0.001**
Day 1		0.211	**0.004**	**<0.001**	**<0.001**
Day 3			**0.014**	**<0.001**	**<0.001**
Day 5				**<0.001**	**<0.001**
Day 7					**<0.001**

Table 5.24 Significant differences between the viability of bone marrow stromal cells following culture in direct contact on low viscosity Type II filled resin composite discs containing 40wt% bioactive glass for 1 day, 3 days, 5 days, 7 days and 12 days (1-way ANOVA, n=3 biological replicates). The culture media was replaced every 2-days. The numbers represent the p value, with the numbers in **bold** showing significant difference between sample conditions.

	Day 1	Day 3	Day 5	Day 7	Day 12
Day 0	**<0.001**	**0.077**	0.595	**<0.001**	**<0.001**
Day 1		0.238	**0.001**	**<0.001**	**<0.001**
Day 3			0.093	**0.001**	**<0.001**
Day 5				**0.039**	**<0.001**
Day 7					**<0.001**

Table 5.25 Significant differences between the viability of bone marrow stromal cells following culture in direct contact on low viscosity Type III filled resin composite discs containing 20wt% bioactive glass for 1 day, 3 days, 5 days, 7 days and 12 days (1-way ANOVA, n=3 biological replicates). The culture media was replaced every 2-days. The numbers represent the p value, with the numbers in **bold** showing significant difference between sample conditions.

	Day 1	Day 3	Day 5	Day 7	Day 12
Day 0	**<0.001**	**<0.001**	**0.044**	0.414	**<0.001**
Day 1		0.700	**0.018**	**<0.001**	**<0.001**
Day 3			0.076	**<0.001**	**<0.001**
Day 5				**0.037**	**<0.001**
Day 7					**<0.001**

Table 5.26 Significant differences between the viability of bone marrow stromal cells following culture in direct contact on low viscosity Type III filled resin composite discs containing 40wt% bioactive glass for 1 day, 3 days, 5 days, 7 days and 12 days (1-way ANOVA, n=3 biological replicates). The culture media was replaced every 2-days. The numbers represent the p value, with the numbers in **bold** showing significant difference between sample conditions.

	Day 1	Day 3	Day 5	Day 7	Day 12
Day 0	**0.022**	0.675	**<0.001**	**<0.001**	**<0.001**
Day 1		0.094	**<0.001**	**<0.001**	**<0.001**
Day 3			**<0.001**	**<0.001**	**<0.001**
Day 5				**<0.001**	**<0.001**
Day 7					**<0.001**

Table 5.27 Significant differences between the viability of bone marrow stromal cells following culture in the absence of filled composite discs for 1 day, 3 days, 5 days, 7 days and 12 days (1-way ANOVA, n=3 biological replicates). The culture media was replaced every 2-days. (1-way ANOVA, n=3 biological replicates). The numbers represent the p value, with the numbers in **bold** showing significant difference between sample conditions.

	Day 1	Day 3	Day 5	Day 7	Day 12
Day 0	**<0.001**	**<0.001**	**<0.001**	0.332	**<0.001**
Day 1		**0.020**	**<0.001**	**<0.001**	**<0.001**
Day 3			**<0.001**	**<0.001**	**<0.001**
Day 5				**<0.001**	**<0.001**
Day 7					**<0.001**

Table 5.28 Significant differences between the viability of bone marrow stromal cells following culture in in direct contact on high viscosity filled resin composite discs containing 80wt% barium silicate filler for 1 day, 3 days, 5 days, 7 days and 12 days (1-way ANOVA, n=3 biological replicates). The culture media was replaced every 2-days. The numbers represent the p value, with the numbers in **bold** showing significant difference between sample conditions.

	Day 1	Day 3	Day 5	Day 7	Day 12
Day 0	**0.001**	0.150	**0.003**	**<0.001**	**<0.001**
Day 1		0.160	**<0.001**	**<0.001**	**<0.001**
Day 3			**0.003**	**<0.001**	**<0.001**
Day 5				**<0.001**	**<0.001**
Day 7					**0.002**

Table 5.29 Significant differences between the viability of bone marrow stromal cells following culture in in direct contact on high viscosity Type I filled resin composite discs containing 23wt% bioactive glass for 1 day, 3 days, 5 days, 7 days and 12 days (1-way ANOVA, n=3 biological replicates). The culture media was replaced every 2-days. The numbers represent the p value, with the numbers in **bold** showing significant difference between sample conditions.

	Day 1	Day 3	Day 5	Day 7	Day 12
Day 0	**0.001**	**<0.001**	**0.004**	**<0.001**	**<0.001**
Day 1		0.624	**<0.001**	**<0.001**	**<0.001**
Day 3			**<0.001**	**<0.001**	**<0.001**
Day 5				**<0.001**	**<0.001**
Day 7					**<0.001**

Table 5.30 Significant differences between the viability of bone marrow stromal cells following culture in in direct contact on high viscosity Type I filled resin composite discs containing 45wt% bioactive glass for 1 day, 3 days, 5 days, 7 days and 12 days (1-way ANOVA, n=3 biological replicates). The culture media was replaced every 2-days. The numbers represent the p value, with the numbers in **bold** showing significant difference between sample conditions.

	Day 1	Day 3	Day 5	Day 7	Day 12
Day 0	0.265	0.435	**<0.001**	**<0.001**	**<0.001**
Day 1		0.185	**<0.001**	**<0.001**	**<0.001**
Day 3			**0.001**	**<0.001**	**<0.001**
Day 5				0.074	**<0.001**
Day 7					**<0.001**

Table 5.31 Significant differences between the viability of bone marrow stromal cells following culture in direct contact on high viscosity Type II filled resin composite discs containing 23wt% bioactive glass for 1 day, 3 days, 5 days, 7 days and 12 days (1-way ANOVA, n=3 biological replicates). The culture media was replaced every 2-days. The numbers represent the p value, with the numbers in **bold** showing significant difference between sample conditions.

	Day 1	Day 3	Day 5	Day 7	Day 12
Day 0	**0.001**	**0.012**	**0.011**	**<0.001**	**<0.001**
Day 1		0.224	**<0.001**	**<0.001**	**<0.001**
Day 3			**0.001**	**<0.001**	**<0.001**
Day 5				0.102	**<0.001**
Day 7					**<0.001**

Table 5.32 Significant differences between the viability of bone marrow stromal cells following culture in direct contact on high viscosity Type II filled resin composite discs containing 45wt% bioactive glass for 1 day, 3 days, 5 days, 7 days and 12 days (1-way ANOVA, n=3 biological replicates). The culture media was replaced every 2-days. The numbers represent the p value, with the numbers in **bold** showing significant difference between sample conditions.

	Day 1	Day 3	Day 5	Day 7	Day 12
Day 0	**0.013**	0.332	**<0.001**	**<0.001**	**<0.001**
Day 1		**0.013**	**<0.001**	**<0.001**	**<0.001**
Day 3			**<0.001**	**<0.001**	**<0.001**
Day 5				**0.001**	**<0.001**
Day 7					**<0.001**

Table 5.34 Significant differences between the viability of bone marrow stromal cells following culture in in direct contact on high viscosity Type III filled resin composite discs containing 23wt% bioactive glass for 1 day, 3 days, 5 days, 7 days and 12 days (1-way ANOVA, n=3 biological replicates). The culture media was replaced every 2-days. The numbers represent the p value, with the numbers in **bold** showing significant difference between sample conditions.

Statistical data of values for non-viable bone marrow stromal cells seeded in the absence/presence of filled resin composites, unfilled resin systems and PMMA

	Day 1	Day 3	Day 5	Day 7	Day 12
Day 0	**0.006**	**0.004**	**0.013**	**0.012**	**0.022**
Day 1		0.305	0.509	0.710	0.661
Day 3			0.774	0.536	0.176
Day 5				0.764	0.326
Day 7					0.461

Table 5.35 Significant differences between non-viable bone marrow stromal cells following culture in the absence of filled resin composite discs for 1 day, 3 days, 5 days, 7 days and 12 days (1-way ANOVA, n=3 biological replicates). The culture media was replaced every 2-days. The numbers represent the p value, with the numbers in **bold** showing significant difference between sample conditions.

	Day 1	Day 3	Day 5	Day 7	Day 12
Day 0	**<0.001**	**<0.001**	**<0.001**	**<0.001**	**<0.001**
Day 1		**0.014**	**0.014**	**<0.001**	**<0.001**
Day 3			>0.999	**0.001**	**<0.001**
Day 5				**0.001**	**<0.001**
Day 7					**<0.001**

Table 5.36 Significant differences between non-viable bone marrow stromal cells following culture in direct contact on discs containing PMMA for 1 day, 3 days, 5 days, 7 days and 12 days (1-way ANOVA, n=3 biological replicates). The culture media was replaced every 2-days. The numbers represent the p value, with the numbers in **bold** showing significant difference between sample conditions.

	Day 1	Day 3	Day 5	Day 7	Day 12
Day 0	**0.004**	**<0.001**	**<0.001**	**<0.001**	**<0.001**
Day 1		**0.015**	**0.005**	**0.004**	**<0.001**
Day 3			0.214	0.555	**0.001**
Day 5				0.401	**0.115**
Day 7					**0.004**

Table 5.37 Significant differences between non-viable bone marrow stromal cells following culture in direct contact on low viscosity filled resin composite discs containing 70wt% barium silicate filler for 1 day, 3 days, 5 days, 7 days and 12 days (1-way ANOVA, n=3 biological replicates). The culture media was replaced every 2-days. The numbers represent the p value, with the numbers in **bold** showing significant difference between sample conditions.

	Day 1	Day 3	Day 5	Day 7	Day 12
Day 0	**<0.001**	**<0.001**	**0.001**	**<0.001**	**<0.001**
Day 1		**<0.001**	**<0.001**	**<0.001**	**<0.001**
Day 3			**0.016**	**<0.001**	**<0.001**
Day 5				**<0.001**	**<0.001**
Day 7					**0.040**

Table 5.38 Significant differences between non-viable bone marrow stromal cells following culture in direct contact on unfilled resin system discs containing 60/40wt% UDMA/TEGDMA for 1 day, 3 days, 5 days, 7 days and 12 days (1-way ANOVA, n=3 biological replicates). The culture media was replaced every 2-days.The numbers represent the p value, with the numbers in **bold** showing significant difference between sample conditions.

	Day 1	Day 3	Day 5	Day 7	Day 12
Day 0	**0.001**	**0.001**	**<0.001**	**<0.001**	**0.013**
Day 1		0.756	0.077	0.265	0.550
Day 3			0.176	0.483	0.394
Day 5				0.372	**0.031**
Day 7					0.106

Table 5.39 Significant differences between non-viable bone marrow stromal cells following culture in direct contact on low viscosity Type I filled resin composite discs containing 20wt% bioactive glass for 1 day, 3 days, 5 days, 7 days and 12 days (1-way ANOVA, n=3 biological replicates). The culture media was replaced every 2-days. The numbers represent the p value, with the numbers in **bold** showing significant difference between sample conditions.

	Day 1	Day 3	Day 5	Day 7	Day 12
Day 0	**0.001**	**<0.001**	**<0.001**	**<0.001**	**<0.001**
Day 1		0.305	0.133	**0.004**	0.229
Day 3			0.461	**0.010**	0.715
Day 5				0.056	0.747
Day 7					**0.033**

Table 5.40 Significant differences between non-viable bone marrow stromal cells following culture in direct contact on low viscosity Type I filled resin composite discs containing 40wt% bioactive glass for 1 day, 3 days, 5 days, 7 days and 12 days (1-way ANOVA, n=3 biological replicates). The culture media was replaced every 2-days. The numbers represent the p value, with the numbers in **bold** showing significant difference between sample conditions.

	Day 1	Day 3	Day 5	Day 7	Day 12
Day 0	**0.003**	**<0.001**	**<0.001**	**0.001**	**0.001**
Day 1		**0.176**	0.051	0.345	0.694
Day 3			0.379	0.750	0.063
Day 5				0.275	**0.018**
Day 7					0.170

Table 5.41 Significant differences between non-viable bone marrow stromal cells following culture in direct contact on low viscosity Type II filled resin composite discs containing 20wt% bioactive glass for 1 day, 3 days, 5 days, 7 days and 12 days (1-way ANOVA, n=3 biological replicates). The culture media was replaced every 2-days. The numbers represent the p value, with the numbers in **bold** showing significant difference between sample conditions.

	Day 1	Day 3	Day 5	Day 7	Day 12
Day 0	**0.003**	**<0.001**	**<0.001**	**0.003**	**0.001**
Day 1		**<0.001**	0.057	0.219	0.694
Day 3			**0.039**	**0.010**	**<0.001**
Day 5				0.536	**0.026**
Day 7					0.122

Table 5.42 Significant differences between non-viable bone marrow stromal cells following culture in direct contact on low viscosity Type II filled resin composite discs containing 40wt% bioactive glass for 1 day, 3 days, 5 days, 7 days and 12 days (1-way ANOVA, n=3 biological replicates). The culture media was replaced every 2-days. The numbers represent the p value, with the numbers in **bold** showing significant difference between sample conditions.

	Day 1	Day 3	Day 5	Day 7	Day 12
Day 0	**0.006**	**0.003**	**0.002**	**0.012**	**0.022**
Day 1		0.444	0.138	0.710	0.661
Day 3			0.394	0.736	0.257
Day 5				0.270	0.079
Day 7					0.461

Table 5.43 Significant differences between non-viable bone marrow stromal cells following culture in direct contact on low viscosity Type III filled resin composite discs containing 20wt% bioactive glass for 1 day, 3 days, 5 days, 7 days and 12 days (1-way ANOVA, n=3 biological replicates). The culture media was replaced every 2-days. The numbers represent the p value, with the numbers in **bold** showing significant difference between sample conditions.

	Day 1	Day 3	Day 5	Day 7	Day 12
Day 0	**0.003**	**<0.001**	**<0.001**	**<0.001**	**0.001**
Day 1		0.106	0.147	**0.014**	0.345
Day 3			>0.999	0.461	0.536
Day 5				0.520	0.576
Day 7					0.176

Table 5.44 Significant differences between non-viable bone marrow stromal cells following culture in direct contact on low viscosity Type III filled resin composite discs containing 40wt% bioactive glass for 1 day, 3 days, 5 days, 7 days and 12 days (1-way ANOVA, n=3 biological replicates). The culture media was replaced every 2-days. The numbers represent the p value, with the numbers in **bold** showing significant difference between sample conditions.

	Day 1	Day 3	Day 5	Day 7	Day 12
Day 0	**0.006**	**0.022**	**0.013**	**0.006**	**0.006**
Day 1		0.661	0.509	>0.999	>0.999
Day 3			0.326	0.661	0.661
Day 5				0.509	0.509
Day 7					>0.999

Table 5.45 Significant differences between non-viable bone marrow stromal cells following culture in the absence of filled resin composite discs for 1 day, 3 days, 5 days, 7 days and 12 days (1-way ANOVA, n=3 biological replicates). The culture media was replaced every 2-days. The numbers represent the p value, with the numbers in **bold** showing significant difference between sample conditions.

	Day 1	Day 3	Day 5	Day 7	Day 12
Day 0	**0.001**	**<0.001**	**<0.001**	**<0.001**	**<0.001**
Day 1		**0.014**	**0.001**	**0.008**	**0.006**
Day 3			0.375	0.609	0.829
Day 5				0.675	0.496
Day 7					0.839

Table 5.46 Significant differences between non-viable bone marrow stromal cells following culture in direct contact on high viscosity filled resin composite discs containing 80wt% barium silicate filler for 1 day, 3 days, 5 days, 7 days and 12 days (1-way ANOVA, n=3 biological replicates). The culture media was replaced every 2-days. The numbers represent the p value, with the numbers in **bold** showing significant difference between sample conditions.

	Day 1	Day 3	Day 5	Day 7	Day 12
Day 0	**0.022**	**0.003**	**<0.001**	**<0.001**	**0.004**
Day 1		0.810	0.211	0.434	>0.999
Day 3			0.255	0.550	0.779
Day 5				0.509	0.138
Day 7					0.345

Table 5.47 Significant differences between non-viable bone marrow stromal cells following culture in direct contact on high viscosity Type I filled resin composite discs containing 23wt% bioactive glass for 1 day, 3 days, 5 days, 7 days and 12 days (1-way ANOVA, n=3 biological replicates). The culture media was replaced every 2-days. The numbers represent the p value, with the numbers in **bold** showing significant difference between sample conditions.

	Day 1	Day 3	Day 5	Day 7	Day 12
Day 0	**<0.001**	**<0.001**	**<0.001**	**<0.001**	**0.001**
Day 1		0.772	0.211	0.747	0.793
Day 3			0.343	>0.999	0.624
Day 5				0.309	0.190
Day 7					0.597

Table 5.48 Significant differences between non-viable bone marrow stromal cells following culture in direct contact on high viscosity Type I filled resin composite discs containing 45wt% bioactive glass for 1 day, 3 days, 5 days, 7 days and 12 days (1-way ANOVA, n=3 biological replicates). The culture media was replaced every 2-days. The numbers represent the p value, with the numbers in **bold** showing significant difference between sample conditions.

	Day 1	Day 3	Day 5	Day 7	Day 12
Day 0	**0.001**	**<0.001**	**<0.001**	**<0.001**	**<0.001**
Day 1		0.063	**0.050**	**0.022**	0.120
Day 3			0.490	0.536	0.747
Day 5				0.821	0.363
Day 7					0.363

Table 5.49 Significant differences between non-viable bone marrow stromal cells following culture in direct contact on high viscosity Type II filled resin composite discs containing 23wt% bioactive glass for 1 day, 3 days, 5 days, 7 days and 12 days (1-way ANOVA, n=3 biological replicates). The culture media was replaced every 2-days. The numbers represent the p value, with the numbers in **bold** showing significant difference between sample conditions.

	Day 1	Day 3	Day 5	Day 7	Day 12
Day 0	**0.003**	**0.002**	**<0.001**	**<0.001**	**0.001**
Day 1		0.394	**0.014**	0.072	0.345
Day 3			0.172	0.346	>0.999
Day 5				0.791	0.133
Day 7					0.313

Table 5.50 Significant differences between non-viable bone marrow stromal cells following culture in direct contact on high viscosity Type II filled resin composite discs containing 45wt% bioactive glass for 1 day, 3 days, 5 days, 7 days and 12 days (1-way ANOVA, n=3 biological replicates). The culture media was replaced every 2-days. The numbers represent the p value, with the numbers in **bold** showing significant difference between sample conditions.

	Day 1	Day 3	Day 5	Day 7	Day 12
Day 0	0.085	0.063	0.063	**0.001**	**0.022**
Day 1		0.710	0.710	0.461	>0.999
Day 3			>0.999	0.176	0.653
Day 5				0.176	0.653
Day 7					0.372

Table 5.51 Significant differences between non-viable bone marrow stromal cells following culture in direct contact on high viscosity Type III filled resin composite discs containing 23wt% bioactive glass for 1 day, 3 days, 5 days, 7 days and 12 days (1-way ANOVA, n=3 biological replicates). The culture media was replaced every 2-days. The numbers represent the p value, with the numbers in **bold** showing significant difference between sample conditions.

Appendix 6 Correlation analysis of unfilled resin systems and filled resin composites

Correlation analysis of unfilled resin systems

	FS	FM	DC	HV US
FM	**0.748**			
DC	**-0.808**	-0.385		
HV US	-0.051	0.475	**0.630**	
HV LS	-0.321	0.217	**0.818**	**0.962**

Table 6.1 Correlations between the flexural strength (FS), flexural modulus (FM), degree of conversion (DC), hardness value for upper surface (HV US) and hardness value for lower surface (HV LS) of unfilled resin systems containing 20/80wt% UDMA/TEGDMA. The numbers represent the Pearson correlation coefficient, with the numbers in **bold** showing a strong correlation between sample conditions.

	FS	FM	DC	HV US
FM	**0.915**			
DC	**-1.000**	**-0.994**		
HV US	-0.364	-0.266	0.369	
HV LS	0.461	0.550	-0.456	**0.659**

Table 6.2 Correlations between the flexural strength (FS), flexural modulus (FM), degree of conversion (DC), hardness value for upper surface (HV US) and hardness value for lower surface (HV LS) of unfilled resin systems containing 30/70wt% UDMA/TEGDMA. The numbers represent the Pearson correlation coefficient, with the numbers in **bold** showing a strong correlation between sample conditions.

	FS	FM	DC	HV US
FM	**0.926**			
DC	0.472	0.368		
HV US	**0.800**	**0.726**	**0.907**	
HV LS	**-0.986**	**-0.960**	**-0.613**	**-0.889**

Table 6.3 Correlations between the flexural strength (FS), flexural modulus (FM), degree of conversion (DC), hardness value for upper surface (HV US) and hardness value for lower surface (HV LS) of unfilled resin systems containing 40/60wt% UDMA/TEGDMA. The numbers represent the Pearson correlation coefficient, with the numbers in **bold** showing a strong correlation between sample conditions.

	FS	FM	DC	HV US
FM	**0.614**			
DC	0.425	0.476		
HV US	**0.673**	**0.714**	**0.956**	
HV LS	**-0.860**	**-0.888**	**-0.828**	**-0.956**

Table 6.4 Correlations between the flexural strength (FS), flexural modulus (FM), degree of conversion (DC), hardness value for upper surface (HV US) and hardness value for lower surface (HV LS) of unfilled resin systems containing 50/50wt% UDMA/TEGDMA. The numbers represent the Pearson correlation coefficient, with the numbers in **bold** showing a strong correlation between sample conditions.

	FS	FM	DC	HV US
FM	0.081			
DC	**-0.999**	**0.788**		
HV US	**-0.852**	**0.989**	**0.870**	
HV LS	**-0.622**	**0.980**	**0.650**	**0.940**

Table 6.5 Correlations between the flexural strength (FS), flexural modulus (FM), degree of conversion (DC), hardness value for upper surface (HV US) and hardness value for lower surface (HV LS) of unfilled resin systems containing 60/40wt% UDMA/TEGDMA. The numbers represent the Pearson correlation coefficient, with the numbers in **bold** showing a strong correlation between sample conditions.

	FS	FM	DC	HV US
FM	**0.958**			
DC	-0.543	-0.572		
HV US	**0.758**	**0.781**	**-0.959**	
HV LS	0.336	0.369	**-0.973**	**0.869**

Table 6.6 Correlations between the flexural strength (FS), flexural modulus (FM), degree of conversion (DC), hardness value for upper surface (HV US) and hardness value for lower surface (HV LS) of unfilled resin systems containing 70/30wt% UDMA/TEGDMA. The numbers represent the Pearson correlation coefficient, with the numbers in **bold** showing a strong correlation between sample conditions.

	FS	FM	DC	HV US
FM	**0.889**			
DC	0.408	0.291		
HV US	**-0.801**	**-0.870**	0.220	
HV LS	0.095	-0.029	**0.948**	0.519

Table 6.7 Correlations between the flexural strength (FS), flexural modulus (FM), degree of conversion (DC), hardness value for upper surface (HV US) and hardness value for lower surface (HV LS) of unfilled resin systems containing 80/20wt% UDMA/TEGDMA. The numbers represent the Pearson correlation coefficient, with the numbers in **bold** showing a strong correlation between sample conditions.

	FS	FM	DC	HV US
FM	**0.830**			
DC	0.115	-0.077		
HV US	0.007	0.197	**-0.993**	
HV LS	-0.458	**-0.620**	**0.830**	**-0.892**

Table 6.8 Correlations between the flexural strength (FS), flexural modulus (FM), degree of conversion (DC), hardness value for upper surface (HV US) and hardness value for lower surface (HV LS) of unfilled resin systems containing 100/0wt% UDMA/TEGDMA. The numbers represent the Pearson correlation coefficient, with the numbers in **bold** showing a strong correlation between sample conditions.

	FS	FM	DC	HV US
FM	**0.807**			
DC	**-0.999**	**-0.987**		
HV US	**1.000**	**0.978**	**-0.999**	
HV LS	-0.067	-0.264	0.108	-0.058

Table 6.9 Correlations between the flexural strength (FS), flexural modulus (FM), degree of conversion (DC), hardness value for upper surface (HV US) and hardness value for lower surface (HV LS) of unfilled resin systems containing 0/100wt% UDMA/TEGDMA. The numbers represent the Pearson correlation coefficient, with the numbers in **bold** showing a strong correlation between sample conditions.

	FS	FM	DC	HV US
FM	**0.734**			
DC	**0.980**	**0.999**		
HV US	-0.334	-0.470	-0.516	
HV LS	**0.773**	**0.670**	**0.630**	0.339

Table 6.10 Correlations between the flexural strength (FS), flexural modulus (FM), degree of conversion (DC), hardness value for upper surface (HV US) and hardness value for lower surface (HV LS) of unfilled resin systems containing 20/80wt% bisGMA/TEGDMA. The numbers represent the Pearson correlation coefficient, with the numbers in **bold** showing a strong correlation between sample conditions.

	FS	FM	DC	HV US
FM	**0.966**			
DC	**1.000**	**0.995**		
HV US	**-0.841**	**-0.794**	**-0.852**	
HV LS	-0.380	-0.305	-0.401	**0.821**

Table 6.11 Correlations between the flexural strength (FS), flexural modulus (FM), degree of conversion (DC), hardness value for upper surface (HV US) and hardness value for lower surface (HV LS) of unfilled resin systems containing 30/70wt% bisGMA/TEGDMA. The numbers represent the Pearson correlation coefficient, with the numbers in **bold** showing a strong correlation between sample conditions.

	FS	FM	DC	HV US
FM	0.322			
DC	**-0.781**	0.040		
HV US	**-0.972**	-0.389	**0.905**	
HV LS	0.383	-0.516	**-0.876**	-0.588

Table 6.12 Correlations between the flexural strength (FS), flexural modulus (FM), degree of conversion (DC), hardness value for upper surface (HV US) and hardness value for lower surface (HV LS) of unfilled resin systems containing 40/60wt% bisGMA/TEGDMA. The numbers represent the Pearson correlation coefficient, with the numbers in **bold** showing a strong correlation between sample conditions.

	FS	FM	DC	HV US
FM	0.573			
DC	**1.000**	**-0.982**		
HV US	**0.998**	**-0.966**	**0.998**	
HV LS	0.579	**-0.730**	0.586	0.529

Table 6.13 Correlations between the flexural strength (FS), flexural modulus (FM), degree of conversion (DC), hardness value for upper surface (HV US) and hardness value for lower surface (HV LS) of unfilled resin systems containing 50/50wt% bisGMA/TEGDMA. The numbers represent the Pearson correlation coefficient, with the numbers in **bold** showing a strong correlation between sample conditions.

	FS	FM	DC	HV US
FM	**0.845**			
DC	**-0.924**	**-0.993**		
HV US	**-0.711**	-0.278	0.388	
HV LS	**-0.759**	-0.345	0.452	**0.997**

Table 6.14 Correlations between the flexural strength (FS), flexural modulus (FM), degree of conversion (DC), hardness value for upper surface (HV US) and hardness value for lower surface (HV LS) of unfilled resin systems containing 60/40wt% bisGMA/TEGDMA. The numbers represent the Pearson correlation coefficient, with the numbers in **bold** showing a strong correlation between sample conditions.

	FS	FM	DC	HV US
FM	**0.925**			
DC	-0.283	-0.551		
HV US	-0.314	-0.023	**-0.822**	
HV LS	**0.995**	**0.924**	-0.189	-0.404

Table 6.15 Correlations between the flexural strength (FS), flexural modulus (FM), degree of conversion (DC), hardness value for upper surface (HV US) and hardness value for lower surface (HV LS) of unfilled resin systems containing 70/30wt% bisGMA/TEGDMA. The numbers represent the Pearson correlation coefficient, with the numbers in **bold** showing a strong correlation between sample conditions.

	FS	FM	DC	HV US
FM	**0.851**			
DC	**0.651**	**0.619**		
HV US	**0.970**	**0.959**	**0.816**	
HV LS	0.001	-0.040	**0.760**	0.245

Table 6.16 Correlations between the flexural strength (FS), flexural modulus (FM), degree of conversion (DC), hardness value for upper surface (HV US) and hardness value for lower surface (HV LS) of unfilled resin systems containing 80/20wt% bisGMA/TEGDMA. The numbers represent the Pearson correlation coefficient, with the numbers in **bold** showing a strong correlation between sample conditions.

	FS	FM	DC	HV US
FM	**0.984**			
DC	**0.983**	**0.998**		
HV US	**0.684**	**0.769**	**0.807**	
HV LS	**-0.883**	**-0.817**	**-0.780**	-0.260

Table 6.17 Correlations between the flexural strength (FS), flexural modulus (FM), degree of conversion (DC), hardness value for upper surface (HV US) and hardness value for lower surface (HV LS) of unfilled resin systems containing 100/0wt% bisGMA/TEGDMA. The numbers represent the Pearson correlation coefficient, with the numbers in **bold** showing a strong correlation between sample conditions.

	FS	FM	DC	HV US
FM	**0.977**			
DC	**-0.911**	**-0.946**		
HV US	0.424	0.508	**-0.759**	
HV LS	0.583	0.502	-0.196	-0.489

Table 6.18 Correlations between the flexural strength (FS), flexural modulus (FM), degree of conversion (DC), hardness value for upper surface (HV US) and hardness value for lower surface (HV LS) of unfilled resin systems containing 30/60/10wt% bisGMA/UDMA/TEGDMA. The numbers represent the Pearson correlation coefficient, with the numbers in **bold** showing a strong correlation between sample conditions.

	FS	FM	DC	HV US
FM	**0.880**			
DC	**0.955**	**0.996**		
HV US	-0.191	-0.388	-0.473	
HV LS	**0.960**	**0.883**	**0.835**	0.090

Table 6.19 Correlations between the flexural strength (FS), flexural modulus (FM), degree of conversion (DC), hardness value for upper surface (HV US) and hardness value for lower surface (HV LS) of unfilled resin systems containing 20/60/20wt% bisGMA/UDMA/TEGDMA. The numbers represent the Pearson correlation coefficient, with the numbers in **bold** showing a strong correlation between sample conditions.

	FS	FM	DC	HV US
FM	**0.892**			
DC	0.284	0.383		
HV US	0.171	0.067	**-0.896**	
HV LS	0.161	0.263	**0.992**	**-0.945**

Table 6.20 Correlations between the flexural strength (FS), flexural modulus (FM), degree of conversion (DC), hardness value for upper surface (HV US) and hardness value for lower surface (HV LS) of unfilled resin systems containing 10/60/30wt% bisGMA/UDMA/TEGDMA. The numbers represent the Pearson correlation coefficient, with the numbers in **bold** showing a strong correlation between sample conditions.

	FS	FM	DC	HV US
FM	**0.639**			
DC	**-0.891**	**-0.811**		
HV US	**-0.988**	**-1.000**	**0.811**	
HV LS	**0.984**	**0.944**	**-0.958**	**-0.944**

Table 6.21 Correlations between the flexural strength (FS), flexural modulus (FM), degree of conversion (DC), hardness value for upper surface (HV US) and hardness value for lower surface (HV LS) of unfilled resin systems containing 40/50/10wt% bisGMA/UDMA/TEGDMA. The numbers represent the Pearson correlation coefficient, with the numbers in **bold** showing a strong correlation between sample conditions.

	FS	FM	DC	HV US
FM	**0.776**			
DC	0.587	**0.632**		
HV US	0.093	0.149	**0.860**	
HV LS	0.558	**0.604**	**0.999**	**0.878**

Table 6.22 Correlations between the flexural strength (FS), flexural modulus (FM), degree of conversion (DC), hardness value for upper surface (HV US) and hardness value for lower surface (HV LS) of unfilled resin systems containing 30/50/20wt% bisGMA/UDMA/TEGDMA. The numbers represent the Pearson correlation coefficient, with the numbers in **bold** showing a strong correlation between sample conditions.

	FS	FM	DC	HV US
FM	**0.817**			
DC	**0.867**	-0.296		
HV US	**0.973**	-0.558	**0.958**	
HV LS	**0.729**	-0.068	**0.973**	**0.866**

Table 6.23 Correlations between the flexural strength (FS), flexural modulus (FM), degree of conversion (DC), hardness value for upper surface (HV US) and hardness value for lower surface (HV LS) of unfilled resin systems containing 20/50/30wt% bisGMA/UDMA/TEGDMA. The numbers represent the Pearson correlation coefficient, with the numbers in **bold** showing a strong correlation between sample conditions.

	FS	FM	DC	HV US
FM	**0.838**			
DC	**-0.780**	-0.209		
HV US	**0.999**	-0.494	**-0.747**	
HV LS	**-0.981**	**0.613**	**0.645**	**-0.990**

Table 6.24 Correlations between the flexural strength (FS), flexural modulus (FM), degree of conversion (DC), hardness value for upper surface (HV US) and hardness value for lower surface (HV LS) of unfilled resin systems containing 10/50/40wt% bisGMA/UDMA/TEGDMA. The numbers represent the Pearson correlation coefficient, with the numbers in **bold** showing a strong correlation between sample conditions.

	FS	FM	DC	HV US
FM	**0.811**			
DC	-0.597	-0.386		
HV US	**-0.965**	**-1.000**	0.365	
HV LS	**-0.618**	-0.411	**1.000**	0.390

Table 6.25 Correlations between the flexural strength (FS), flexural modulus (FM), degree of conversion (DC), hardness value for upper surface (HV US) and hardness value for lower surface (HV LS) of unfilled resin systems containing 50/40/10wt% bisGMA/UDMA/TEGDMA. The numbers represent the Pearson correlation coefficient, with the numbers in **bold** showing a strong correlation between sample conditions.

	FS	FM	DC	HV US
FM	0.470			
DC	-0.409	**0.816**		
HV US	**0.795**	-0.376	0.228	
HV LS	**0.895**	-0.544	0.040	**0.982**

Table 6.26 Correlations between the flexural strength (FS), flexural modulus (FM), degree of conversion (DC), hardness value for upper surface (HV US) and hardness value for lower surface (HV LS) of unfilled resin systems containing 50/30/20wt% bisGMA/UDMA/TEGDMA. The numbers represent the Pearson correlation coefficient, with the numbers in **bold** showing a strong correlation between sample conditions.

	FS	FM	DC	HV US
FM	**0.851**			
DC	**0.931**	0.504		
HV US	**-0.990**	**-0.864**	**-0.870**	
HV LS	**-0.696**	-0.101	**-0.910**	0.588

Table 6.27 Correlations between the flexural strength (FS), flexural modulus (FM), degree of conversion (DC), hardness value for upper surface (HV US) and hardness value for lower surface (HV LS) of unfilled resin systems containing 50/20/30wt% bisGMA/UDMA/TEGDMA. The numbers represent the Pearson correlation coefficient, with the numbers in **bold** showing a strong correlation between sample conditions.

	FS	FM	DC	HV US
FM	**0.904**			
DC	0.416	0.260		
HV US	-0.018	0.147	**-0.917**	
HV LS	0.316	0.468	**-0.731**	**0.943**

Table 6.28 Correlations between the flexural strength (FS), flexural modulus (FM), degree of conversion (DC), hardness value for upper surface (HV US) and hardness value for lower surface (HV LS) of unfilled resin systems containing 50/10/40wt% bisGMA/UDMA/TEGDMA. The numbers represent the Pearson correlation coefficient, with the numbers in **bold** showing a strong correlation between sample conditions.

Correlation analysis of filled resin composites

	FS	FM
FM	**0.625**	
DC	-0.018	**-0.265**

Table 6.29 Correlations between the flexural strength (FS), flexural modulus (FM) and degree of conversion (DC) of 60/40wt% UDMA/TEGDMA filled resin composites containing 70wt% barium silicate filler. The numbers represent the Pearson correlation coefficient, with the numbers in **bold** showing a strong correlation between sample conditions.

	FS	FM
FM	0.569	
DC	-0.147	0.348

Table 6.30 Correlations between the flexural strength (FS), flexural modulus (FM) and degree of conversion (DC) of 60/40wt% UDMA/TEGDMA filled resin composites containing 80wt% barium silicate filler. The numbers represent the Pearson correlation coefficient.

	FS	FM
FM	**0.751**	
DC	0.012	0.106

Table 6.31 Correlations between the flexural strength (FS), flexural modulus (FM) and degree of conversion (DC) of PMMA. The numbers represent the Pearson correlation coefficient, with the numbers in **bold** showing a strong correlation between sample conditions.

	FS	FM
FM	-0.070	
DC	-0.187	0.096

Table 6.32 Correlations between the flexural strength (FS), flexural modulus (FM) and degree of conversion (DC) of 60/40wt% UDMA/TEGDMA filled resin composites containing 60wt% barium silicate filler and 10wt% Type I silanated filler. The numbers represent the Pearson correlation coefficient.

	FS	FM
FM	**0.677**	
DC	0.261	0.280

Table 6.33 Correlations between the flexural strength (FS), flexural modulus (FM) and degree of conversion (DC) of 60/40wt% UDMA/TEGDMA filled resin composites containing 50wt% barium silicate filler and 20wt% Type I silanated filler. The numbers represent the Pearson correlation coefficient, with the numbers in **bold** showing a strong correlation between sample conditions.

	FS	FM
FM	0.317	
DC	-0.138	-0.052

Table 6.34 Correlations between the flexural strength (FS), flexural modulus (FM) and degree of conversion (DC) of 60/40wt% UDMA/TEGDMA filled resin composites containing 40wt% barium silicate filler and 30wt% Type I silanated filler. The numbers represent the Pearson correlation coefficient.

	FS	FM
FM	0.385	
DC	0.516	0.388

Table 6.35 Correlations between the flexural strength (FS), flexural modulus (FM) and degree of conversion (DC) of 60/40wt% UDMA/TEGDMA filled resin composites containing 30wt% barium silicate filler and 40wt% Type I silanated filler. The numbers represent the Pearson correlation coefficient.

	FS	FM
FM	0.565	
DC	-0.436	0.186

Table 6.36 Correlations between the flexural strength (FS), flexural modulus (FM) and degree of conversion (DC) of 60/40wt% UDMA/TEGDMA filled resin composites containing 60wt% barium silicate filler and 10wt% Type II non-silanated filler. The numbers represent the Pearson correlation coefficient.

	FS	FM
FM	0.584	
DC	0.017	-0.363

Table 6.37 Correlations between the flexural strength (FS), flexural modulus (FM) and degree of conversion (DC) of 60/40wt% UDMA/TEGDMA filled resin composites containing 50wt% barium silicate filler and 20wt% Type II non-silanated filler. The numbers represent the Pearson correlation coefficient.

	FS	FM
FM	0.584	
DC	0.017	-0.363

Table 6.38 Correlations between the flexural strength (FS), flexural modulus (FM) and degree of conversion (DC) of 60/40wt% UDMA/TEGDMA filled resin composites containing 40wt% barium silicate filler and 30wt% Type II non-silanated filler. The numbers represent the Pearson correlation coefficient.

	FS	FM
FM	**0.746**	
DC	0.324	-0.038

Table 6.39 Correlations between the flexural strength (FS), flexural modulus (FM) and degree of conversion (DC) of 60/40wt% UDMA/TEGDMA filled resin composites containing 30wt% barium silicate filler and 40wt% Type II non-silanated filler. The numbers represent the Pearson correlation coefficient, with the numbers in **bold** showing a strong correlation between sample conditions.

	FS	FM
FM	0.306	
DC	-0.576	-0.308

Table 6.40 Correlations between the flexural strength (FS), flexural modulus (FM) and degree of conversion (DC) of 60/40wt% UDMA/TEGDMA filled resin composites containing 60wt% barium silicate filler and 10wt% Type III non-silanated filler. The numbers represent the Pearson correlation coefficient.

	FS	FM
FM	0.226	
DC	**0.951**	0.281

Table 6.41 Correlations between the flexural strength (FS), flexural modulus (FM) and degree of conversion (DC) of 60/40wt% UDMA/TEGDMA filled resin composites containing 50wt% barium silicate filler and 20wt% Type III non-silanated filler. The numbers represent the Pearson correlation coefficient, with the numbers in **bold** showing a strong correlation between sample conditions.

	FS	FM
FM	-0.377	
DC	-0.539	0.455

Table 6.42 Correlations between the flexural strength (FS), flexural modulus (FM) and degree of conversion (DC) of 60/40wt% UDMA/TEGDMA filled resin composites containing 40wt% barium silicate filler and 30wt% Type III non-silanated filler. The numbers represent the Pearson correlation coefficient.

	FS	FM
FM	0.335	
DC	0.579	-0.409

Table 6.43 Correlations between the flexural strength (FS), flexural modulus (FM) and degree of conversion (DC) of 60/40wt% UDMA/TEGDMA filled resin composites containing 30wt% barium silicate filler and 40wt% Type III non-silanated filler. The numbers represent the Pearson correlation coefficient.

	FS	FM
FM	0.341	
DC	-0.440	-0.058

Table 6.44 Correlations between the flexural strength (FS), flexural modulus (FM) and degree of conversion (DC) of 60/40wt% UDMA/TEGDMA filled resin composites containing 69wt% barium silicate filler and 11wt% Type I silanated filler. The numbers represent the Pearson correlation coefficient.

	FS	FM
FM	**0.699**	
DC	-0.371	0.253

Table 6.45 Correlations between the flexural strength (FS), flexural modulus (FM) and degree of conversion (DC) of 60/40wt% UDMA/TEGDMA filled resin composites containing 57wt% barium silicate filler and 23wt% Type I silanated filler. The numbers represent the Pearson correlation coefficient, with the numbers in **bold** showing a strong correlation between sample conditions.

	FS	FM
FM	**0.701**	
DC	0.451	0.361

Table 6.46 Correlations between the flexural strength (FS), flexural modulus (FM) and degree of conversion (DC) of 60/40wt% UDMA/TEGDMA filled resin composites containing 45wt% barium silicate filler and 34wt% Type I silanated filler. The numbers represent the Pearson correlation coefficient, with the numbers in **bold** showing a strong correlation between sample conditions.

	FS	FM
FM	0.052	
DC	0.141	-0.430

Table 6.47 Correlations between the flexural strength (FS), flexural modulus (FM) and degree of conversion (DC) of 60/40wt% UDMA/TEGDMA filled resin composites containing 45wt% barium silicate filler and 34wt% Type I silanated filler. The numbers represent the Pearson correlation coefficient.

	FS	FM
FM	**0.883**	
DC	0.021	0.159

Table 6.48 Correlations between the flexural strength (FS), flexural modulus (FM) and degree of conversion (DC) of 60/40wt% UDMA/TEGDMA filled resin composites containing 11wt% barium silicate filler and 69wt% Type II non-silanated filler. The numbers represent the Pearson correlation coefficient, with the numbers in **bold** showing a strong correlation between sample conditions.

	FS	FM
FM	0.522	
DC	-0.035	-0.494

Table 6.49 Correlations between the flexural strength (FS), flexural modulus (FM) and degree of conversion (DC) of 60/40wt% UDMA/TEGDMA filled resin composites containing 57wt% barium silicate filler and 23wt% Type II non-silanated filler. The numbers represent the Pearson correlation coefficient.

	FS	FM
FM	**0.748**	
DC	**-0.806**	**-0.666**

Table 6.50 Correlations between the flexural strength (FS), flexural modulus (FM) and degree of conversion (DC) of 60/40wt% UDMA/TEGDMA filled resin composites containing 45wt% barium silicate filler and 34wt% Type II non-silanated filler. The numbers represent the Pearson correlation coefficient, with the numbers in **bold** showing a strong correlation between sample conditions.

	FS	FM
FM	0.585	
DC	-0.273	**-0.663**

Table 6.51 Correlations between the flexural strength (FS), flexural modulus (FM) and degree of conversion (DC) of 60/40wt% UDMA/TEGDMA filled resin composites containing 34wt% barium silicate filler and 45wt% Type II non-silanated filler. The numbers represent the Pearson correlation coefficient, with the numbers in **bold** showing a strong correlation between sample conditions.

	FS	FM
FM	0.176	
DC	**0.610**	0.539

Table 6.52 Correlations between the flexural strength (FS), flexural modulus (FM) and degree of conversion (DC) of 60/40wt% UDMA/TEGDMA filled resin composites containing 69wt% barium silicate filler and 11wt% Type III non-silanated filler. The numbers represent the Pearson correlation coefficient, with the numbers in **bold** showing a strong correlation between sample conditions.

	FS	FM
FM	**0.801**	
DC	0.134	0.009

Table 6.53 Correlations between the flexural strength (FS), flexural modulus (FM) and degree of conversion (DC) of 60/40wt% UDMA/TEGDMA filled resin composites containing 57wt% barium silicate filler and 23wt% Type III non-silanated filler. The numbers represent the Pearson correlation coefficient, with the numbers in **bold** showing a strong correlation between sample conditions.

	FS	FM
FM	-0.292	
DC	0.031	-0.288

Table 6.54 Correlations between the flexural strength (FS), flexural modulus (FM) and degree of conversion (DC) of 60/40wt% UDMA/TEGDMA filled resin composites containing 45wt% barium silicate filler and 34wt% Type III non-silanated filler. The numbers represent the Pearson correlation coefficient. , with the numbers in **bold** showing a strong correlation between sample conditions.